



National Library of Canada

Cataloguing Branch
Canadian Theses Division

Ottawa, Canada
K1A 0N4

Bibliothèque nationale du Canada

Direction du catalogage
Division des thèses canadiennes

NOTICE

AVIS

The quality of this microfiche is heavily dependent upon the quality of the original thesis submitted for microfilming. Every effort has been made to ensure the highest quality of reproduction possible.

If pages are missing, contact the university which granted the degree.

Some pages may have indistinct print especially if the original pages were typed with a poor typewriter, ribbon or if the university sent us a poor photocopy.

Previously copyrighted materials (journal articles, published tests, etc.) are not filmed.

Reproduction in full or in part of this film is governed by the Canadian Copyright Act R.S.C. 1970, c. C-30. Please read the authorization forms which accompany this thesis.

**THIS DISSERTATION
HAS BEEN MICROFILMED
EXACTLY AS RECEIVED**

La qualité de cette microfiche dépend grandement de la qualité de la thèse soumise au microfilmage. Nous avons tout fait pour assurer une qualité supérieure de reproduction.

Si il manque des pages, veuillez communiquer avec l'université qui a conféré le grade.

La qualité d'impression de certaines pages peut laisser à désirer, surtout si les pages originales ont été dactylographiées à l'aide d'un ruban usé ou si l'université nous a fait parvenir une photocopie de mauvaise qualité.

Les documents qui font déjà l'objet d'un droit d'auteur (articles de revue, examens publiés, etc.) ne sont pas microfilmés.

La reproduction, même partielle, de ce microfilm est soumise à la Loi canadienne sur le droit d'auteur, SRC 1970, c. C-30. Veuillez prendre connaissance des formules d'autorisation qui accompagnent cette thèse.

**LA THÈSE A ÉTÉ
MICROFILMÉE TELLE QUE
NOUS L'AVONS REÇUE**

MECHANICAL PERFORMANCE OF SNOW UNDER LOADING

by

Masaharu Fukue

A Thesis submitted to the Faculty of Graduate Studies and
Research in partial fulfillment of the requirements
for the degree of Doctor of Philosophy

Department of Civil Engineering & Applied Mechanics
McGill University
Montreal, Quebec
February 1977

MECHANICAL PERFORMANCE OF SNOW UNDER LOADING

by

Masaharu Fukue

Department of Civil Engineering
and Applied Mechanics

Ph.D.

ABSTRACT

As a basic concept in snow mechanics, the adhesion theory was developed. The adhesion theory requires assumption that contact area between snow grains increases with the local flow deformation of solid near the contacts and the adhesion at contacts increases with the size of contact area. The results obtained from the microscopic and macroscopic experiments show that the adhesion theory is applicable to snow.

The deformation mechanisms of snow under confined compression were microscopically studied by using a microscope and thin section method. The experimental results showed that the type of deformation depends upon the deformation rate applied.

For the requirements in snow mechanics, simple testing techniques, i.e., unconfined compression, single load confined compression, increment load confined compression, progressive load confined compression, direct shear, thin blade penetration and rectangular rigid plate penetration tests were examined by using various types of snow. In addition, the mechanical response characteristics of various snow were

studied by performing the mechanical tests. The experimental results showed that the behaviour of snow under the mechanical tests was well explained by the adhesion theory developed in this study.

The test results obtained from confined compression testing, and observations made in regard to physical performance of the test specimens, illustrated the need for establishment of critical density and threshold density. These quantities give the significant changes in the behaviour of snow below and beyond these points.

The failure modes depend on the type of testing, snow type and size of specimen. The experimental results show that the conventional shear theory is not always applicable to snow.

On the basis of the present research, snow classification based on the important factors governing snow properties for engineering purposes was proposed.

FONCTIONNEMENT DE LA NEIGE SOUS PÉSSION

par

Masaharu Fukue

Département de Génie Civil
et de Mécaniques Appliquées

Ph.D.

RESUME

La théorie de l'adhésion fut développée comme concept de base dans la mécanique de la neige. La théorie de l'adhésion requiert la supposition que la surface de contact entre les grains de neige s'accroît en même temps que la déformation locale de l'écoulement des solides près des points de contact et que l'adhésion aux contacts s'accroît avec la dimension de la surface du contact. Les résultats obtenus pendant des expériences microscopiques et macroscopiques montrent que la théorie de l'adhésion peut s'appliquer à la neige.

La mécanique de la déformation de la neige sous compression avec étreinte latérale fut étudiée par l'usage du microscope et de la méthode de la section mince. Les résultats des expériences montrent que le type de déformation dépend de l'allure de la déformation utilisée.

Pour les exigences de la mécanique de la neige, de simples techniques d'essai, telles que la compression simple, la compression avec étreinte latérale à charge unique, la compression avec étreinte latérale à charge augmentée, la compression avec étreinte latérale à charge progressive, le cisaillement direct, la pénétration de la lame mince et la pénétration de la plate rigide rectangulaire furent

examinées dans l'utilisation de divers types de neige. De plus, les caractères de la réponse mécanique des différents genres de neige furent étudiés par les essais mécaniques. Les résultats des expériences montrent que le comportement de la neige dans les essais mécaniques pouvait bien s'expliquer par la théorie de l'adhésion développée dans cette recherche.

Les résultats obtenus lors de la compression avec étreinte latérale, et les observations à l'égard du fonctionnement physique des échantillons, ont illustré le besoin de l'établissement d'une densité critique et d'une densité du seuil. Ces quantités produisent des changements significatifs dans le caractère de la neige à l'intérieur et au de là de ces densités.

Les manières de la rupture dépendent du type d'essai, du type de neige et de la dimension de l'échantillon. Les résultats des expériences montrent que la théorie conventionnelle du cisaillement n'est pas toujours applicable à la neige.

Ayant pour base la présente recherche, une classification de la neige établie sur les facteurs importants contrôlant les caractéristiques, est proposée pour les fins de l'ingénierie.

ACKNOWLEDGEMENTS

The author wishes to express his gratitude to his research director, Professor R.N. Yong, Director of the Geotechnical Research Centre of McGill University of his guidance and suggestions throughout the course of this research.

He also wishes to thank Professor J.C. Osler and Professor R.D. Japp for their invaluable suggestions during entire period of this research.

Some apparatuses were made by Mr. P.V. Janiga and the technical staff of the Department of Civil Engineering, to them the author expresses his gratitude.

He wishes to thank Dr. A. Sethi, Dr. A.S. Baweja and Mr. C.H. Cheung for their assistance in the preparation of the manuscript.

He also wishes to thank Mrs. Boonsinsuk for typing the manuscript.

This thesis study was conducted with financial support from the mobility contract. Full acknowledgement is accorded to DREO and the Project Officer, Mr. I.S. Lindsay, for financial support arrangements with the Department of Supply and Services, Canada.

LIST OF FIGURES

<u>Figure No.</u>		<u>Page</u>
1,1	General flow chart for snow mechanics	2
1,2	Organization of the study for the adhesion theory	8
1,3	Organization of the study for mechanical properties of snow	9
2,1	Diagram of transformation for snow type	17
2,2	Actual snow failure under rigid plate with dead load, showing cutting shear and compression shear	19
2,3	General shear failure for dense assemblage	21
3,1	Various snow models	24
3,2	Adhesion of clean steel ball on a clean indium surface	26
3,3	Increase in contact area between grains	28
3,4	Various load conditions for granular snow	30
3,5	Various load conditions for semi-bonded snow	37
3,6	Various load conditions for sintered snow	37
4,1	Typical grain structure of polycrystalline solid	42
4,2	Organization of the study in Chapter IV	44
4,3	Mathematical model of spherical particles in contact for interpretation of increase in contact area under relative movement (e_r)	45
4,4	Increase in contact area between spherical particles as a function of relative movement (e_r)	46
4,5	Uniform deformation of cylindrical specimen under parallel loading	50

LIST OF FIGURES (cont'd)

<u>Figure No.</u>		<u>Page</u>
4,6	Interpretation of local flow deformation as a function of contact angle and axial deformation	53
4,7	Theoretical relationship between $(\frac{\xi}{r})^2$ and strain	56
5,1	Organization of experimental study	58
5,2	Grain size distribution of snows used in the study	60
5,3	Illustration of ice pulverizer apparatus for manufacture of laboratory snow	61
5,4	Typical snow crystal used in the study	63
5,5	Preparation of thin section of snow sample	66
5,6	A possible thin sectioned-grain size and the true grain size	67
5,7	Illustration of apparatus for unconfined compression test	72
5,8	Apparent and true stresses on ideal failure plane in snow	75
5,9	Illustration of apparatus for dead load confined compression test	77
5,10	Illustration of apparatus for direct shear test	81
6,1	Organization of the microscopic study on deformation mechanism of snow	87
6,2	Compressed snow sample used in thin section method	89
6,3	Three dimensional and two dimensional grain sizes, contact angle, and contact area	90
6,4	Comparison between thin sectioned-grain size and true grain size in microscope analysis	91
6,5	Thin sectioned - internal structure of compressed snow under confined compression	95

LIST OF FIGURES (cont'd)

<u>Figure No.</u>		<u>Page</u>
6,6	Theoretical relationship between $(\frac{\xi}{r})^2$ and ψ	97
6,7	Statistical comparison between experimental $(\frac{\xi}{R})_{ex.}^2$ and theoretical $(\frac{\xi}{r})_{theo.}^2$	98
6,8	Frequency distribution of ψ obtained from thin section method	100
6,9	Contact number per grain obtained from thin section method	100
6,10	Thin sectioned - internal structure of compressed snow under confined compression	105
7,1	Typical stress-strain curve of snow in relation to deformation rate	107
7,2	Typical brittle and ductile stress-strain curves of snow in relation to bonding and deformation rate	110
7,3	Typical semi-brittle stress-strain curve of snow	111
7,4	Typical failure modes for snow in unconfined compression test	113
7,5	Relationships between unconfined compressive strength and deformation rate for variously age hardened snow	116
7,6	Relationship between unconfined compressive strength and failure strain for variously age hardened snow at a compressive velocity of 0.98 mm/sec	119
7,7	Relationship between compressive modulus and unconfined compressive strength for snow	121
7,8	Density change of variously age hardened snows	124
7,9	Volume change of granular snow in confined loading tests using constant load	130

LIST OF FIGURES (cont'd)

<u>Figure No.</u>		<u>Page</u>
7,10	Volume change relationships for snow in confined compression tests using incremental loading.	132
7,11	Various deformation types for snow in dead load confined compression	134
7,12	Typical stress-density relationship for confined compression with controlled deformation rates	137
7,13	Stress-density change curves as a function of various initial densities	139
7,14	Relationship between strain rate and threshold density for granular snow	140
7,15	Relationship between "stress-density modulus" and threshold density	142
7,16	Threshold and critical densities of artificial snow	144
7,17	Stress, density and strain rate surface for snow	145
7,18	Simple structure model of loose snow for confined compression performances showing various deformation mechanisms in relation to density changes as a function of loading rate	149
7,19	Relationships between shear stress and shear deformation for snow in direct shear test	153
7,20	General shear failure of snow in direct shear test	154
7,21	Typical tensile failure mode for snow without normal pressure or with relatively lower normal pressure in direct shear test	156
7,22	Irregular failure mode of snow in direct shear test when the thickness of specimen is insufficient	156
7,23	Shear force as a function of thickness of snow specimen in direct shear test	157
7,24	Relationships between shear strength and normal pressure for granular snow in direct shear test at shear velocities, 0.065 and 0.31 cm/sec	159

LIST OF FIGURES (cont'd)

<u>Figure No.</u>		<u>Page</u>
7,10	Volume change relationships for snow in confined compression tests using incremental loading.	132
7,11	Various deformation types for snow in dead load confined compression	134
7,12	Typical stress-density relationship for confined compression with controlled deformation rates	137
7,13	Stress-density change curves as a function of various initial densities	139
7,14	Relationship between strain rate and threshold density for granular snow	140
7,15	Relationship between "stress-density modulus" and threshold density	142
7,16	Threshold and critical densities of artificial snow	144
7,17	Stress, density and strain rate surface for snow	145
7,18	Simple structure model of loose snow for confined compression performances showing various deformation mechanisms in relation to density changes as a function of loading rate	148
7,19	Relationships between shear stress and shear deformation for snow in direct shear test.	153
7,20	General shear failure of snow in direct shear test	154
7,21	Typical tensile failure mode for snow without normal pressure or with relatively lower normal pressure in direct shear test	156
7,22	Irregular failure mode of snow in direct shear test when the thickness of specimen is insufficient	156
7,23	Shear force as a function of thickness of snow specimen in direct shear test	157
7,24	Relationships between shear strength and normal pressure for granular snow in direct shear test at shear velocities, 0.065 and 0.31 cm/sec	159

x

LIST OF FIGURES (cont'd)

<u>Figure No.</u>		<u>Page</u>
7,25	Effect of normal pressure in direct shear test	162
7,26	General stress condition at grain contact	164
7,27	Illustration of shear strength from the adhesion theory	166
7,28	Relationships between shear strength and normal pressure for variously age hardened snow in direct shear test	168
7,29	Typical shearing responses of snow in direct shear test in relation to snow type	172
7,30	Illustration of thin blade penetration performance	179
7,31	Speed effect of thin blade penetration into age hardened snow	180
7,32	Prediction of snow behaviour under thin blade penetration	183
7,33	Relationship between unconfined compressive strength and thin blade penetrating force	185
7,34	Illustration of rectangular rigid plate penetration performance (glass-sided experiment)	189
7,35	Plate penetration into fresh snow	190
7,36	Relationships between penetrating force and depth for fresh snow, in rectangular rigid plate penetration (glass-sided experiment)	191
7,37	Plate penetration into granular snow	193
7,38	Illustration of apparent snow responses under plate penetration	195
7,39	Relationship between penetrating force and depth for granular snow in rectangular rigid plate penetration test (glass-sided experiment)	196

LIST OF FIGURES (cont'd)

<u>Figure No.</u>		<u>Page</u>
7,40	Illustration of thin blade penetration performance into snow previously compressed by plate penetration	199
7,41	Blade penetrating force contours for granular snow previously compressed by plate penetration with a speed of 0.097 mm/sec	200
7,42	Blade penetrating force for snow previously compressed by plate penetration with a speed of 0.98 mm/sec	201
7,43	Profiles of blade penetrating force for snow previously compressed by plate penetration obtained from Figs. 7,41 and 7,42	202
7,44	Plate penetration into age hardened snow for 3 days	205
8,1	Adhered snow specimen under confined compression	208
8,2	Unconfined compressive strength of snows previously compressed under confined condition	210
8,3	Typical rate effect of deformation in confined compression	211
8,4	Microscopic model for various deformation types of snow	213
8,5	Macroscopic model of snow for direct shear test	215
8,6	Various snow nature in relation to unconfined compressive strength and density	219
A-1	International snow classification (see Table A-1)	228
B-1	Stress condition in snow under compression	230
B-2	Intergranular slippage condition under uniaxial true stress P_z at contact between grains	232
B-3	Depositing performance of granular material	234

LIST OF FIGURES (cont'd)

<u>Figure No.</u>		<u>Page</u>
B-4	Intergranular slippage condition under biaxial true stress condition	236
C-1	Depositing performance of snow into a cup through a sieve	239
C-2	Apparent depositing features of (a) fresh snow and (b) two year old snow into cups through a sieve	240
D-1	A comparison between grain size distributions obtained from the microscope and the sieve analyses	243
D-2	Frequency distribution of shape factor (D_s/D_1) in uniformly graded snow	244
E-1	Mohr's envelope	247
F-1	Illustration that e_s equals to $e \cos \phi$ if $\Delta \phi$ is assumed to be small	248

LIST OF TABLES

<u>Table No.</u>		<u>Page</u>
6,1	Mechanical properties of snows used for thin sections	94
7,1	Critical density, γ_{cr} , for uniformly and well graded snows	127
8,1	Snow classification based on the study	222
A-1	International snow classification (see Fig. A-1)	227
C-1	Depositing density and H^*/R^* of snow	241

LIST OF SYMBOLS

A_c	adhesion per unit area
A_d	adhesion per contact
A_s	adhesion by sintering
D_l	long diameter of grain
D_s	short diameter of grain
$d, \Delta d$	deformation
e, e_p	deformation per particle
F	force
F_c	tangential force required to initiate slide on contact between grains
h^*	height of cone shape deposits
h_0, L, l	initial height of specimen
N	normal force acting on contact between grains
n, n'	number of particles or grains
P	force acting on contact between grains
R	radius of curvature
R^*	radius of circular bottom of cone shape deposits
r	radius of spherical particle
S, S_c, S'	contact area between particles or grains
S_e	effective contact area
t	time
V	volume

$\Delta \gamma$	increment of density
γ_{cr}	critical density of snow
γ_0	initial density of snow
γ_{th}	threshold density of snow
e	axial strain
e	relative strain of particles, $e / 2r$
r	radius of contact area
r^*	radius of contact area in thin section
ϵ	$\sqrt{r^2 - r^{*2}}$
n_{th}	stress-density modulus in confined compression
σ	stress
$\Delta \sigma$	increment of stress
σ_c	unconfined compressive strength
σ_n	normal force acting on shear plane
τ	shear strength
ϕ	macroscopic inherent angle of friction for granular snow
ϕ'	macroscopic apparent angle of friction for granular snow
ϕ_e	microscopic inherent angle of friction for sintered snow
ϕ_i	microscopic inherent angle of friction for granular snow
ψ	contact angle
ψ^*	contact angle in thin section
B.P.E.	thin blade penetrating force

CONTRIBUTIONS

1. An adhesion theory for snow has been developed using both microscopic and macroscopic evidence obtained from this study.
2. The deformation mechanisms of snow were studied using a microscope and thin section techniques to aid in provision of explanations regarding the basic mechanical behaviour of snow.
3. The analysis of results from simple mechanical testing techniques applied to several types of snow shows that loading rate is of utmost significance. Loading rate can change the total character of both material property and response performance.
4. The mechanical response characteristics of various types of snow have been examined using simple mechanical tests and the results expand the present knowledge of the mechanical response characteristics of snow.
5. Since the difficulty in the study of snow lies in the varied nature of snow, the classification of snow for engineering purposes has been proposed in this study.

6. For field testing, the thin blade penetrating technique was developed in this study. By using the thin blade penetrating technique with other factors, such as grain characteristics, density and external factors, the approximate mechanical properties and behaviour of snow may be predicted using the classification proposed in this study.
7. The contribution of this study includes the presentation of new problems which will be encountered in snow mechanics in the future. The entire study indicates that further engineering study of snow should be undertaken.
8. The establishment of critical and threshold densities as specific properties of snow characteristic of (a) method of test loading, (b) grain size distribution of the snow, and (c) initial density, is a significant contribution to the evaluation of snow performance under loading.

TABLE OF CONTENTS

ABSTRACT	i
RESUME	iii
ACKNOWLEDGEMENTS	v
LIST OF FIGURES	vi
LIST OF TABLES	xiii
LIST OF SYMBOLS	xiv
CONTRIBUTIONS	xvi
<u>CHAPTER</u>	<u>Page</u>
I INTRODUCTION	1
II NATURE OF SNOW AND ICE IN RELATION TO PROBLEM UNDER STUDY	11
II-1 Grain Shape	12
II-2 Grain Size	13
II-3 Intergranular Force of Snow	14
II-4 Density of Snow	16
II-5 Some Problems in Low Density Snow	18
PART I	
THEORETICAL CONSIDERATION ON DEFORMATION MECHANISM OF SNOW	
III ADHESION AND FRICTION OF SNOW	22
III-1 Introduction	22
III-2 Adhesion between Solids	25
III-3 Fresh Snow	27
III-4 Granular Snow	28

CHAPTER

Page

III Continued

III-5	Semi-bonded Snow	34
III-6	Sintered Snow	36

IV INCREASE IN CONTACT AREA BETWEEN SNOW GRAINS UNDER VISCOUS DEFORMATION OF CRYSTALS

IV-1	Introduction	40
IV-2	Relation between Contact Area and Relative Strain	43
IV-3	Relationship between Microscopic Relative Strain and Macroscopic Axial Strain	49
IV-4	Increase in Contact Area between Particles as a Function of Macroscopic Axial Strain and Contact Angle	54

PART 2

EXPERIMENTAL INVESTIGATION

V EXPERIMENTATION

V-1	Description of Material	59
V-2	Preparation of Thin Section of Snow Sample	64
V-3	Method of Compressive Loading	68
V-4	Mechanical Tests	70
V-4.1	Unconfined Compression Test	70
V-4.2	Confined Compression Test	73
V-4.3	Direct Shear Test	79
V-4.4	Penetration Test	82
V-5	Sample Preparation	83

CHAPTER

Page

VI	MICROSCOPIC STUDY ON DEFORMATION MECHANISMS OF SNOW	
VI-1	Change in Internal Structure of Snow under Ductile Confined Compression	85
VI-1.1	Introduction	85
VI-1.2	Results and Discussion	94
VI-2	Change in Internal Structure of Snow under Brittle Confined Compression	103
VI-2.1	Introduction	103
VI-2.2	Results and Discussion	104
VII	RESULTS AND DISCUSSION ON MECHANICAL PROPERTIES AND BEHAVIOUR OF SNOW	
VII-1	Unconfined Compression Performance	106
VII-1.1	Stress-Strain Relationship	106
VII-1.2	Apparent Failure Mode for Snow in Brittle Unconfined Compression Performance	112
VII-1.3	Unconfined Compressive Strength of Snow as a Function of Compressive Velocity and Age of Sintering	115
VII-1.4	Relationship between Unconfined Compressive Strength and Failure Strain at a Given Brittle Compressive Velocity	118
VII-2	Confined Compression Performance	123
VII-2.1	Confined Compression under a Single Fixed Load	123
VII-2.2	Microfracture and Creep Deformation of Snow in Confined Compression	129
VII-2.3	Snow Behaviour under Progressive Load (Confined Compression Test with Controlled Deformation Rate)	135

CHAPTER

Page

VI MICROSCOPIC STUDY ON DEFORMATION MECHANISMS OF SNOW

VI-1	Change in Internal Structure of Snow under Ductile Confined Compression	85
VI-1.1	Introduction	85
VI-1.2	Results and Discussion	94
VI-2	Change in Internal Structure of Snow under Brittle Confined Compression	103
VI-2.1	Introduction	103
VI-2.2	Results and Discussion	104

VII RESULTS AND DISCUSSION ON MECHANICAL PROPERTIES AND BEHAVIOUR OF SNOW

VII-1	Unconfined Compression Performance	106
VII-1.1	Stress-Strain Relationship	106
VII-1.2	Apparent Failure Mode for Snow in Brittle Unconfined Compression Performance	112
VII-1.3	Unconfined Compressive Strength of Snow as a Function of Compressive Velocity and Age of Sintering	115
VII-1.4	Relationship between Unconfined Compressive Strength and Failure Strain at a Given Brittle Compressive Velocity	118
VII-2	Confined Compression Performance	123
VII-2.1	Confined Compression under a Single Fixed Load	123
VII-2.2	Microfracture and Creep Deformation of Snow in Confined Compression	129
VII-2.3	Snow Behaviour under Progressive Load (Confined Compression Test with Controlled Deformation Rate)	135

CHAPTER

Page

VII Continued

VII-3	Direct Shear Performance of Snow	152
VII-3.1	Shear Stress-Deformation Relationship	152
VII-3.2	Apparent Failure Modes in Direct Shear Performance	152
VII-3.3	Effect of Shear Velocity	155
VII-3.4	Effect of Initial Bonding of Snow in Direct Shear Test	167
VII-4	Penetration Performance	176
VII-4.1	Thin Blade Penetration Performance into Snow	176
VII-4.2	Rectangular Rigid Plate Penetration Performance	187

VIII GENERAL DISCUSSION AND CONCLUDING REMARKS 206

VIII-1	Discussion on the Adhesion Theory	206
VIII-2	Proposition of Snow Classification for Engineering Purpose	216
VIII-3	Concluding Remarks	223

APPENDICES

A	INTERNATIONAL CLASSIFICATION OF FRESH SNOW	227
B	INTERGRANULAR SLIPPAGE BETWEEN SNOW GRAINS	229
C	DEPOSITING CHARACTERISTICS OF SNOW WITH RESPECT TO ITS GRAIN SIZE DISTRIBUTION AND GRAIN SHAPE	238

APPENDICES

Continued

Page

D	TRUE GRAIN SIZE OF SNOW OBTAINED FROM THE MICROSCOPE ANALYSIS AND APPARENT GRAIN SIZE FROM THE SIEVE ANALYSIS	242
E	NOHR'S ENVELOPE	245
F	ILLUSTRATION OF Eq. (4,8)	247
	BIBLIOGRAPHY	248

CHAPTER I

INTRODUCTION

General Problem Development

The behaviour of snow under load falls within the consideration of snow mechanics. Figure 1,1 shows a general flow chart which portrays the involvement of snow in various kinds of activities. The need for a proper and basic study of the behaviour of snow under loading in the case of this thesis arises from a realization of the fact that in off-road vehicle mobility on snow covered terrain, the influence of snow cover properties on vehicle performance is very significant. For proper positive traction development between vehicular tracks and snow (for tracked vehicles), the following conditions need to be fulfilled:

- (a) integral adhesion or bonding (no slip) between the mechanical traction device and snow to allow for generation of propulsion, and
- (b) stable snow compression, i.e.; compression of underlying snow without yield or failure, to provide for support of the vehicle.

Thus, proper positive traction performance requires that a minimum amount of input energy is expended on non productive work-thereby

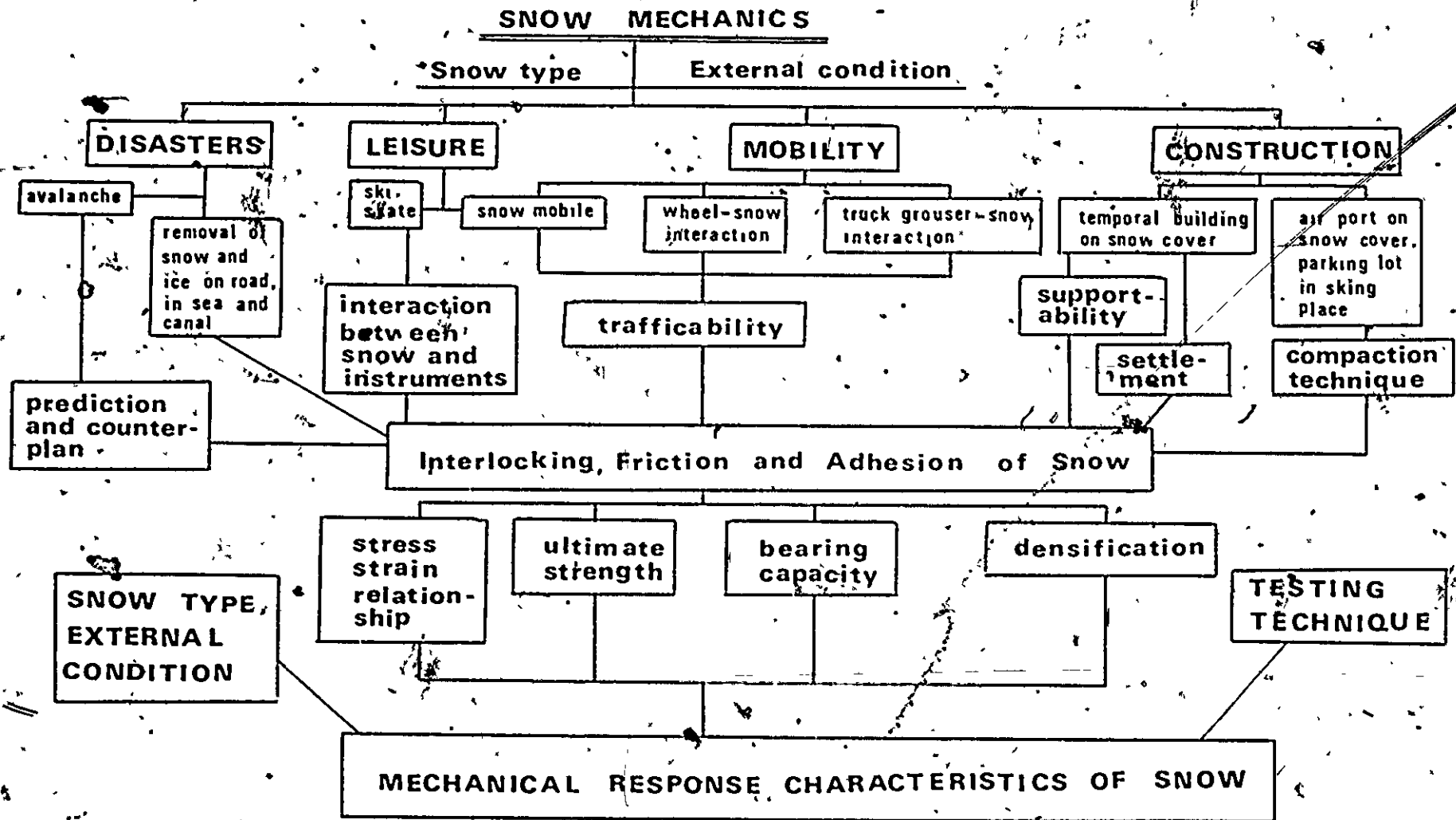


Fig. 1,1 General Flow Chart for Snow Mechanics

producing optimum drawbar pull.

Changes in the state and character of snow from a stressed region to an unstressed can be easily observed in a study of snow performance under load. Types of shear failure in snow are difficult to characterize or evaluate - both qualitatively and quantitatively. The reasons for this are due to the extremely varied nature of snow properties and characteristics which are climatic, physiographic, temperature, and pressure dependent. Thus for example, variations or difference in snow properties and characteristics are found between tree-line snow and prairie snows, coastal as opposed to alpine, arctic as opposed to subarctic snows, etc. Taking into account the influence of climatic and physiographic factors, and other conditions such as time and local pressure which will contribute to the metamorphic processes in snow, it becomes obvious that for a proper appreciation of snow properties, it is necessary to recognize:

- (a) the problem of appropriate and valid characterization of snow and
- (b) the fact that response performance of snow is conditioned by the type of snow but also by the nature and manner of physical testing.

The problem of determination of snow properties thus becomes obvious.

It is therefore clear as to the nature of the investigation required in this thesis study.

When the original grain structure is disrupted or destroyed the snow is considered to have failed, and the maximum stress mobilized in failure is taken as the "ultimate strength" of the snow.

The ultimate strength of snow has generally been considered a function of intergranular bonds established in the snow or density. Keeler (1969), Jellinek (1959) and Gow and Ramseier (1963) in studying bonding effects described that snow strength increases with the bonding area developed in the snow.

The shear strength of snow is related to density, temperature, and grain structure of snow (as other strength properties are) and in addition, is also dependent upon the pressure normal to the shear direction. Attempts have been made to apply Coulomb's equation (being used in soil mechanics) to describe the failure condition of the snow. Experimental results obtained by Butkovich (1956) and University of Minnesota (1951) show, however, that the relationship between shear strength and normal pressure for bonded snow is not linear because of the compressibility of the snow. Ballard and McGaw (1965) and Ballard and Feldt (1966) assumed from the results of their studies on snow strength that the external stress on a snow mass produces a uniform stress condition in the internal structure of snow and that failure occurs when these internal snow structures are stressed to the ultimate strength of ice.

Although it has been acknowledged that the mechanical properties and behaviour of snow are influenced by the multiple factors governing the nature of snow, most investigators have confined their

studies of snow properties to a consideration of a single factor, i.e., density, bonds or grain size. To illustrate the limitations in single factor considerations, it should be noted that, in most instances, different densities of natural snows demonstrate different snow grain characteristics and different types of bonds between the snow grains.

This means that the effect of density as a factor included the effect of snow grain characteristics and bonding relationships. Thus, for example, the mechanical properties and behaviour of a bonded snow is easily distinguishable from that of a sugar snow (for the same density). To provide for a proper characterization of the behaviour of snow under loading, it is thus necessary to examine the mechanical properties and behaviour for a specified snow condition (relation to the multiple factors) by proper test techniques.

Basis for Thesis Study

It is noted that the concern for a basic development of the study of snow properties is motivated by.

- (a) the lack of adequate physical mechanical results and data leading to a rational characterization of snow,
- (b) the incomplete understanding of snow behaviour in relation to snow nature and type, test method and conditions and lack of rational correlations between compression and shear performance vis-a-vis snow strength and stability.

Snow factors worthy of consideration are:

- (1) Snow properties change with time even under constant temperature. (see Chapter II). This means that laboratory testing on snow specimens obtained from the field is not necessarily useful because the test results obtained from the laboratory tests cannot necessarily be directly applied to the field snow.
- (2) There may be difficulty in analyses of in-situ test data because of the inadequate appreciation of the dominant factors operative in the field problem, i.e., unknown snow conditions, effect of changing temperature, etc.

Organization of Thesis

Recognizing many of the difficulties, a possible systematical study of snow can be achieved with the following procedures:

- (1) Simple tests should be performed in the laboratory for the purpose of examination of both test technique and snow properties. The nature of snow should be established prior to testing.
- (2) The important factors governing snow properties should be established from procedure (1).
- (3) Based on the examination of the physical performance of various types of snow, a scheme for classification of snow,

from the quantitative mechanical properties and qualitative mechanical behaviour, may be established. To provide this, it is expected that the study may require many years.

- (4) Development of proper test techniques using information obtained from procedures (1), (2) and (3) for determination of snow properties and behaviour. With such a procedure, it is expected that a proper appreciation of the nature and types of snow in field in so far as mechanical behaviour and performance may be achieved. From the snow classification established through procedure (3), the mechanical properties and behaviour of field snow may be predicted.

These procedures have been followed in two separate but interrelated study schemes in this thesis. Figures 1.2 and 1.3 show the two schemes used together with the format for presentation in the thesis and the basic organization of the study material.

In physical presentation of the thesis, Chapter II describes the nature of snow and ice as required necessary background material. Chapter III develops the adhesion theory to describe the mechanical response characteristics of snow. An important assumption in the adhesion theory is that two solids i.e., snow particles adhere as a result of a plastic junction similar to that proposed by Bowden and Tabor (1950, 1964). Chapter IV provides a theoretical examination of the increase in contact area between particles as required in the adhesion theory. Chapters V through VIII describe the experimental investigation taken

ADHESION THEORY OF SNOW

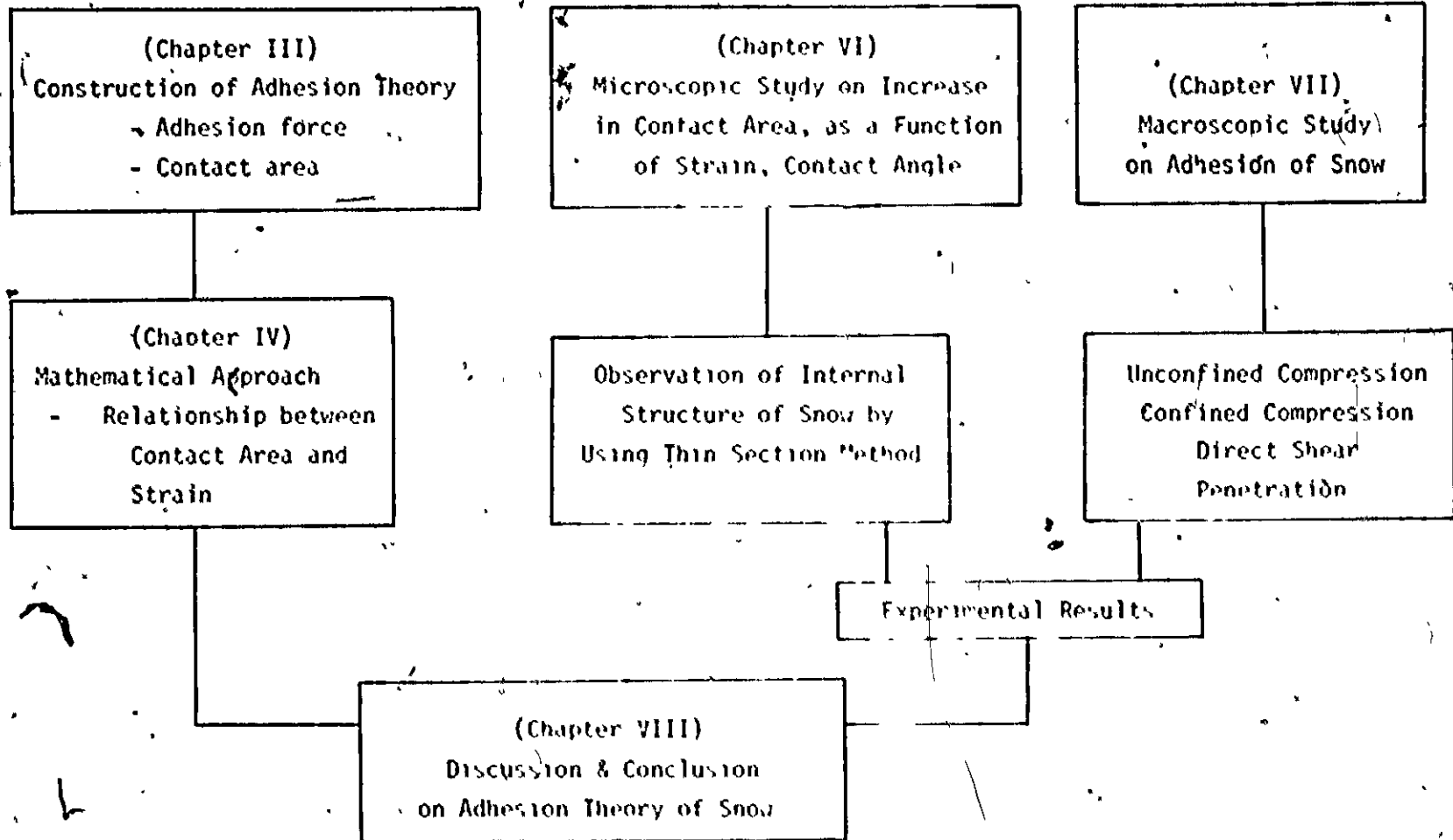


Fig. 1,2 Organization of the Study for the Adhesion Theory

MECHANICAL PROPERTIES OF SNOW

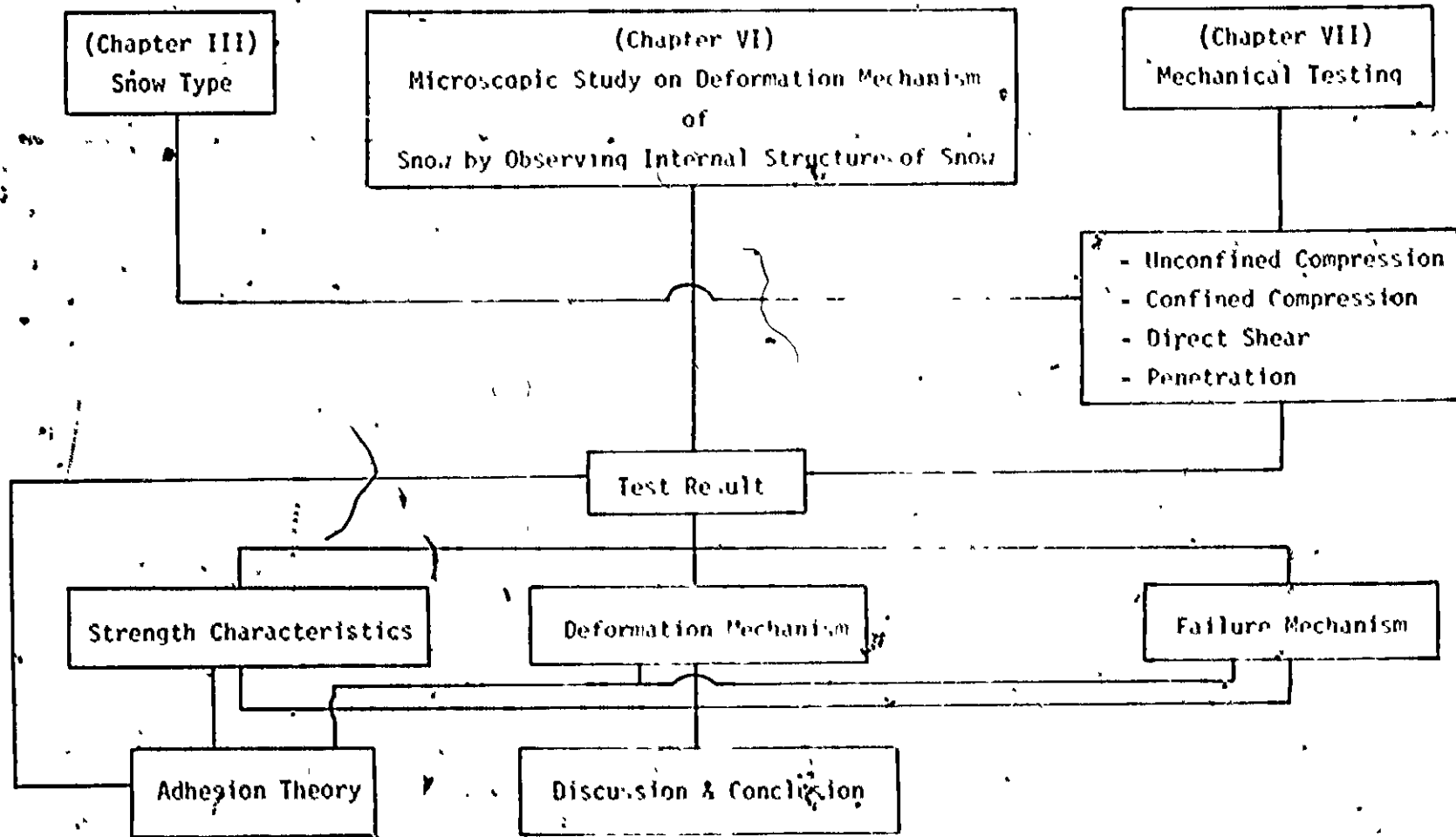


Fig. 1,3 Organization of the Study for Mechanical Properties of Snow

in the research. Chapter V describes the experimental procedure and materials used in the research. Chapter VI discusses the experimental results on the deformation and failure mechanisms of snow. Chapter VII discusses the physical and mechanical response characteristics of snow from the mechanical test results obtained in the study. Chapter VIII discusses the adhesion theory based on the experimental results, and snow classification based on its demonstrated mechanical properties and behaviour.

CHAPTER II

NATURE OF SNOW AND ICE IN RELATION TO PROBLEM UNDER STUDY

The objects of this chapter are to:

- (a) provide for the necessary background for the proper appreciation of the nature of snow from the review of literature,
- (b) consider the main factors governing snow structure, and
- (c) prepare background for the other chapters in this thesis.

We might expect that the mechanical properties of snow are primarily dependent on snow nature which is characterized by (a) grain characteristics, (b) interaction force and (c) density.

Since snow varies from freshly fallen one to ice as a function of time, temperature and pressure (Sommerfeld and LaChapelle, 1970, LaChapelle, 1969 and Shumskii, 1964), it is necessary to understand the whole process of snow transformation. Therefore, this chapter briefly describes the variations in snow nature with respect to grain characteristics, interaction force between grains and density and points out some problems with respect to snow nature.

CHAPTER II

NATURE OF SNOW AND ICE IN RELATION TO PROBLEM UNDER STUDY

The objects of this chapter are to:

- (a) provide for the necessary background for the proper appreciation of the nature of snow from the review of literature;
- (b) consider the main factors governing snow structure, and
- (c) prepare background for the other chapters in this thesis.

We might expect that the mechanical properties of snow are primarily dependent on snow nature which is characterized by (a) grain characteristics, (b) interaction force and (c) density.

Since snow varies from freshly fallen one to ice as a function of time, temperature and pressure (Sommerfeld and LaChapelle, 1970, LaChapelle, 1969 and Shumskii, 1964), it is necessary to understand the whole process of snow transformation. Therefore, this chapter briefly describes the variations in snow nature with respect to grain characteristics, interaction force between grains and density and points out some problems with respect to snow nature.

II-1 Grain Shape

The shape of snow crystal or grain varies in newly fallen snow. In crystallography, single crystal is any single ice particle which has a common orientation of the orderly array of molecules which make up its solid structure. In this sense, single crystal and grain often coincide.

The most widely used classification is that proposed by the International Commission on Snow and Ice in 1961. In this classification, there are seven main crystal types, such as plates, stellar crystal, columns, needles, spatial dendrites, capped columns and irregular forms (see Appendix A). However, there are many variations within the categories which are not identified by the International Snow classification.

From the engineering point of view, the classification for newly fallen snow is not always useful because it is too difficult to consider the shape effect of crystals, such as plates, needles, etc., on the mechanical response characteristics.

From the thermodynamic point of view, newly fallen snow crystals have very unstable shapes because of their large specific surfaces. A large specific surface (i.e., a large ratio of surface area to volume) means that the surface molecules of the crystal have a high potential energy. The natural tendency of thermodynamic process is to reduce the surface free energy to a minimum. The ideal shape to achieve this minimum shape is a sphere (LaChapelle, 1969). This process is called "equi-temperature metamorphism" in snow, and is strongly time and temperature dependent.

In the process of metamorphism, two main types, i.e., fresh snow (non-metamorphic snow) and metamorphic snow (old grain-snow), are distinguished by the shape characteristics.

II-2 Grain Size

Fresh snow crystals commonly range in size from a fraction of a millimeter to a few millimeters. When dry snow is blown by strong wind, some fragmentation occurs and smaller grains form. The grain sizes for cold blown snow mainly range from 0.1 to 1.0 mm equivalent diameter.

After deposition of fresh snow, the first process of equi-temperature metamorphism is the decrease of curvature of the sharp point of crystal. A little later, but still within the same step, the small necks of crystal disappear, causing the snow crystal to lose most of its complicated shape and to break up into smaller grains with less total surface area. During the next step in the metamorphic process, the total surface area is further decreased as the grains become more equi-dimensional. Needles become shorter and wider. plates become thicker while their major diameters decrease. The first step, (breaking up of crystal into smaller grains), is called "equi-temperature destructive metamorphism" of snow. After the destructive metamorphism, the grains become more equi-dimensional and larger. This increase in grain size of snow is called "grain growth" of snow crystals. Thus grain size of snow first decreases and it increases later under natural environment.

II-3 Intergranular Force of Snow

In the previous sections, an individual snow grain has been described. In this section, intergranular force of snow is considered.

At very cold temperature, as was described by Kingery (1960), packing of snow grains may bring on the state of frictional interaction and interlocking of grains. Snow (usually spherical grain) in this state is defined as granular snow, sometimes sugar snow. Early investigators observed that ice did not readily adhere at temperatures well below the melting point. However, Nakaya and Matsumoto (1954) observed that, at a temperature of -7°C , ices adhered together due to a liquid-like film. The experimental result obtained by Hosler and Jensen (1957) shows that cohesive force between two ice spheres is approximately 650 dynes at the melting point and rapidly decreases with decreasing temperature. Their result shows that cohesive force between ice grains vanished at temperature of approximately -5°C in dry environment, whereas cohesive force exists in saturated environment with respect to ice down to -30°C . Below these temperatures, granular condition is obtained for snow.

There is evidence that granular snow and semi-bonded (with liquid-like film) become bonded snow with time. For instance, Kingery (1960), Kuroiwa (1961), Hobbs and Mason (1964) and Ramsefer and Keeler (1966) studied the process by which snow and ice particles bond together with time at temperature below the melting point. In experiments utilizing small spheres of ice brought in contact under controlled conditions, Kingery thought that surface diffusion was the

principal mechanism of mass transfer whereas Kuroiwa concluded that volume diffusion was primarily responsible at temperature above -15°C , and surface diffusion below that temperature. Hobbs and Hason (1964) pointed out that evaporation-condensation is the major mechanism by which intergranular bond proceeds under normal atmosphere conditions. Ramseier and Keeler (1966) measured unconfined compressive strength as a function of intergranular bonds from the age hardening of snow in both samples under a saturated atmosphere and immersed in silicon oil. They deduced from the experimental results that the evaporation-condensation is the major mechanism for the intergranular bond formation. Thus, it is deduced that the bond formation of snow at temperature well below the melting point, is due to sublimation (evaporation-condensation) with diffusion. This process of the bond formation, at temperature below the melting point, is termed as "sintering" in analogy with the phenomenon known in powder metallurgy. A united view in sintering process of snow is that if the snow is very cold the sintering will be promoted very slowly; but if it is close to the melting point it can be promoted very rapidly.

As mentioned earlier, the mainly three types of intergranular force in snow are as follows:

1. friction and interlocking of grain without sintering at cold temperature (fresh and granular snow)
2. adhesion force due to water-like film of grain surface, without sintering at relatively high temperature (semi-bonded snow), and
3. bonding due to sintering, as a function of time and temperature, (sintered snow).

It is found that the mechanical response characteristics of any assembled material are dependent on the intergranular interaction. The response characteristics of snow are also dependent on the type of intergranular force. In this sense, at least four main types of snow, consisting of various intergranular interactions mentioned earlier, should be examined for the study of mechanical response characteristics. Those are as follows:

- (a) fresh snow (with original crystal shape),
- (b) granular snow,
- (c) semi-bonded snow (with water film), and
- (d) sintered snow.

As mentioned earlier, these types of snow change one to another with time and temperature as shown in Fig. 2,1. Fresh snow becomes sintered snow with time and granular snow becomes semi-bonded snow with temperature and becomes sintered snow with time as shown in the figure. Note that this transformation of snow type is often accompanied by changes in density and grain characteristics as a function of time, temperature and pressure.

II-4 Density of Snow

Snow structure may be described by the density knowing the other factors, such as grain characteristics, and intergranular force.

Density of snow is defined as:

$$\gamma \text{ (g/cm}^3\text{)} = \frac{\text{Weight of snow mass}}{\text{Volume of snow mass}}$$

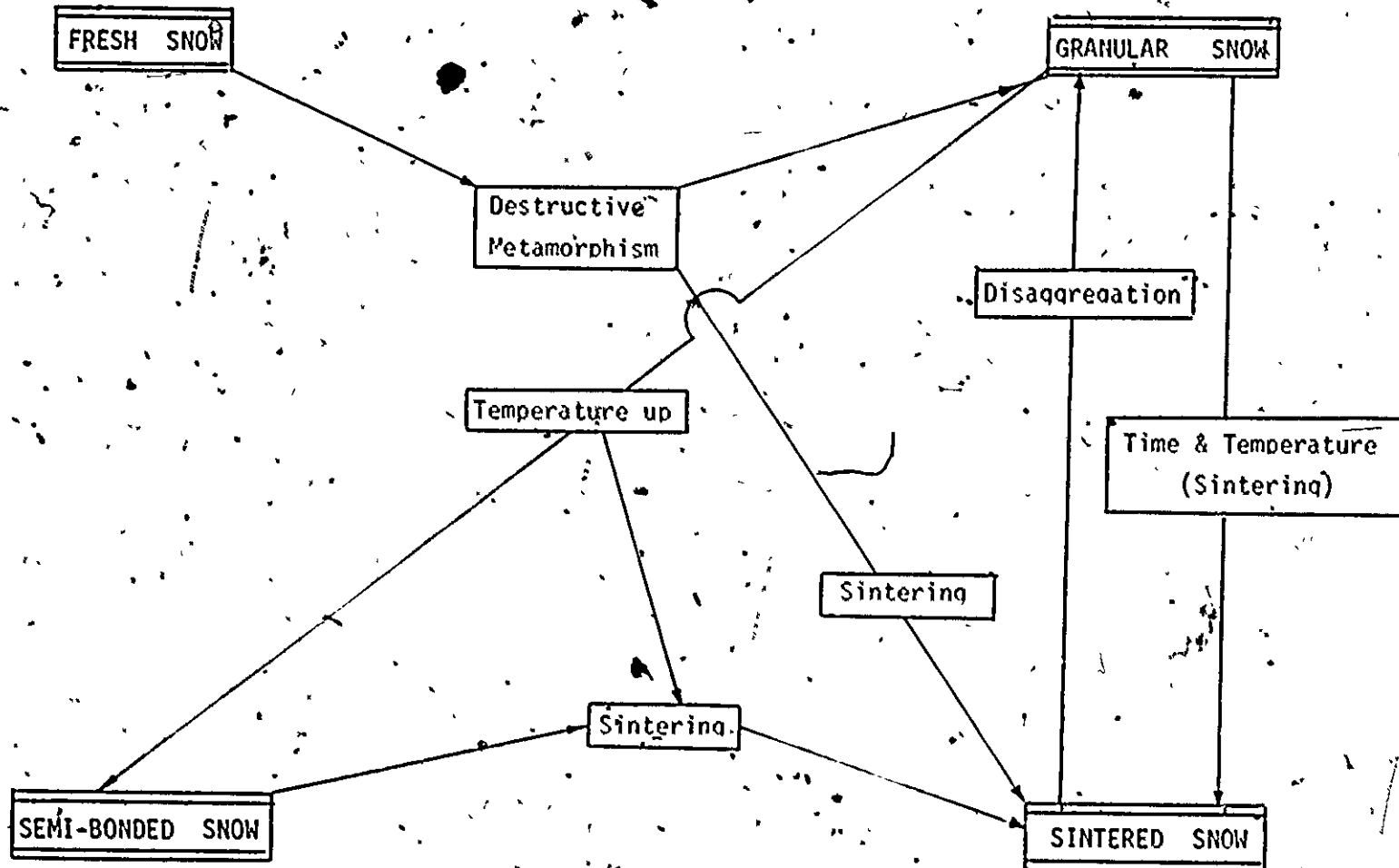


Fig. 2.1. Diagram of Transformation for Snow Type

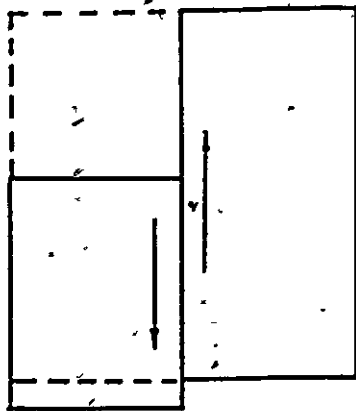
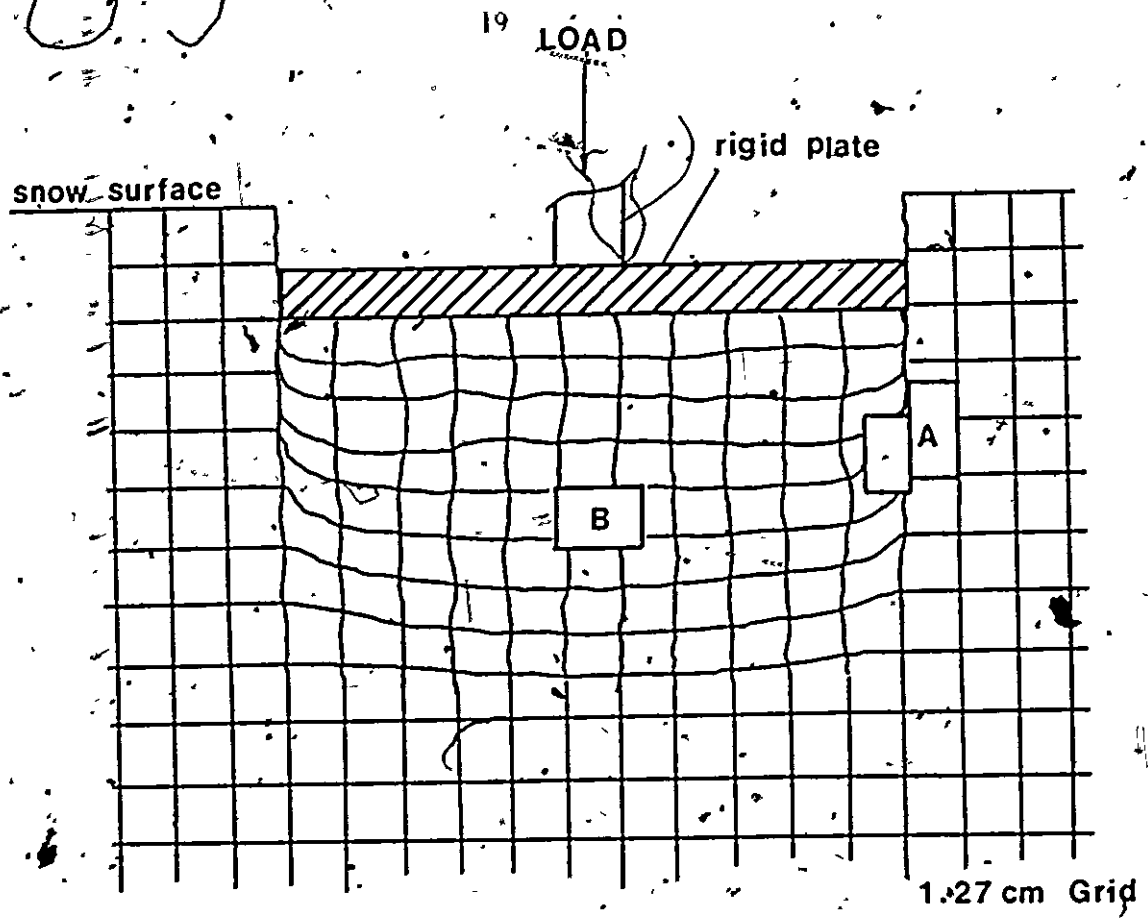
Deposited snow ranges, in density, from less than 0.1 g/cm^3 for fresh snow to more than 0.7 g/cm^3 for snow which has been soaked with water or densified. Density of snow has been used as an indicator of mechanical properties of snow by many investigators, however, it is doubted that snow properties can be indicated by density alone. This can be examined by the mechanical tests in Chapter VII.

II-5 Some Problems in Low Density Snow

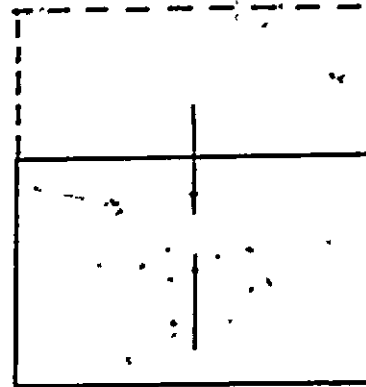
From the mechanical point of view, difficulty of study for low density snow lies in irrecoverable density change which causes the parameters to change, such as compressive modulus, Poisson's Ratio, coefficient of viscosity, etc.

It is hereby considered that change in density of snow results from the collapse of pores. For example, Fig. 2.2 shows change in density of loose snow under rigid plate with a constant dead load. This change in density is considered to occur as a result of failure of snow. Note that the apparent feature of failure shown in the figure is distinguished from the general shear failure commonly found in soils which is shown in Fig. 2.3.

Whether or not failure of snow occurs is dependent on the snow strength and load intensity. The analyses of supportability of snow are estimated from the strength at the failure. Therefore, the study of failure mechanism is of great importance in the engineering practice. The distinct differences between those failure modes illustrated in Fig. 2.2, and Fig. 2.3 may be dependent on the loose



ELEMENT A



ELEMENT B

Fig. 2,2 Actual Snow Failure under Rigid Plate with Dead Load, Showing Cutting Shear and Compression Shear

or dense state of any material. It is found that loose sand fails into the so-called local shear failure which is not too dissimilar to the apparent failure mode as shown in Fig. 2.2. The problem here is that the high compressibility failure shown in Fig. 2.2 does not follow the conventional failure theories. In Fig. 2.2, the macroscopic mechanical response of snow is divided mainly into two types; i.e., (a) cutting shear at the edge of plate, and (b) compression shear beneath the plate. These two mechanisms are apparently distinguishable. For instance, at the edge of rigid plate, "the cutting shear" occurs to the direction of maximum stress axis while "the compression shear" occurs across the maximum stress axis as shown in the figure. At the present, there is no rational relationship between the cutting shear and compression shear. Therefore, these mechanisms are studied in this research. The cutting shear of snow is studied by direct shear test while the compression shear is studied by the unconfined and confined compression tests in Chapter VII-3 and Chapter VII-1 & 2, respectively.

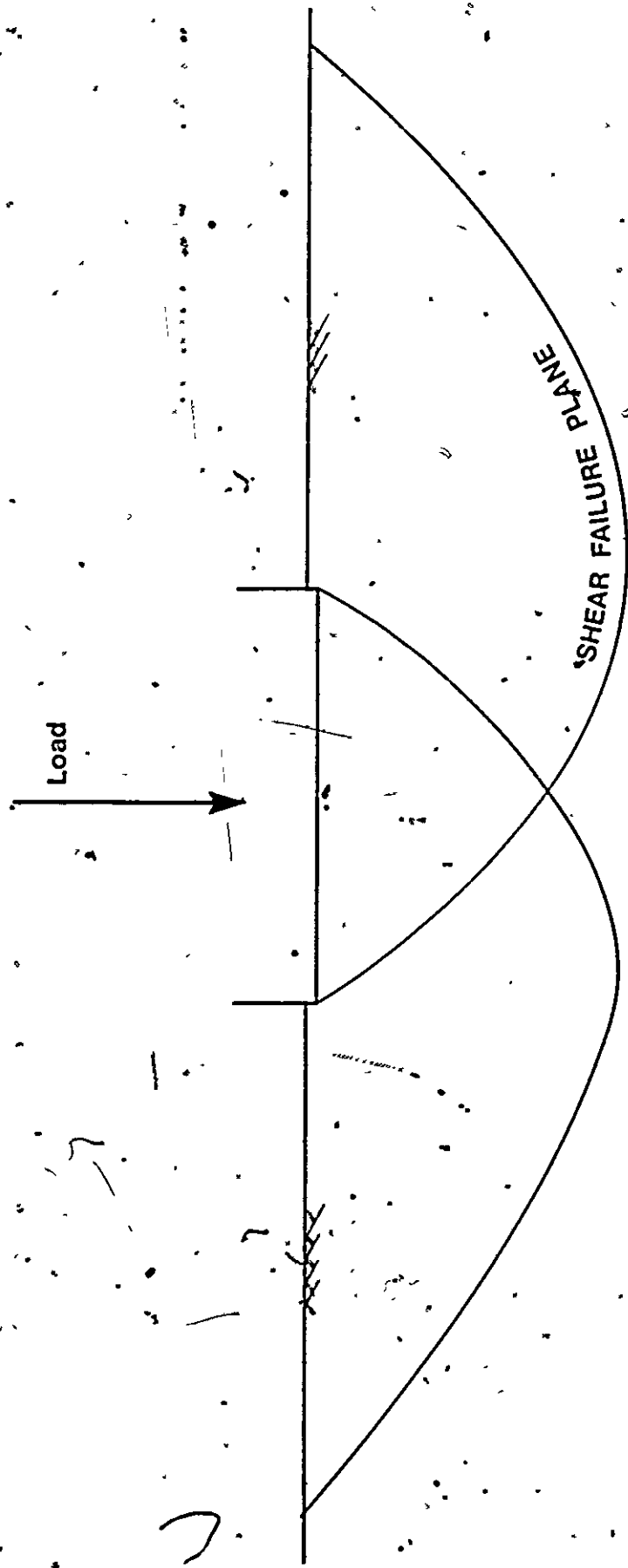


Fig. 2.3 General Shear Failure for Dense Assemblage

PART 1

THEORETICAL CONSIDERATION ON DEFORMATION MECHANISM OF SNOW

CHAPTER III

ADHESION AND FRICTION OF SNOW

III-1 Introduction

At very low temperature snow consists of ice particles and air. On the other hand, at relatively higher temperature snow consists of ice particles, water and air. Snow structure composes of either particle-particle contact, bonding between particles or particle-water system. In this sense, mechanical response characteristics of snow depend on nature of snow and properties of ice.

Mechanical properties of ice are generally described in terms of elastic, plastic and viscous components and are very complicated in terms of "time-dependence". In the case of a prolonged increasing load, the elastic limit decreases sharply, the elastic deformation is overlapped by residual deformation and the more prolonged the loading is, the greater will be the amount of elastic deformation that becomes residual (Shumskii, 1964).

Under this condition, the mechanical properties of snow are very complicated in terms of complicated properties of ice particle and the fact that snow is composite material.

It is felt that the present poor understanding and confusion on the properties and behaviour of snow result from the improper appreciation of snow type.

Snow varies from fresh to near ice. This variation in snow nature may correspond with sand to sandstone or clay to shale. This means that the mechanical properties of snow also varies between extreme limits. Thus, it may be too difficult to describe mechanical properties of snow in general way.

From the engineering point of view, below the melting point, snow may be classified into four types, i.e., (a) fresh snow, (b) granular snow, (c) semi-bonded snow and (d) sintered snow, as shown in Fig. 3.1.

Fresh snow consists of the original crystals which are needle, plane, stellar, etc., (see Appendix A), and the internal structure is very complicated in terms of "interlocking" of crystals, as illustrated in Fig. 3.1(a). Granular snow consists of discrete ice particles or grains and the apparent feature in terms of structure may not be dissimilar to ordinary sand except snow porosity is often very large (Fig. 3.1 (b)). Semi-bonded snow is described in terms of grain-water film system as shown in Fig. 3.1 (c). This type of snow can be obtained at relatively high temperature but below the melting point (Chapter II). Sintered snow (Fig. 3.1 (d)) may be identified as the ordinarily bonded snow or processed snow. Grains of sintered snow are basically same for granular snow or semi-bonded snow unless transition from snow grain to ice grain occurs. These types of snow have partially been described previously. The problem is that

It is felt that the present poor understanding and confusion on the properties and behaviour of snow result from the improper appreciation of snow type.

Snow varies from fresh to near ice. This variation in snow nature may correspond with sand to sandstone or clay to shale. This means that the mechanical properties of snow also varies between extreme limits. Thus, it may be too difficult to describe mechanical properties of snow in general way.

From the engineering point of view, below the melting point, snow may be classified into four types, i.e., (a) fresh snow, (b) granular snow, (c) semi-bonded snow and (d) sintered snow, as shown in Fig. 3.1.

Fresh snow consists of the original crystals which are needle, plane, stellar, etc., (see Appendix A), and the internal structure is very complicated in terms of "interlocking" of crystals, as illustrated in Fig. 3.1(a). Granular snow consists of discrete ice particles or grains and the apparent feature in terms of structure may not be dissimilar to ordinary sand except snow porosity is often very large (Fig. 3.1 (b)). Semi-bonded snow is described in terms of grain-water film system as shown in Fig. 3.1 (c). This type of snow can be obtained at relatively high temperature but below the melting point (Chapter II). Sintered snow (Fig. 3.1 (d)) may be identified as the ordinarily bonded snow or processed snow. Grains of sintered snow are basically same for granular snow or semi-bonded snow unless transition from snow grain to ice grain occurs. These types of snow have partially been described previously. The problem is that

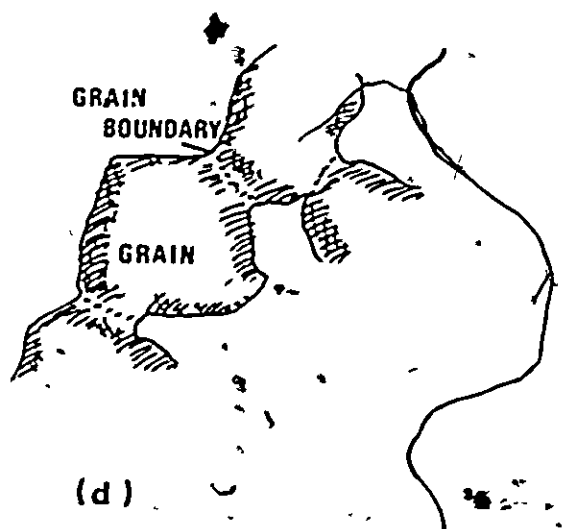
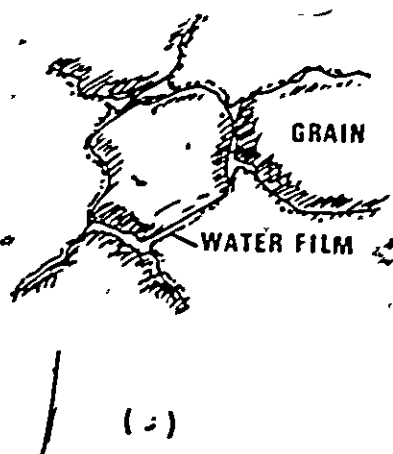
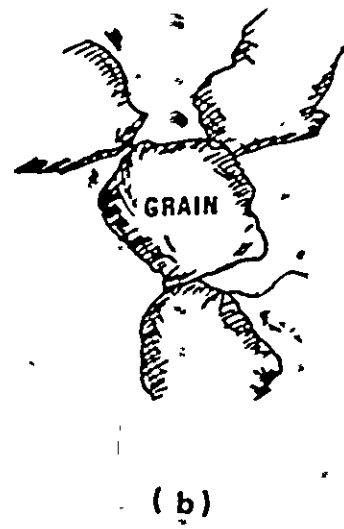


Fig. 3.1

Various Snow Models Showing:

- (a) Fresh Snow With Original Crystal Shape,
- (b) Granular Snow
- (c) Semi-Bonded Snow with Water Film, and
- (d) Sintered Snow

mechanical response characteristics of snow may depend on the types of snow. Therefore, it is necessary to examine these types of snow.

III-2 Adhesion between Solids

Snow is composite material. Therefore, interaction between each constituent may play an important role in understanding the mechanical response characteristics.

Bowden and Tabor (1950, 1964) pointed out that creep deformation of metal plate under metal ball with load will produce adhesion force between the plate and ball. They found that adhesion force was directly proportional to the size of contact area between the plate and ball, as shown in Fig. 3.2. Taylor (1948) described that, when loads are applied to a solid, some type of intrinsic attraction or bond either exists or comes into action to resist the relative displacement of adjacent particles. The shearing strength which any material possesses by virtue of its intrinsic pressure is given the general name "cohesion". A similar concept has been used by Trollope (1960) in his shear strength theory of soils.

This concept is introduced to snow in order to describe mechanical properties and behaviour of snow. Any theory requires certain assumptions which often are true only to a limited degree.

Thus, the preceding mention may bring us to consider adhesion force as a function of contact area between ice particles even if snow is initially in a granular condition (point contact) because it is quite possible that irreversible increase in contact area may occur

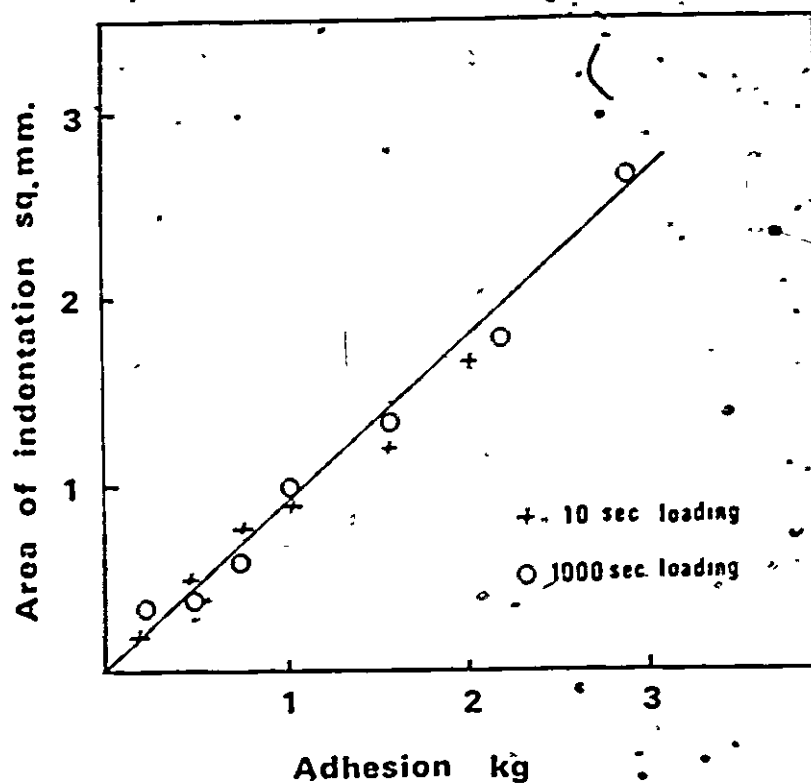


Fig. 3,2 Adhesion of Clean Steel Ball on a Clean Indium Surface

The adhesive force is directly proportional to the size of indentation formed, whether the time of loading is 10 sec. or 1,000 sec. This suggests that the increase in adhesion with time is essentially a creep effect (after Bowden and Tabor).

due to either local melting or creep, or plastic deformation under loads.

This chapter, therefore, mainly considers failure and deformation mechanisms of various types of snow, with respect to adhesion as a function of contact area between grains and friction and also prepares for the experimental investigation.

- Hypothesis -

Consider initially point contact of two particles (or grains) as shown in Fig. 3.3. Under compressive stress, irreversible increase in contact occurs under viscous, plastic or creep deformation but not elastic deformation. As found in metal (Fig. 3.2) the relationship between adhesion force and contact area is assumed to be given by:

$$A_d = A_c S_c \quad \text{----- (3, 1)}$$

Where A_d is total adhesion force

A_c is the adhesion per unit area with respect to contact area

S_c is the contact area.

III-3 Fresh Snow

Theoretical consideration of mechanical response characteristics of fresh snow is rather difficult because of its extremely complicated crystal shape. Therefore, fresh snow is only examined by the

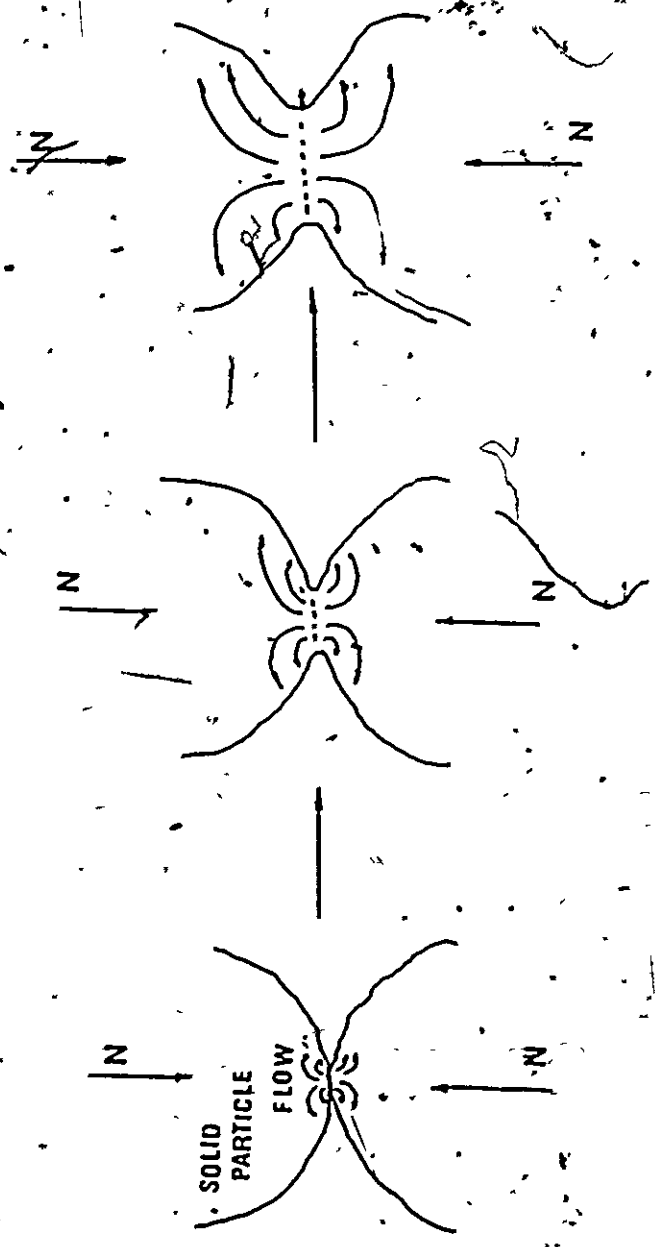


Fig. 3,3 Increase in Contact Area between Grains

experimental investigation. The results obtained are compared with the other types of snow and discussed in Chapter VII.

III-4 Granular Snow

It was mentioned that granular snow may not be dissimilar to other granular materials, which is partially true. Fig. 3.4 illustrates possible relative movement of two discrete snow particles under various load application. Figure 3.4(a) illustrates the separation of two particles which is identified as tensile strength of snow. Since granular snow consists of discrete grains as defined earlier the contact area is assumed as a point contact or very small. In this condition, the normal force required to separate two grains may be negligible. This is quite true for sugar snow. Figure 3.4(b) illustrates relative displacement (slip) of two particles. In the case of slide without normal pressure the force required to cause slide is very small for granular condition. Because the contact area is very small as mentioned above the adhesion force presented in Fig. 3.1 is negligible. This assumption is valid and is examined experimentally (Chapter VII). The tangential force required to cause slip between two grains under normal force is not negligible because of frictional resistance. The concept of friction of materials is known as Amonton's law which is widely being used in many fields.

Suppose that two bodies with an approximately plane surface of contact of apparent area A are pressed together by force N normal

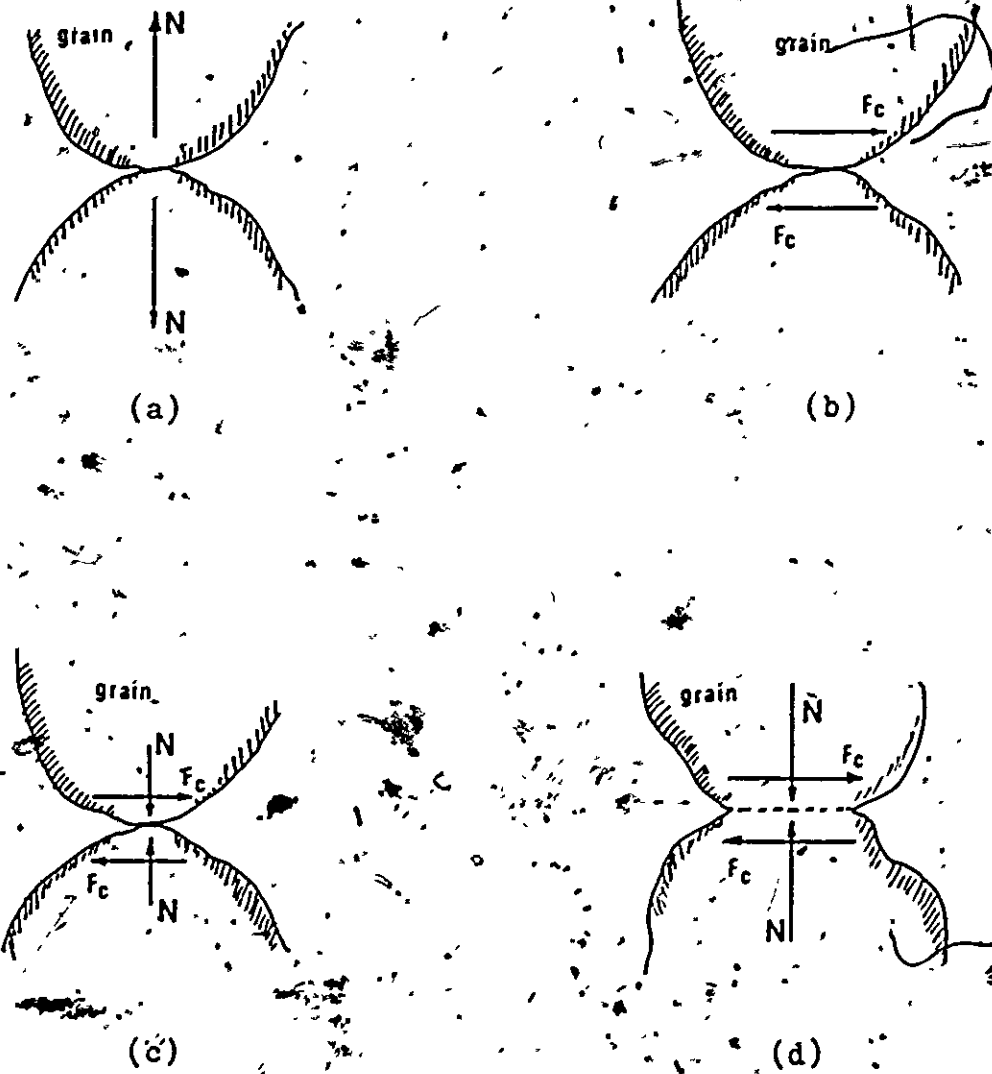


Fig. 3, 4. Various Load Conditions for Granular Snow:

(a) Separation

(b) Sliding without Normal Stress

(c) Sliding with Normal Stress, and

(d) Sliding under Increase in Contact Area.

to the plane of contact, and the tangential force F_c parallel to the surface of contact necessary to initiate sliding on it is measured. The relationship between F_c and N may be written into Amonton's law:

$$F_c = \mu N \quad \text{-----} \quad (3,2)$$

Where μ is called the coefficient of friction, μ depends on the nature of the materials and the finish and state of the surface in contact. μ might also be expected to depend on A and N , but experiment has shown that, to a reasonable approximation, it is independent of both these quantities.

However, compressive normal force acting on the contact may provide for an increase in contact area (Fig. 3.4 (d)). Hertz has developed theoretical relationship between increase in contact area and normal pressure in the case of elastic spherical particles in contact. Nevertheless, Bowden and Tabor pointed out that, from their experimental result obtained by using lead, copper and steel particles, the load required to reach the elastic limit is extremely small. Perutz (1950) also described that ice had no clearly defined elastic limit with constant load at 0°C , provided that the resistance to-shear the elastic limit does not exceed 0.1 kg/cm^2 . At low temperatures, however, the elastic part of deformation increases considerably. Even at 0°C , shear does not become perceptible until the ice is subjected to stresses of around 1 kg/cm^2 . As a first approximation ice may be regarded as a plastic substance with an elastic limit of the order of 1 kg/cm^2 (Perutz, 1950), by considering that;

- (a) elastic limit of ice is not high under low rate of deformation,
- (b) elastic deformation of crystal is very small, and
- (c) true stresses at point contact under even small apparent stress is very high.

The large deformation of ice particles is mainly plastic or viscous. This suggests that the contact area under deformation occurs irreversibly. Therefore, Hertz equation is not applicable for the large deformation of snow. This assumption is examined by the experimental investigation. By combining Eqs. (3,1) and (3,3), we get the tangential force required to initiate slip:

$$F_c = A_c S_c + \mu N \quad (3,3)$$

Where F_c is the tangential force required to initiate slip
 A_c is the adhesion force per unit area with respect to contact area
 S_c is the contact area when slip initiates
 μ is the frictional coefficient
 N is the normal force acting on the contact.

S_c is not constant but variable. If S_c is negligible tangential force required to initiate slip is presented by Eq. (3,2) which may be rewritten in forms of::

$$F_c = N \tan \phi_i \quad (3,4)$$

Where ϕ_i is the angle of internal friction.

In sand, the cohesion force between soil is generally neglected. This means that the cohesion between sand grains may be small or the contact area between sand grains is assumed to be negligible. Therefore, similar equation to Eq. (3,1) is being used in sand (Coulomb-Navier theory).

In most cases the slip strength of grains can be expressed by:

$$F_c = A_c S_c + N \tan \phi_i \quad \text{----- (3,3)}$$

where F_c is the tangential force required to initiate relative sliding of two grains

A_c is the adhesion force per unit area of contact

S_c is the contact area which is variable as a function of viscous, plastic or creep deformation, under load

N is the force acting normal to contact surface and

ϕ_i is the frictional angle

(see Appendix B).

Increase in contact area between spherical particles as a function of deformation is mathematically treated in Chapter IV and is compared with the experimental result. General discussion on the adhesion of snow is presented in Chapter VIII.

III-5. Semi-bonded Snow

Earlier work by Shaw and Leavey (1930)[†] has shown that strong adhesion may occur between surfaces which have been cleaned and freed of adsorbed surface films, but if the surfaces are exposed to air no adhesion is observed. On the other hand, the work of Budgett (1911)[†], Bowden and Tabor (1950, 1964) and other workers have shown that marked adhesion between solid surfaces can occur in the presence of water or other liquid films. Bowden and Tabor considered that the adhesion due to water film between solid results from surface tension of liquid. Their simple calculation based on the surface tension quite agrees with experimental results obtained on glass heads.

As mentioned in Chapter II, ice particle holds water-like film on its surface at relatively high temperature at even below the melting point (Nakaya and Matsumoto, 1954; Hosler and Jensen, 1957, Kuroiwa et al., 1967, Jellinek, 1967, and Flecher, 1973). Thus, adhesion due to water film of snow may cause the tensile strength of the snow. It is expected that mechanical response characteristics of semi-bonded snow are distinguished from the others, such as fresh, granular, or sintered snow. Therefore, in this section theoretical considerations in relation to mechanical response of semi-bonded snow are discussed.

Figure 3,5(a) illustrates separation of two adhered grains due to the water film. This case may be identified as mechanical tensile performance in semi-bonded snow. According to Hosler and Jensen (1957), adhesion force between two ice particles exists in a range of

[†] see Bowden and Tabor [1950,1964]

temperature from the melting point to approximately -5°C for dry environment while for humid environment, adhesion is observed even at -30°C (see Chapter II).

Figure 3.5(b) illustrates sliding of two adhered grains due to water film. In this case, the tangential force required to initiate sliding is considered to be dependent on temperature, grain size and surface tension of water.

In the more general case (Fig. 3.5 (c)), the situation may not be too dissimilar to the clay-water system. To initiate sliding, it is required that tangential force must overcome adhesion force resulting from water film. If sufficient normal force is acting on contact surface the water film may break and thus result in an increase in contact area due to deformation which is normal to the contact surface coupled with the mechanism mentioned for granular snow earlier.

This may cause increase in total adhesion on the contact. Thus tangential force required to initiate relative sliding is dependent on:

- (a) adhesion force due to water film,
- (b) friction,
- (c) normal pressure,
- (d) increase in adhesion resulting from increase in contact area, and
- (e) temperature.

III-6 Sintered Snow

The fourth type of snow to be examined is sintered snow. Sintered snow is obtained from the sintering process mentioned in Chapter II. Note that the process of sintering is strongly dependent on time and temperature. Sintered snow is identified as "bonded snow" which differs from the other types of snow. In natural condition, sintered snow varies in density from, about 0.25 g/cm^3 to 0.8 g/cm^3 . The important role of sintering is a hardening of the snow by the mechanism of evaporation-condensation as mentioned in Chapter II. Figure 3,6(a) illustrates separation of sintered snow grains. From the macroscopic point of view, this is identified as tensile performance. The tensile strength of very high density snow (0.8 g/cm^3) at a temperature of -10°C is approximately 20 kg/cm^2 (Butkovich, 1956). This suggests that adhesion due to sintering is very high.

In the general case, relative sliding of two adhered grains (Fig. 3,6 (b)) is possibly dependent on the adhesion force resulting from sintering, and normal force: If the initial bond strength between grains is sufficiently high so that an additional increase in contact is not expected, the tangential force required to initiate relative sliding of a mass can be expressed from the macroscopic point of view by Mohr theory (Appendix E):

$$\tau = f(\sigma_n)$$

Where sliding force τ is a function of normal force σ_n .

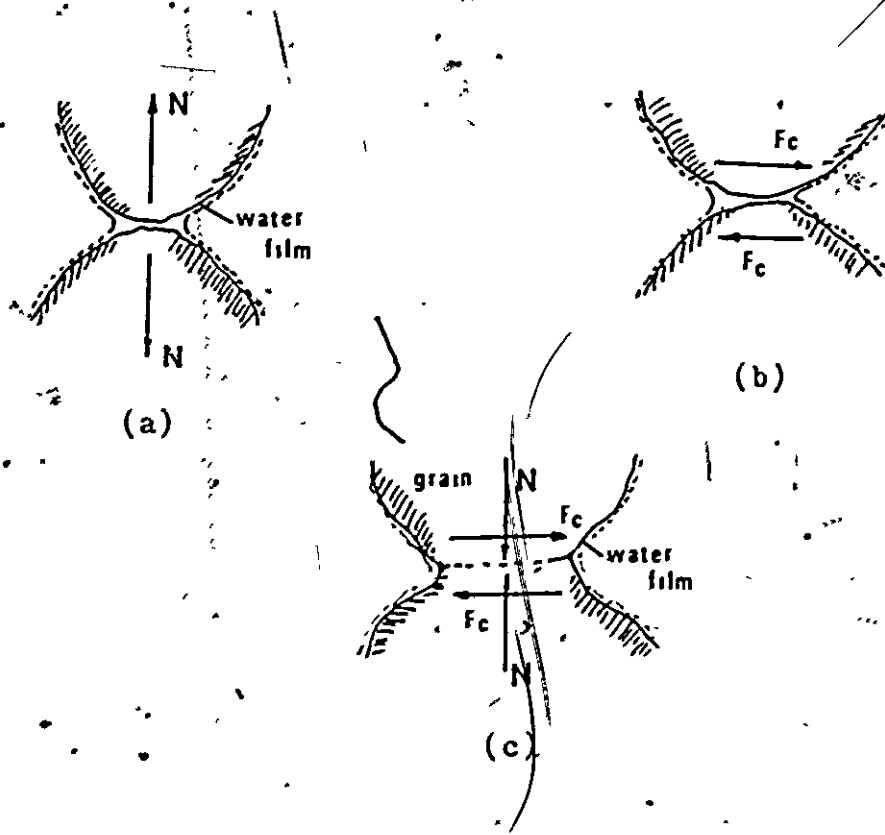


Fig. 3.5 Various Load Conditions for Semi-Bonded Snow.

- (a) Separation, (b) Sliding without Normal Stress, and
(c) Sliding with Normal Stress under Increase in Contact Area.

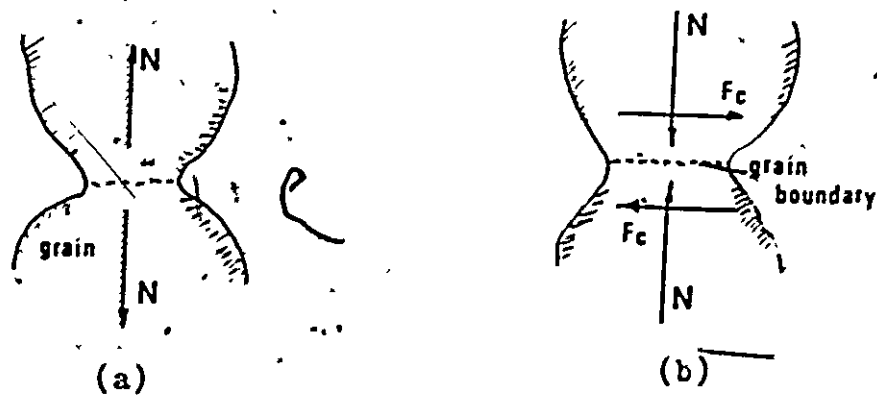


Fig. 3.6 Various Load Conditions for Sintered Snow.
(a) Separation and (b) Sliding with Normal Stress under Increase in Contact Area.

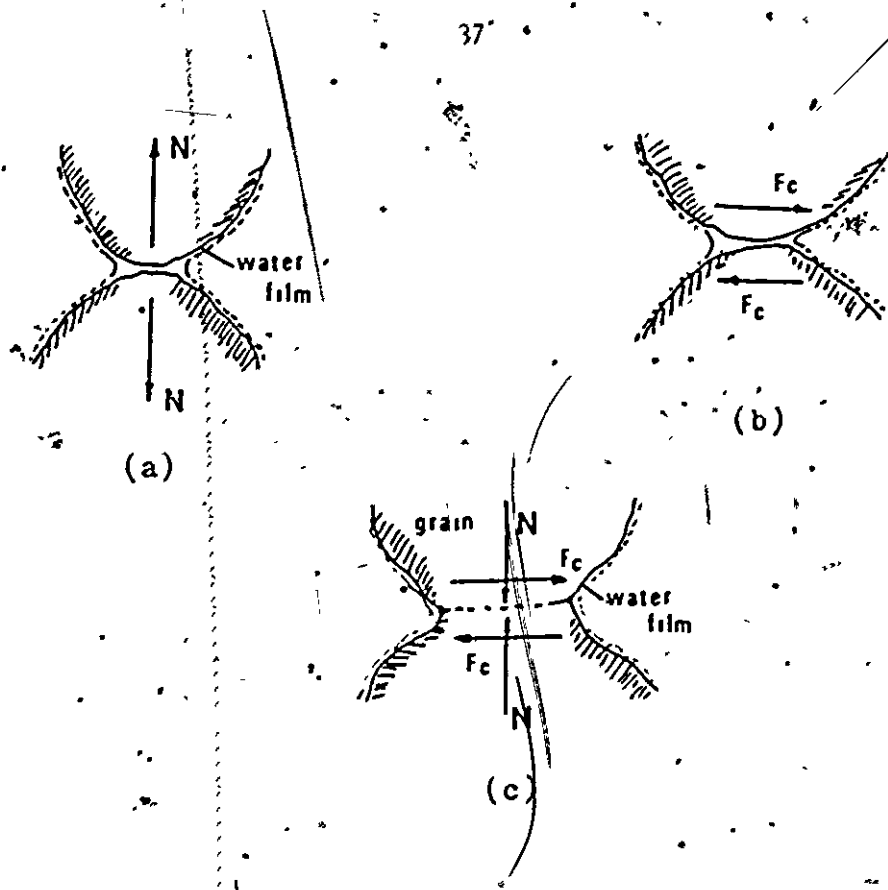


Fig. 3.5 Various Load Conditions for Semi-Bonded Snow.
 (a) Separation, (b) Sliding without Normal Stress, and
 (c) Sliding with Normal Stress under Increase in Contact Area.

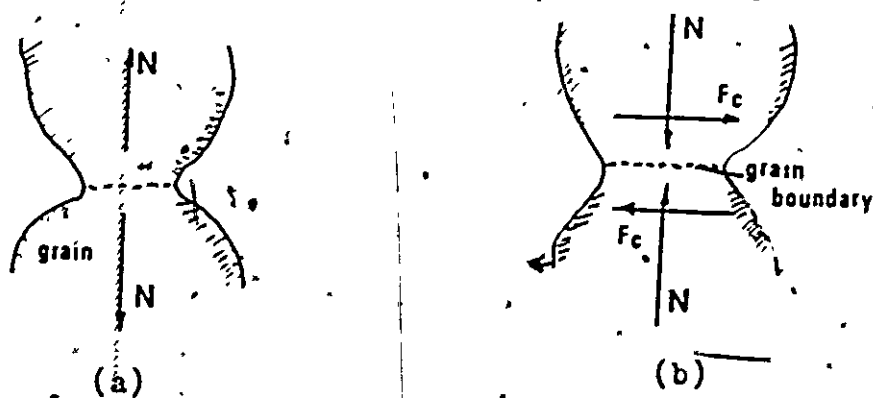


Fig. 3.6 Various Load Conditions for Sintered Snow.
 (a) Separation and (b) Sliding with Normal Stress under Increase in Contact Area.

From the microscopic point of view, the tangential force required to initiate grain slip can be written by:

$$F_c = A_s S_c + N \tan \phi_e \quad \text{----- (3,5)}$$

Where A_s is the adhesion force per unit area resulting from sintering of snow
 N is the compressive force normal to the sliding surface
 S_c is the bonding area
 ϕ_e is the angle of internal friction for sintered snow.

There is no idea whether A_s is equal to A_c however it is expected that A_s is higher than A_c .

If bond between grains is not sufficient enough, increase in contact area possibly occurs under normal force acting on sliding surface because of local deformation near contact. This may cause either disturbance of initial ordinary bond or increase in adhesion force with respect to increase in contact area.

The above mentioned equations are based on the assumption that failure occurs as a result of intergranular slippage. Equation (3,5) may be valid if adhesion force between grains is not too strong, so that intergranular slippage can occur without breaking of grains. Thus, intergranular interaction and the corresponding sliding mechanism depend on snow type.

Equations (3,1) through (3,5) indicates the tangential force required to initiate relative sliding between two grains based on the adhesion and friction.

To provide for the necessary background of experimental investigation, for the adhesion theory, the mathematics describing the increase in contact area as a function of strain is presented in Chapter IV. Chapter IV prepares for the experimental investigation which is presented in Chapter VI. The adhesion theory is therefore examined through experimentation in Chapter V through Chapter VIII. Chapters IV and VI deal mainly with the study of increase in contact area between grains and Chapter VII deals with the adhesion and friction by experimentation and Chapter VIII discusses the adhesion theory.

CHAPTER IV

INCREASE IN CONTACT AREA BETWEEN SNOW GRAINS
UNDER VISCOUS DEFORMATION OF CRYSTALS

The object of this chapter is to develop a relationship between increase in contact area of snow grains and viscous strain for the requirement in the adhesion theory.

V-1 Introduction

Firstly, it should be noted that "crystalline flow" differs from granular flow in terms of physical features. Crystalline flow is the flow of atoms or molecule in crystal while granular flow occurs as a result of intergranular slippage. The distinction between crystalline and granular flow is extremely important, so far as comprehensive behaviour of snow is concerned. In this section, the fundamental features of crystalline flow are described in order to develop the constitutive relationship of snow densification.

Any crystal can change its shape by self-diffusion in such a way as to yield to an applied shearing stress, and this can cause the macroscopic behavior of polycrystalline solid to be like that of a viscous fluid (Nabarro, 1948). This phenomenon may cause the creep of crystalline solid at very high temperature and very low stresses, though not under more usual conditions for metals (Herring, 1950).

Diffusion, which will cause "diffusional flow" of crystal, can be divided into two aspects: (1) the crystallographic and geometrical features and (2) the effect of temperature. Firstly, diffusion almost certainly takes place in elementary steps of length approximately one atomic diameter, i.e., few angstrom units. The atoms or molecules move in discrete jumps from one atomic or molecular lattice position to an adjacent one. These elementary jumps, when added together, permit the molecules to travel large distances. Once these postulate are accepted, the question remains of the detailed mechanism by which the individual molecular jump occurs. Several possibilities exist, vacancy motion, interstitial motion, or some sort of atom or molecule - interchange mechanism (Wert and Thomson, 1970). The possibility of viscous creep resulting from such vacancy migration was suggested by Nabarro (1949), and theory was worked out in a more refined manner by Herring (1950). According to Hayden et al (1965), at temperature close to the melting point, where the equilibrium concentration of vacancies is very high and self-diffusion is rapid, polycrystalline solid may deform by a diffusional creep mechanism rather than slip.

Figure 4.1(a) shows the self-diffusional currents of mosaic grain structure which is found in metals (after Herring, 1950, and Hayden et al, 1965). Figure 4.1(b) shows the self-diffusional currents to be expected when the loose grain structure is subjected to stress.

Therefore, we assume that increase in contact area occurs at grain contact due to the diffusional flow in crystal. It is an

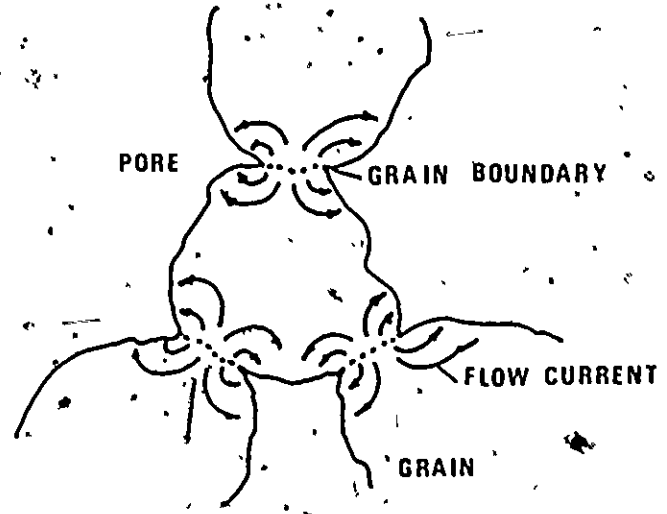
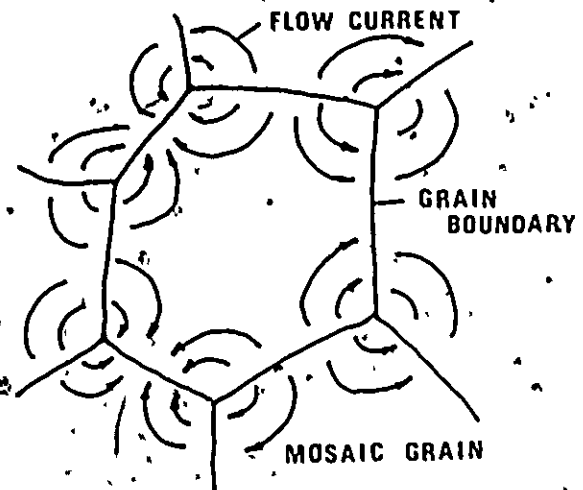


Fig. 4.1 Typical Grain Structure of Polycrystalline Solid, Showing the Self-Diffusion Currents to be Expected when Solid is Subjected to Stress, (a) Mosaic Grain Structure (after Herring, 1959) and (b) Loose Grain Structure.

important assumption in the adhesion theory (Chapter III) that increase in contact area directly increases adhesion between grains. This is proved through the experimental investigation (Chapters V and VII). In this chapter, increase in contact area with respect to strain is mathematically developed. The summary of this chapter is shown in Fig. 4,2.

IV-2 Relation between Contact Area and Relative Strain

Consider a contact between two spherical particles with radius of r as shown in Fig. 4,3. The figure demonstrates that the upper particle under loading moves downward without relative slip, consequently the increase in contact area between the particles occurs. In the figure, e^o denotes the deformation with respect to Z axis (direction of loading), e_ψ denotes the relative movement with respect to V axis, ψ is defined as the contact angle and $\Delta\psi$ is the increase in contact angle in relation to the deformation.

We assume volume V_1 , which is the overlapped portion by the particles as shown in Fig. 4,2, flows to the neck, i.e., shaded portion shown in the figure. The volume of shaded portion (i.e., wedge - sectioned ring) is V_2 . From the assumption, we may write $V_1 = V_2$. Thus the increase in contact area can be described in terms of ϵ as shown in Fig. 4,4.

Volume V_1 can be obtained with the integration method with respect to U and V axes, i.e.,

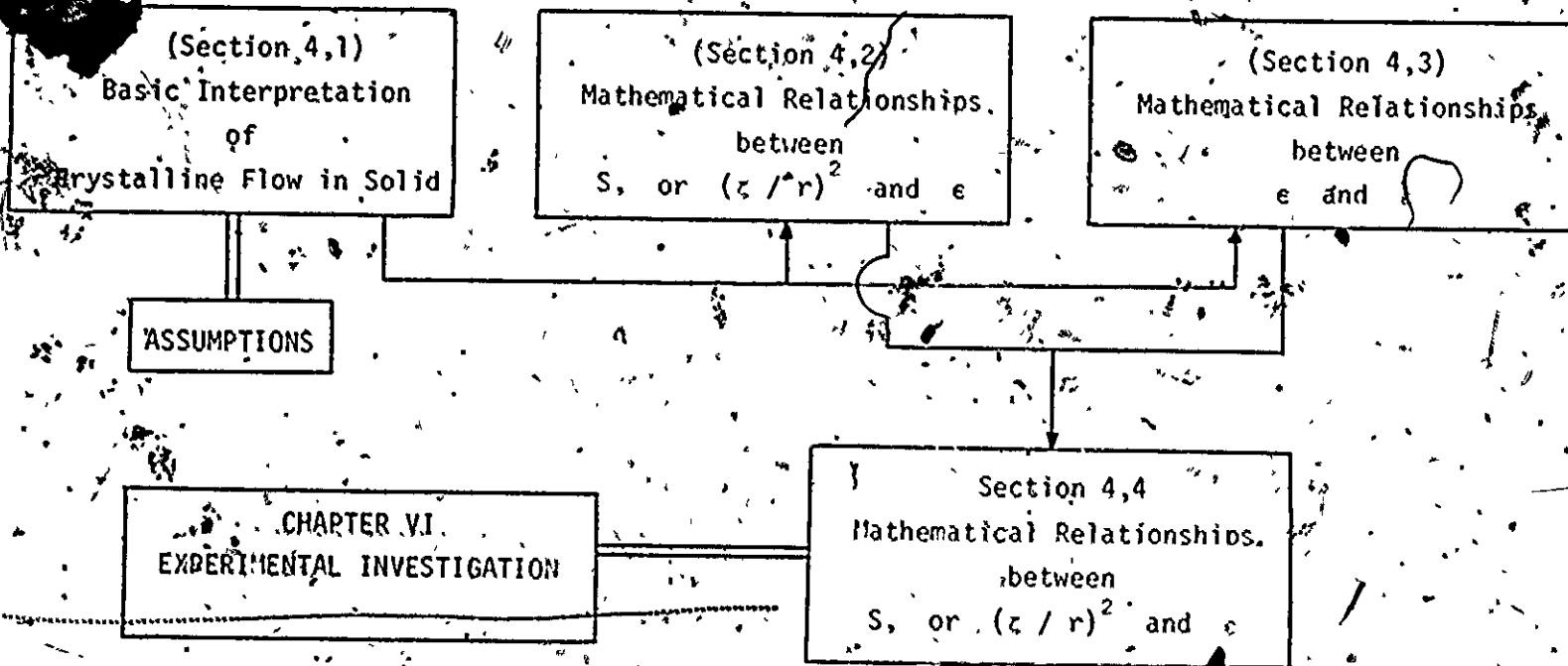


Fig. 4,2 Organization of the Study in Chapter IV

S is contact area
 e is the relative strain of particle
 ϵ is the macroscopic axial strain

z is the radius of circular contact
 r is the radius of spherical particle

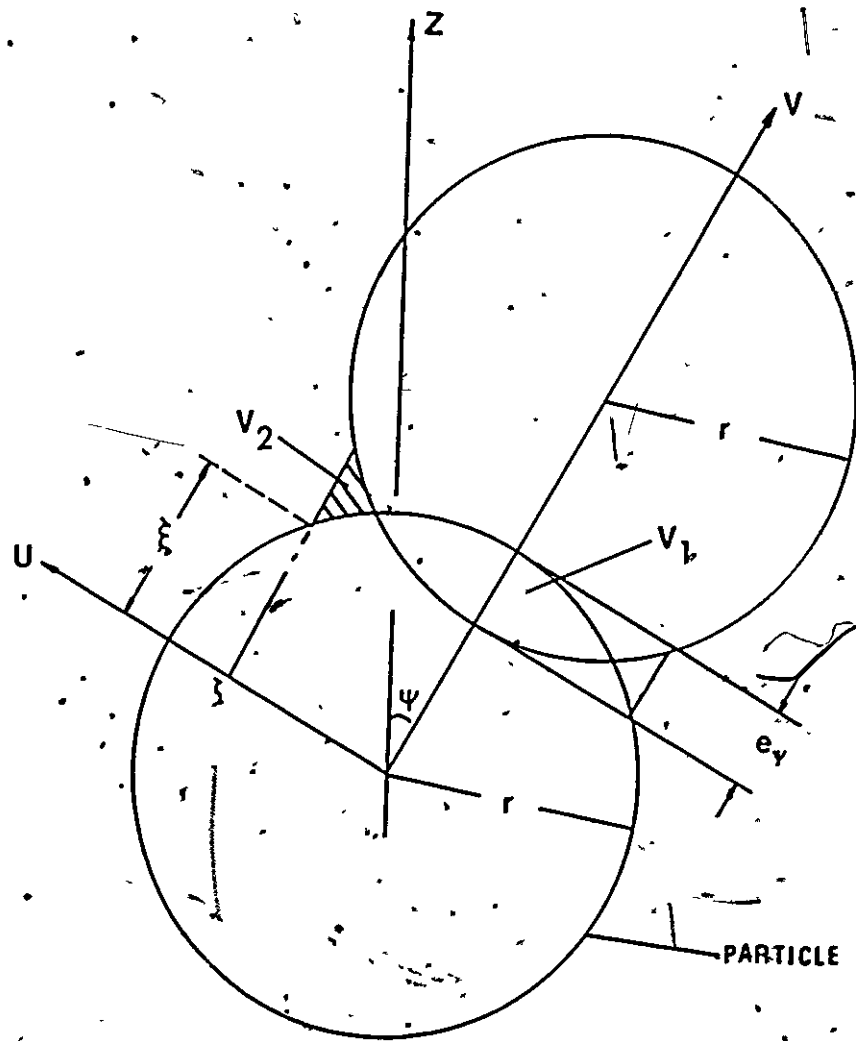


Fig. 4,4 Increase in Contact Area between Spherical Particles as a Function of Relative Movement (e_y) Based on Simple Assumption (at $\Delta x = 0$).

$$V_1 = 2\pi \int_{\frac{e}{2}}^{r - \frac{e}{2}} \left(r^2 - (V - 2r + e)^2 \right) dV$$

$$= 2\pi \left(r - \frac{r^3}{3} \right) - 2\pi \left(r^2 \left(r - \frac{e}{2} \right) - \frac{\left(r - \frac{e}{2} \right)^3}{3} \right)$$

$$= 2\pi \left(r \left(\frac{e}{2} \right)^2 - \frac{1}{3} \left(\frac{e}{2} \right)^3 \right) \quad (4.1)$$

Where e is the relative movement of two particles

r is the radius of spherical particle as shown in Fig. 4.4.

Volume V_2 is given by:

$$V_2 = 2\pi \int_{\xi}^{r - \frac{e}{2}} \left(\xi^2 - (r^2 - V^2) \right) dV$$

Where $\xi = \sqrt{r^2 - \zeta^2}$

ζ is the radius of circular contact.

Then,

$$V_2 = 2\pi \left(\xi^2 r - \xi^2 \left(\frac{e}{2} \right) + \frac{2}{3} r^3 - r \left(\frac{e}{2} \right)^2 - \frac{1}{3} \left(\frac{e}{2} \right)^3 \right) - \frac{2}{3} \sqrt{r^2 - \zeta^2} (r^2 - \zeta^2) \quad (4.2)$$

Taking V_1, V_2 from Eqs. (4,1) and (4,2)

$$\frac{2}{3} r^2 - \frac{2}{3} r^3 + \frac{2}{3} \sqrt{r^2 - r^2} (r^2 - r^2) - r^2 \left(\frac{e}{2r}\right) = 0 \quad \dots (4,3)$$

or

$$\frac{e}{2r} = 1 + \frac{2}{3} \sqrt{1 - \left(\frac{r}{S}\right)^2} \left(\left(\frac{r}{S}\right)^2 - 1\right) - \frac{2}{3} \left(\frac{r}{S}\right)^2 \quad \dots (4,4)$$

We define relative strain as $e = \frac{e}{2r}$. e denotes the ratio of relative movement e to diameter of particle. Therefore, the contact area by using $S = r^2$ is given by:

$$e = 1 + \frac{2}{3} \sqrt{1 - \frac{S}{r^2}} \left(\frac{r^2}{S} - 1\right) - \frac{2}{3} \left(\frac{r^2}{S}\right) \quad \dots (4,5)$$

With approximation,

$$S = r^2 (3.9 e - 1.789 e^2) \quad \dots (4,5)$$

Eqs. (4,5) and (4,5) denote the relationships between contact area and relative strain e . The equations show that contact area increases with increasing relative strain e .

Snow consists of large number of grains (ice particles) and the arrangement of grains is considered to be random. Experimentally, it is difficult to obtain the relative strain e , i.e., $\frac{e}{2r}$. We may assume that relative strain is a function of both the macroscopic axial strain and the contact angle. Therefore, in the next section, relationship between relative strain and macroscopic axial strain based on simple assumptions is mathematically developed.

IV-3 Relationship between Microscopic Relative Strain and Macroscopic Axial Strain

In the preceding section, increase in contact area between two spherical particles is expressed in terms of the relative strain $\frac{e}{2r}$ where e is the relative movement of particles and r is the radius of particle as shown in Fig. 4,4.

Consider a circular specimen consisting of large number of particles as shown in Fig. 4,5. The specimen has sectional area of A and height of L . If deformation d of the specimen occurs under loading the axial strain is defined as:

$$\frac{d}{L} \dots (4,6)$$

From the microscopic point of view, materials consisting of particles are never homogeneous in point size. Nevertheless, if specimen consists of sufficient number of particles it may be regarded as homogeneous. This statement is a basic assumption which is being used in mechanics. This suggests that we may assume that, under uniformly applied stress, the deformation exerted is also uniform but not to point size. In this study, the minimum scale for which deformation is valid may be the deformation per particle. The deformation of particles themselves may be very complicated in terms of the local deformation. It has been assumed earlier that the viscous deformation near contact (local deformation) will increase contact area.

Consider horizontal sections B and C in the specimen as shown in Fig. 4,5. We may assume that the distributions of contact angle ψ on the sections are similar. This assumption may be valid if sufficient number of contacts lies on the sections.

IV-3 Relationship between Microscopic Relative Strain and Macroscopic Axial Strain

In the preceding section, increase in contact area between two spherical particles is expressed in terms of the relative strain $\frac{e}{2r}$ where e is the relative movement of particles and r is the radius of particle as shown in Fig. 4.4.

Consider a circular specimen consisting of large number of particles as shown in Fig. 4.5. The specimen has sectional area of A and height of L . If deformation, d of the specimen occurs under loading the axial strain is defined as:

$$\frac{d}{L} \dots (4.6)$$

From the microscopic point of view, materials consisting of particles are never homogeneous in point size. Nevertheless, if specimen consists of sufficient number of particles, it may be regarded as homogeneous. This statement is a basic assumption which is being used in mechanics. This suggests that we may assume that, under uniformly applied stress, the deformation exerted is also uniform but not to point size. In this study, the minimum scale for which deformation is valid may be the deformation per particle. The deformation of particles themselves may be very complicated in terms of the local deformation. It has been assumed earlier that the viscous deformation near contact (local deformation) will increase contact area.

Consider horizontal sections B and C in the specimen as shown in Fig. 4.5. We may assume that the distributions of contact angle θ on the sections are similar. This assumption may be valid if sufficient number of contacts lies on the sections.

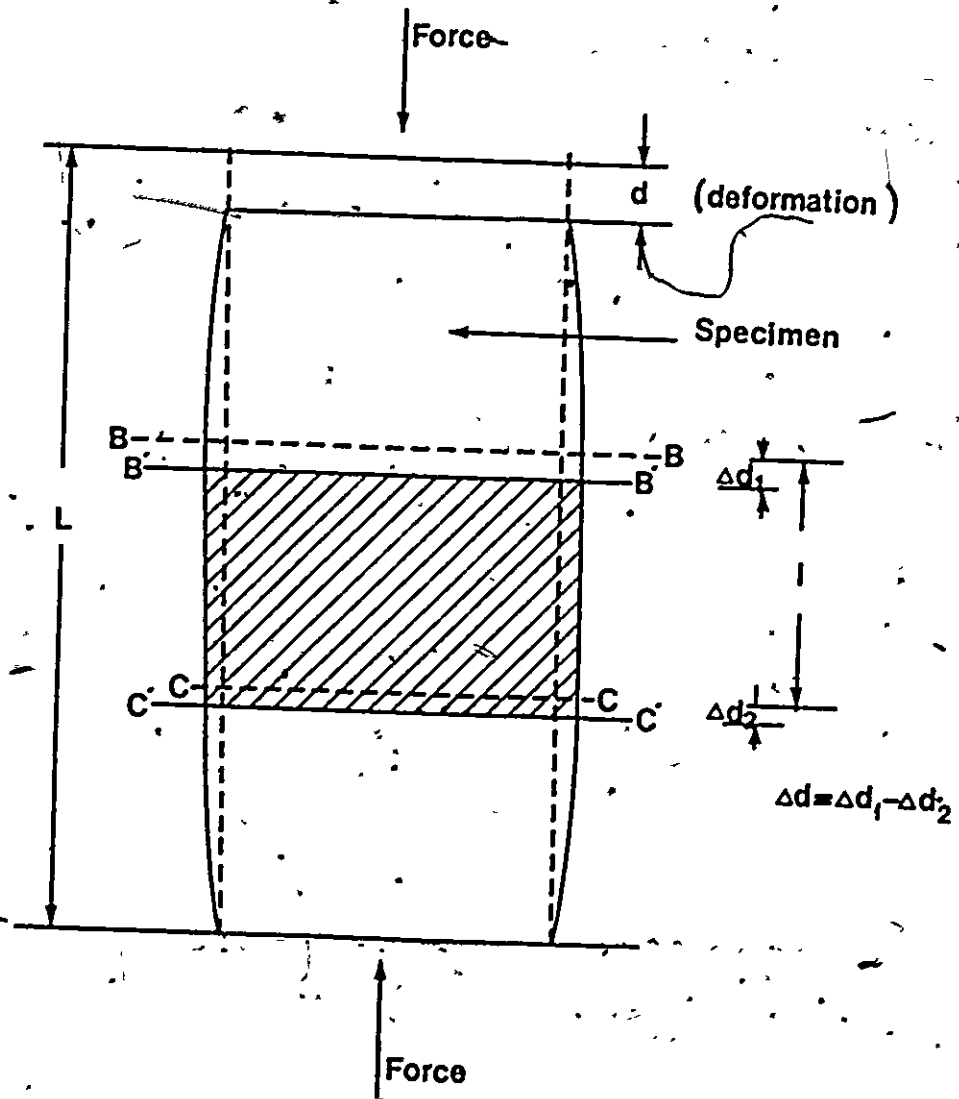


Fig. 4.5 Uniform Deformation of Cylindrical Specimen under Parallel Loading

Note that, for snow the lateral expansion is very small.

Then, condition can be written by

$$\frac{\Delta d}{L} = \frac{\Delta d}{l}$$

where Δd is the total axial deformation

L is the height of specimen

Δd is the vertical deformation of the column B - C with length of l .

Consider arrangement of particles as shown in Fig. 4,5. In the simplest case, i.e., all the contact angle are zero, deformation without intergranular slip can be written by

$$\Delta d = e n$$

where e is the deformation of a particle with respect to Z axis

n is the number of particles between sections B and C, as shown in Fig. 4,6(a).

Since initial height of column B - C is given by

$$l = 2 r n$$

the strain of column is given by dividing deformation by the initial height, i.e.,

$$\frac{\Delta d}{L} = \frac{e n}{2 r n} = \frac{e}{2 r}$$

In the preceding section, the ratio of deformation to diameter of particle is defined as relative strain.

Since $\epsilon = \frac{d}{L} = \frac{\Delta d}{L}$ and $e = \frac{e}{2r}$ (at $\psi = 0$) ... (4,7)

Thus, macroscopic axial strain accords with the microscopic relative strain, if all contact angles are zero. However, this is not valid if contact angle is not zero.

Consider the case of ψ' as shown in Fig. 4,6(b). The number of particles between sections B and C is

$$n' = \frac{n}{\cos \psi'}$$

Where n' is particle number at ψ'

n is the number of particles at $\psi = 0$.

If we assume ψ' (Fig. 4,6(b)) is small deformation e_y with respect ψ axis can approximately be given as:

$$e_y = e \cos \psi' \quad (4,8) \quad \text{(see Appendix F)}$$

Since $\Delta d = e n'$ and $L = 2r n' \cos \psi'$,

$$\frac{\Delta d}{L} = \frac{e}{2r \cos \psi'}$$

$$\frac{e_y}{2r \cos^2 \psi'}$$

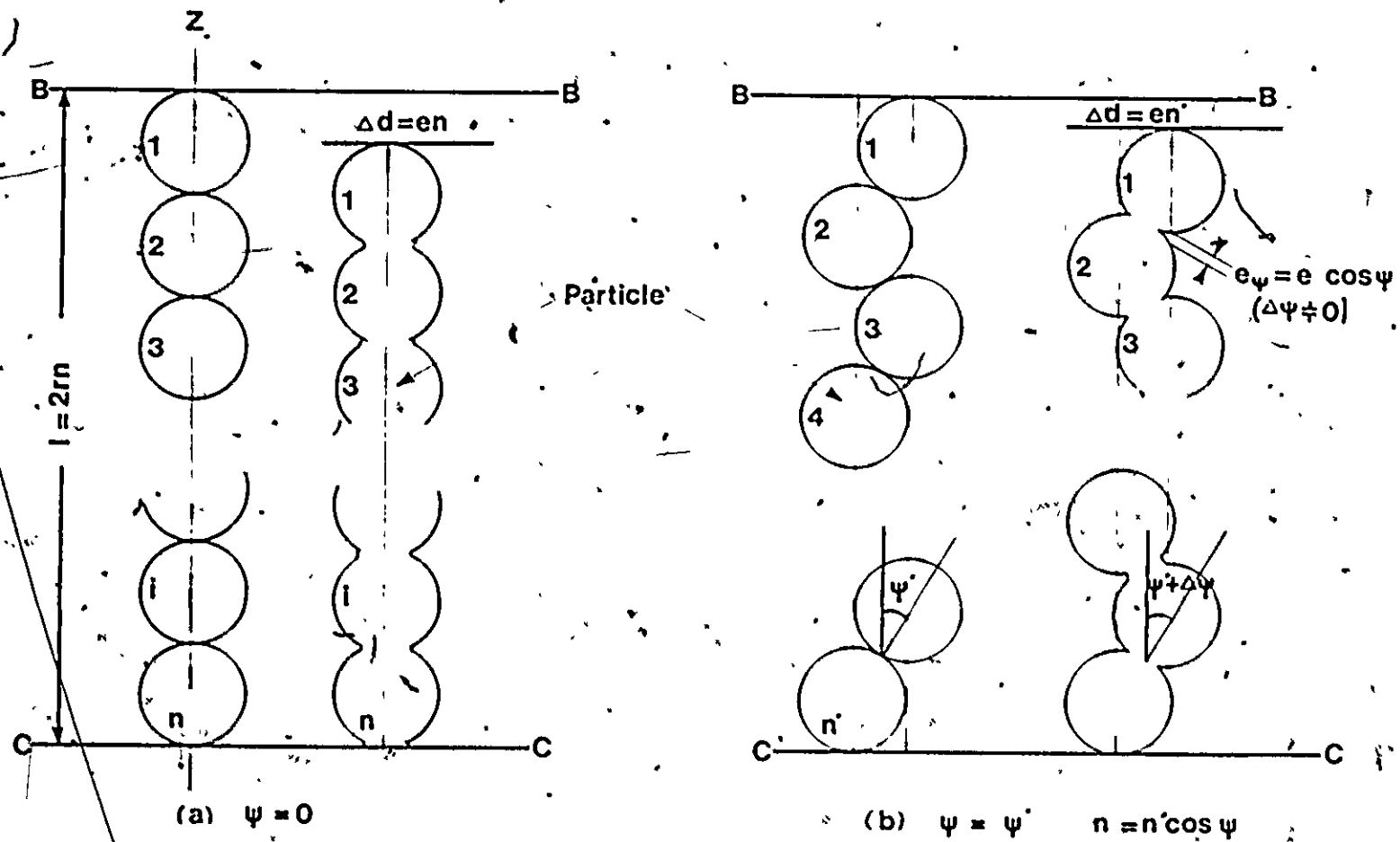


Fig. 4,6 Interpretation of Local Flow Deformation as a Function of Contact Angle and Axial Deformation

Therefore,

$$\frac{\epsilon}{\cos^2 \theta}$$

or

$$\epsilon = \epsilon' \cos^2 \theta \quad (\text{at } \theta = \theta') \quad \dots (4,9)$$

Where ϵ' is the macroscopic axial strain
 ϵ is the relative strain of particles.

Equation (4,9) denotes the relationship between the macroscopic axial strain and microscopic relative strain. The equation shows that relative strain ϵ decreases with increasing θ . This is true because of condition of no lateral deformation. Therefore, if $\theta = 90^\circ$ degree the relative strain ϵ must be zero. Equation (4,9) denotes the general case of Equation (4,7).

IV-4 Increase in Contact Area between Particles as a Function of Macroscopic Axial Strain and Contact Angle

The relationship between relative strain ϵ and radius of contact area r can be described by Eq. (4,4) and the relationship between the relative strain and macroscopic axial strain can be expressed by Eq. (4,9), as follows:

$$\epsilon = \frac{e}{2r} = 1 + \frac{2}{3} \sqrt{1 - \left(\frac{r}{r_0}\right)^2} \left(\left(\frac{r}{r_0}\right)^2 - 1\right) - \frac{2}{3} \left(\frac{r}{r_0}\right)^2 \quad (4,4)$$

and

$$e = \epsilon \cos^2 \alpha \quad \dots (4.9)$$

From Eq. (4,4) and Eq. (4,9)

$$\cos^2 \alpha = 1 + \frac{2}{3} \sqrt{1 - \left(\frac{\xi}{r}\right)^2} \left(\frac{r}{\xi}\right)^2 - 1 + \frac{2}{3} \left(\frac{r}{\xi}\right)^2 \quad \dots (4,10)$$

The calculation of $\left(\frac{r}{\xi}\right)^2$ versus ϵ and α from Eq. (4,10) is presented in Fig. 4,7. The figure shows that $\left(\frac{r}{\xi}\right)^2$ increases with strain ϵ and it decreases with increasing α for any strain.

Equation (4,10) can be rewritten with the approximate fitting as:

$$S = r^2 (3.9 \epsilon \cos^2 \alpha - 1.785 \epsilon^2 \cos^4 \alpha) \quad \dots (4,11)$$

Where S is contact area, i.e., πr^2

ϵ is the macroscopic axial strain

α is the contact angle defined in Fig. 4,4.

Equation (4,11) denotes that S increases with axial strain.

Equation (4,10) is experimentally examined, and the results are discussed in Chapter VI.

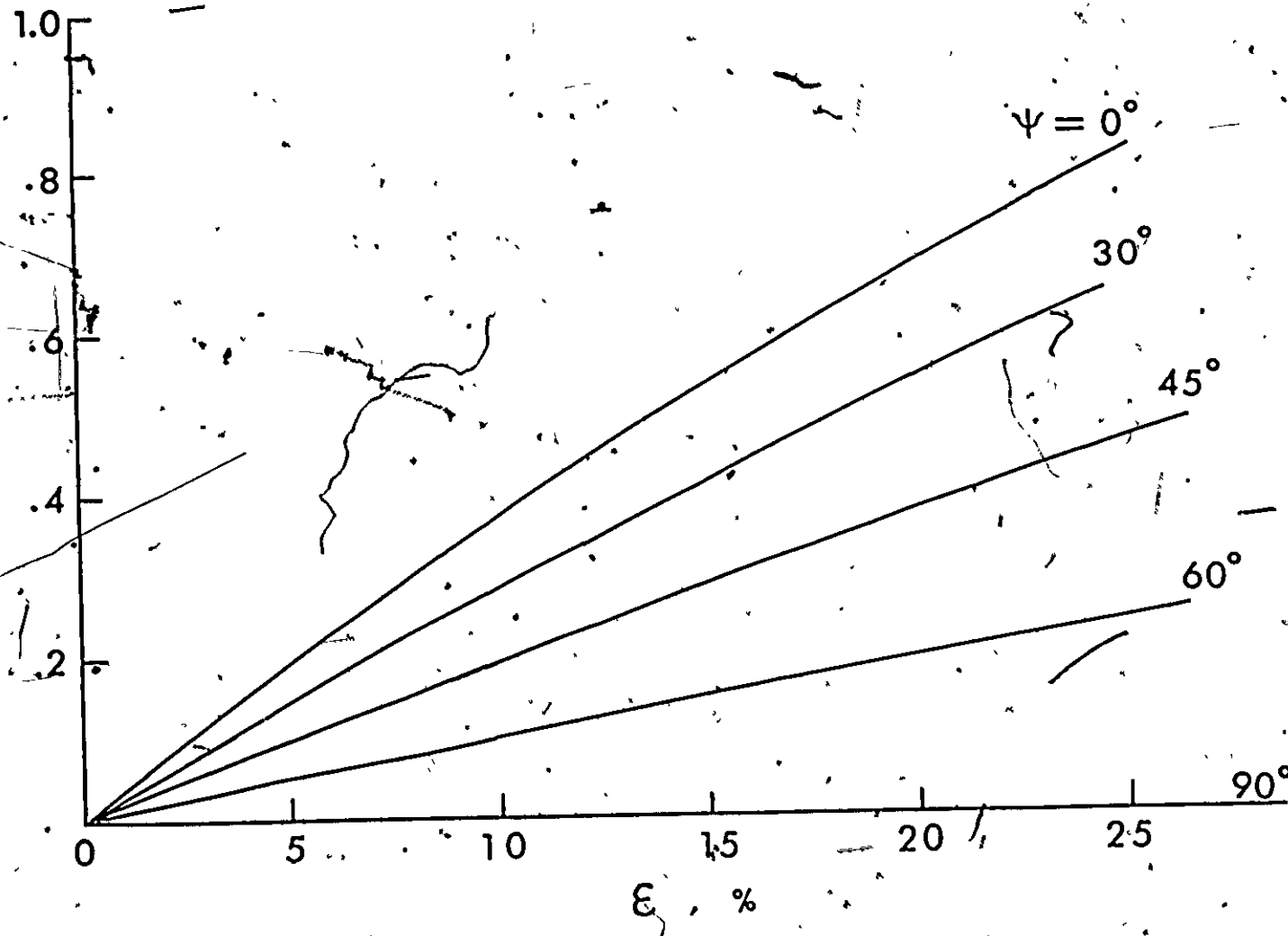


Fig. 4,7 Theoretical Relationship between $(\tau / r)^2$ and Strain



PART 2

EXPERIMENTAL INVESTIGATION

CHAPTER V

EXPERIMENTATION

The experimental investigation in this thesis comprises of some characteristics studied as shown in Fig. 5.1, with objective:

- (a) to examine the adhesion theory developed in Chapter III.

(The adhesion theory is examined by the microscopic observation of internal structure of snow by means of thin section method. The macroscopic study, by performing mechanical tests, also examines the adhesion theory.)

- (b) to examine the simple mechanical tests themselves which will be popular in snow mechanics, and
- (c) to develop a simple technique for the evaluation of in-situ snow properties. (This requires the basic properties and behaviour of snow.)

This chapter, therefore, provides for the necessary background of the experimental investigation and its critical evaluation.

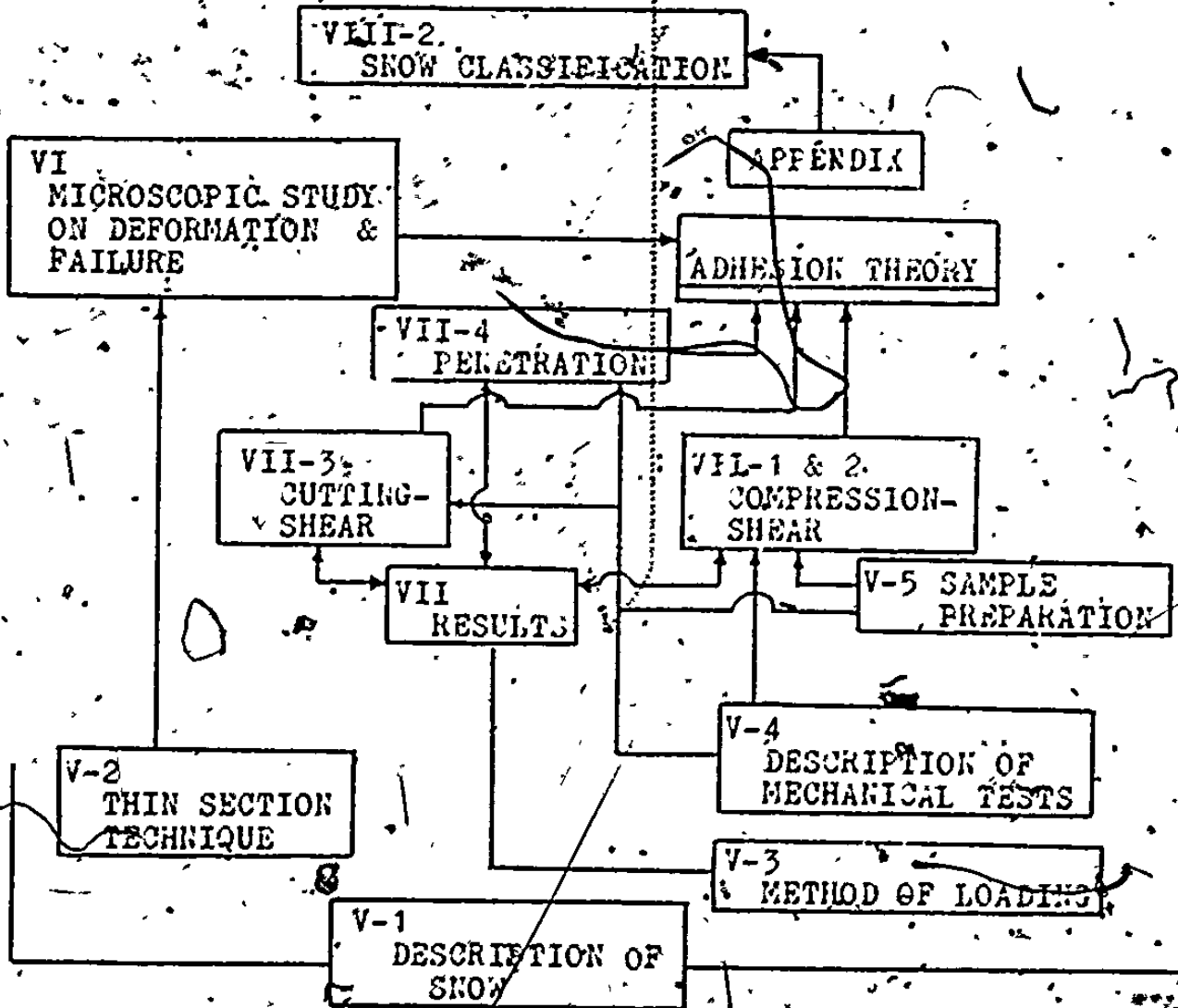


FIG: 5,1
 ORGANIZATION OF EXPERIMENTAL STUDY.

This chapter is divided into following five sections:

(1) descriptions of the snow used in the experiments,

(2) method of preparation of thin section of snow.

As mentioned above, the thin section method is used for the observation of internal structure of snow.

(3) discussion of the methods of loading which are normally employed,

(4) description of various tests performed in this research, and finally,

(5) the method of preparation of snow specimens used for mechanical tests.

These sections are discussed in detail as follows:

V-1 Description of Material

For the reason described previously, various types of snow should be examined. The materials used in the study consisted of

(a) seasonal fresh snow (curve A in Fig. 5,2), (b) seasonal snow aged for three weeks (curve B in Fig. 5,2), (c) seasonal snow aged for two years (curve C in Fig. 5,2), (d) uniformly graded snow obtained from aged snow (curves D, E, and F in Fig. 5,2) obtained by crushing ice by a pulverizer. The laboratory pulverizer is shown in Fig. 5,3. The reasons for using artificial snow lie mainly in the fact that this kind of snow was easier to produce and its grain size distribution could be more reliably predicted and controlled.

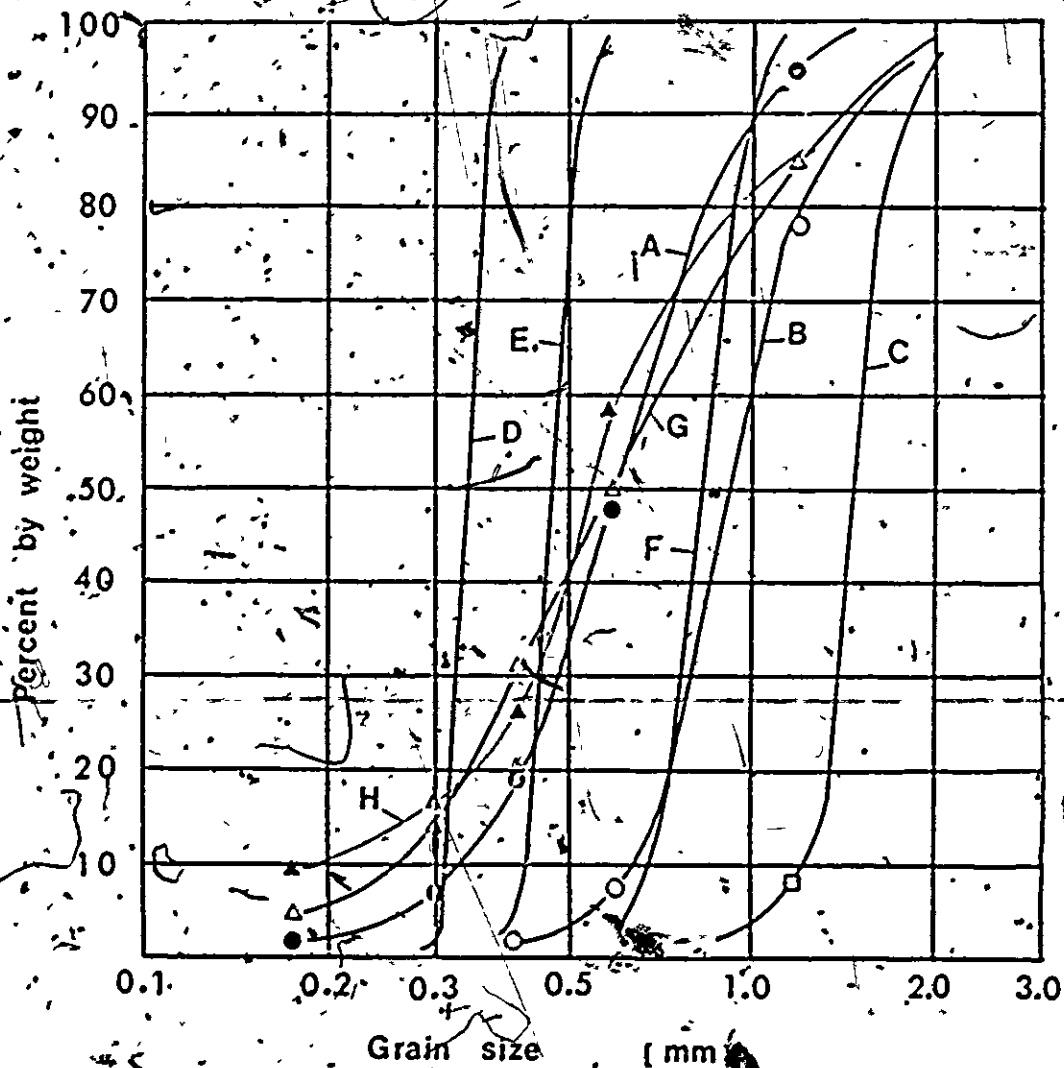


FIG. 5,2

GRAIN SIZE DISTRIBUTION OF SNOWS USED IN THE STUDY OBTAINED FROM THE SIEVE ANALYSIS. A = FRESH SNOW, B = THREE WEEK OLD SNOW, C = TWO YEAR OLD SNOW, D, E AND F = UNIFORMLY GRADED SNOW, G AND H = ARTIFICIAL SNOW OBTAINED FROM LABORATORY PULVERIZER.

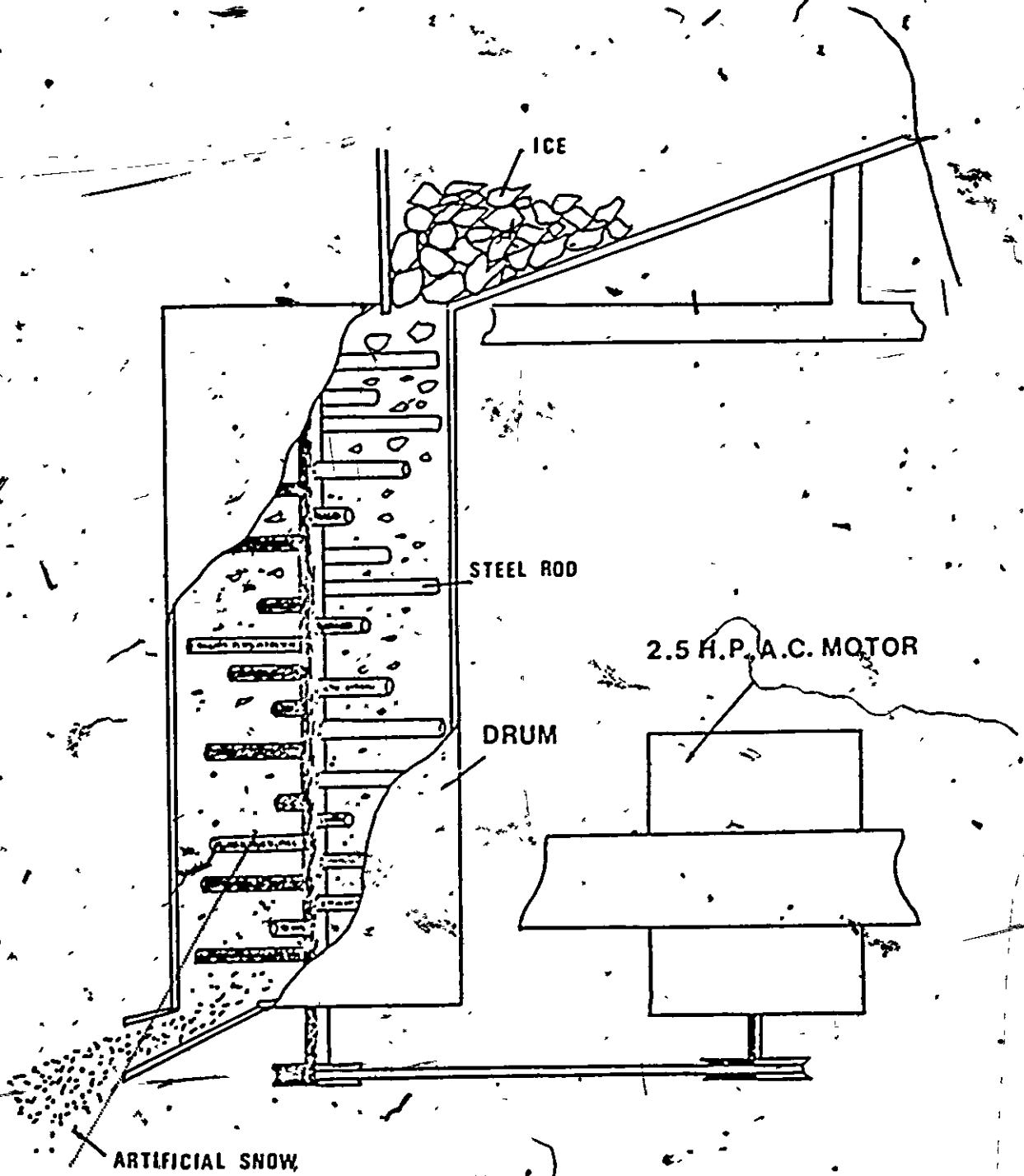


FIG. 5, 3

ILLUSTRATION OF ICE PULVERIZER APPARATUS FOR MANUFACTURE OF LABORATORY SNOW.

From the engineering point of view, the grain composition of two main types of snow should be examined.

1. Fresh Snow (Non-Metamorphic Grains)

In comparison with metamorphic grains, the grain shape of this kind of snow is considered to be more important factor on the control of engineering properties than the grain size. The initial size and shape of crystal (especially needle and plate crystal) are easily breakable. As a result of fragmentation by external and internal conditions, initial snow crystals become smaller and granular.

2. Metamorphic Grains (Aged Grains)

Aged snow approaches sphericity in shape and thermodynamically speaking is more stable because it has a minimum surface energy. Generally the longer the age of snow, the greater the grain size. From the point of view of mechanics of snow, grain size or size distribution of this type should be examined.

The typical morphology of three types of snow, i.e., (a) fresh snow, (b) seasonal snow aged for three weeks and (c) seasonal snow aged for two years are shown in Fig. 5,4.

From a different point of view, i.e., intergranular interaction, snow can be divided into three types, i.e., (a) granular snow, (b) semi-bonded snow, and (c) sintered snow, as mentioned in Chapter III. In the experiment, both granular and sintered snows were used. Granular snow was obtained from the disaggregation of snow while sintered snow was obtained from the sintering process of the snow. Semi-bonded snow

From the engineering point of view, the grain composition of two main types of snow should be examined.

1. Fresh Snow (Non-Metamorphic Grains)

In comparison with metamorphic grains, the grain shape of this kind of snow is considered to be more important factor on the control of engineering properties than the grain size. The initial size and shape of crystal (especially needle and plane crystal) are easily breakable. As a result of fragmentation by external and internal conditions, initial snow crystals become smaller and granular.

2. Metamorphic Grains (Aged Grains)

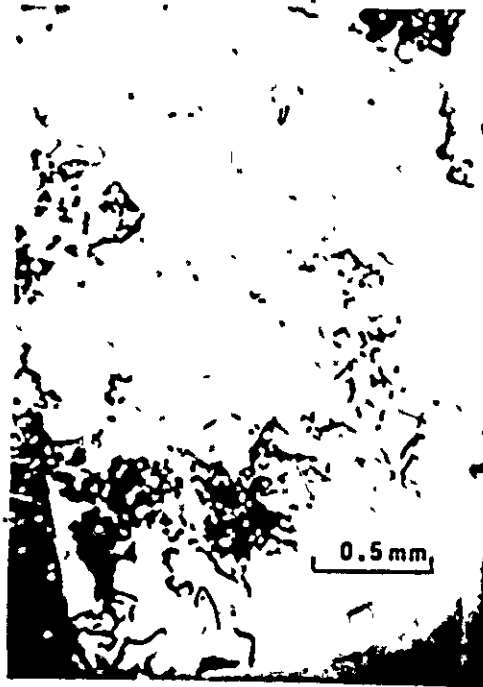
Aged snow approaches sphericity in shape and thermodynamically speaking is more stable because it has a minimum surface energy.

Generally the longer the age of snow, the greater the grain size.

From the point of view of mechanics of snow, grain size or size distribution of this type should be examined.

The typical morphology of three types of snow, i.e., (a) fresh snow, (b) seasonal snow aged for three weeks and (c) seasonal snow aged for two years are shown in Fig. 5.4.

From a different point of view, i.e., intergranular interaction, snow can be divided into three types, i.e., (a) granular snow, (b) semi-bonded snow, and (c) sintered snow, as mentioned in Chapter III. In the experiment, both granular and sintered snows were used. Granular snow was obtained from the disaggregation of snow while sintered snow was obtained from the sintering process of the snow. Semi-bonded snow



(a)



(b)



(c)

Fig. 5.4 Typical Snow Crystal Used in the Study,

(a) Fresh Snow,

(b) Three Week Old Snow

(c) 2 Year Old Snow (at temperature of -13°C)

was not examined in this research because elevated low temperature of -13°C used does not provide for semi-bonded snow condition as mentioned in Chapter II.

V-2 Preparation of Thin Section of Snow Sample

In the adhesion theory (Chapter III), it was the basic assumption that irreversible increases in contact area between snow grains, under plastic, viscous, or creep deformation except elastic deformation, occurs.

In Chapter IV, the mathematical treatment with increase in contact area, based on simple assumptions, was made.

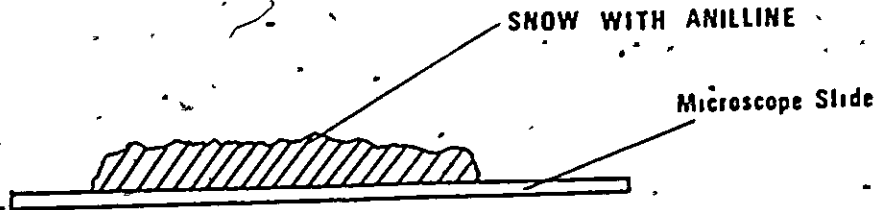
The assumption can be proved directly by the observation of internal structure of snow. Basically, the observation of internal structure of snow can be made on the thin section of snow specimens. Therefore, this section in this chapter describes the technique to prepare thin section of snow. The experimental results and discussion on the observation of internal snow structure by this technique are presented in Chapter VI.

Most methods of preparing thin sections of snow require the preliminary filling of the pore spaces which facilitates mounting and as well reinforces the structure against breakage during sectioning. Various kinds of liquid have been described in the literature, i.e., tetrabromoethane (Bader et al, 1939), diethylphthalate (Schytt, 1958) and aniline (Kinosita and Wakahama, 1959). Aniline was used in this study.

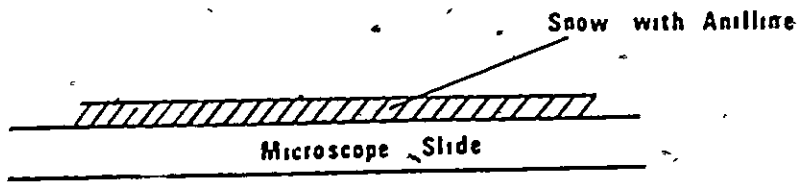
Thin sections were prepared in essentially the same manner as described by Kinoshita and Wakahama (1959). The main procedure is as follows:

- (1) Small blocks of snow sample, approximately $3 \times 3 \times 1$ cm. were immersed in water saturated aniline at approximately -7°C (above the melting point of aniline) and were allowed to freeze at -20°C (below the melting point of aniline). Water saturated aniline was obtained by placing ice rock in aniline liquid.
- (2) One side of block sample was made to be flat by a sharp blade plane and was attached to a microscope slide with liquid aniline (Fig. 5.5 (a)). After that, the sample with the microscope slide was frozen again. Note that lucite plates were used for the microscope slide and were made to be lightly rough surface by a fine sand paper because rough surface will provide for the better cementation between snow sample and the microscope slide when aniline is frozen.
- (3) After freezing, the other side of the prepared sample was planed until the thickness of snow becomes approximately $0.1 \sim 0.2$ mm. (Fig. 5.5 (b)).
- (4) Aniline was allowed to melt at approximately -7°C . Then aniline became transparent. (Fig. 5.5(c)).

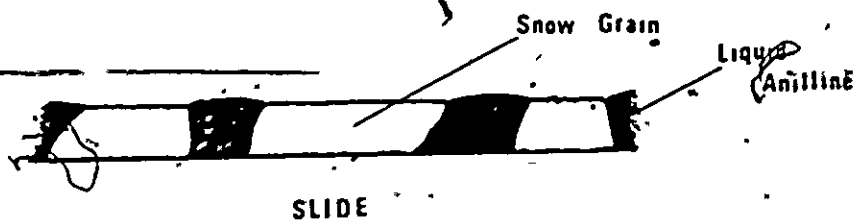
There are both advantages and disadvantages in the use of thin section method. Main advantage is that direct observation of,



(a)



(b)



(c)

Fig. 5,5 Preparation of Thin Section of Snow Sample

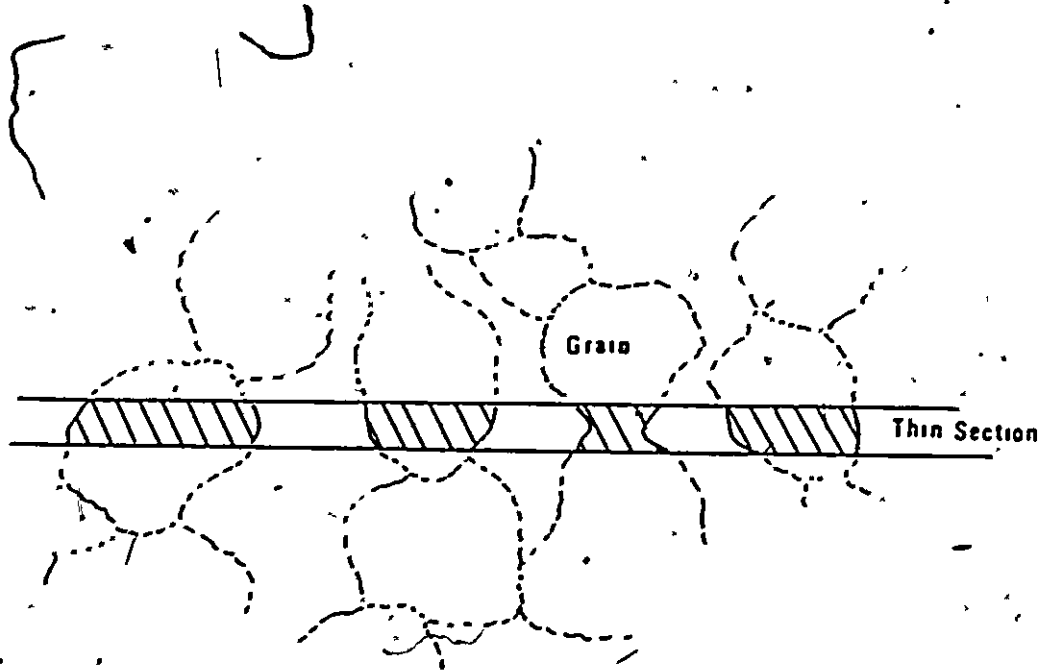


Fig. 5,6 A Possible Thin Sectioned-Grain Size and the True Grain Size

snow structure can be achieved. It is the disadvantage that the observation of internal structure is always made on two dimensional section of snow structure. This will cause probable errors for the measurement of grain size, grain shape or pore size because thin section can be made across a given section of grains as shown in Fig. 5,6. Therefore, grain size obtained from the thin section is relatively smaller than the true grain size (Fig. 6,4).

It should be noted that aniline is poisonous. Therefore, it must be avoided to breathe the vapor of aniline.

V-3 Method of Compressive Loading

The method of compressive loading in particular influences the behaviour of snow under stress. Whilst there are many ways in which stress may be applied to snow, it is observed that for most purposes it is sufficient to distinguish the typical types of loading as follows:

(a) Dead load application

This is basically a dynamic loading generally identified in terms of a sudden loading. This situation occurs when "dead load" is suddenly placed upon the snow mass. Most instances of sudden loading are actually instances of very quick progressive loading.

(b) Removal of load

Typically, a load or stress is applied and wholly or partially removed or reversed.

(c) Creep loading

Most materials will creep or flow to some extent under constant stress or decreasing stress. This tendency is strongly temperature dependent. In the case of loose snow, a volumetric creep (i.e., density increasing) must be taken into account.

(d) Short time static loading

In testing, the load is increased progressively until failure including micro-failure occurs, and total time required to produce failure is not more than few minutes. The ultimate strength, yield point and yield strength of materials are usually determined by short-time static loading test.

It is felt that the present confusion of snow properties and behaviour is due to the poor understanding of the physical aspects of deformation mechanism of snow in relation to the loading rate and density changes. In the application to the problem, it is necessary to examine deformation mechanism of snow under various loading conditions.

V-4 Mechanical Tests

V-4.1 Unconfined Compression Test

In engineering practice, the loads most often applied are compressive. In this sense, the compressive response characteristics of snow may be one of the most important.

The unconfined compression test, in which right circular cylinders are compressed parallel to their longitudinal axis, is the simplest test, and continues to be one of the most convenient and useful ways for determining the mechanical properties of snow. The examination of types of failure for snow may also be achieved by performing unconfined compression tests.

Generally stress-strain relationship of materials is the most basic concept in mechanics. Stress is basically part of statics and strain is a part of geometry. The mechanical properties of snow, such as strength, yield stress, compressive modulus (often Young's modulus), etc., for the requirement for engineering analyses or designs may be obtained from the stress-strain relationship of snow.

Therefore, the first attempt in this research is to appreciate the stress-strain relationships of various types of snow. Secondly, the type of failure of various types of snow is examined.

Another object of performing unconfined compression tests on snow is to obtain important factors governing snow properties, by using various known snow.

The apparatus used for the unconfined compression test was the same type being used for soil testing, as shown in Fig. 5.7. The deformation rate on snow was controlled by a 1.5 H.P. AC motor with pulleys as shown in the figure. The evaluation of stress and ultimate strength of snow in the unconfined compression test were calculated by dividing the force recorded by the sectional area of specimens. Basically, the force exerted was recorded by a heat type-pen recorder through a proving ring and transducer as shown in the figure.

The size of specimens were chosen as 5 cm in diameter and 15 cm high. This dimension is not uncommon for the unconfined compression test for soils.

Specimens for the unconfined compression tests were basically obtained from the artificial redepositing manner through a sieve into lucite cylinders. After a certain time, which provides for the age hardening of snow sample in the lucite cylinders, the snow samples were pushed out by a piston made of paraffin wax.

Note that time will cause the hardening of snow from the sintering process as mentioned in Chapter II. Therefore, effect of initial bond in snow is obtained from aging after the preparation of specimens.

The experimental results and discussion on unconfined compression test is presented in Chapter VII-1.

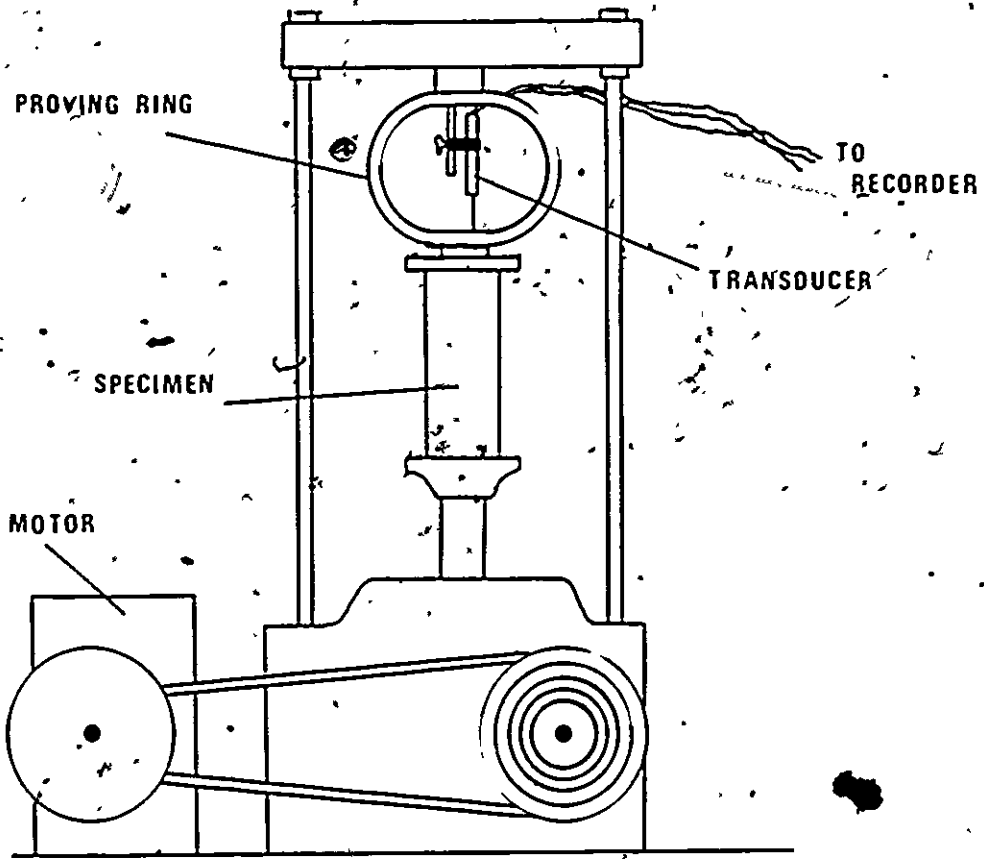


Fig. 5,7 Illustration of Apparatus for Unconfined Compression Test

V-4.2 Confined Compression Test

The most practical type of test in soil mechanics may be the triaxial compression test which establishes the influence of confining pressure.

In general procedure, the result obtained in the triaxial test can be plotted into Mohr-Coulomb circle envelope which is being widely used as the failure criterion.

Triaxial test, however, requires an assumption that the specimen does not fail by the confining pressure applied. However, loose-sintered snow has possibility to fail under confining pressure. In addition any snow possibly has the volumetric creep deformation under confining pressure applied. Note that the volumetric creep deformation changes internal structure of snow. Under this condition, the proper analysis and appreciation of triaxial test on snow are quite difficult.

The compression shear of snow (Fig. 2.2) illustrates the crushing behaviour under the load application. This response characteristics of snow is major difficulty of the progress in snow mechanics because;

- (a) compression shear is considered to be micro-failure which does not follow the conventional failure theories in the macroscopic scale, as mentioned previously.
- (b) this failure mechanism may only be explained by the microscopic considerations.

In the condition illustrated in Fig. 2.2, the confining pressure acting on the ideal failure plane can be illustrated in Fig. 5.8.- In fact, confining pressure P_1 indicated in the figure is dependent on the intensity of load applied and Poisson's Ratio of snow. In the figure, confining pressures P_2 and P_3 apparently depend on applied force F . Note that the failure under P_3 are not common in a dense assembly. This is identified as the micro-failure of snow. The importance is that confining pressures P_1 , P_2 and P_3 are never constant in actual case, but they are variables which are dependent on the method of load application. Under dead load application, the confining pressures, P_1 , P_2 and P_3 exerted on the ideal failure plane, increase very quickly. Under progressive load application, the confining pressures, P_1 , P_2 and P_3 , may be exerted progressively. Thus, in actual case, the confining pressure in snow depends on the type of load application. This suggests that the standard triaxial test is not necessarily useful for snow because usual procedure of triaxial test, the application of confining pressure prior to the axial load application, may change snow properties. In addition, snow may fail by confining pressure as mentioned above. Thus, the soil testing is not always applicable in snow mechanics. Thus, snow testing requires very careful consideration based on the properties and behaviour of snow. At present, since the properties and behaviour of snow has not yet been understood sufficiently, the testing performance for snow is very difficult. Therefore, it may be suggested that simple tests should be performed for the purpose of proper appreciation of snow properties.

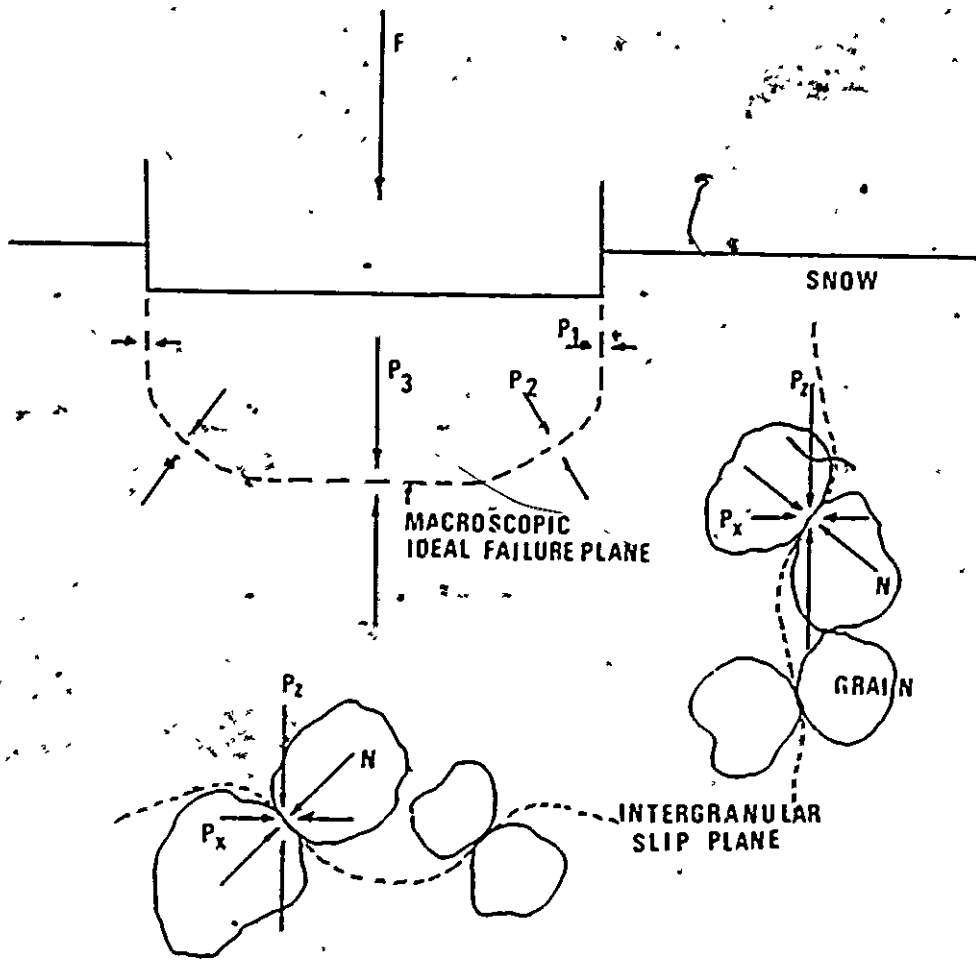


Fig. 5.8 Apparent and True Stresses on Ideal Failure Plane in Snow

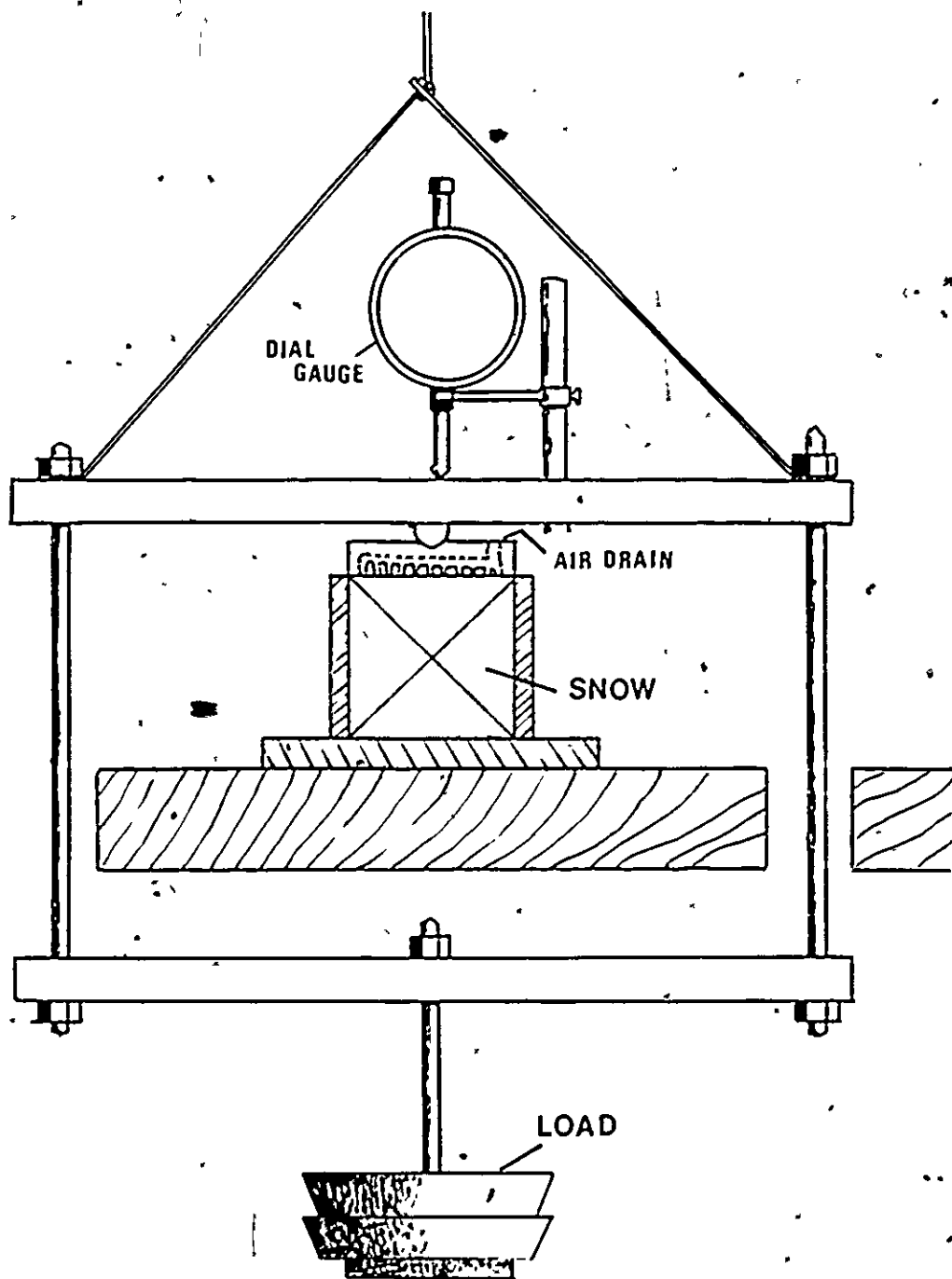
For these reasons, the confined compression test techniques were used in this research. Two types of confined compression tests used in the research are as follows:

(a) Dead Load Confined Compression Test

This test apparently examines the snow behaviour under dead load application which is more realistic in actual case of load application in field. The illustration of the dead load confined compression test apparatus is shown in Fig. 5.9. This test type is rather similar to "consolidation test" being used in soil mechanics. This type of test enables one to obtain both the instantaneous deformation and consequent creep deformation characteristics of snow. In this test, various terminologies, i.e., confined compression (by Costes, 1963), consolidation (by Feldt and Ballard, 1966) and confined creep (by Mellor and Hendrickson, 1963) have been used. However, there are various combinations of dead loads application, which are described as below:

(i) Single Dead Load Application

This method of loading provides for one increment for loading. By using similar snow specimens and various dead loads, relationship between deformation and load intensity can be obtained. Note that this relationship is not necessarily same to that obtained from dead loads increment test.



• Fig. 5,9 Illustration of Apparatus for Dead Load Confined Compression Test

(ii) Volumetric Creep Loading

By similar tests mentioned above, relationship between deformation and time for snow can be obtained. This is identified as "confined creep" or "consolidation" test performance. Note that confined creep of snow means volumetric creep deformation.

(iii) Dead Load Increments

By adding dead loads in increments on a snow specimen, relationship between snow deformation and time can be obtained. However, this loading method differs from the single dead load application. Mechanical response characteristics of snow under these three types of loading are examined and presented in Chapter VII-2.

(b) Progressive Load Confined Compression Test

This type of test provides for the condition that the axial load is progressively applied and the confined pressure is progressively exerted. For the reason mentioned in the last section, the mechanical response characteristics of snow under this condition are examined.

For the confined compression tests with controlled deformation rates, the sizes of specimen, 4.6, 7.3 and 13 cm were examined. The diameter of specimens was 5 cm. The apparatus for the confined compression with controlled deformation rates was basically same to that used for the unconfined compression tests, except the confining

device (standard lucite test cylinder).

Because the confinement provided by the lucite cylinder in the confined compression tests cannot be properly measured or evaluated, it must be considered as an experimental constraint that need to be duplicated for all confined compression tests. Since all the test specimens were similarly prepared for the same kind of test, and since the technique for confined compression was always maintained as standard, it can be reasonably assumed that with similar density measurements during compressive straining, and the developed confinement between specimens would not be too dissimilar. It is observed that whilst the lucite cylindrical confinement effect does not provide for an exact duplication of the confining effect, there is a basis for introducing the confined compression study. Generally speaking, the lateral expansion during vertical compression depends on the Poisson's ratio of material. Therefore, it may be a function of density of material.

V-4.3 Direct Shear Test

Direct shear test, which determines shear strength of materials, is one of the most popular in soil mechanics.

According to Mohr theory, shear strength of materials can be presented by:

$$\tau = f(\sigma_n)$$

Where τ is the shear strength of material

$f(\sigma_n)$ is some function to the normal pressure acted on the shear plane.

For sand, the equation by Coulomb-Navier theory is written by:

$$\tau = \sigma_n \tan \phi'$$

Where ϕ' is the angle of internal friction of material.

As mentioned previously, one of the snow behaviour under pressure is described in terms of "cutting shear" which is the shearing on a plane between two assembled masses. It is found that the function $f(\sigma_n)$ for snow is very complicated (Butkovich, 1956, University of Minnesota, 1951). At present, however, there is a considerable lack of examination of shearing characteristics of snow. For this reason, direct shear test is performed in this research and shearing response of snow is examined.

The object is to obtain the unknown function $f(\sigma_n)$ for snow as a function of snow type and shearing velocity.

The apparatus used for direct shear test is illustrated in Fig. 5,10. The shear boxes used were made of transparent lucite which enable to observe apparent failure mode in snow specimens. The size of shear boxes is $7.6 \times 7.6 \text{ cm}^2$ ($3 \times 3 \text{ sq.in.}$). The shearing was promoted by 1.5 H.P. A.C. motor as shown in the figure.

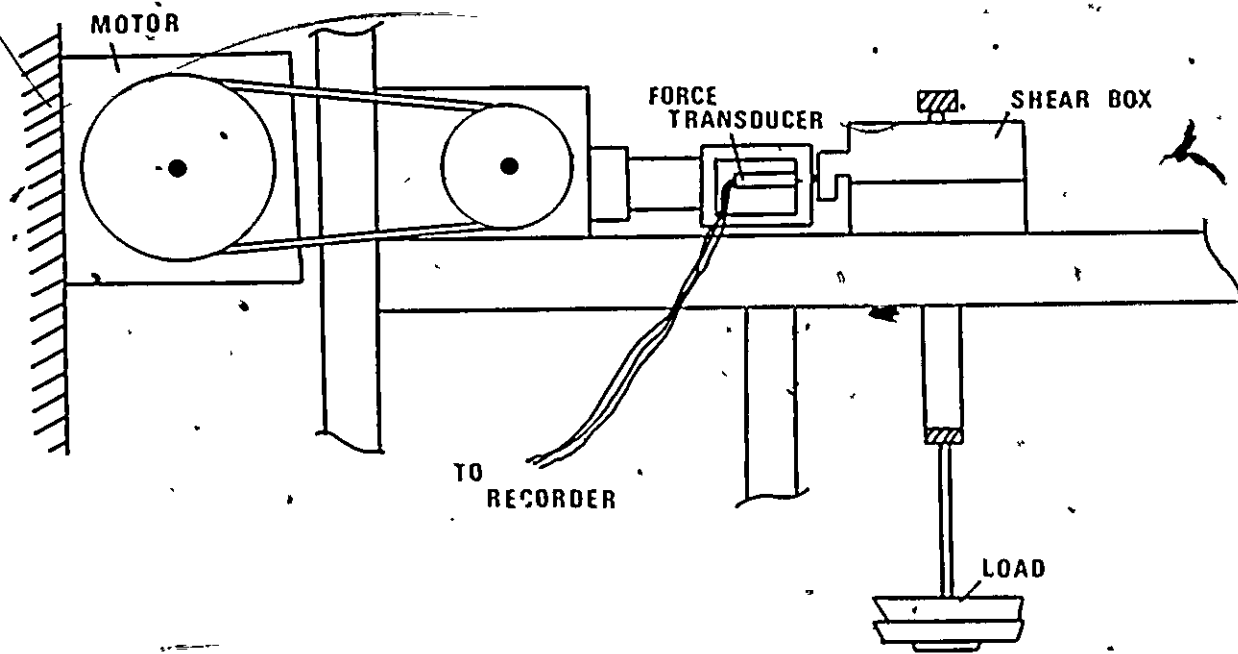


Fig. 5,10 Illustration of Apparatus for Direct Shear Test

The shear stress was calculated by dividing the maximum force required to shear by the constant sectional area of specimen. The specimens for the direct shear test were prepared by the mechanical depositing manner (see Chapter V-4.5). The results and discussion on the direct shear test are presented in Chapter VII-3.

V-4.4 Penetration Test

Although penetration techniques have been used for the evaluation of snow properties, the analyses have not always been successful because penetration response characteristics of snow have been poorly understood. In fact, the analyses for penetration test results require a basic mechanics based on the behaviour of materials or need some relationship between the results obtained from the penetration test and the other test results obtained from an established test technique.

To develop a simple technique, for evaluation of snow properties especially in the field, a thin blade penetration was examined (see Chapter VII-4). A rectangular plate penetration tests were performed. The details are described in

The snow layers for the penetration tests were basically obtained by the mechanical redepositing of snow. The test result and discussion on the penetration performance are presented in Chapter VII-4.

V-5 Sample Preparation

Laboratory tests usually consist of simple experiments appropriate to the nature of snow in which important quantities, often stress and strain or strain and time, are determined. On the other hand the mechanical behaviour of snow is investigated by performing simple tests. Because of considerable lack of the information of snow properties, and lack of the examination of simple experiments, mechanical tests should be performed on known snow conditions. A point which deserves more attention than it has generally received is the extent to which the measured behaviour of snow specimens depends upon the experimental system. The extrapolation of behaviour induced by the system to different circumstances can be most misleading, and every effort must be made to distinguish between the properties of the snow and those of the experimental system.

The structure of snow and its mechanical nature are partially mentioned in the earlier Chapters. Its mechanical properties may depend upon the grain size, grain shape, interaction between grains and density, as found in other materials. Therefore, the most basic mechanical properties of snow are those of a specimen of a size sufficient to contain a large number of constituent grains but small enough to exclude major structural discontinuities, so that it possesses homogeneous properties. Specimens of snow with dimensions of a several centimeters are usually adequate for this purpose and can conveniently be tested in a laboratory.

There are two methods for sampling of snow with different objects. One is the sampling from the field snow condition. Field sampling basically provides for the properties evaluation for a particular snow in the glaciological context. Because of considerable variation of snow properties in field, and the difficulties for the elimination of some of factors governing snow properties, it may be difficult to do systematical examination of the mechanical behaviour of snow by this method. Another method is to obtain snow sample by an artificial depositing manner by using natural fallen snow or artificially prepared snow (fine ice particles) under the specified snow condition. This method will take into account the factors governing snow structure. Since some factors are eliminated or controlled in this method it is easier to analyze and compare the test results. In this research, artificial manner for sample preparation was used.

The basic snow obtained for fabrication of the test specimens were obtained as the various types of snow, i.e., fresh snow, metamorphic-snow and artificially prepared snow as stated in the previous section.

Thus basically all the specimens used in the mechanical tests mentioned above were prepared from the artificial depositing of snow samples into the lucite test cylinder, shear boxes and penetration boxes.

CHAPTER VI

MICROSCOPIC STUDY ON DEFORMATION MECHANISMS OF SNOW

The objects of this chapter are to:

- (a) observe internal grain structure of snow,
- (b) examine experimentally an increase in contact area between snow grains under confined compression, and
- (c) compare the test results with the theoretical values presented in Chapter IV.

VI-1 Change in Internal Structure of Snow under Ductile Confined Compression

VI-1.1 Introduction

The increase in contact area between spherical particles as a function of grain size, contact angle and strain can be expressed mathematically by Eq. (4,10):

$$e \cos^2 \theta = 1 + \frac{2}{3} \sqrt{1 - \left(\frac{r}{r_0}\right)^2} \left\{ \left(\frac{r}{r_0}\right)^2 - 1 \right\} - \frac{2}{3} \left(\frac{r}{r_0}\right)^2$$

Where e is the macroscopic axial strain which is assumed to be uniform through specimen during ductile confined compression

- c is the radius of circular contact area
- r is the radius of spherical grain
- θ is the contact angle as defined in Chapter IV.

The term "ductile compression" indicates that no apparent fracture or abrupt decrease in stress in snow takes place during the compression. The detail is discussed in Chapter VII. In this chapter, the irreversible increase in contact area between snow grains under ductile confined compression is experimentally studied.

In Eq. (4,10), snow grains are assumed as spherical, however, actual shape of snow grain is not ideal sphere. For fresh snow, which has original complicated shape, the assumption is apparently invalid. In metamorphic grains the assumption may be more valid though the shape of grains is not ideal (see Appendix D). In this Chapter, therefore, increase in contact area between grains for metamorphic snow under ductile compression is observed by using microscope and thin section technique. The technique of preparing thin sections has been described in Chapter V-2.

Figure 6,1 shows the organization of experimental study done in this Chapter. The study consists of:

- (1) sample preparation for thin section of snow. Snow specimens (curve F in Fig. 5,2) were compressed at a compressive speed of 0.097mm/sec. in the standard confined compression cylinder up to various strain, i.e., 6, 10, 17 and 25 percent.

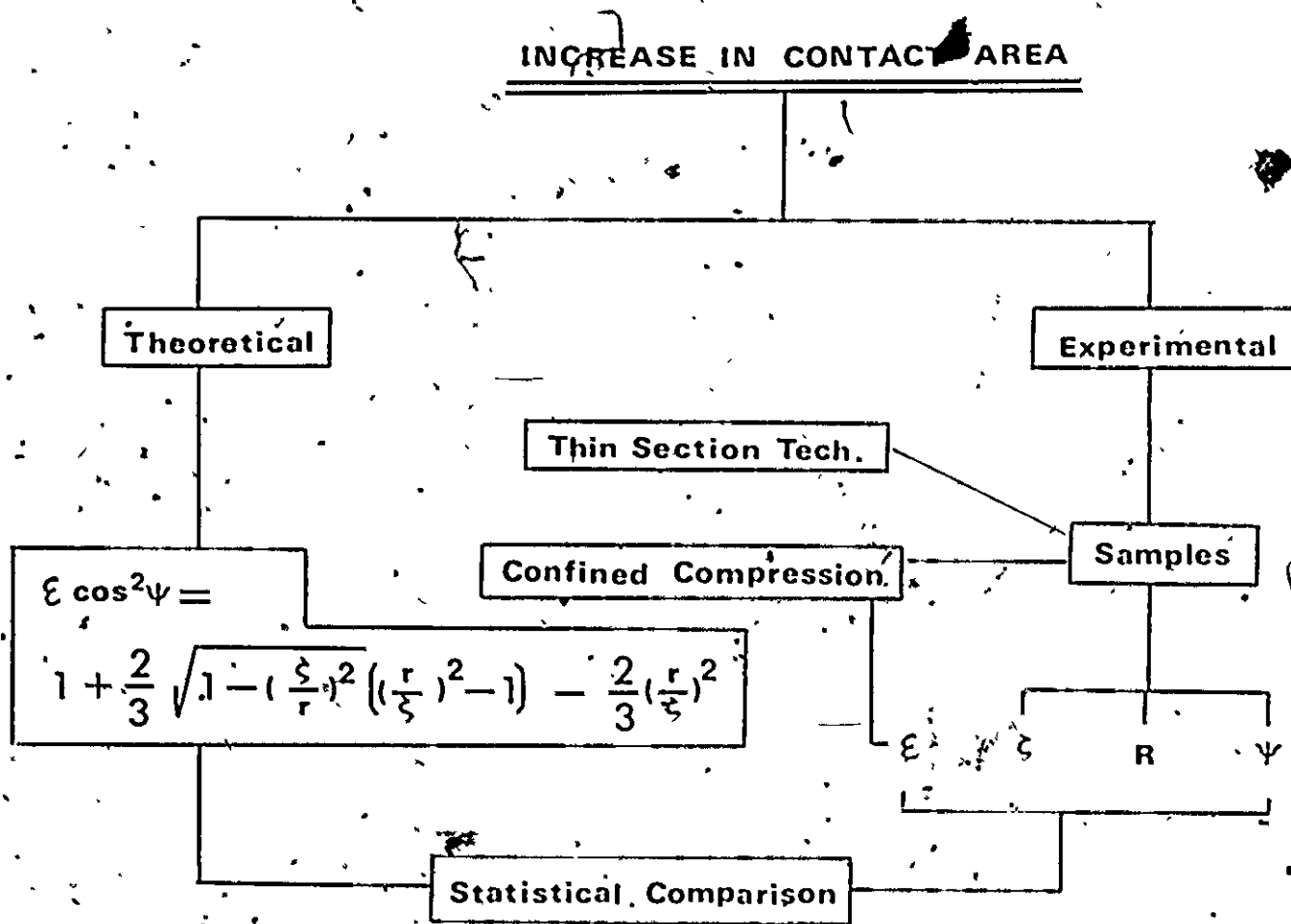


Fig. 6.1 Organization of the "Microscopic Study on Deformation Mechanism of Snow"

(2) snow blocks were cut off from the each compressed specimen as shown in Fig. 6,2.

(3) the blocks were subjected to make the thin sections and then the microscopic-photographs were taken. Note that the direction of force applied should be known in the thin sections because of the need for evaluation of contact angle ψ^* :

(4) the measurements of ψ^* , R and ζ^* were made on the microscopic-photographs and a statistical comparison between the experimental $(\bar{r})_{ex.}$ and the theoretical $(\bar{r})_{theo.}$ with respect to contact angle and strain was made.

An example of evaluation for ψ^* , R and ζ^* is shown in Fig. 6,3. There was an extreme difficulty of evaluation for R of some grains because of their complicated shape (see Appendix D). Therefore, the evaluation was made on grains which were relatively spherical (strictly speaking, circular because of thin section in two dimension). Statistically grain size obtained from thin section is relatively smaller than the true grain size as shown in Fig. 6,4. The both distribution curves were obtained by using microscope analysis (See Appendix D). This is because the thin section does not often cross over the maximum diameter of grains as shown in Fig. 5,6.

A similar situation can be cited for the evaluation of ζ^* . R was evaluated by an approximate way, i.e., by taking smaller curvature near the contact for the reason:

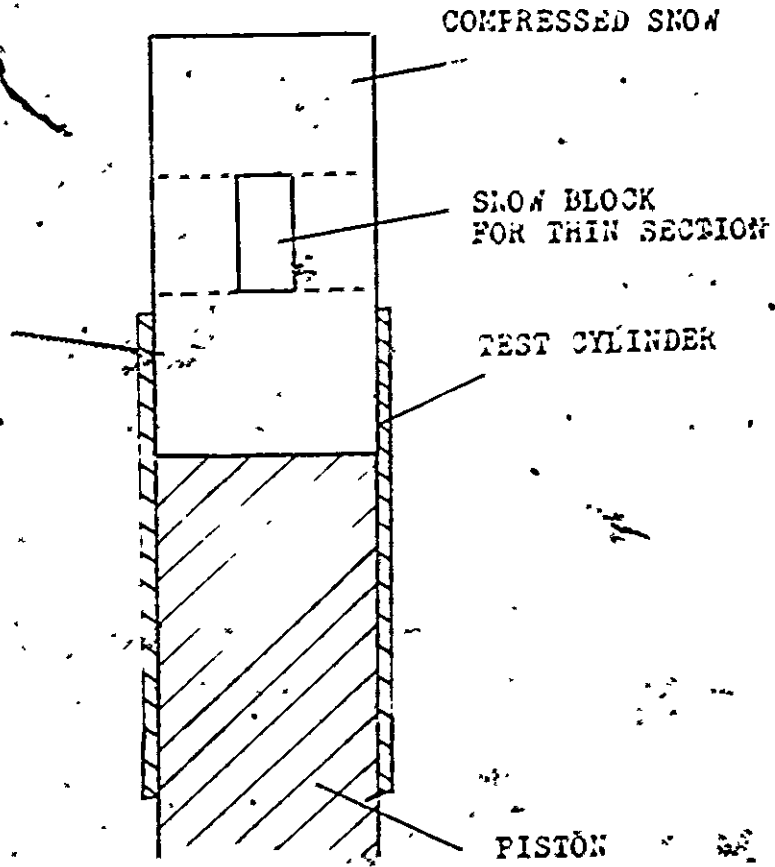


Fig. 6.2 Compressed Snow Sample Used in Thin Section Method

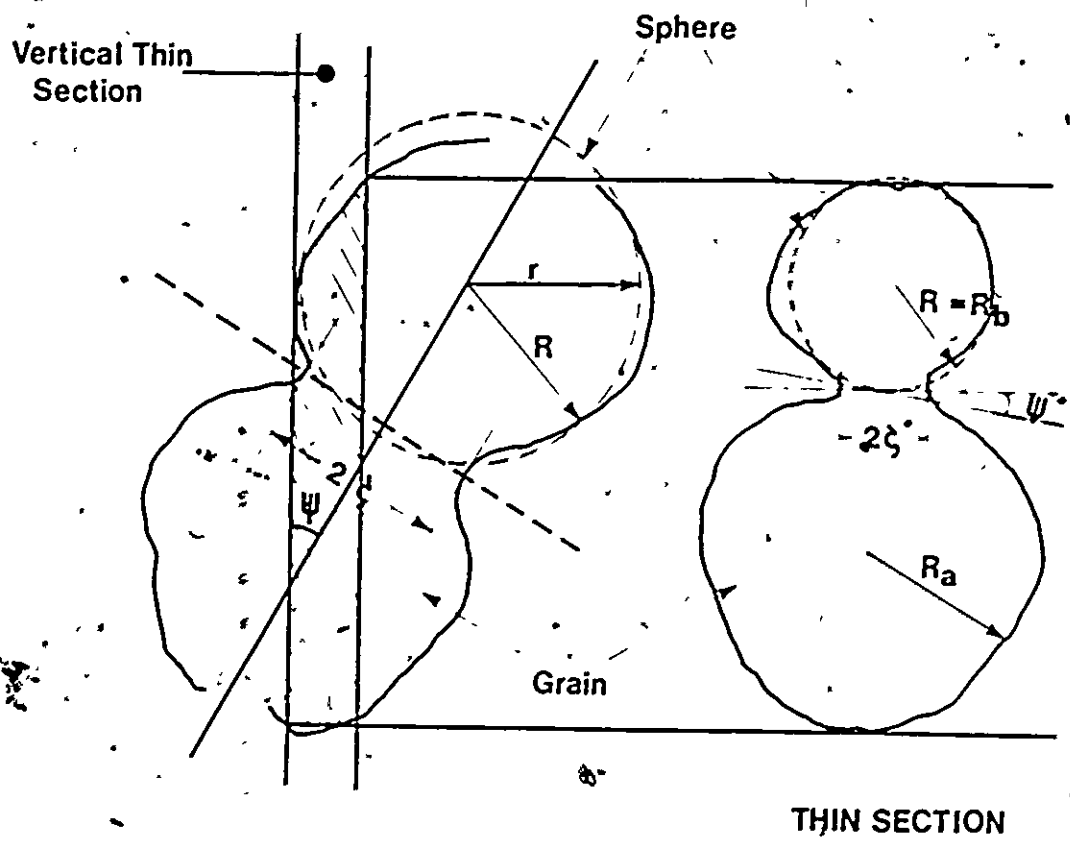


Fig. 6.3 Three Dimensional and Two Dimensional Grain Sizes, Contact Angle, and Contact Area.

- r - radius of sphere
- R - equivalent radius of curvature of grain
- R_b - smaller radius of grains in thin section
- ψ - actual contact angle
- ψ^* - contact angle in thin section
- ζ - actual radius of contact area
- ζ^* - radius of contact area in thin section

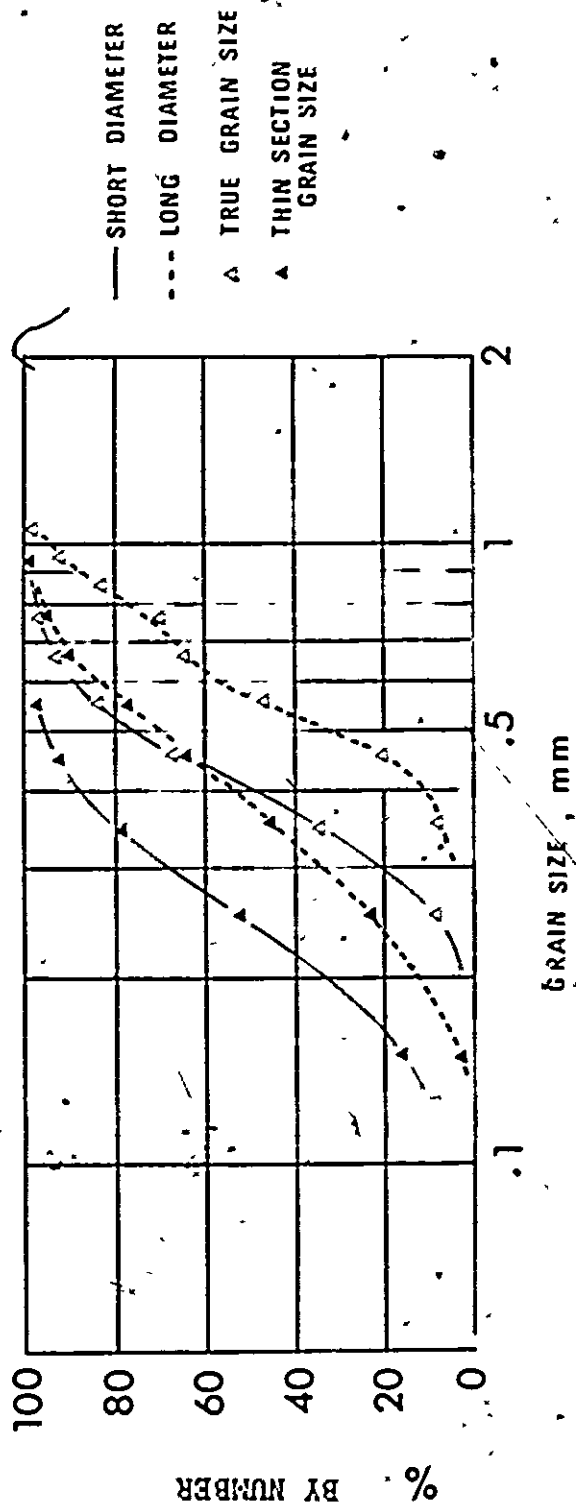


Fig. 6.4 Comparison between Thin Section and True Grain Size in Microscope Analysis

In Fig. 6.3(a), the condition can be cited:

$$R_b < R_a$$

and

$$\zeta^* < \zeta$$

apparently

$$\frac{\zeta^*}{r} \equiv \frac{\zeta^*}{R_a} > \frac{\zeta^*}{R_b}$$

However

$$\frac{\zeta^*}{R_b} > \frac{\zeta^*}{R_a}$$

Therefore, we assume

$$\frac{\zeta^*}{r} \equiv \frac{\zeta^*}{R_b} \equiv \frac{\zeta^*}{R}$$

ζ^* was measured by using a protractor.

A crucial circumstance is that the experimental ζ^* cannot be transferred to three dimension and varies from zero to \dots . However, if ζ^* is always 90 degrees with respect to vertical thin section.

Since the aim of study in this chapter rather lies in the qualitative observation of increase in contact area with respect to strain, a statistical comparison between the experimental $(\frac{\zeta^*}{R})_{ex}^2$

and the theoretical $(\frac{r}{r})_{\text{theo.}}^2$ is made and the trend is discussed.

The statistical comparison basically consists of:

- (a) evaluation of $(\frac{r^*}{R})_{\text{ex.}}^2$ with respect to r^* and R
- (b) evaluation of $(\frac{r}{r})_{\text{theo.}}^2$ (Eq. 4,10) with respect to r^* and r (Fig. 6,6),
- (c) calculation of the relative ratio $\left| \frac{(\frac{r^*}{R})_{\text{ex.}}^2}{(\frac{r}{r})_{\text{theo.}}^2} \right|$ with respect to r^* and r , and
- (d) plotting of contact number versus the ratio

$$\frac{(\frac{r^*}{R})_{\text{ex.}}^2}{(\frac{r}{r})_{\text{theo.}}^2} \quad (\text{Fig. 6,7}).$$

The results are discussed later in this section.

The mechanical properties of snows used for thin sections are presented in Table 6.1.

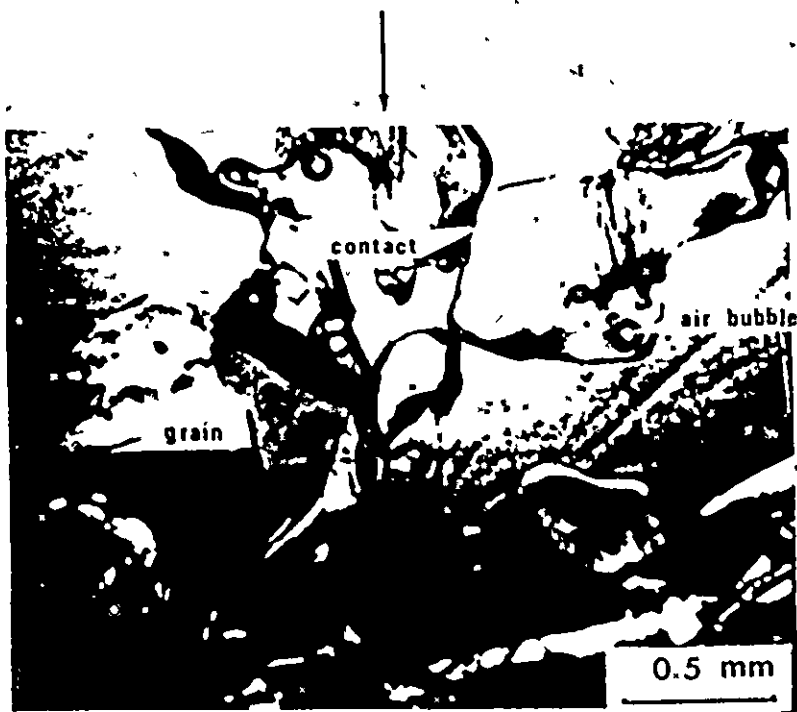
TABLE 6.1 Mechanical Properties of Snows
Used For Thin Sections

(Basic snow: uniformly graded
snow, i.e., curve F in Fig.
5.2. Compressive velocity:
0.097 mm/sec.)

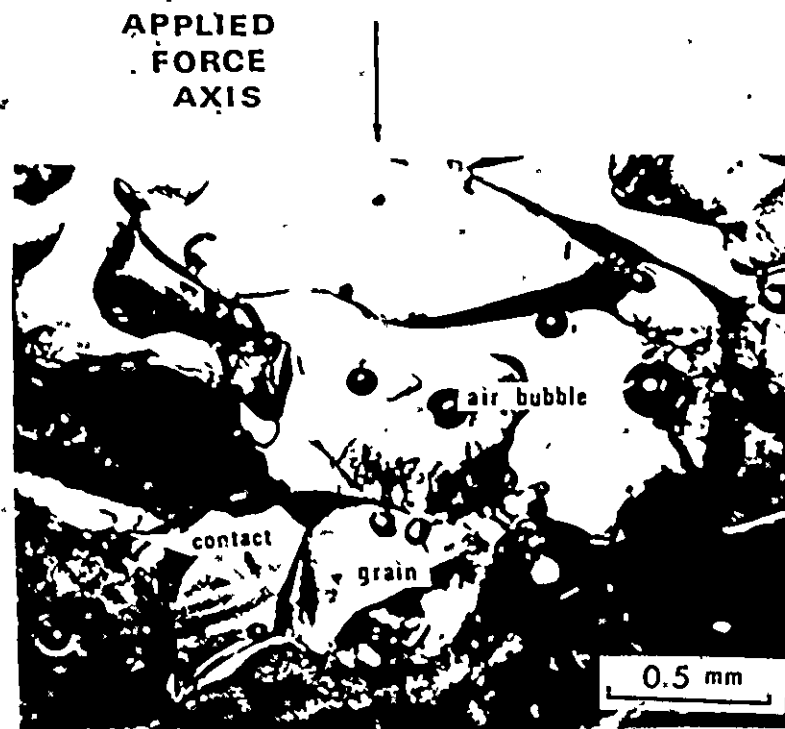
Specimen no.	Initial density, (g/cm ³)	Final density (g/cm ³)	Strain, ϵ (%)	Final stress (kg/cm ²)
1	0.43	0.47	10.1	1.10
2	0.42	0.52	17.7	1.45
3	0.43	0.57	25.3	2.50

VI-1.2 Result and Discussion

Figure 6.5 shows typical vertical internal structure of snow obtained from the thin section technique. Figure 6.5(a) indicates the structure of compressed snow up to 6% axial strain while Figure 6.5(b) shows the structure for 25% axial strain. The major differences between these two figures are in pore size and contact area between grains. It may be realized that the pore size decreases with strain



(a)



(b)

Fig. 6.5 Thin Sectioned - Internal Structure of Compressed Snow under Confined Compression

(a) Axial Strain, 6%

(b) 25%. Compressive Velocity, 0.097 mm/sec.

and the contact area increases with strain.

Theoretically, from Eq. (4.10), $(\frac{\zeta}{r})_{\text{theo.}}^2$ increases with axial strain and decreases with contact angle, as shown in Fig. 6.6.

If α equals to 90 degree,

$(\frac{\zeta}{r})_{\text{theo.}}^2$ is always zero for any axial strain.

This provides for the assumption that no lateral contraction of snow occurs. Therefore, Fig. 6.6 can be valid only for uniaxial compression or laterally constraint condition. The assumption used for obtaining Fig. 6.6 is presented in Fig. 4.2.

Figure 6.7 shows the distribution of ratio $\frac{(\frac{\zeta^*}{R})_{\text{ex.}}^2}{(\frac{\zeta}{r})_{\text{theo.}}^2}$

with respect to contact numbers for (a) 10 axial strain (b) 17.7 axial strain and (c) 25.3 axial strain, respectively. In the figure, in the range of zero to one for $\frac{(\frac{\zeta^*}{R})_{\text{ex.}}^2}{(\frac{\zeta}{r})_{\text{theo.}}^2}$ ratio, the

percent of contact number for 10, 17.7 and 25.3 axial strain are 87, 81 and 74.5, respectively. As mentioned earlier, the theoretical $(\frac{\zeta}{r})_{\text{theo.}}^2$ increases with the axial strain. This means that the experimental $(\frac{\zeta^*}{R})_{\text{ex.}}^2$ also increases with the axial strain for a given

ratio $\frac{(\frac{\zeta^*}{R})_{\text{ex.}}^2}{(\frac{\zeta}{r})_{\text{theo.}}^2}$.

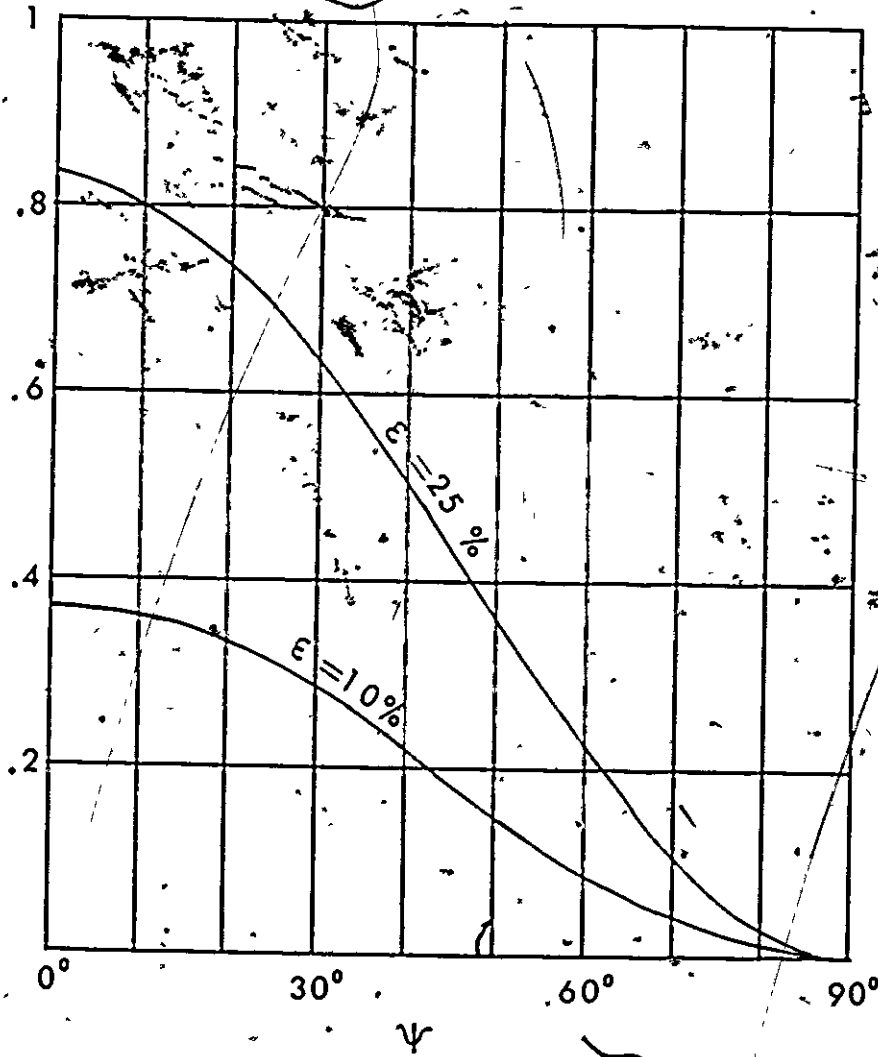
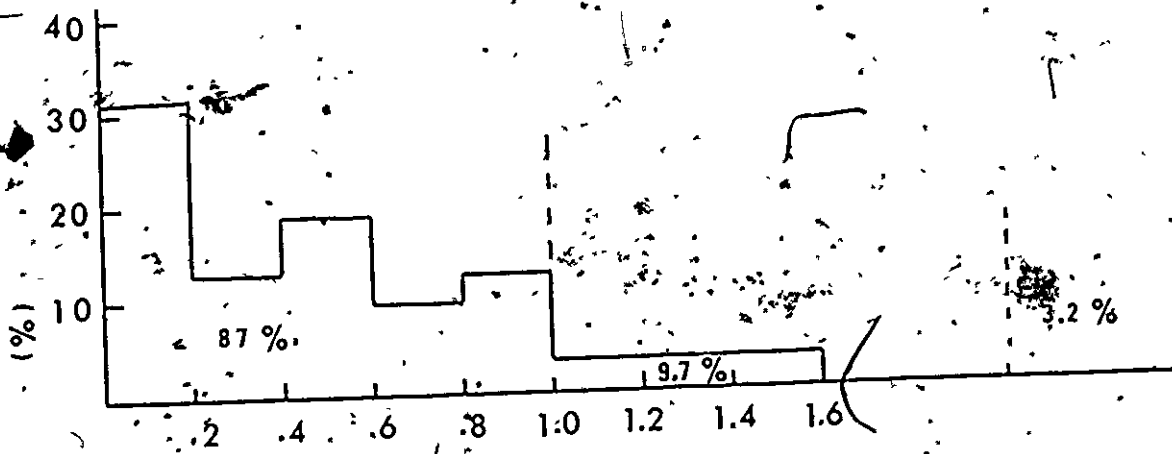
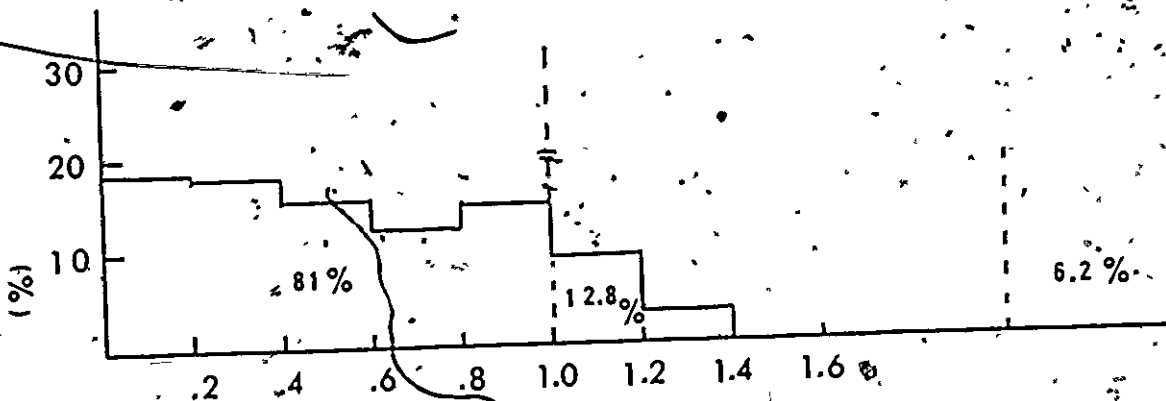


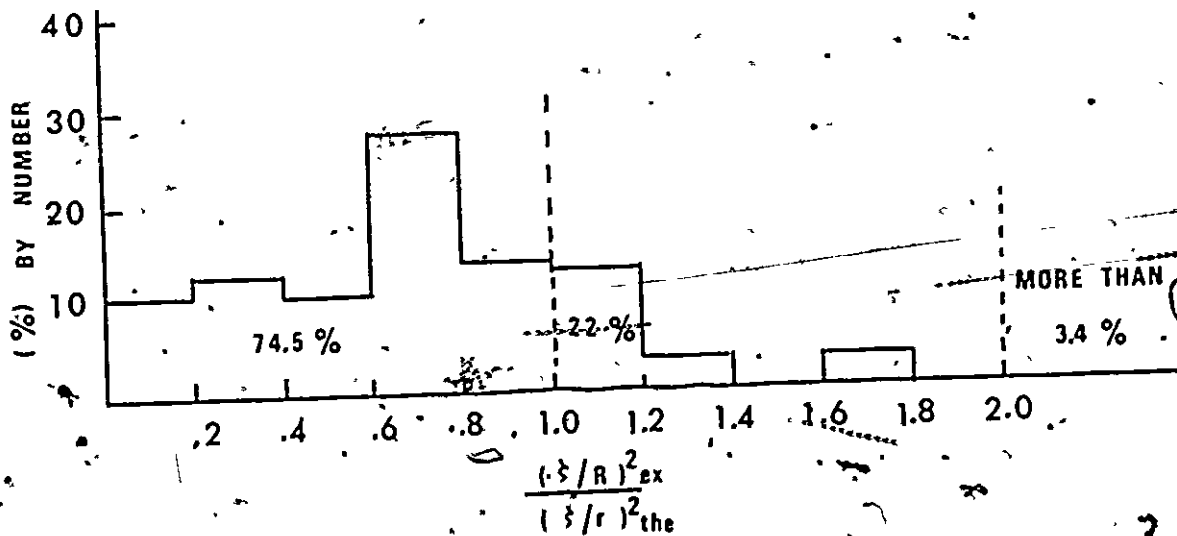
Fig. 6,6 Theoretical Relationship between $(\epsilon / r)^2$ and ψ



(a) $\epsilon = 10\%$



(b) $\epsilon = 17\%$



(c) $\epsilon = 25\%$

Fig. 6.7 Statistical Comparison between Experimental $(\tau / R)_{ex}^2$ and Theoretical $(\tau / r)_{theo}^2$.

(a) $\epsilon = 10\%$, (b) $\epsilon = 17\%$ and (c) $\epsilon = 25\%$.

There may be mainly three reasons why the distribution shown in Fig. 6,7 spreads mainly between the relative ratio of zero to one:

- 1) some of the contacts were initially idle and then the stress applied did not transmit through those grains. This consequently results in no relative strain between grains. Some of the contacts may be made under compression but the true relative strain will be smaller than that of the corresponding macroscopic strain.
- 2) there was an error in the measurement because of two dimensional thin section; as mentioned previously.
- 3) there was a true variation because of varied nature in shape and size of snow grains in comparison with the theoretical approach.

Figure 6,8 shows the frequency distribution of the contact angle, ψ^* , in the snow specimens. As can be seen in the figure, the frequency distribution decreases with the value of ψ^* increasing. This may be packing characteristics of snow (see Appendix C).

The increase in contact number per grain under the confined compression is shown in Fig. 6,9. The figure shows that the number of contacts slightly increases with the axial strain increasing. It should be noted that both the frequency distribution of ψ^* and the number of contacts were directly obtained from the thin sections and these values cannot be actual values in three dimensional consideration.

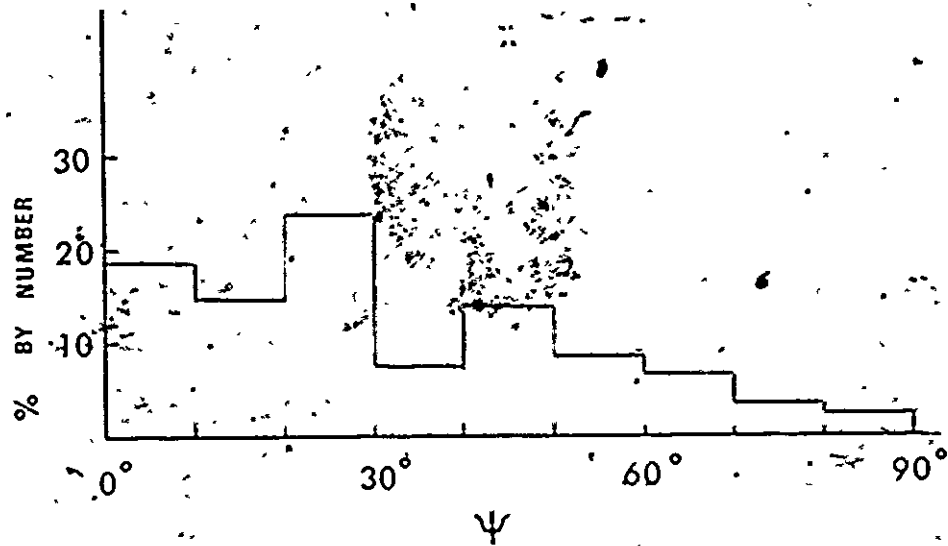


Fig. 6,8 Frequency Distribution of Ψ Obtained from Thin Section Method

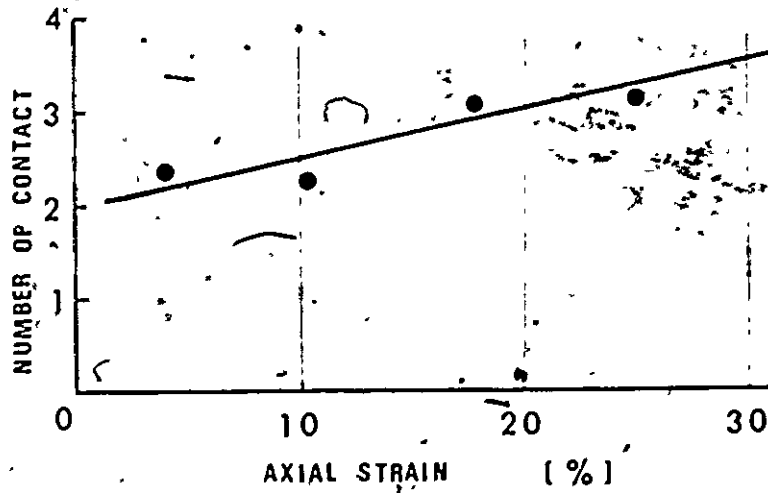


Fig. 6,9 Contact Number per Grain Obtained from Thin Section Method

It is therefore expected that the actual number of contacts is relatively greater than that shown in the figure.

The increase in yield stress (final stress) with respect to the axial strain (Table 6.1) under the ductile compression can be described in terms of increase in contact area (Fig. 6,7) and the increase in contact number (Fig. 6,9). In fact, the rate of increase in yield stress is also influenced by the strain rate, because crystalline flow is dependent on the viscosity of crystal (Herring, 1950).

Thus, the ductile compression of snow can be qualitatively described as:

- (a) increase in contact area between grains as a function of grain size, axial strain and contact angle,
- (b) increase in contact number as a function of axial strain or density, and
- (c) viscous behaviour as a function of temperature.

It should be noted that if snow is initially of strongly sintered nature the situation may be partially or totally changed.

From the mechanical point of view, the constitutive equation for ductile confined compression may be in form of:

$$\sigma = f(S, n, \psi, \dot{\epsilon})$$

Where σ is the stress, which is a function of contact area, S ,

n , is contact number

- n, is the coefficient of viscosity of ice
- θ is contact angle
- $\dot{\epsilon}$ is strain rate.

Many researchers have regarded density as a function of ductile compressive stress from the macroscopic point of view. However, it should be noted that the increase in contact area between grains should be taken into account. This is discussed in Chapter VII. The fact, that increase in contact area occur under ductile confined compression, is extremely important for the development of the adhesion theory which may be the most basic concept in snow mechanics. As described earlier, one of the objects of the research is to develop and confirm the adhesion theory. Therefore, for next step, it is necessary to examine that the adhesion force with increase in contact area will increase. This is examined through the mechanical tests presented in Chapter VII and the details are summarized and discussed in Chapter VIII.

In next section, a change in internal structure of snow under brittle confined compression is discussed from the experimental results.

VI-2 Change in Internal Structure of Snow under Brittle Confined

Compression

VI-2.1 Introduction

As presented in Fig. 2.2, loose snow possibly fails by micro-failure. Similarly loose snow fails in cylinder if relatively high deformation rate is applied on snow. This behaviour of snow is defined as brittle behaviour of snow. The experimental results in relation to brittle behaviour in confined compression are presented in Chapter VII-2 and the detail is discussed in also Chapter VII-2.

It is of importance to examine physical aspects of brittle behaviour of snow for comparison with the ductile behaviour shown in the previous section. From the microscopic point of view, brittle compressive behaviour of snow is examined in this section. The experimental procedure is basically similar to the one described in the previous section, i.e., VI-1.

Snow specimen (initially granular snow) was compressed in the standard lucite test cylinder at a velocity of 0.98 m/sec. This velocity provides for the brittle behaviour of the snow. Note that the effect of compressive velocity is one of the most important factors governing snow behaviour. This is discussed in Chapter VII. The deformation rate used in this section is ten times higher than that used in the ductile compression presented in Section VI-1.

In the cylinder, the brittle behaviour changed into the ductile at axial strain of 13 percent. When the axial strain reached to 22 percent, the specimen was pushed out by a piston made of

paraffin wax and was used to make thin sections. The thin section technique has been described in Chapter V-2.

VI-2.2 Result and Discussion

The internal structure of snow, which has been subjected to brittle confined compression, is shown in Fig. 6,10. In the figure, many breakages of grains and cracks within grains are seen.

It was described in Chapter III that ice is viscous material. Viscous materials under extremely rapid loading behave like rigid material. This idea has well been established in the rheology (ref. Reiner, 1960). This means that the more rapid the deformation applied on snow, the more rigidly the grains behave. If snow grain behaves like rigid, the deformation of grain can be neglected. Therefore, the deformation applied must be dissipated into either grain breakage or intergranular slippage to the exclusion of significant crystalline-flow found in the ductile confined compression presented in Chapter VI-1.

Thus, the brittle mechanism of snow is distinguished from the ductile. Since both mechanisms may accompany with density changes under compression, the effects of change in density should also be described in terms of brittle or ductile.

In summarizing, it may be concluded that snow response characteristics under compression can be divided into mainly two mechanisms, i.e., (a) ductile and (b) brittle. However, general deformation mechanisms of snow may be dependent on grain characteristics, initial density, bonding strength, temperature, etc. Some of these factors are examined by performing the mechanical tests and discussed in Chapter VII.



Fig. 6,10 Thin Sectioned - Internal Structure of Compressed Snow under Confined Compression.

Axial Strain, 22

Compressive Velocity, 0.98 mm/sec

CHAPTER VII

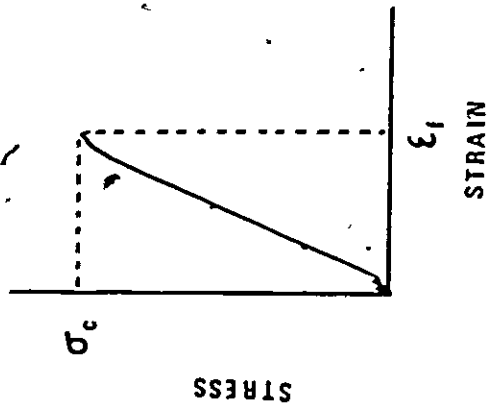
RESULTS AND DISCUSSION ON MECHANICAL PROPERTIES
AND BEHAVIOUR OF SNOWVII-1 Unconfined Compression PerformanceVII-1.1 Stress-Strain Relationship

Nearly 200 cylindrical snow specimens, of known characteristics, were compressed under unconfined condition at various compressive velocities, i.e., 0.037, 0.176, 0.227, 0.508 and 0.980 mm/sec.

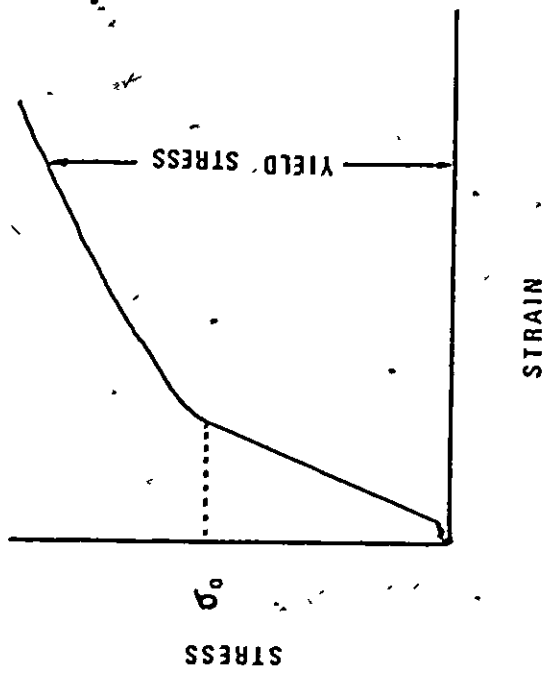
From the experimental results, the relationship between stress and strain of snow under unconfined compression is divided into many types in terms of deformation rate and snow type.

Figure 7.1 shows typical stress-strain curves in relation to the compressive velocities. The curve as shown in Fig. 7.1(a) can be obtained for relatively higher compressive velocity while the curve (Fig. 7.1(b)) can be obtained for lower velocity.

Figure 7.1(a) demonstrates that the stress increases almost proportionally with the axial strain and abruptly decreases down to zero when the stress reaches to a certain point. The apparent feature of this typical curve is similar to other brittle materials. Therefore, this behaviour of snow is defined as the "brittle behaviour" of snow. While, Fig. 7.1(b) demonstrates that the stress increases with the initially high gradient and then slowly. This behaviour is defined



(a)



(b)

Fig. 7.1 Typical Stress-Strain Curve of Snow in Relation to Deformation Rate

- (a) High Rate of Deformation
- (b) Low Rate of Deformation

as "the ductile behaviour" of snow, which is opposed to brittle behaviour. It is noted that a little difference between snow and other ductile materials lies in the yield stress in relation to the axial strain. For example, the stress in ductile behaviour of snow increases continuously with the increasing axial strain while the yield stress of other ductile materials generally starts to decrease when the progressive shear failure occurs. As examined in Chapter VI, the ductile behaviour of snow will increase the contact area between snow grains. Since the idea is that the increase in contact area results from the viscous flow of crystals, it can be said that the ductile behaviour of snow is rather viscous. This suggests that the concept of failure is not applicable for ductile behaviour of snow.

The unconfined compressive strength, σ_c , is defined as the maximum stress in the brittle type of stress-strain curve as shown in Fig. 7.1(a). When the stress reaches the ultimate strength, the stress decreases abruptly as mentioned earlier. This abrupt drop of stress is identified as the "failure" or "fracture" of snow. σ_c increases with bonding as shown in the figure. This is discussed in the next section.

As mentioned in Chapter VI, the failure of snow (i.e., brittle behaviour of snow) may be described in terms of intergranular slippage or/and grain breakage.

For the ductile behaviour of snow, the "yield point", σ_y , may be defined as the stress where the clear change in slope of stress-strain curve occurs as shown in Fig. 7.1(b). The yield point is very

dependent on the bonding of snow. This is discussed later in this section.

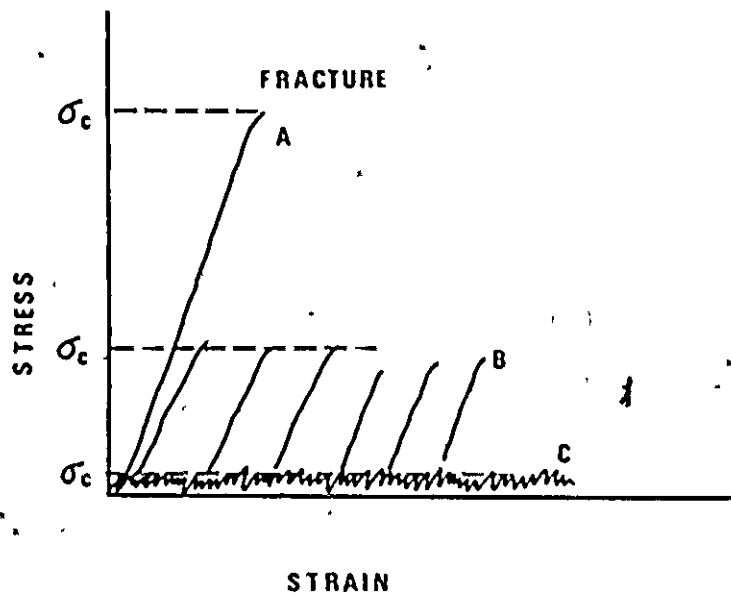
It was mentioned in Chapter II that the bonding of snow is dependent on time and temperature (sintering process). The longer the sintering time, the stronger the snow bonding.

The bonding effect on stress-strain relationship of snow is shown in Fig. 7.2. Because of the effect of compressive velocity as pointed out earlier, the stress-strain relationship in relation to the bonding is also divided into brittle and ductile types.

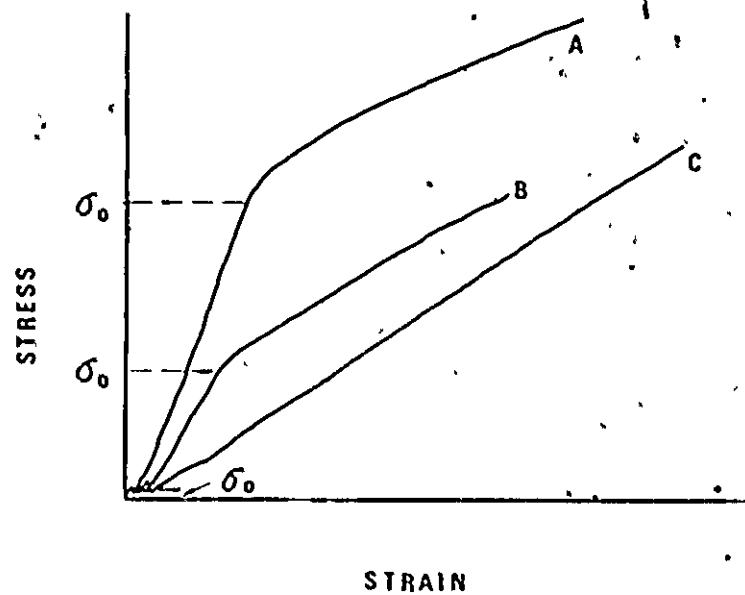
In Fig. 7.2(a), Curve A indicates the stress-strain relationship of strongly bonded snow, Curve B indicates a typical saw-toothed type stress-strain relationship of moderately bonded snow, and Curve C indicates a typical chattering effect of poorly bonded snow. The types of failure mode concerning with the Curves A, B and C are discussed in the next section. As mentioned earlier, the unconfined compressive strength, σ_c , is defined as the maximum stress as shown in the figure.

In Fig. 7.2(b), Curves A, B and C indicate the ductile stress-strain relationship of strongly bonded snow, moderately bonded snow and poorly bonded snow respectively. The figure demonstrates that the yield point, σ_0 , defined earlier, increases with the increasing bonding.

At medium compressive velocity, the combined behaviour of brittle and ductile for snow is obtained as shown in Fig. 7.3. This behaviour is defined as the semi-brittle or semi-ductile behaviour of snow. The apparent feature of semi-brittle behaviour of snow is that



(a) brittle



(b) ductile

Fig. 7,2 Typical Brittle and Ductile Stress-Strain Curves of Snow in Relation to Bonding and Deformation Rate.

- A Strongly Bonded Snow
- B Moderately Bonded Snow
- C Poorly Bonded Snow

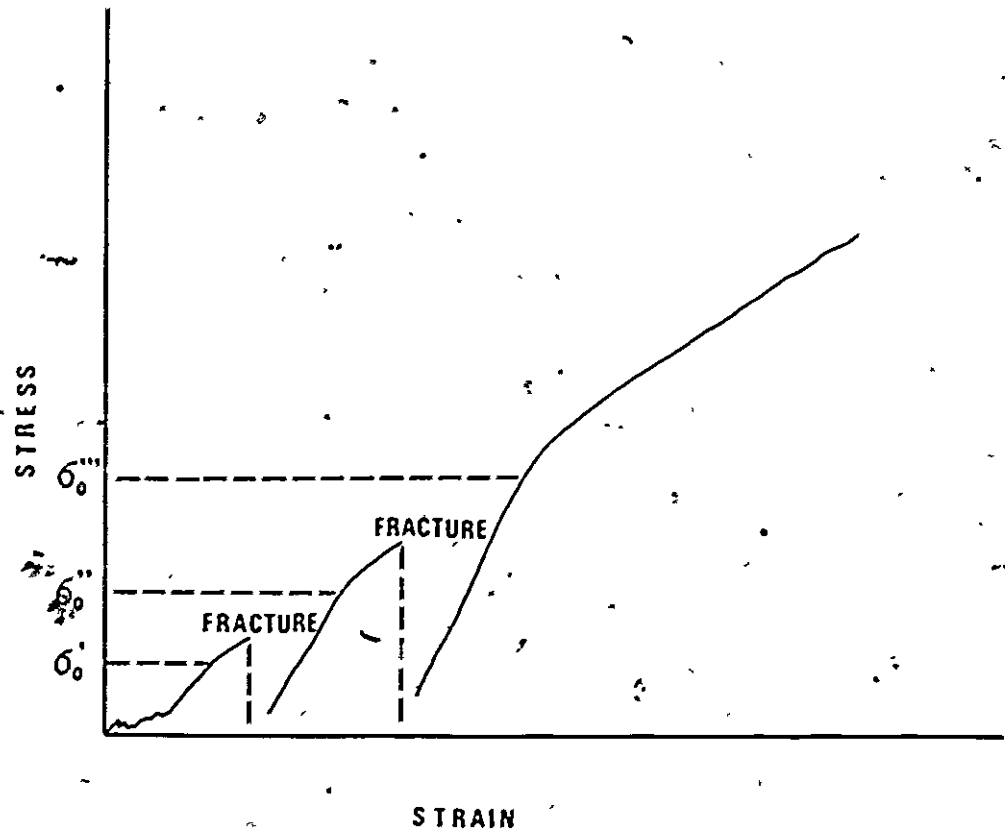


Fig. 7.3 Typical Semi-Brittle Stress-Strain Curve of Sn.

a few or several abrupt stress drops occur during the unconfined compression but finally the behaviour becomes ductile. Thus, the stress-strain relationship of snow is divided mainly into two types, i.e., brittle and ductile, and additionally semi-brittle or semi-ductile with respect to the deformation rate and snow type. This is further discussed later in this chapter.

VII-1.2 Apparent Failure Mode for Snow in Brittle Unconfined Compression Performance

Apparent failure mode is obtained in brittle unconfined compression. Typical types of failure performances corresponding with Fig. 7,2(a) are illustrated in Fig. 7,4 as follows:

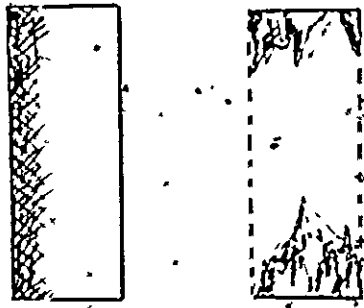
Type 1: Complete and distinct fracture with an observable failure surface concentrated near the end platens.

This is like the brittle performance known by other materials.

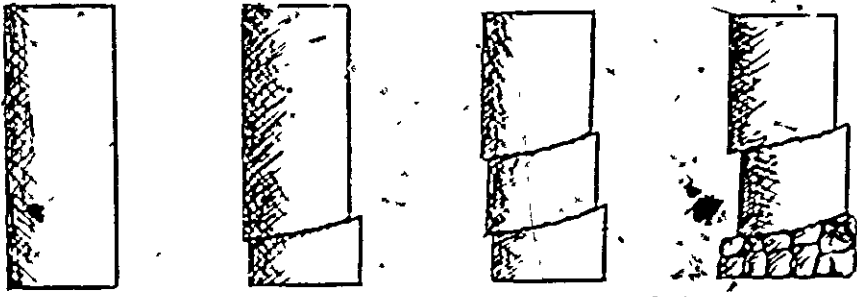
Type 2: Multiple plane fracture surfaces as observed in confined compression tests. The results of confined compression tests are presented in Chapter VII-2.

Type 3: Local crushing and dislocation of snow particles and aggregate groups at the end platens.

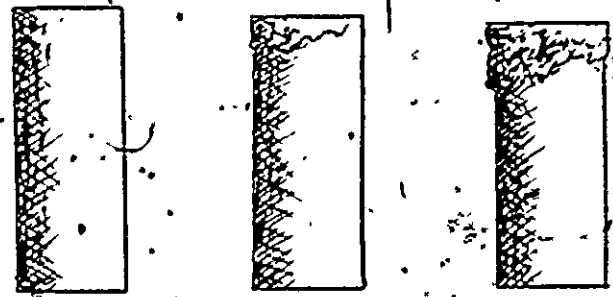
The failure observed in Type 1 is typical of strongly bonded snow (i.e., for longer time in sintering). This type is similar to those



Type 1



Type 2.



Type 3

Fig. 7.4 Typical Failure Modes for Soil in Unconfined Compression Test

obtained in high density-naturally processed snow by Butlovich (1956). When bond development is not strong enough, the medium or loose snow failure performance is characterized by multiple plane fracture surfaces as shown in Type 2. The stress-strain relationship shows abrupt stress release when a plane fracture occurs. Stress build-up occurs again as the test specimen regains rigidity and it is apparently due to the collapse of pores on initial failure surface which does not permit further failure development along that particular rupture surface. In other words, inhomogeneous density change produced by plane failure may result in the high supportability on the failure plane against further failure. Another failure occurs on a plane which is the weakest part under new stress development. When another rupture surface is generated, an abrupt stress release occurs (Fig. 7,2(a)), thus, producing the saw-toothed pattern (Curve B) of the stress-strain curve.

Type 3 failure is typical of a very poorly bonded snow. This is generally the case for low density snows. Local crushing for loose snow occurs at the loading surface (platen). This phenomenon will propagate into the specimen since there is little continuity in stress propagation and distribution in view of loose assembly and poor bonding. Thus, continued local crushing will occur in the face of advancing loading surface. The stress-strain pattern (Fig. 7,2(a), Curve C) shows a typical chattering effect of local rupture due to crushing effects.

VII-1.3 Unconfined Compressive Strength of Snow as a Function of Compressive Velocity and Age of Sintering

As mentioned earlier, unconfined compressive strength of snow is defined as the maximum stress, only in brittle stress-strain curve. The result of unconfined compression tests on the artificial snow during sintering for 30 minutes, 1 hour, 2 hours, 3 days and 6 days is shown in Fig. 7,5. The sintering process in snow is presented in Chapter II. In the figure, the points indicated by the triangle, square and circle show the unconfined compressive strength obtained from the brittle type stress-strain curves. The figure indicates three important facts, namely:

- (a) unconfined compression performance on snow is divided into main two types, i.e., brittle and ductile,
- (b) unconfined compressive strength of snow is influenced by the compressive velocity, and
- (c) unconfined compressive strength of snow increases with the age of sintering.

The brittle and ductile zones with respect to the stress-strain curves are indicated in the figure. As described earlier, brittle curves are obtained for higher compressive velocity while ductile behaviour of snow is obtained for relatively lower compressive velocity (see Fig. 7,2).

The boundary (i.e., the broken line indicated in Fig. 7,5)

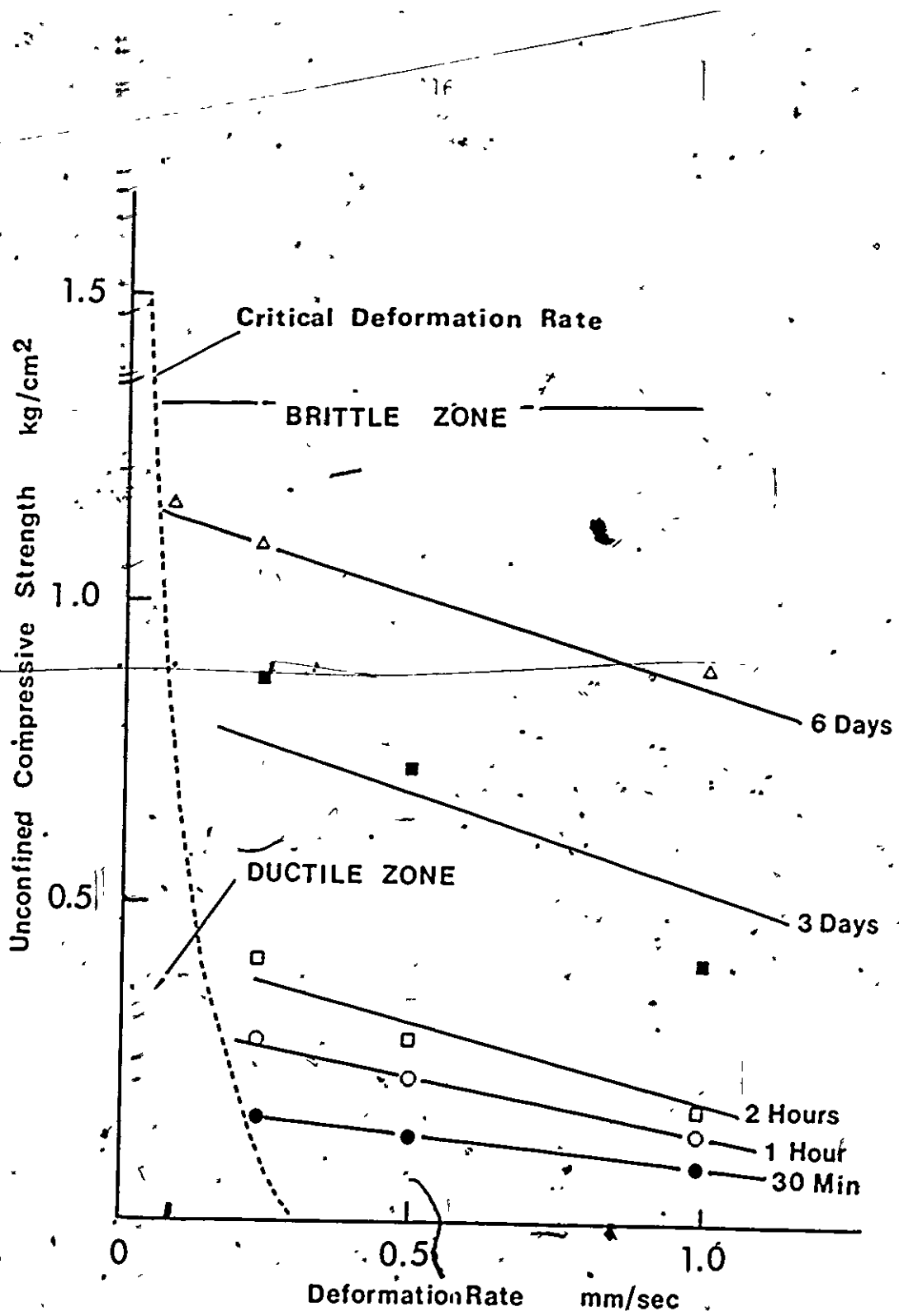


Fig. 7.5 Relationships between Unconfined Compressive Strength and Deformation Rate for Variously Age Hardened Snow

between the ductile and brittle zones may be defined as "critical deformation rate" or "critical velocity" as proposed by Yosida (1963). Note that, at or near the critical deformation rate, semi-brittle stress-strain curves were obtained. The critical deformation rate seems to be a function of unconfined compressive strength (i.e., snow type with respect to sintering time). The figure shows that the critical deformation rate decreases with increasing unconfined compressive strength. Yosida (1963) described that critical deformation rate increases with increasing temperature. By comparison, the metal transition is a function of deformation rate, temperature and grain size (Pasmore, 1965 and Armstrong, 1969). Thus, the transition between ductile and brittle behaviour of materials may be dependent on many factors. It is deduced that the problem of transition for snow is dependent on the internal and external conditions, such as grain size, bonding, temperature and lateral constraint. The effect of lateral constraint for the transition problem of snow is discussed in Chapter VII-2.

Figure 7.5 shows that the unconfined compressive strength increases with bonding (i.e., sintering time) and decreases with increasing compressive velocity. Since the density changes of snow specimens were not obtained during the sintering process of 6 days for initially granular condition, the increase in unconfined compressive strength with respect to sintering time as shown in the figure is almost entirely due to the bond development. Note that the density of each specimen was almost constant during sintering because

the specimen was kept more or less in a closed system in view of mass transfer, and basic snow sample used was not fresh snow.

The trend that unconfined compressive strength decreases with increasing deformation rate as mentioned earlier (Fig. 7,5) is uncommon to other materials. This effect of deformation rate may be very complicated in terms of deformation and failure mechanisms. However, it is considered that time until failure under load may affect the unconfined compressive strength. This is discussed with other test results in Chapter VII-3 and Chapter VIII-1.

In summarizing, it may be concluded that unconfined compression performance of snow is strong function of deformation rate and bonding strength (sintering time). Therefore, these factors must be taken into account for the unconfined compressive strength of snow. In the next section, a relationship between unconfined compressive strength and failure strain of snow is discussed.

VII-1.4 Relationship between Unconfined Compressive Strength and Failure Strain at a Given Brittle Compressive Velocity

Figure 7,6 shows a relationship between unconfined compressive strength, σ_c , and the strain at failure, ϵ_f , for a compressive velocity of 0.98 mm/sec, which provides for the brittle behaviour of snow at temperature of -13°C as shown in Fig. 7,5.

The stress is measured through the proving ring and deformation transducer as described in Chapter V. The total deformation (i.e., compressive velocity \times time) consists of the deformation of

both the proving ring and snow specimen. The deformation of snow specimen alone, therefore, must be corrected by subtracting the deformation of proving ring from the total deformation recorded.

Therefore, the corrected line indicated in Fig. 7,6 indicates the actual unconfined compressive strength-failure strain relationship.

In Fig. 7,6, the higher strength for a given density means the longer age in sintering process as mentioned earlier. The result shows that the failure strain ranges from near zero for poorly bonded snow to approximately 1.0 percent for snow with unconfined compressive strength of 1.4 kg/cm^2 .

There are two important features in Fig. 7,6. Firstly, the relationship between unconfined compressive strength and failure strain seems to be independent of the density. Secondly, the unconfined compressive strength of snow increases with the increasing failure strain. Figure 7,7 shows the compressive modulus, $\frac{\sigma_c}{\epsilon_f}$, as a function of unconfined compressive strength. The result shows that the compressive modulus of poorly bonded snow is approximately 80 kg/cm^2 and it increases with the increasing unconfined compressive strength. Note that the unconfined compressive strength of snow is a strong function of bonding.

It may be concluded that unconfined compressive strength of snow is greatly dependent upon the bonding of snow but not upon the density. The effect of bonding is much more obvious than that of density in the unconfined compression performance. Nevertheless, many researchers have obtained the fact that unconfined compressive strength

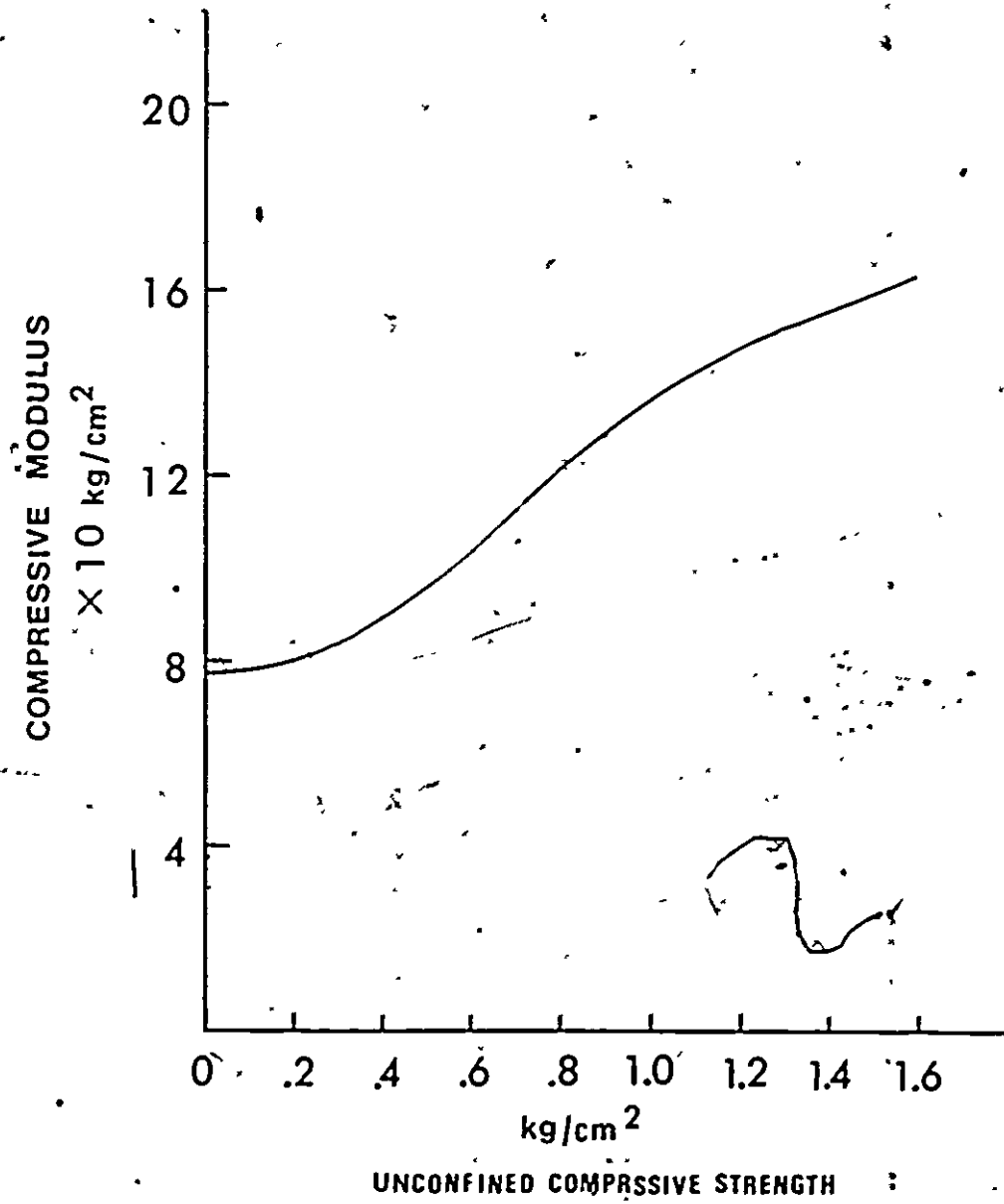


Fig. 7,7 Relationship between Compressive Modulus and Unconfined Compressive Strength for Snow :

of in-situ snow is a quite function of density. It may be considered that there is some correlation between bonding and density for the in-situ snow.

The axial strain at the failure in unconfined compressive test is very small in comparison to other assembled materials. For example, the axial strain at failure in ordinary sand often exceeds 3 percent (Taylor, 1948) in the triaxial test. The experimental result shown in Fig. 7.6 shows that, for almost granular condition, the failure strain may be neglected. This means that the failure of very poorly bonded snow occurs immediately when the load is applied as mentioned earlier.

The failure strain of snow increases with increasing bonding strength as mentioned earlier. The failure of bonded snow occurs abruptly when the stress reaches to the ultimate strength as mentioned earlier. This mechanism may be described entirely in terms of brittle behaviour of snow.

VII-2 Confined Compression Performance

VII-2.1 Confined Compression under a Single Fixed Load

The use of single loading confined compression tests on individual duplicate snow specimens provides a basis for studying the effects of rapid compression of snow. For the snow used in this test series, bonding between snow grains was established through age-hardening of the test specimens for 1, 3, and 24 hours. The cylindrical test specimens of snow were 5 cm in diameter and 4.6 cm in height as mentioned previously. The tests were performed in the drained condition which was accomplished by providing a large number of holes on the upper loading cap as illustrated in Fig. 7,8 (to allow for escape of air). This technique is not uncommon in testing of snow. To ensure uniformity in the snow samples for testing, eight specimens were prepared at the same time. These were then subjected to confined compression tests, each with its own individual single load ranging from 0.1 to 1.08 kg/cm². For a known initial specimen density, a change in density was computed from the axial deformation measured immediately after load application. With this procedure, no creep deformation was included in the computation. This was confirmed by a continuous monitoring of the load-deformation phenomenon for the individual samples. Extrapolation of the standard creep curves obtained confirms the viability of instantaneous deformation measurements as rapid compression deformation (Fig. 7,9).

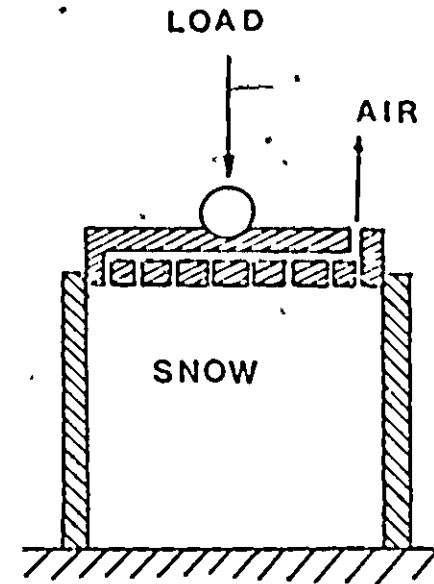
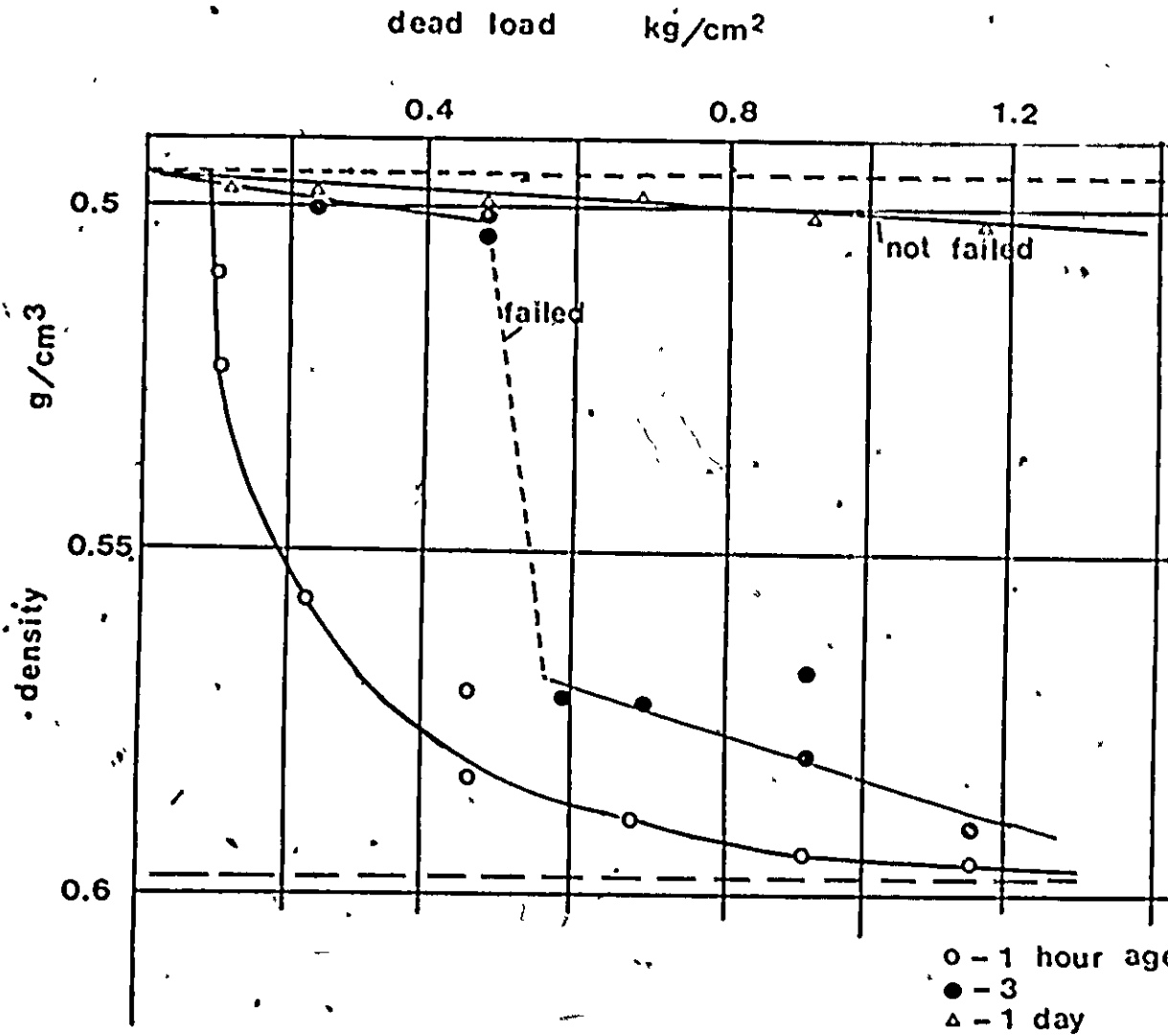


Fig. 7,8 Density Change of Variously Age Hardened Snows; for 1 hour, 3 hours and 24 hours; for Confined Compression under Single Loading

The relationship between load and resultant density obtained after rapid dead load compression for the various snows tested is shown in Fig. 7.8. It is noted that each data point shown represents an individual test. The apparent yield strength in the rapid dead load confined compression test for metamorphic snow that had been age-hardened for one hour is seen to be 0.1 kg/cm^2 . This is represented by the initial break point in the curve. The apparent yield strength is seen to increase to about 0.45 kg/cm^2 for a three hour age-hardened snow, as shown by the abrupt break in the curves given in Fig. 7.8.

Whilst the apparent yield strength increases with time after deposition, it should be noted that age itself is not totally responsible for the apparent yield strength. This is because age-hardening of snow is dependent on characteristics of initial snow grains (size, shape and texture), initial density (number of contacts between grains per unit mass considered), and bond intensity development as a function of time and temperature.

As can be seen in Fig. 7.8, application of any load larger than apparent yield strength will produce a considerable increase in density. Experimental observations show that this increase in density occurs almost instantaneously when load is applied. As shown in this figure for applied loads greater than the apparent yield strength, the resultant density tends to an asymptotic value which can be defined as the "critical density" of snow. This critical density is seen to be a function of age-hardening of snow and initial snow characteristics. Bearing in mind that each data point represents a single sample

test, it is observed that reproducibility of test constraints and specimen control was obtained - as testified by the continuity of the resultant test curve. The significance of the critical density obtained by this procedure is that it not only distinguishes loose snow from dense snow, but it also denotes the amount of irrecoverable compressibility of the snow in relation to the initial density. It is noted that the phenomenon of irrecoverable compression under dead load is in essence a kind of local failure which occurs as a result of collapse of pores in the snow.

When the snow was age-hardened for 24 hours it did not fail under the level of dead load up to 1.2 kg/cm^2 because of the high bonding effect. This is obvious from the results obtained in the unconfined compression tests mentioned previously.

The critical density of the various snow types using the same procedure for evaluation as described earlier, in Fig. 7,8 is presented in Table 7.1. All the test samples shown in this Table were established as initially poorly bonded snow.

TABLE 7.1 Critical Density, γ_{cr} , of Uniformly and Well-Graded Snows
(G denotes the size of grains)

Grain size or snow type	Critical density, γ_{cr} (g/cm ³)
2 year old grains (disaggregated)	0.57
artificial snow A (well-graded)	0.60
G = 2.38 mm (disaggregated) (3 week-old)	0.47
G = 1.19 mm (disaggregated) (3 week-old)	0.50
1.19 mm < G < 2.38 mm (disaggregated) (3 week old)	0.45

As can be seen in Table 7.1, the uniformity of grain size plays an important role in the development of the critical density (γ_{cr}), a high critical density for the well-graded snow and a low critical density for the uniformly graded snow. It is noted that this trend is common in the packing of other kinds of granular materials. For comparison, a density corresponding to maximum packing was reported by [1964] for Peter Snow to be 0.55 g/cm³. Note that values of greater than 0.6 g/cm³ have been obtained and that values of from 0.52 to 0.57 g/cm³ had been obtained by Tusima (1973) from repeated loading test for seasonal deposited snow. The density of snow below critical

density values can be widely found in natural snow covers. For example, the density of snow found on the surface to 7 m depth of the Greenland Ice Cap is less than 0.5 g/cm^3 . At approximately 20 m depth, the density value is about 0.6 g/cm^3 (Takaya and Kurohira, 1967). In relatively warm regions, it is noted that low density zones are separated by a few ice layers which form as a result of cycles of melting and refreezing.

From a mechanistic point of view, it can be noted that the high density changes occurring under large load increments are due to the collapse of pores resulting from the breaking of intergranular bonds. This mechanism can be identified as intergranular slippage and is like the sudden collapse of a loose granular mass under rapid or sudden loading. It is expected that some local shearing of the snow grains will also occur during the compression process. This total process which is denoted as the compressive microfracture of snow can be related to bonding force, density and load intensity. Experimental observations showed that if snow density is initially higher than the critical density, very little compressive microfractures occur during compression in the confined condition. It is noted that if creep deformation is excluded, no increase in densification beyond the critical density can be achieved in rapid single load confined compression tests.

VII-2.2 Microfracture and Creep Deformation of Snow in Confined Compression

The results for two separate load intensities (0.227 and 0.341 kg/cm²) for confined compression tests on natural medium coarse grained snow (with specified constant dead loads) are shown in Fig. 7,9. As noted in the Figure, with an initial specimen density of 0.39 g/cm³, the immediate compression volume change obtained from a dead load intensity of 0.341 kg/cm² was 9.34 percent, whilst the corresponding immediate compressive volume change for the 0.227 kg/cm² dead load intensity was 6.22 percent.

In Fig. 7,9, the volume change creep portions of the curves for two loads have been plotted from a common zero point - after correcting for the immediate compression are shown. It is noted that the apparent amount of creep deformation for the lower load intensity (0.227 kg/cm²) is in actual fact higher than the test specimen with the higher load. If one accounts for the fact that:

- (a) the associated immediate compressions (microfractural deformation) produced a lower resultant density for the lower load, and a higher resultant density for the higher load, (unless load is sufficient to densify up to the critical density, as shown in Fig. 7,8) and
- (b) the total compressive strain, i.e., immediate and creep strains, is higher with higher load at any time,

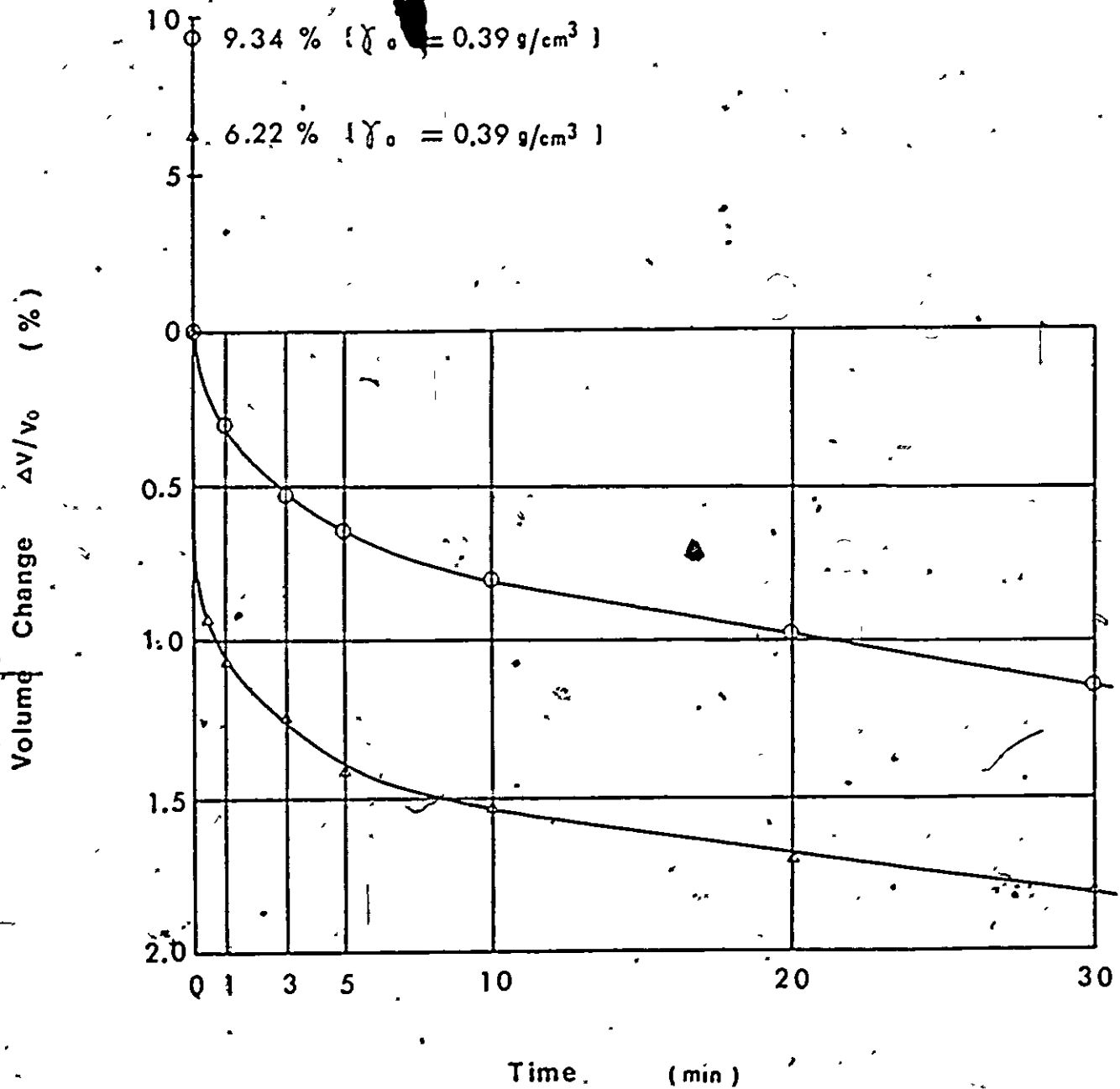


Fig. 7.9 Volume Change of Granular Snow in Confined Loading Tests
Using Constant Load

Line through circles are from a loading of 0.341 kg/cm^2

Triangular points are from a loading of 0.227 kg/cm^2

the results in the Figure indicate that beyond about five minutes, the rate of creep deformation for the two curves are similar. This phenomenon appears valid so long as the loads applied are not sufficient to cause resultant density changes attaining critical density. Thus, with the preceding informations, snow behaviour under a dead load can be described in terms of immediate compressive microfracture and creep in the confined state. For conditions where initial densities are higher or equal to the critical density, it follows that the loaded deformation process is describable in terms of creep for the single loading test.

Figure 7,10, shows a typical incremental loading and unloading curve sequence for a dead load confined compression test on a natural medium coarse-grained snow similar to that used for presentation in Fig. 7,9, with an initial density of 0.39 g/cm^3 . A total of seven separate load increments were used to arrive at a final load intensity of 0.5 kg/cm^2 . The seven load increments were applied over a period of two and a half minutes. The four points below the first volume change point under a load intensity of 0.5 kg/cm^2 indicate continued deformation (volumetric creep) obtained at one-minute intervals after final load increment to 0.5 kg/cm^2 . The unload sequence in Fig. 7,10 shows approximately 12.5 percent of total volumetric strain recovered. Considering a confined creep situation with constant cross-section area, the volumetric strain is indicated by the vertical (axial) strain. During the seven load increments, the volume change (axial strain) consisted of immediate compression and creep deformation under each load increment.

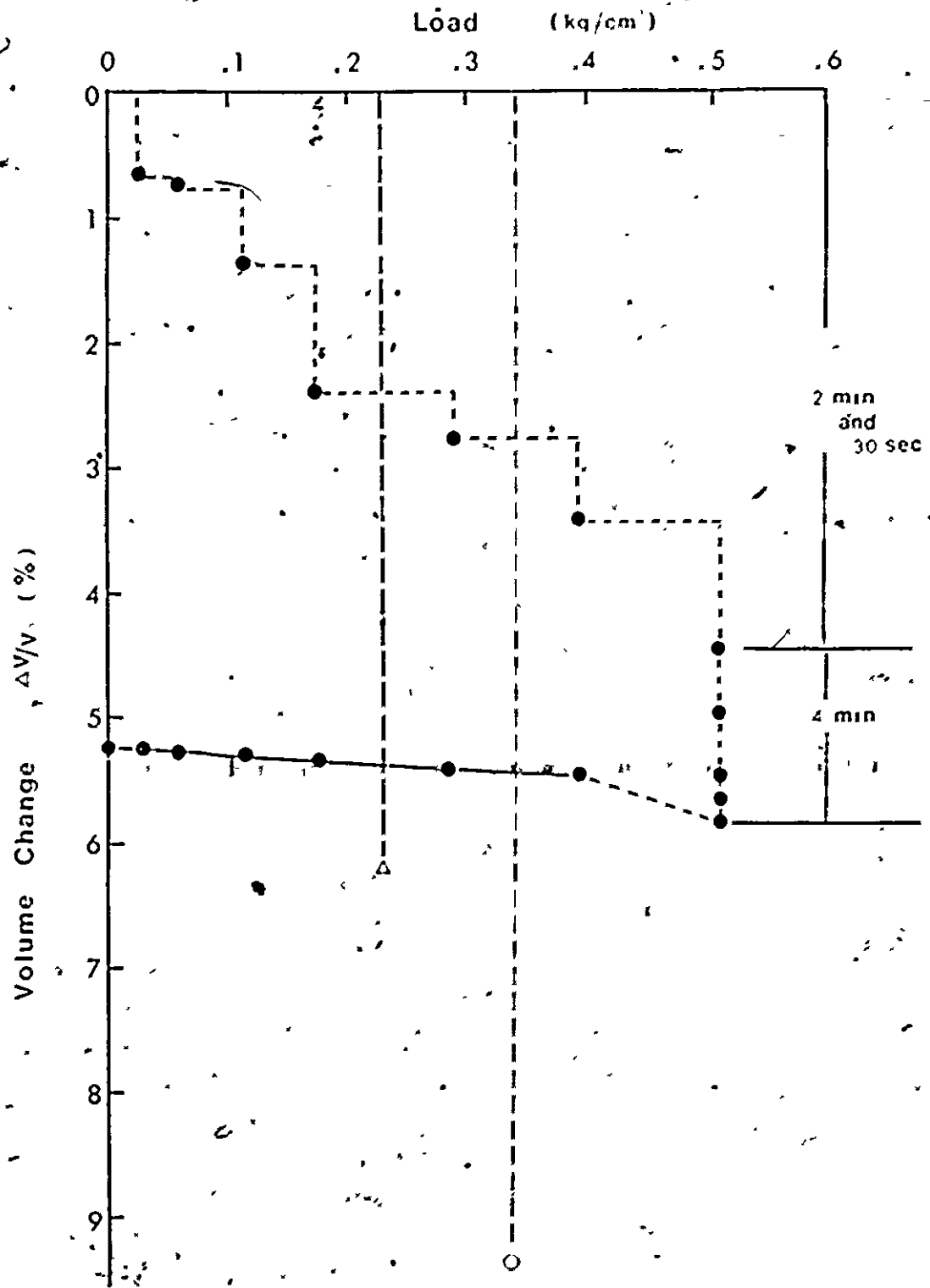


Fig. 7,10 Volume Change Relationships for Snow in Confined Compression Tests Using Incremental Loading

Open triangle and Open circle indicate single loading

If one superposes the volume change results from the single instantaneous or rapid dead load test as shown in Fig. 7.10, the results show that the volume changes from the single loading confined compression tests are considerably higher than those obtained in step-wise load increments for the corresponding loads. The volume change under a single dead load of 0.341 kg/cm^2 is 9.34 percent while that of five incremental loads to a load intensity of 0.34 kg/cm^2 is only three percent. Similar comparisons can be made for the 0.227 kg/cm^2 loading as shown in Fig. 7.10. The dependence on stress-path is indeed obvious.

The various deformation types of snow in dead load confined compression is schematically shown in Fig. 7.11. The figure shows that, in general case (bonded snow), there are basically two types of deformation mechanisms for snow, i.e., failure and no-failure performances. It has mentioned previously whether or not snow fails is dependent on mainly the strength characteristics of snow and load intensity. If initial density (ρ_0) of snow is lower than the critical density (ρ_{cr}), snow fails under the sufficient dead load. However, if initial density (ρ_0) is greater than the critical density (ρ_{cr}) snow will not fail. In the past, most of study on creep behaviour of snow has been concerned in the case of no-failure performance. However, as shown in the figure, the many cases in relation to snow type including the initial and critical densities and load intensity should be taken into account in the consideration of confined compressive behaviour of snow under dead load.

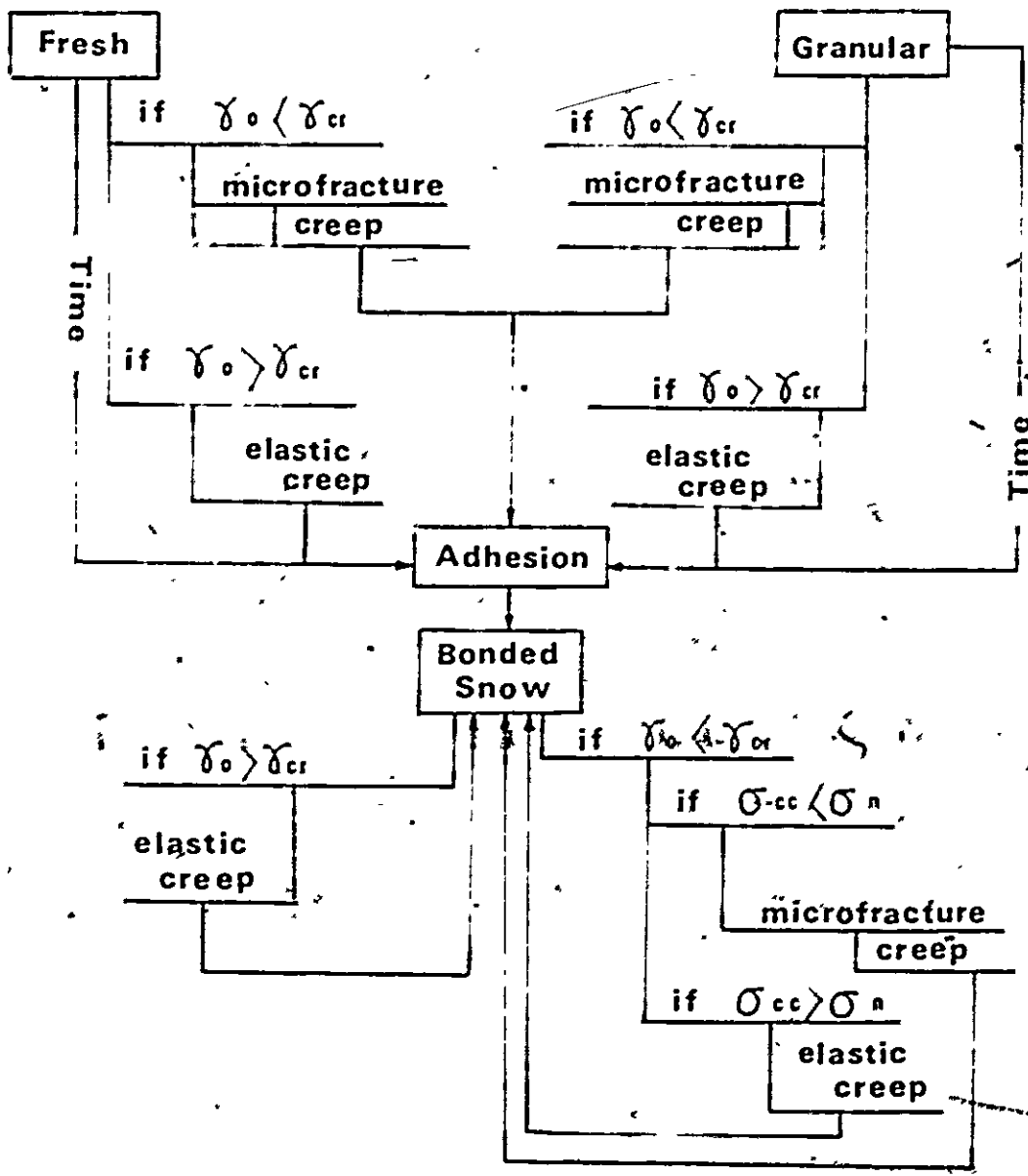


Fig 7.11 Various Deformation Types for Snow in Dead Load Confined Compression

σ_{cc} is the confined compressive strength

To provide for a more detailed examination of compression performance, in view of the volumetric strain (axial strain) influences on generation of succeeding snow properties, it is necessary to examine controlled strain characteristics in confined compression. This provides not only further insight into snow behaviour, but also begins to simulate the transient load conditions on snow as for example, in track-snow or wheel-snow interaction.

VII-2.3 Snow Behaviour under Progressive Load (confined Compression Test with Controlled Deformation Rate)

In this test series, the specimen size used was 5 cm diameter and 4, 6, 7 or 13 cm high. Tests conducted on both artificial and natural snows showed little difference in performance. Differences observed in compression response performance was more a result of differences in grain size distribution and not type of snow (natural granular or artificial granular). The stress-strain performance of a test specimen can be evaluated in terms of stress-density, by converting the deformations obtained in terms of resultant specimen density since the cross-sectional area remains constant. The typical curves obtained from the controlled deformation rate tests are shown in Fig. 7, 12. Curve A indicates the typical deformation behaviour obtained under a controlled low deformation rate compression test on initially semi-bonded loose snow, while Curve B shows a typical result obtained from high compression rates. It is noted that the application of a controlled high deformation rate produces microfracture in the

initially loose snow state. This is evident in Curve B where an abrupt stress release (as demonstrated by the sharp drop in stress) is obtained when microfracture occurs. Continued loading (straining) will see a subsequent stress build-up and another stress release when microfracture occurs again leading to the saw-toothed effect shown in Fig. 7,12. Continued compression beyond the phase of microfracturing will produce a condition of straining or densification without any apparent fracture where the stress-density (or alternatively, stress-strain) curve will show an increasing value. The backward projection of Curve B shown in Fig. 7,12 on to the density axis intersects the axis at a density boundary which may be defined as the threshold density, ρ_{th} . The threshold density may thus be defined as that density which will not develop microfractures when subjected to confined deformation rate controlled compression testing. It is to be noted that this threshold density, ρ_{th} is not similar or equal to the critical density, ρ_{cr} . The critical density, ρ_{cr} for a given snow may be considered to be unique, while the threshold density, ρ_{th} cannot be uniquely determined because it is dependent on the deformation rates. In essence, one could obtain a separate value for ρ_{th} for each separate deformation rate used provided the characteristics of Curve B are obtained as shown in Fig. 7,12. Figure 7,14 shows the variable ρ_{th} as a function of deformation (strain) rates.

To evaluate the influence of compression (deformation) rate on the magnitude of ρ_{th} , one could begin by comparing Curves A and B in Figure 7,12. On the basis of the mechanism associated with the

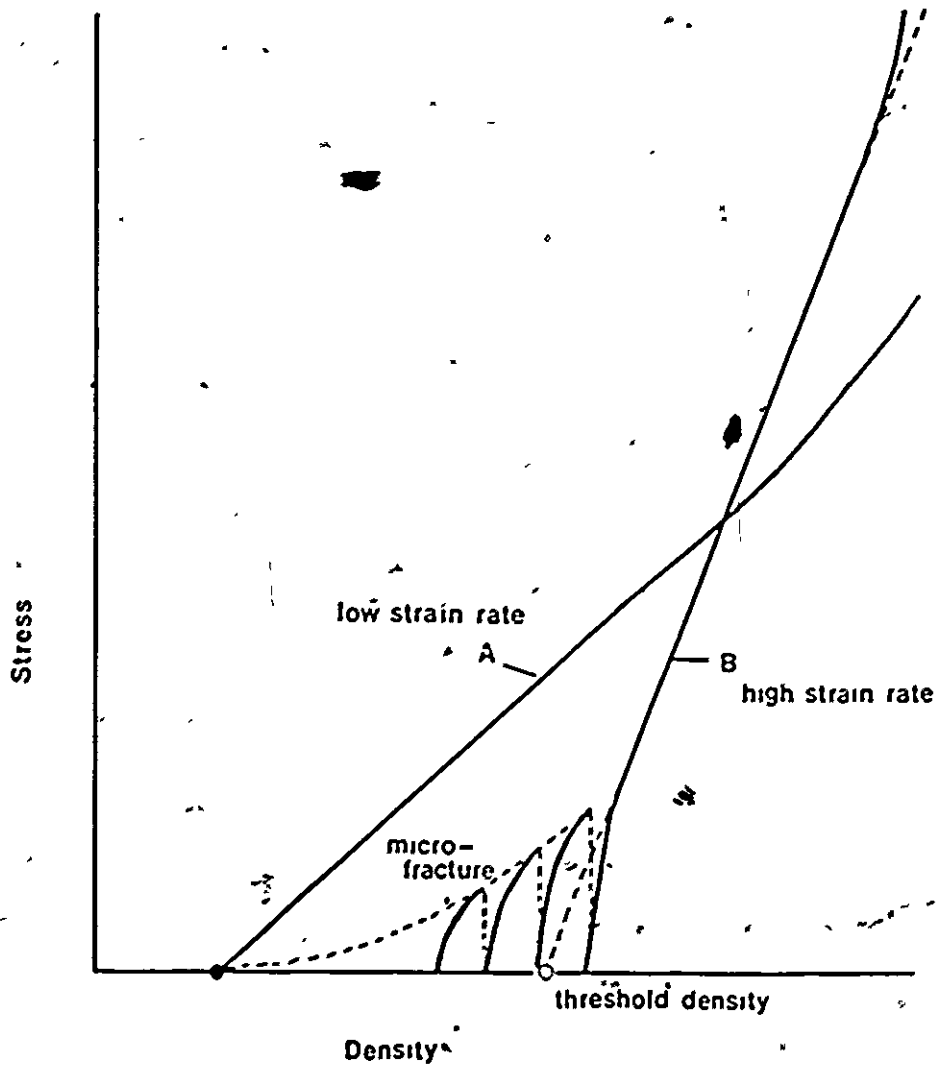


Fig. 7,12 Typical Stress-Density Relationship for Confined Compression with Controlled Deformation Rates

characterization of the threshold density ρ_{th} , i.e., saw-toothed stress development as shown by Curve B, the initial density ρ of the stress-density (stress-deformation) Curve A shown in Fig. 7.12 obtained as a result of low compression rate testing can be taken to be equal to or above the threshold density in view of the absence of saw-toothed/stress-density or stress-strain performance.

Figure 7.13 shows the stress-density relationship for snow with varying initial density, tested at a common constant strain rate of 0.075 per second at a temperature of -13 C. In addition to the deformation rate, the following factors seem to be influencing the ρ_{th} :

- (a) grain size distribution,
- (b) temperature,
- (c) initial density, and
- (d) method of test assessment.

The range of deformation rates producing from, for example, Curve A in Figure 7.12 for compression under a low deformation rate to Curve B which is a result of compression under a high deformation rate can be examined vis-a-vis development or characterization of the threshold density. Figure 7.14 shows the influence of strain rate on establishment of the threshold density for granular snow, where G denotes snow grain size from a sieve analysis. The results indicate that with a well-graded snow as shown by the triangular and solid points, the threshold densities developed as a function of strain rate

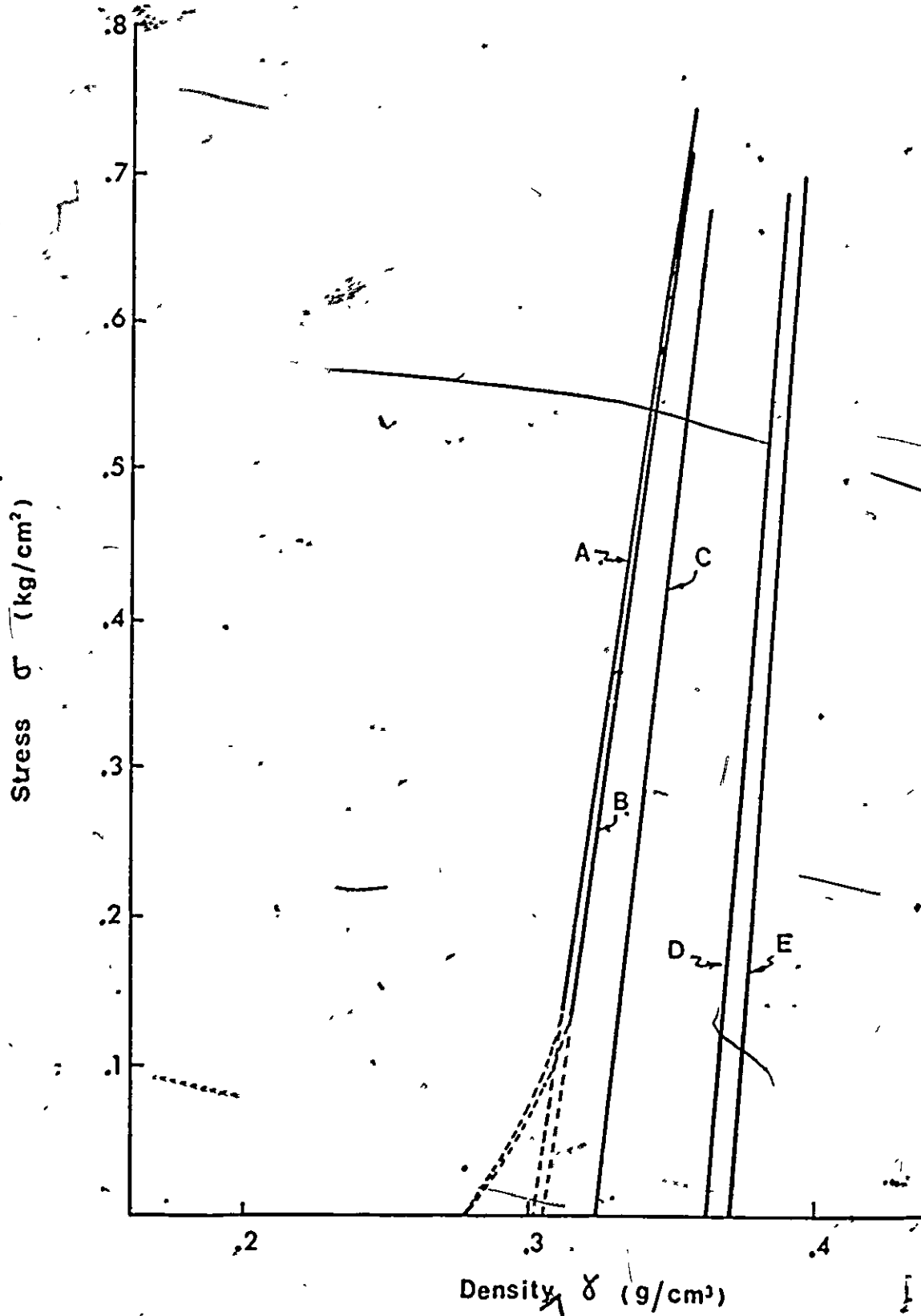


Fig. 7.13 Stress-Density Change Curves as a Function of Various Initial Densities

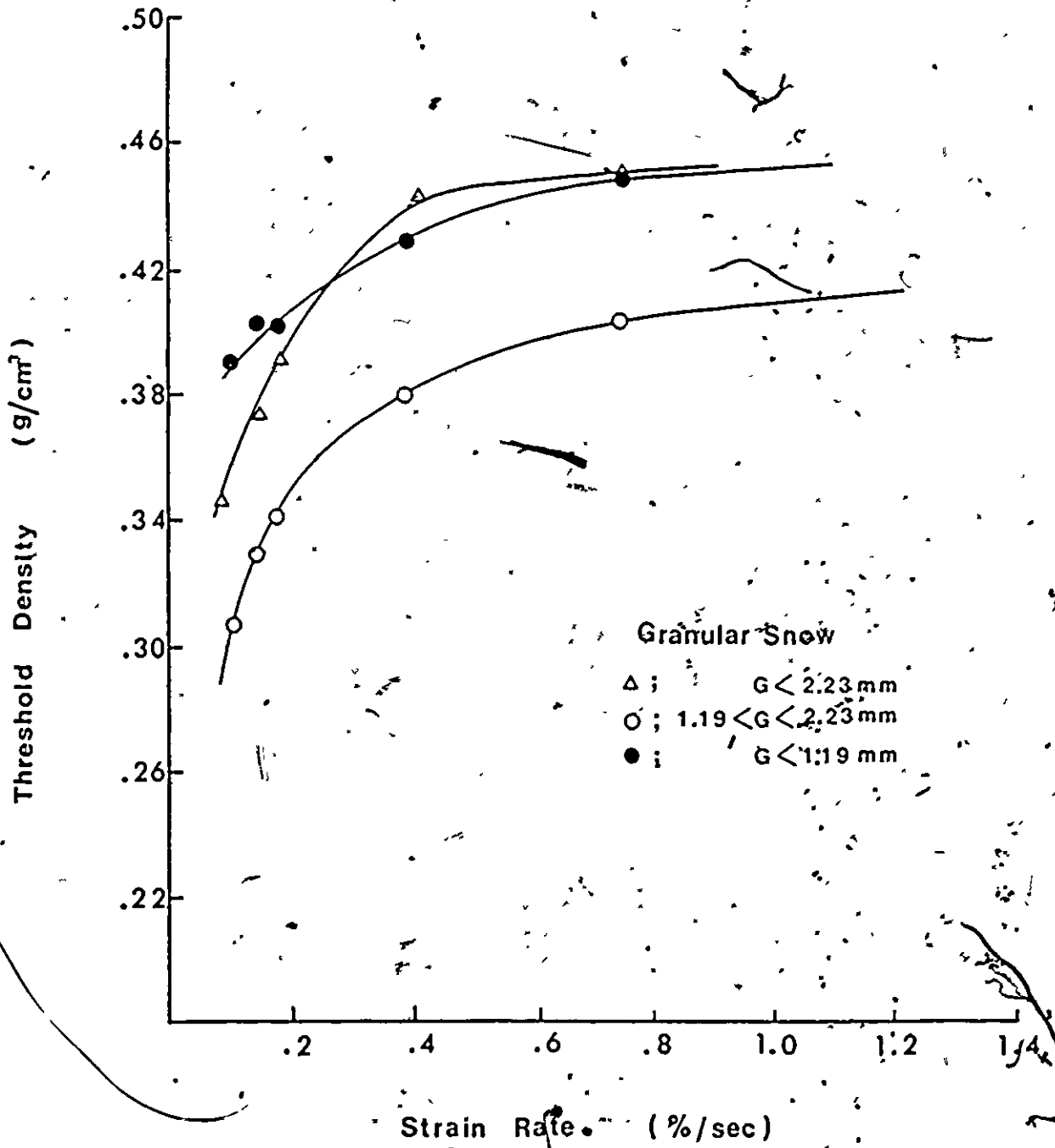
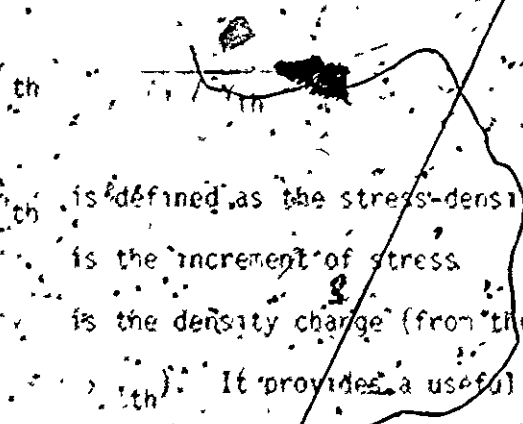


Fig. 7,14 Relationship between Strain Rate and Threshold Density for Granular Snow

are essentially larger than that obtained from the more uniformly graded snow, as shown by the open circle points.

The ratio of the increase in stress, $\Delta \sigma$, to the density ratio, $\Delta \rho / \rho_{th}$, i.e., "stress-density modulus", apparently characterizes the type of curves as shown in Fig. 7.12. The relationship is as following:



Where

ρ_{th} is defined as the stress-density modulus
 $\Delta \sigma$ is the increment of stress
 $\Delta \rho$ is the density change (from threshold density, ρ_{th})

It provides a useful basis for examining the characteristics of the threshold density. Figure 7.15 shows the relationship between ρ_{th} and ρ_{cc} for both fresh snow and granular snow. The influence of the granular nature of the aged snow can be seen in terms of the non-linearity in ρ_{th} and ρ_{cc} .

It is noted that as the controlled deformation rate of testing is increased, a point is reached where the deformation rate approaches that of the rapid "dead" incremental load (rate). Thus with greater and greater deformation rates, the threshold density is seen to asymptote to a constant value as shown in Fig. 7.14. From the experimental results, it is apparent that the asymptotic value may not be dissimilar to the critical density, ρ_{cc} , values obtained from the single loading confined compression tests as presented in Table 7.1.

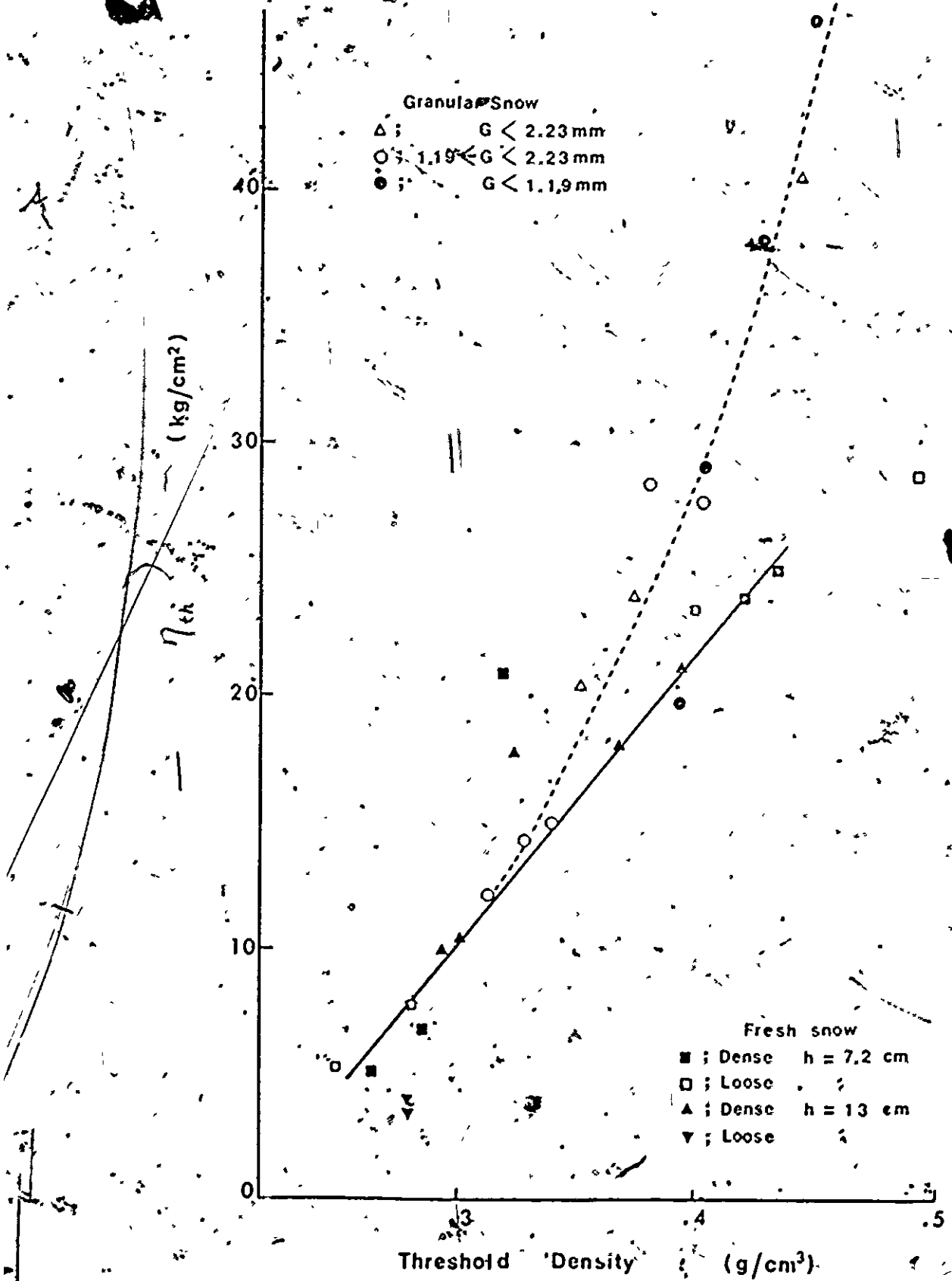


Fig. 7,15 Relationship between "Stress-Density Modulus" and Threshold Density

In Fig. 7,16; the critical and threshold densities of artificially well graded snow and uniformly graded snow are shown. The critical densities were obtained from the "single load confined compression" while the threshold densities were obtained from the "progressive load confined compression". The figure indicates that:

- (a) threshold density of snow is a strong function of deformation rate,
- (b) threshold densities do not exceed the critical density for a given type of snow, and
- (c) size of snow specimen does not strongly affect the threshold and critical densities.

The inter-relationships described between stress, strain rate, initial and threshold densities may be seen in the three-dimensional representation as shown in Fig. 7,17. It is apparent in this figure that, as strain rate increases the threshold density reaches an asymptotic limiting value. This is demonstrated by the near vertical plane rising from the threshold density line (at the base). It should be noted here that the stress-density relationship becomes steeper not only because threshold density increases but also because deformation rate increases.

As has been indicated by the results, the deformation of snow under confined compression due to microfracturing is different from that obtained in creep performance. In rapid constant "dead" loading confined compression tests, microfracturing was seen to occur

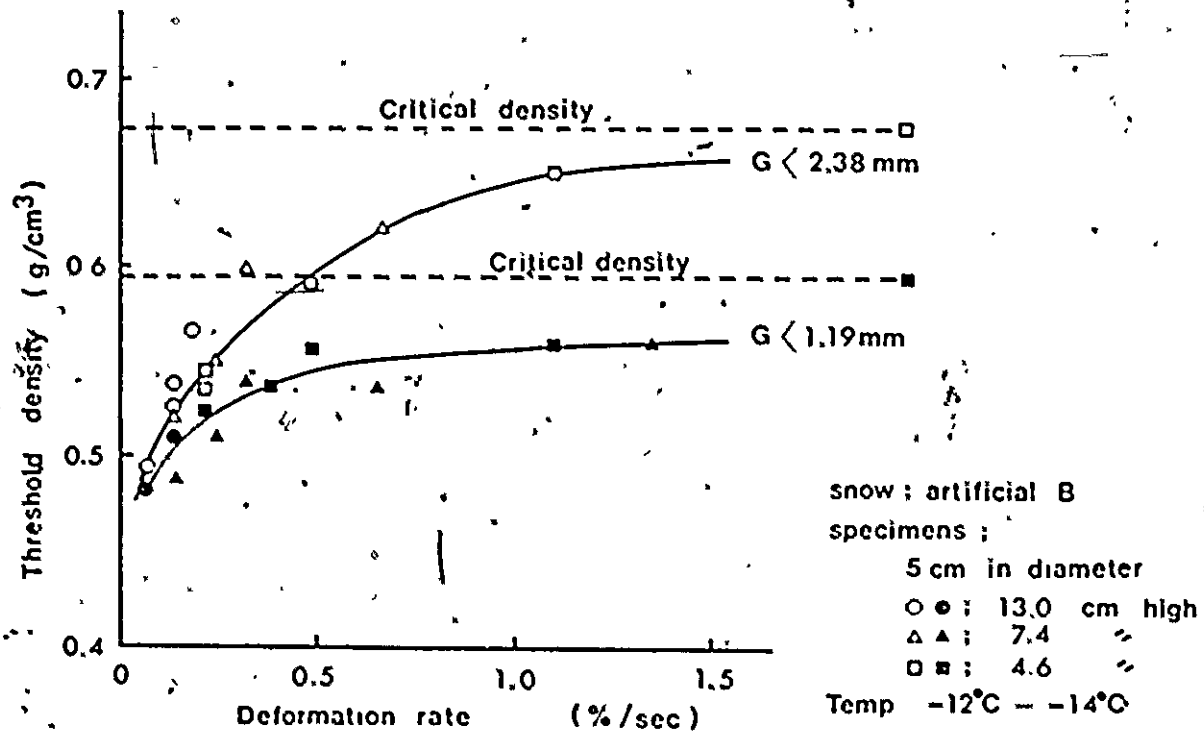


Fig. 7.16: Threshold and Critical Densities of Artificial Snow

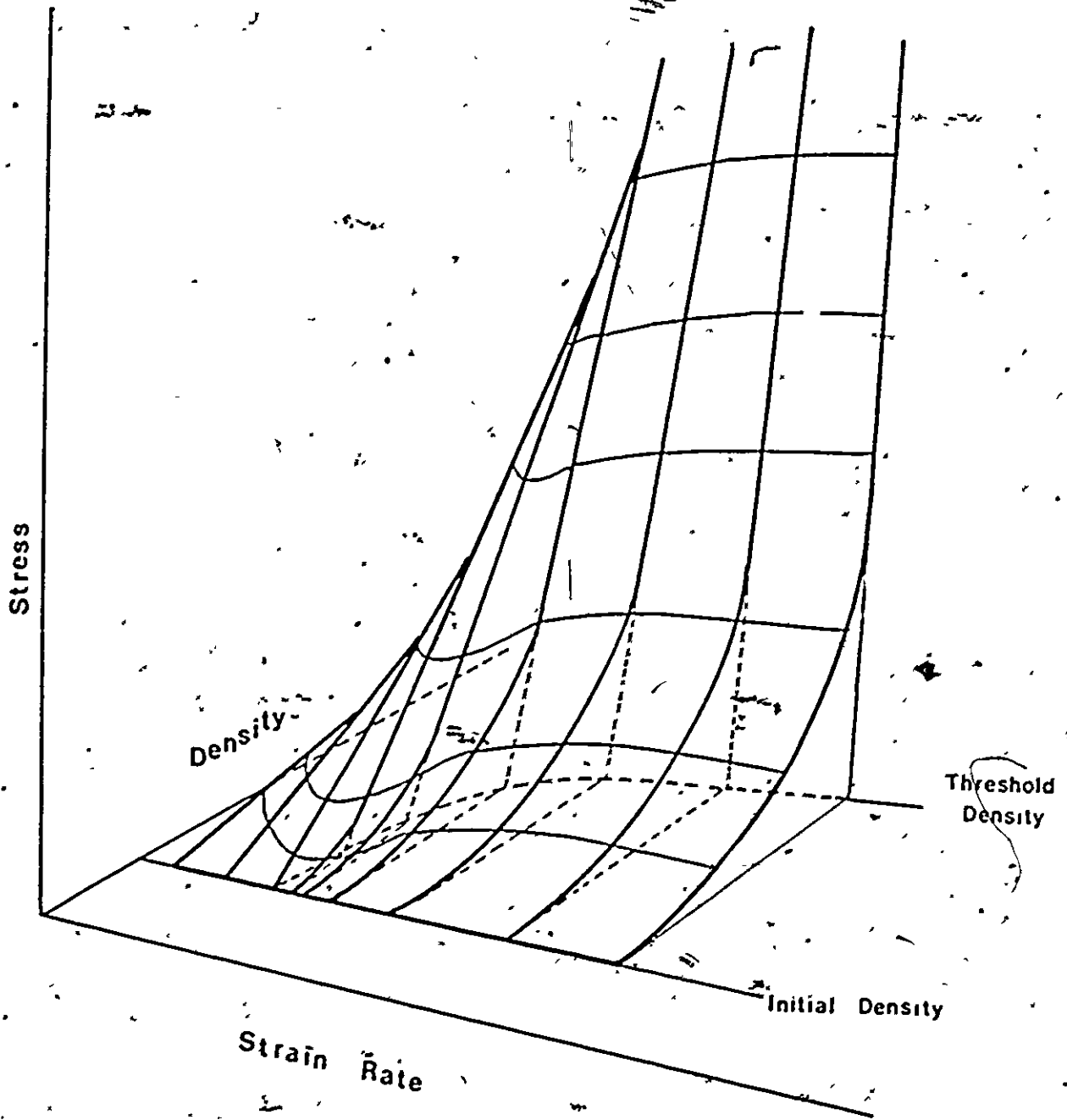


Fig. 7,17 Stress, Density and Strain Rate Surface for Snow

instantaneously, whilst microfracturing in controlled deformation rate compression tests occurred discontinuously. Intuitively, one would expect that the nature of deformation of snow is strongly time dependent.

As has been observed, snow behaviour in the controlled deformation rate compression test for initial densities higher than threshold density (load-density or load-deformation performance) is similar to creep deformation. Under a 10^{-2} rate compression (0.075 per sec), the increase of initially granular snow specimens, with axial strain, was observed as shown in Chapter VI. The results also indicated that in continuous deformation (ductile) of snow with initial densities higher than threshold density, an increase in number of contacts and contact area between snow grains are obtained, especially for initially poorly bonded snow.

In Chapter VI, the results also indicated that a microphotograph of a test specimen under an axial strain of 22 percent, as compressed from an initial density below threshold density to a density above the threshold value at a compression rate of 0.75 /sec (0.98 m/sec). Some fragmentation of snow grains can be seen in the picture (Fig. 6,10), produced as a result of microfracturing under rapid compression.

On the basis of the two kinds of compression tests, results obtained, and photomicrographs viewed for test samples subjected to both kinds of compression procedures, a mechanistic model of confined compression of snow can be proposed. The postulated simple model

shown in Fig. 7.18 is somewhat like that proposed by Terzaghi (1927) for consolidation of clay. As can be seen in the figure, the schematic analogous structural model of snow consists of parallel rigid plates and supporting bars between parallel rigid plates. The properties of the supporting bars cannot be uniquely or simply identified because the snow behaviour is complicated by the loading rate effect. However, in the extreme cases, the supporting bar properties may not be too dissimilar to that of ice. Since air permeability of relatively loose snow is very high, pore pressures developed during compression in drained conditions will be negligible.

In Fig. 7.18, the process of very rapid compression, identified as A, produces an immediate deformation (microfracture). This situation is typified by compression under sudden loading obtained from the single load compression test where microfracture occurs instantaneously.

The compression process B (Fig. 7.18) indicates discontinuous microfracturing in controlled deformation rate compression testing. Typically, the density of the snow sample may be considered to be initially below the threshold value. From the experimental results, process B is more likely in high controlled deformation rate compression tests.

Sweeping clockwise from process B to D, the compression rate is decreased to the point where process D is the compression process typified as creep. Process C indicates no microfracture occurring in compression performance because of the very slow rate of

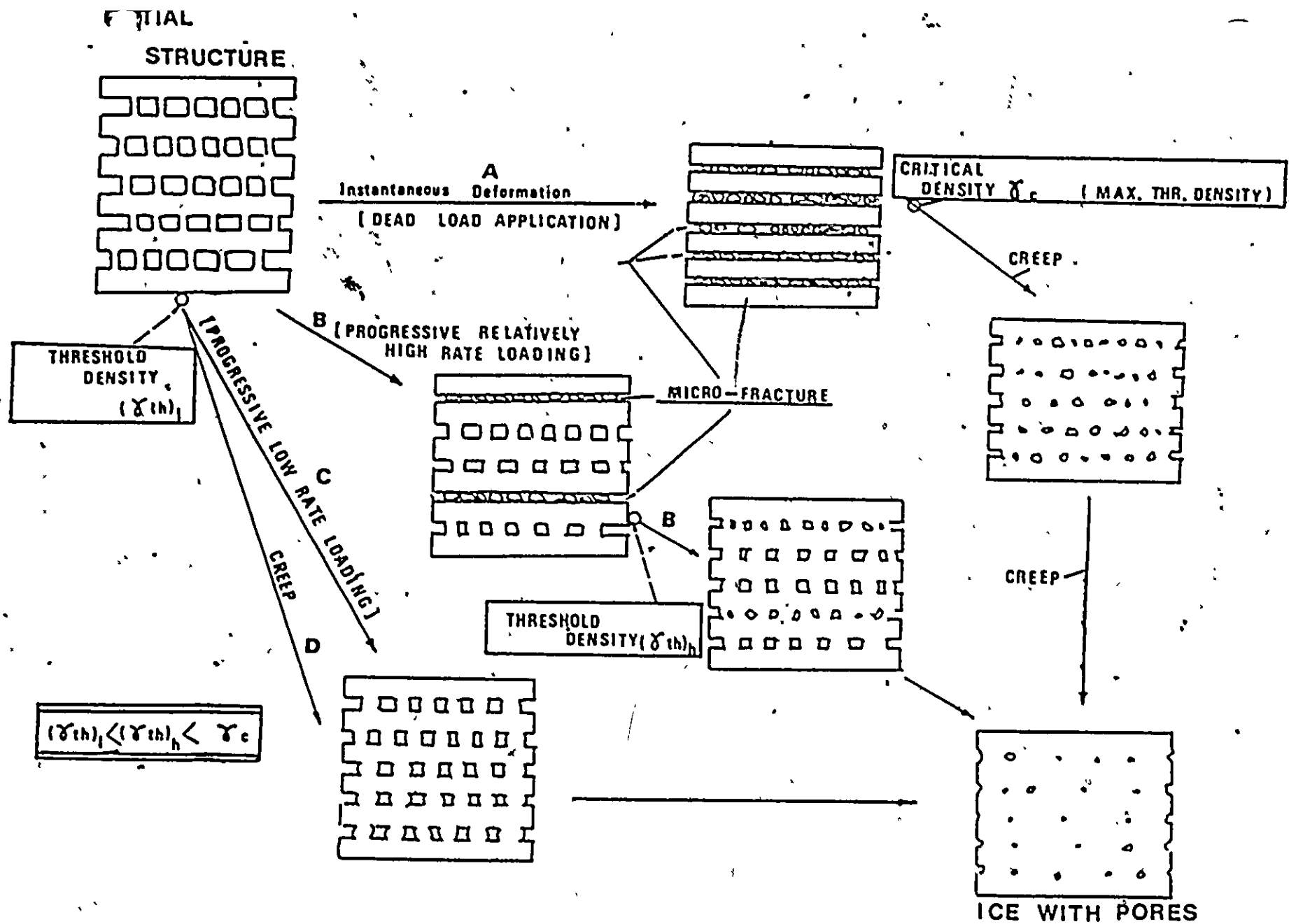


Fig. 7,18 Simple Structural Model of Loose Snow for Confined Compression Performances Showing Various Deformation Mechanisms in Relation to Density Changes as a Function of Loading Rate

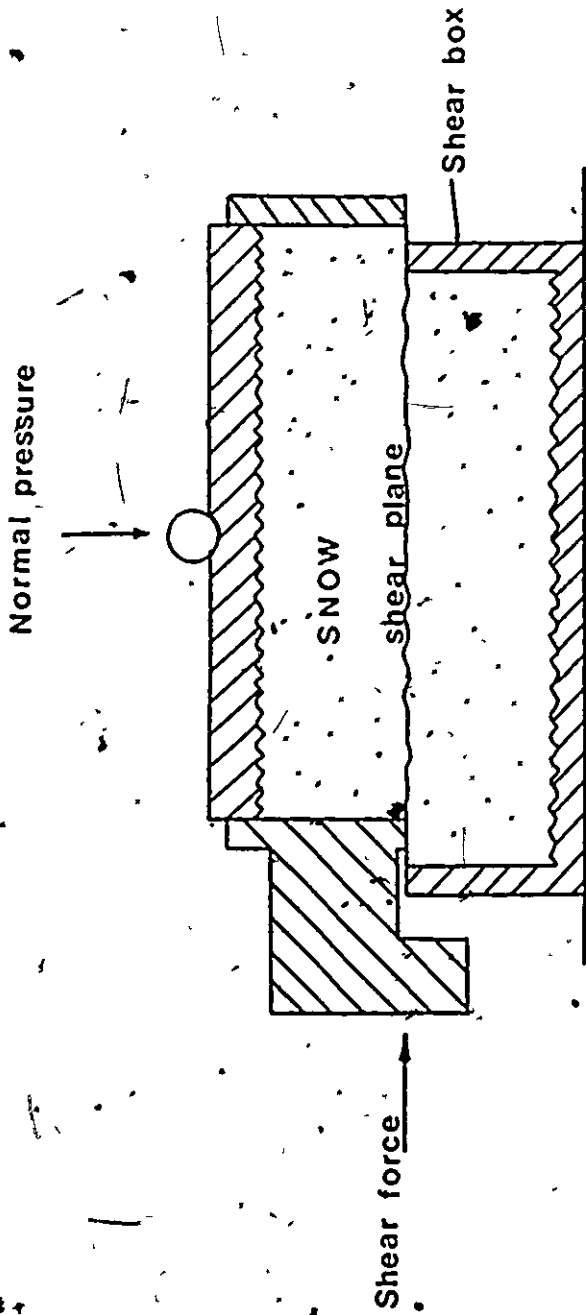


Fig. 7.20 General Shear Failure of Snow in Direct Shear Test.

due to ageing are vital to characterization of response performance. Since snow structure depends on temperature, ageing process, in-place load conditions, time, etc., it is evident that for a proper analysis of the constitutive performance of snow, a comprehensive programme of study should be undertaken.

In light of the above, this study was undertaken to examine the characteristics of the deformation mechanisms, from the confined compression testing point of view. The test results and observations made in regard to physical performance of the test specimens in the confining lucite cylinder illustrate the need for the establishment of the threshold density and critical density in relation to loading rate effect. The experimental results showed that the deformation mechanism of loose snow is strongly dependent upon loading rate, snow type and initial density at a temperature of -13°C . The compressive deformation mechanism under load can be divided into two typical types:

- (a) significant collapse of internal structure of snow (at high loading rate), and.
- (b) hardening of structure due to the increase in grain boundaries (at low loading rate, including creep loading).

The distinction between the physical aspects of deformation mechanisms (a) and (b) can be made by the threshold density. The threshold density in actuality defines the region which provides the separation point where bonding in the snow becomes significant. The disappearance of micro-fractures for snow densities above the threshold

density attests to this fact. At and beyond this point, significant increases in stress can be sustained by progressively changing the structure of snow. Experimental observations and test results indicate that micro-fracture, which occurs only in the loose state of snow, cannot be demonstrated by the conventional shear theory.

The physical aspects of deformation mechanism (b) noted above in fact are described in terms of the adhesion theory developed in Chapters III and IV. The fact that the increase in contact area between grains produced by the ductile deformation will cause an increase in adhesion force were partially shown previously and are further shown in Chapter VIII. The general discussion on the adhesion theory is presented in Chapter VIII.

VII-3 Direct Shear Performance of Snow

VII-3.1 Shear Stress-Deformation Relationships

Figure 7,19 shows shear stress-deformation curves for initially granular snow (basic snow was artificial), obtained under normal pressures of (a) 0.08 kg/cm^2 (upper), (b) 0.16 kg/cm^2 (middle) and (c) 0.47 kg/cm^2 (bottom). All curves shown in the figure show a chattering type.

Shear strength of snow, in the direct shear test, is defined as the maximum stress of envelope for the chattering curves as shown in Fig. 7,19. It is obvious that the shear strength increases with the increasing normal pressure. This trend is very common to other materials. This is discussed later in Section 3.3.

VII-3.2. Apparent Failure Modes in Direct Shear Performance

For granular snow, the failure mode in the direct shear performance is the "cutting shear" as shown in Fig. 7,20 as well as other granular materials. However, if snow is well sintered (bonded), the failure mode, without normal pressure or with relatively lower normal pressure, differs from the ordinary shear failure mode, as shown in Fig. 7,21. This failure mode may be identified as "tension failure" of well sintered snow in direct shear tests. Butkovich (1956) described that, for double shear ring test, tension break of snow specimens was obtained. In fact, tension failure of rocks in direct shear and unconfined compression performances is not uncommon.

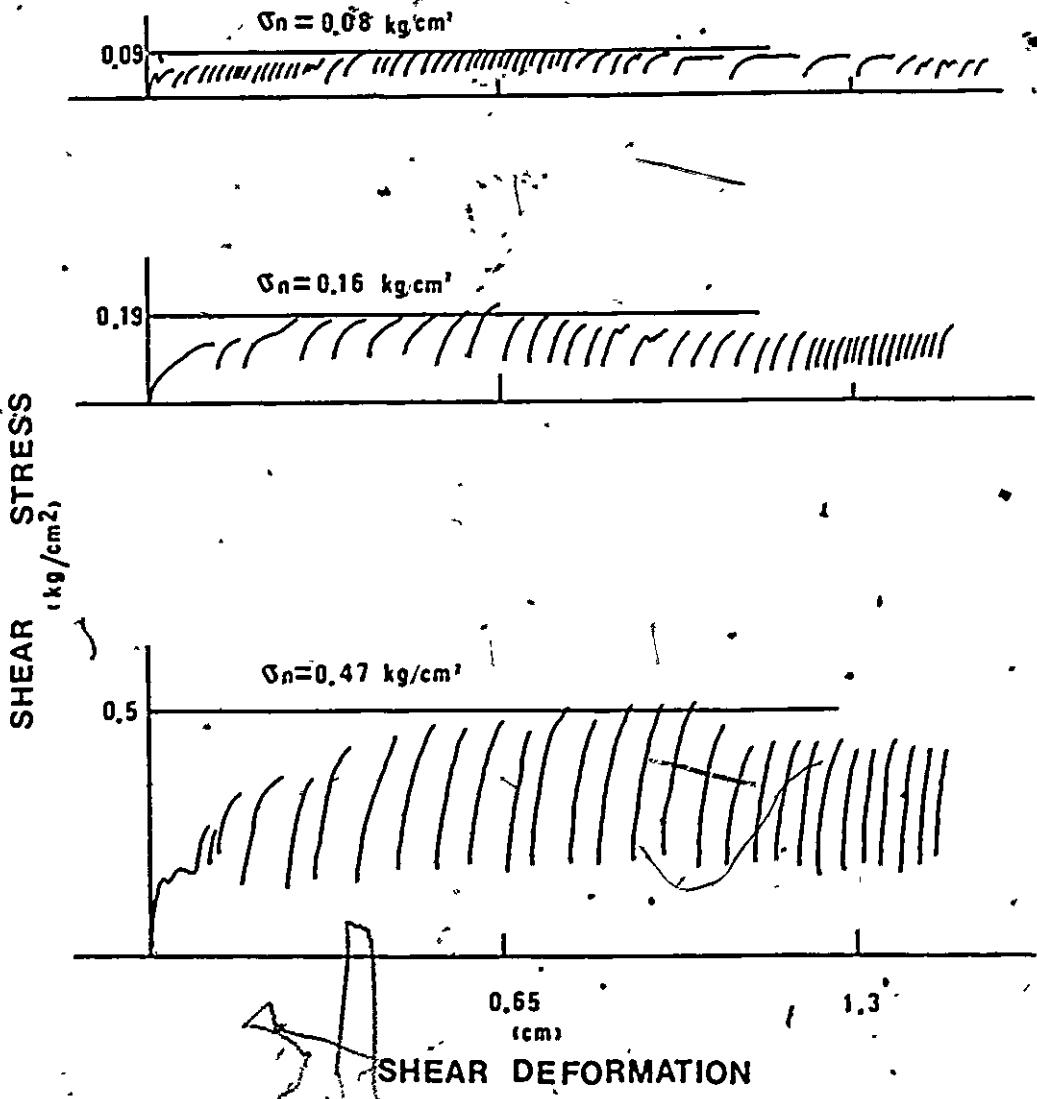


Fig. 7.19 Relationships between Shear Stress and Shear Deformation for Snow in Direct Shear Test

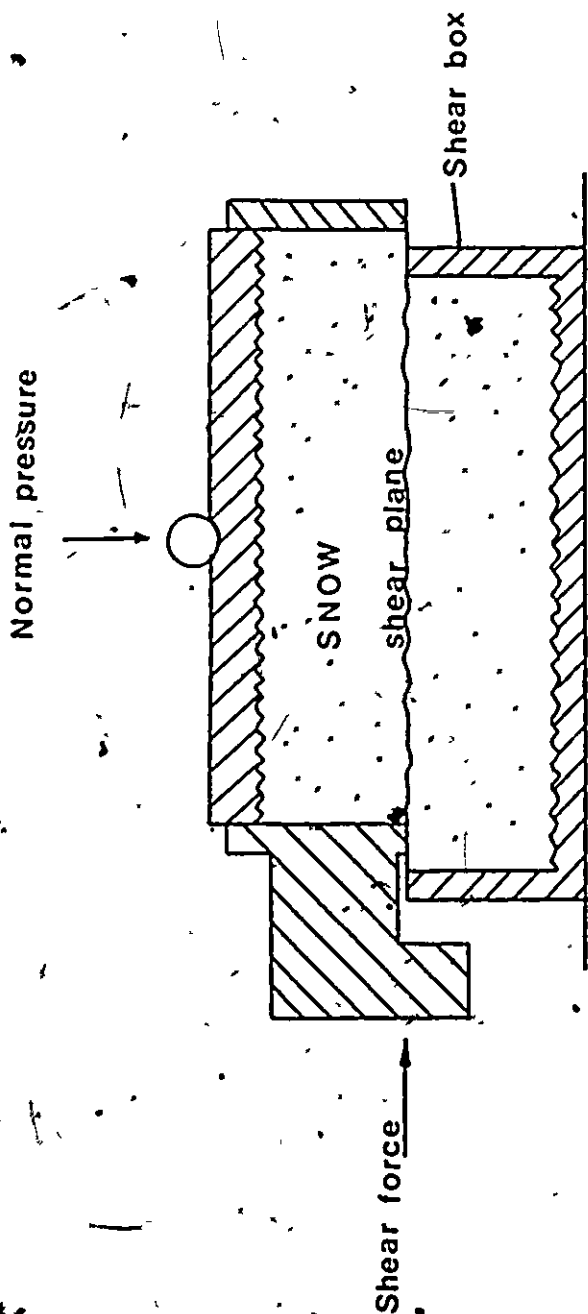


Fig. 7,20 General Shear Failure of Snow in Direct Shear Test

Under sufficient confining pressure, the failure mode of sintered snow shows the ordinary shear identified as the case shown in Fig. 7,20. This effect of confining pressure is also very common for mechanical performances of rock.

Figure 7,22 shows an irregular type of failure mode when the thickness of snow specimen, from the expected shear plane for the ordinary shear to the upper snow surface, is insufficient. Apparently, the occurrence of this irregular failure leads the very low shear resistance in comparison with the ordinary shear failure performance. The effect of thickness of snow specimen in the direct shear performances is shown in Fig. 7,23. The experimental result shows that the shear resistance in thickness of 1.5 cm is very small in comparison with the thicker snow specimens. For the thickness more than 2.0 cm, shear force seems to be almost constant as shown in the figure. Thus the size of snow specimen in the direct shear test performance is of great importance. In this research, therefore, the thickness of snow specimens was taken as 2.5 to 3 cm in the upper layer above the shearing plane.

VII-3.3 Effects of Shear Velocity

Figure 7,24 shows the relationship between shear strength and normal pressure for artificial granular snow at two ranges of shear velocities, e.g. 0.065 and 0.31 cm/sec. The open circles indicate the shear strength obtained from the standard procedure mentioned previously for granular condition at shear velocity of 0.065 cm/sec, while the

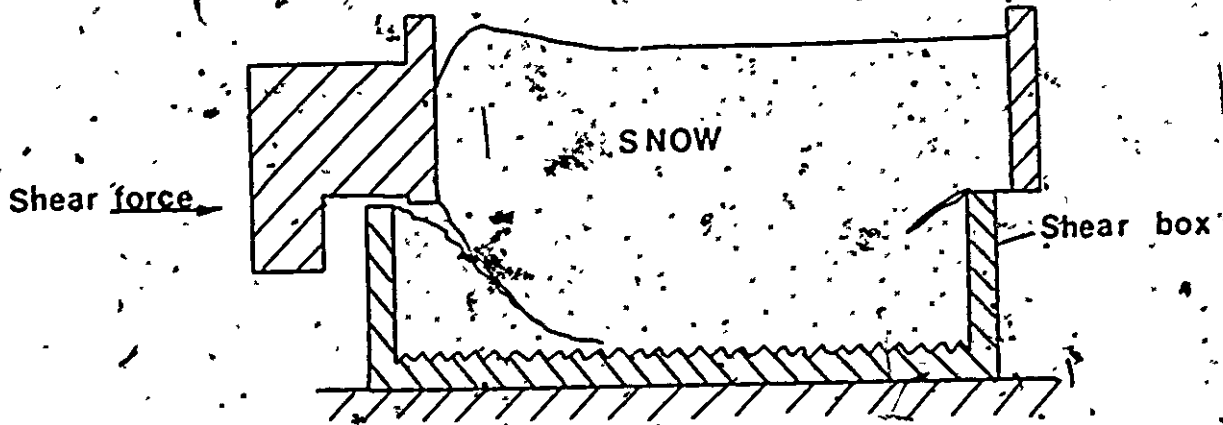


Fig. 7,21 Typical Tensile Failure Mode for Snow Without Normal Pressure or with Relatively Lower Normal Pressure in Direct Shear Test

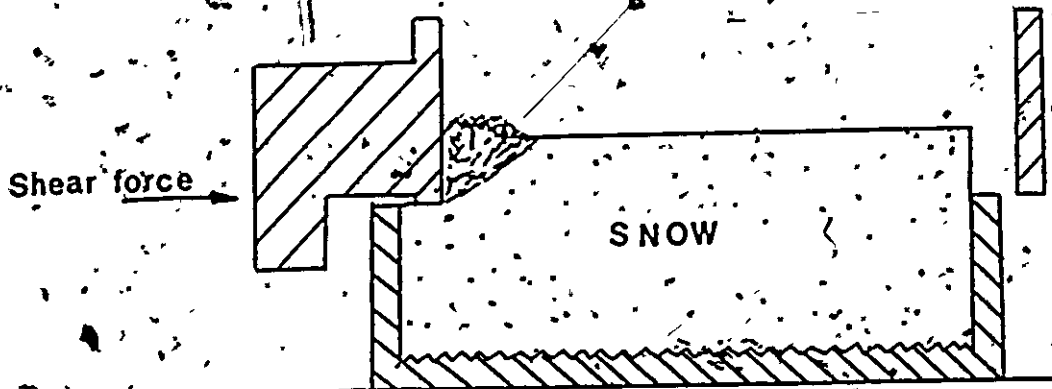


Fig. 7,22 Irregular Failure Mode of Snow in Direct Shear Test when the Thickness of Specimen is Insufficient

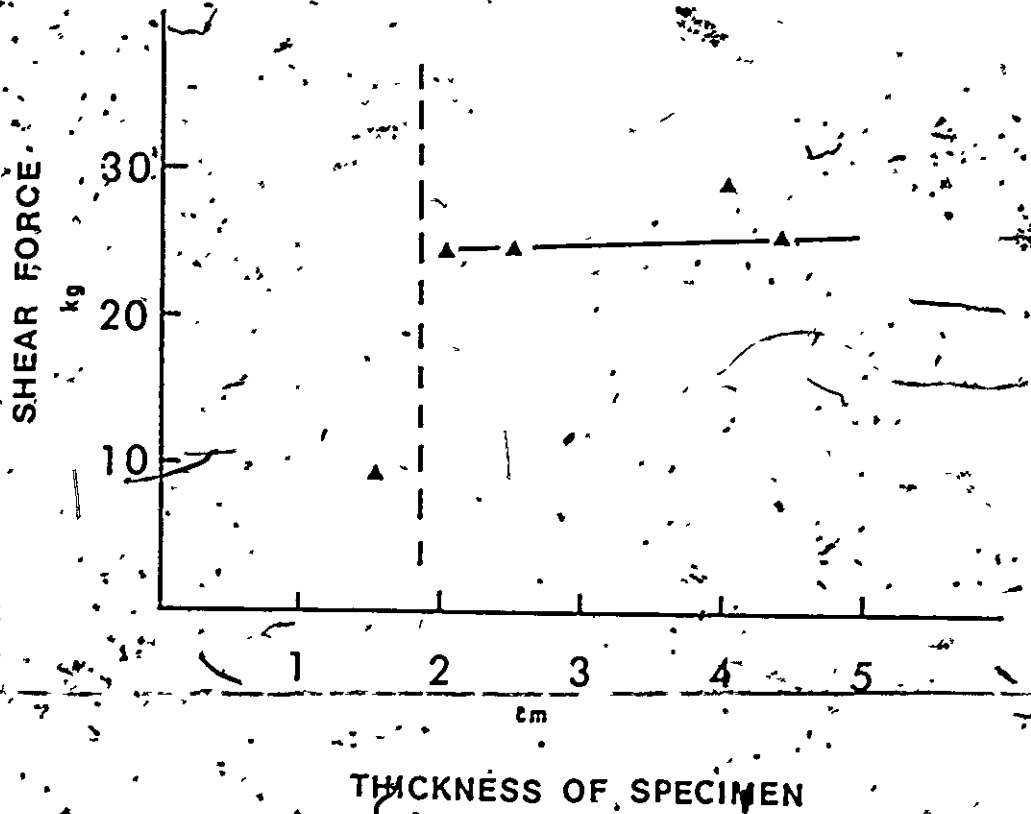


Fig. 7.23 Shear Force as a Function of Thickness of Snow Specimen in Direct Shear Test

black circles indicate shear strength for the same snow condition but at a different shear velocity of 0.31 cm/sec.

The results show that the relationship between shear strength, τ , and normal pressure, σ_n , is almost linear at both shear velocities of 0.065 and 0.31 cm/sec. This trend is actually common for sugar snow and other granular materials.

In the similar manner with soil mechanics, the relationship between shear strength and normal pressure may be given by the Coulomb-Navier theory:

$$\tau = \sigma_n \tan \phi$$

Where

τ is the shear strength

σ_n is the normal pressure acting on the shear plane

ϕ is the apparent angle of internal friction.

As shown in Fig. 7.24, the apparent frictional angle, ϕ , is strongly dependent upon the shear velocity. The experimental results show that the apparent frictional angle, ϕ , is 46 degrees in the direct shear performance at a shear velocity of 0.065 cm/sec, while ϕ is 33 degrees at the performance of a shear velocity of 0.31 cm/sec. This suggests that the shear strength of snow decreases with the increasing shear velocity. This trend, however, is not common to other materials. In the previous section, it is pointed out that the unconfined compressive strength of snow decreases as the compressive velocity increases

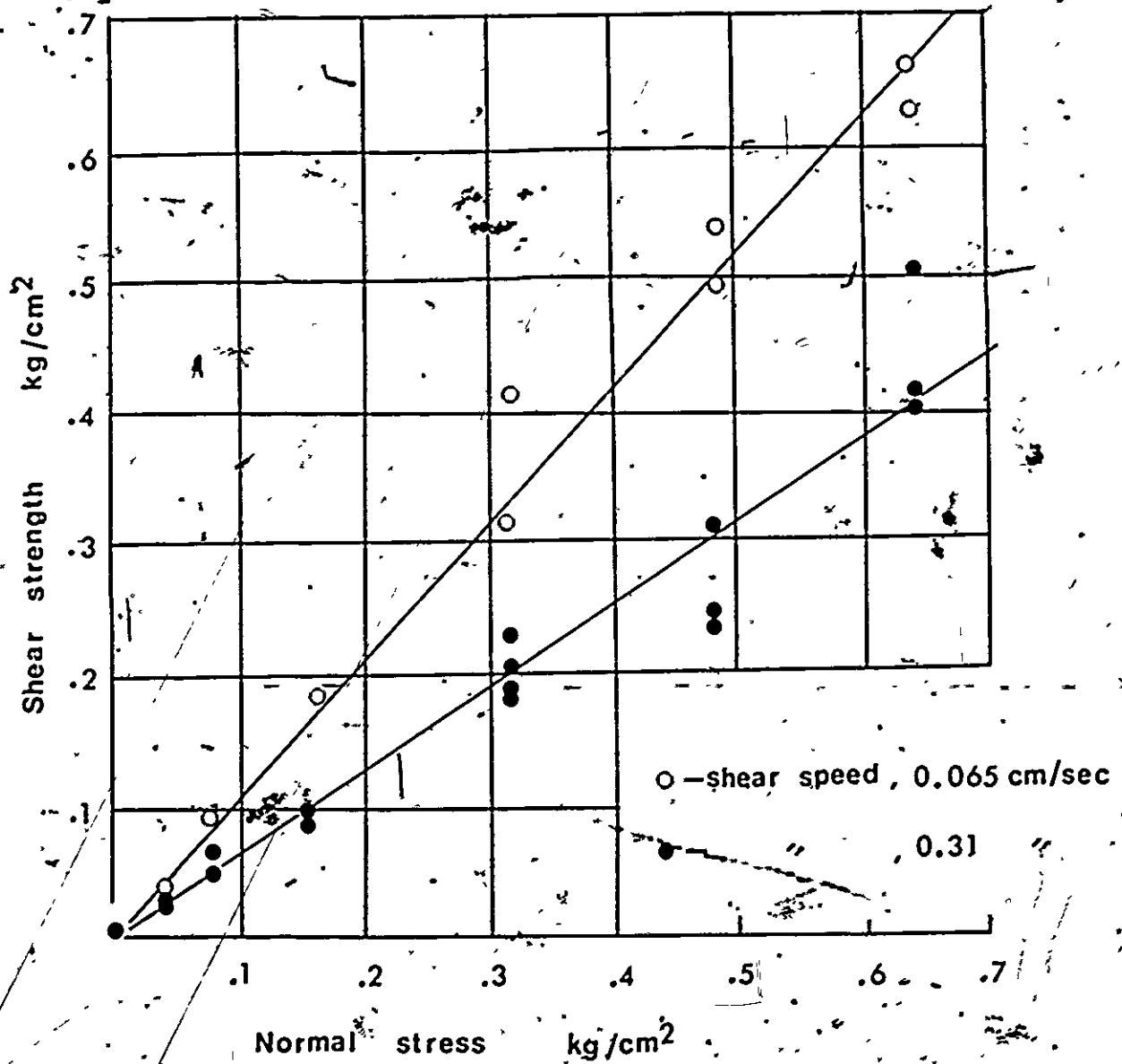


Fig. 7.24 Relationships between Shear Strength and Normal Pressure for Granular Snow in Direct Shear Test at Shear Velocities, 0.065 and 0.31 cm/sec

(Fig. 7,5). Therefore, it is expected that the shear velocity effects on the strength is caused by the same mechanism as found in the unconfined compression performances. These mysterious phenomena in relation to the deformation rates may confirm the adhesion theory developed in Chapter III. The shearing mechanism of snow, from the adhesion theory, is discussed herein and is further discussed in Chapter VIII.

It was found in Chapter VI that the contact area between snow grains increases with the irrecoverable deformation except intergranular slippage. Firstly, a point contact between two grains is considered as shown in Fig. 7,25. This figure illustrates the relationship between contact area and time under a certain constant load. Apparently, if time, t , is zero, the contact area for granular condition is negligible as mentioned earlier.

When $t = t_1$, it is considered that the contact area increases up to S_1' . Similarly, when $t = t_2$, the contact area becomes S_2' as shown in the figure. In direct shear performances, t_1, t_2, \dots, t_n with regard to different shear velocities are actually dependent upon time until the relative slippage of grains or shear failure occurs (see Fig. 7,20). It is noted that, at lower shear velocity, longer time is required for the slippage or shear failure to occur. As shown in the figure, if we assume that time t_1 until slip is required for the higher shear velocity, while t_2 is required to initiate slip for the lower shear velocity, tangential forces (Eq.(3,3)) required to initiate slippage between two grains may be given by,

for $t = t_1$

$$F_{c1} = A_c S_1' + \mu \tan \delta_1$$

for $t = t_2$

$$F_{c2} = A_c S_2' + \mu \tan \delta_1$$

Where F_{c1} and F_{c2} are the tangential forces to initiate slip when $t = t_1$ and $t = t_2$ respectively

A_c is the adhesion per unit area on the contact,
 S_1' and S_2' are contact areas in relation to t_1 and t_2 respectively

μ is the normal pressure acting on the contact
 δ_1 is the inherent angle of internal friction for initially granular snow.

From the preceding statements, apparently, the condition can be written by.

$$F_{c1} < F_{c2}$$

Thus, the higher the shear velocity, the smaller the tangential force required to initiate slip between grains. This idea can be extended to the similar phenomenon in the unconfined compression performances presented in Fig. 7.5.

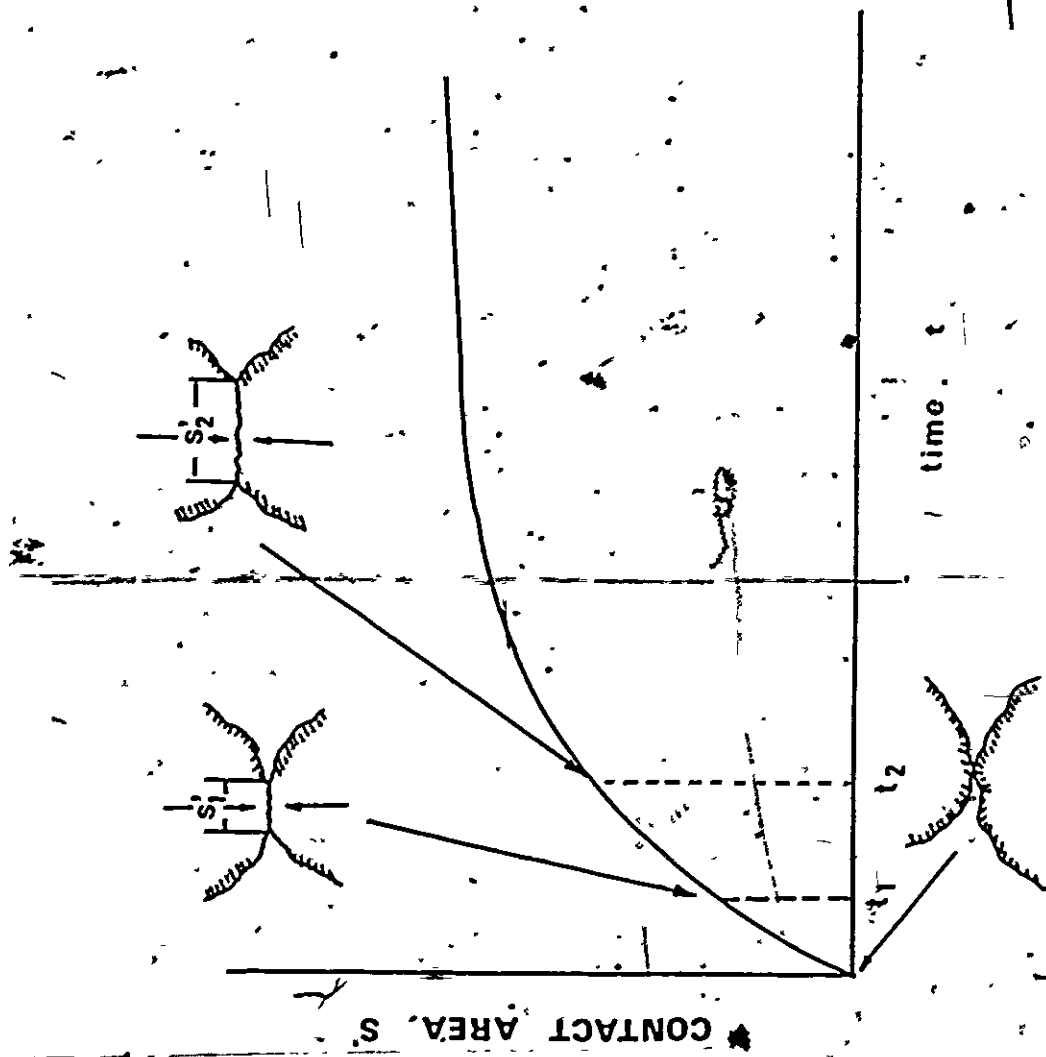


Fig. 7.25 Effect of Normal Pressure in Direct Shear Test

In more general case as shown in Fig. 7.26, the contact area between grains for initially point contact can be expressed as a function of grain size, strain and contact angle, as mentioned in Chapters IV and VI. From Eq. (4.11), contact area is given by,

$$S' = r^2 (3.9 \epsilon \cos^2 \psi - 1.785 \epsilon^2 \cos^4 \psi)$$

Where S' is the contact area

r is the radius of spherical grain

ψ is the contact angle

ϵ is the strain (see Chapter IV).

It should be noted that S' does not include elastic strain and intergranular slippage. From Eqs. (3.3) and (4.11), we obtain:

$$F_c = A_c r^2 (3.9 \epsilon \cos^2 \psi - 1.785 \epsilon^2 \cos^4 \psi) + N \tan \phi_i \quad \dots (7.1)$$

Equation (7.1) demonstrates that the tangential force required to initiate intergranular slip is dependent upon adhesion force, A_c , grain size, r , strain, ϵ , contact angle, ψ , normal force, N , acting on the contact and inherent angle of friction, ϕ_i . However, the transfer from the microscopic scale to the macroscopic scale is very complicated in terms of number of contacts and arrangement of grains (see Appendix B). Nevertheless, from the macroscopic point of view, the shear strength of snow may be expressed by,

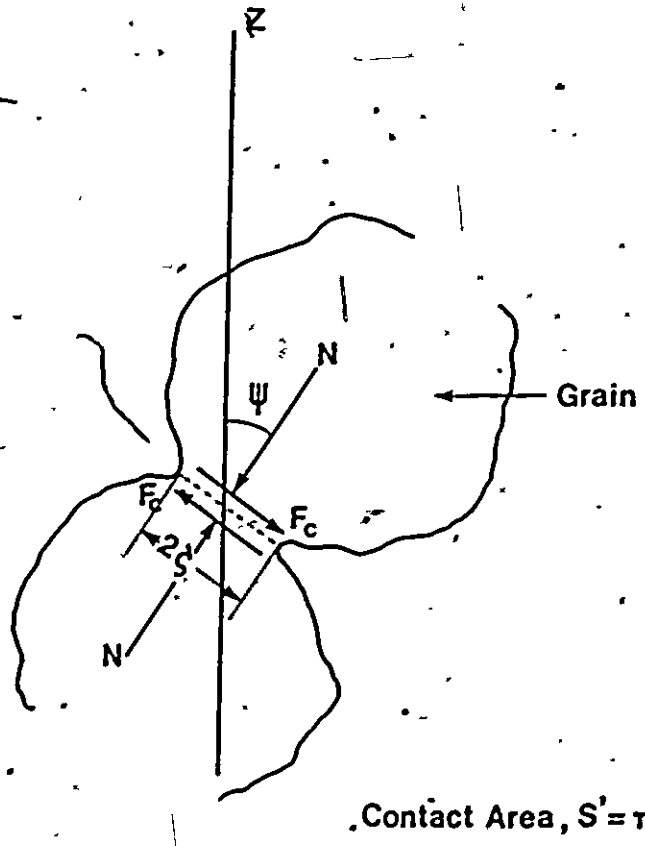


Fig. 7,26 General Stress Condition at Grain Contact

$$\tau = A_c S_e + \sigma_n \tan \phi \quad \dots(7,2)$$

Where

τ is the shear strength

A_c is the adhesion per unit area

S_e is the "effective contact area" of the specimen

σ_n is the normal force acting on the shear plane

ϕ is the inherent angle of friction for initially granular condition from the macroscopic point of view.

The effective contact area may be concerned with the microscopic contact area and σ_n may be quantitatively dependent upon the stress applied. Generally, the inherent angle of friction can be assumed to be constant as in other materials (Trollope, 1960). In addition, it is empirically established that coefficient of friction between solids is independent of the area and normal force applied. ~~we~~ we assume that ϕ is constant, then the experimental results obtained are explainable as shown in Fig. 7,27. The figure demonstrates that the shear strength of snow consists of the frictional and adhesive resistance. Since the adhesive force is assumed to be proportional to the effective contact area (Eq. 3,1), it increases as the failure time increases because longer time provides for a greater contact area as mentioned earlier. As mentioned earlier, higher shear velocity provides for a shorter time until snow fails. Therefore, the minimum shear strength of snow can be obtained at a very high shear velocity so that the intergranular slip can occur without sufficient development

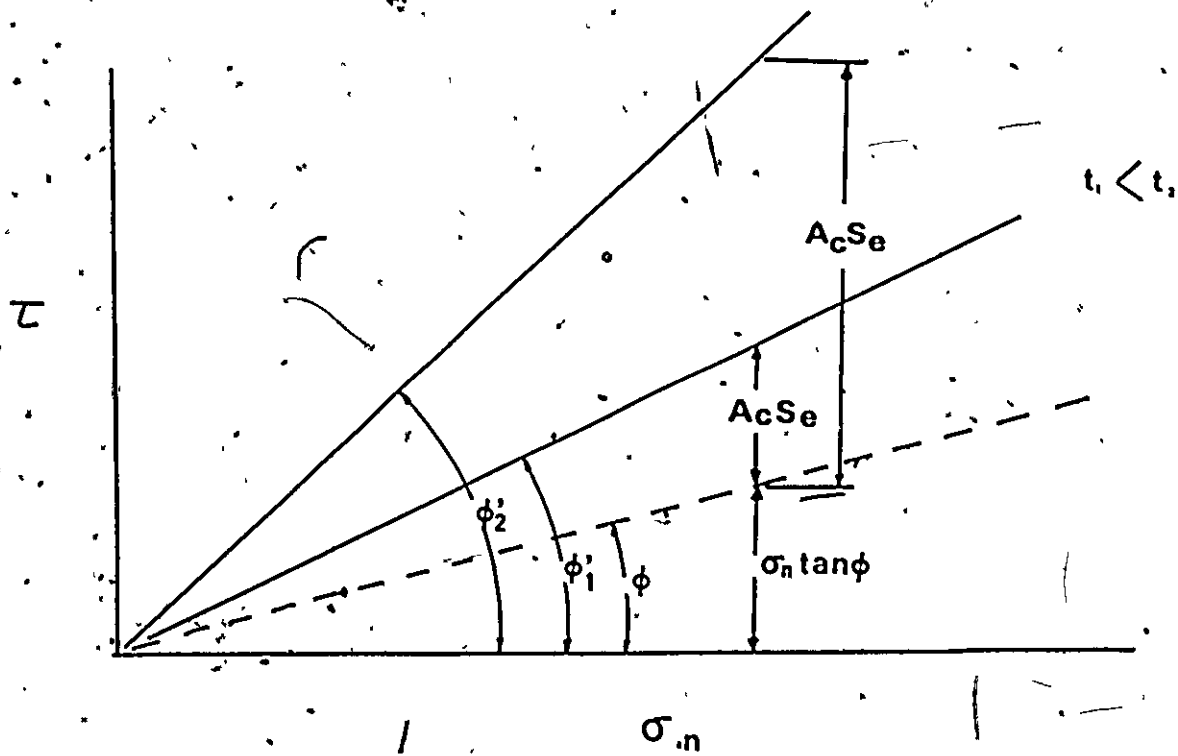


Fig. 7.27 Illustration of Shear Strength from the Adhesion Theory

of the contact area between snow grains. Under this condition, the shear strength can be described in terms of $\sigma_n \cdot \tan \phi$. This concept apparently satisfies the effect of deformation rate that the strength of snow decreases as the deformation rate increases (Fig. 7,5 and Fig. 7,24). Thus, the shear strength in relation to both the adhesion and friction should be taken into account.

Through the entire study, the effect of deformation rate is very obvious. This effect can only be explained by the adhesion theory of snow developed in Chapter III. Here, the shear velocity effect was interpreted by the adhesion theory. The evidence shown in this section may not be sufficient, therefore, complete discussion on the adhesion theory with further evidence is presented in Chapter VIII.

VII-3.4 Effect of Initial Bonding of Snow in Direct Shear Test

Figure 7,28 shows relationships between shear strength and normal stress obtained from differently age hardened snow. In these test series, various snows, i.e., granular snow, age-hardened snow for 2 hours and age-hardened snow for 3 days were examined. The basic snow was artificial snow (See Chapter V-1). Granular snow is identified as an assemblage with discrete grains while age-hardened snow is identified as sintered snow as mentioned in Chapter III. The details on snow type are presented in Chapter III. The apparent relationship between shear strength, τ , and normal stress, σ_n , for granular snow is almost linear and the apparent angle friction, ϕ' , is approximately 33 degrees for a shear velocity of 0.31 cm/sec as described in the preceding section.

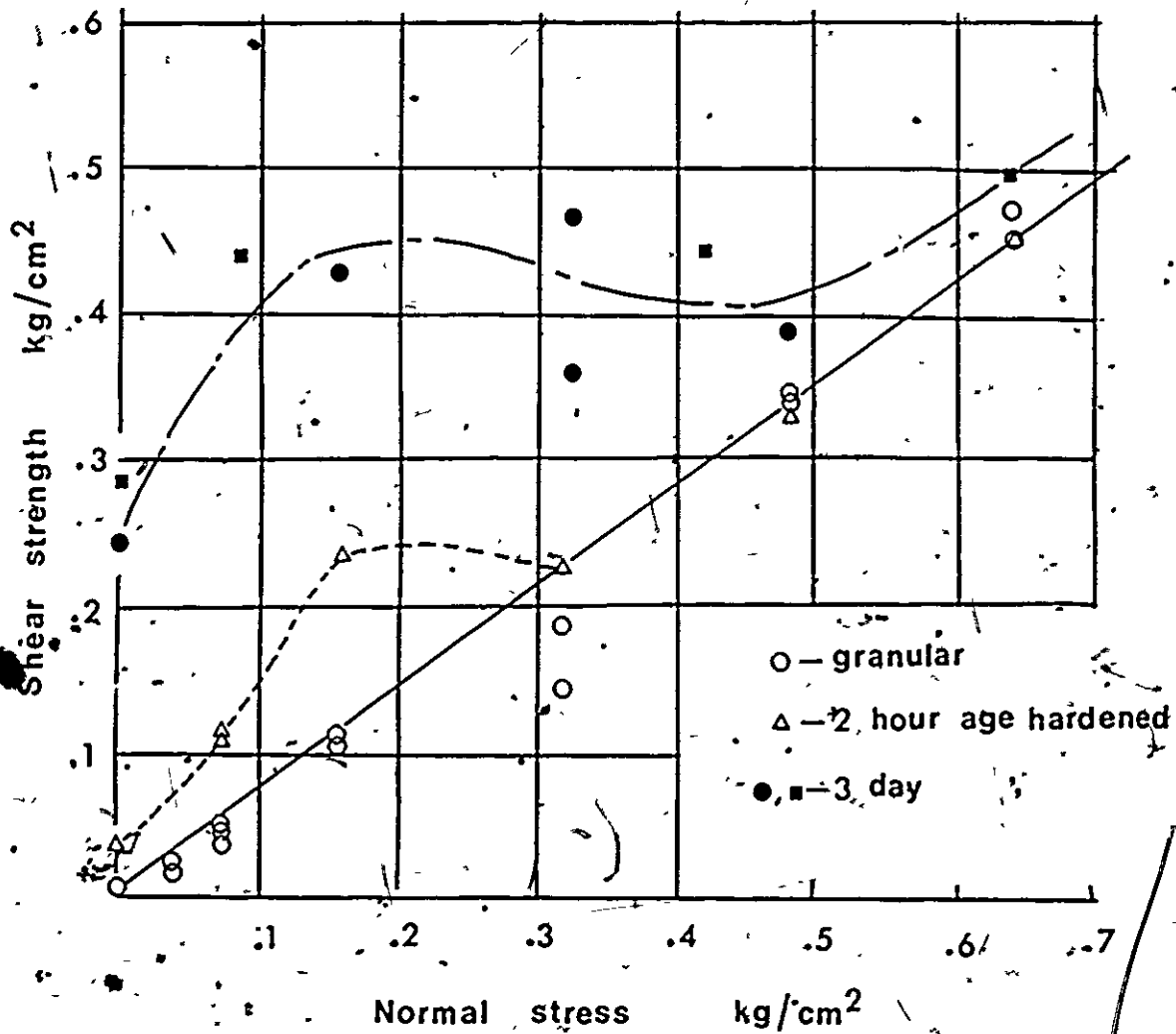


Fig. 7,28 Relationships between Shear Strength and Normal Pressure for Variously Age Hardened Snow in Direct Shear Test

The $\tau - \sigma_n$ curve of aged snow for 2 hours (indicated by triangles) is not totally linear as shown in Fig. 7,28. The results show that the non-linear part of curve for the aged snow appears under normal pressures of less than 0.3 kg/cm^2 . Under pressures greater than that normal pressure, the relationship between τ and σ_n is almost linear as shown in the figure. For age-hardened snow for 3 days, the relationship shows the non-linearity under normal pressures of less than 0.55 kg/cm^2 . Since the age means the bond development here (see Chapter II), the non-linearity of the curve is dependent upon the bonding strength-normal pressure relationship. The relationship between bonding strength and normal pressure was mentioned in terms of the structure change of snow under dead load application in the confined compression performances (see Fig. 7,11). In the confined compression performances, the following summary is drawn:

- (1) if dead load intensity is relatively insufficient in relation to the bonding strength of snow, the elastic deformation overlapped by the creep deformation of snow occurs under the load. Under this condition, no microfracture of snow occurs, and
- (2) if dead load applied is relatively greater than the bonding strength of snow, the sudden microfractures of snow occur when the dead load is applied. The breakage of intergranular bonds resulting from the microfractures creates a granular condition of snow through the change of density. Under this

condition, the consequent creep deformation of snow occurs (Process A in Fig. 7,18).

Thus, there are two main types of snow response characteristics under dead load application. Strictly speaking, the items presented are also dependent on the initial density of snow (Fig. 7,11). The shear strength of snow can be measured under the condition, i.e., item (1) or item (2). It is noted that, under item (1), the shear strength can be obtained from the almost initial properties of snow but, under item (2), the shear strength can be obtained from the completely changed properties of snow, especially for bonding strength and density, as mentioned earlier. It is considered that the $\tau - \sigma_n$ relationship under item (1) becomes non-linear. Whilst the linear $\tau - \sigma_n$ curve can be obtained under item (2) because the snow approaches to granular condition as mentioned earlier. It should be noted that non-linear $\tau - \sigma_n$ curve for rocks is not uncommon and linear $\tau - \sigma_n$ curve is common for sands. In addition, in the experiment, almost linear $\tau - \sigma_n$ curves were obtained from the granular snow (Fig. 7,24 and Fig. 7,28). The shearing characteristics of granular snow were discussed in the preceding section.

It is interesting to note that the results shown in Fig. 7,28 show exactly the same trends of strength envelope as for sensitive clays (LaRoche and Lefebvre, 1971, and Lo and Morin, 1972). Basically the non-linear $\tau - \sigma_n$ curves for both snow and sensitive clays are entirely dependent upon the following factors:

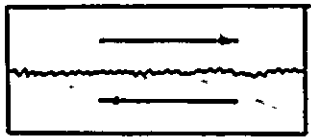
- (a) both materials are loose,
- (b) bonding strength - normal pressure relationship plays an important role, and
- (c) bonds between grains for both materials are breakable under pressure.

Generally sneaking, sensitive clays as well as snow show a similar behaviour, and were identified as brittle-like materials (Lo and Morin, 1972). The failure strain for St. Louis clays in consolidated-undrained triaxial tests is almost 1.0 percent. This value is comparable with that for snow in the unconfined compression tests (see Fig. 7,5).

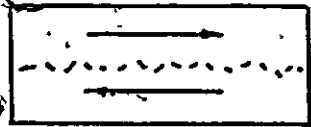
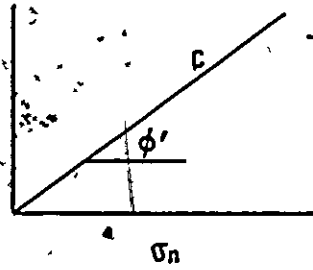
Thus, the shear response behaviour of snow is dependent upon the following factors:

- 1) snow type,
- 2) normal pressure acting on the shear plane,
- 3) shear velocity, and
- 4) temperature.

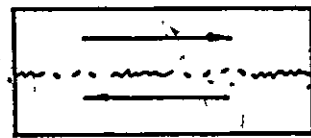
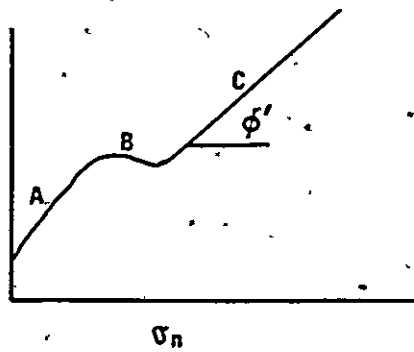
In summary, a structure model to explain the shear behaviour with respect to both snow type and normal pressure effects is developed as shown in Fig. 7,29. Figure 7,29(a) illustrates the simple model for shearing characteristics of granular snow. The model shows that the shear plane of granular snow is initially indicated as discontinuity which means no bonding between grains. From the engineering point of view, at relatively low temperatures, the water film effect is not too



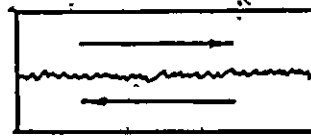
(a)



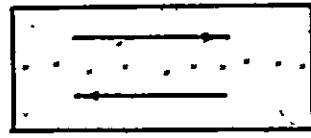
TYPE, A (b)



TYPE, B (c)



TYPE, C (d)



(e)

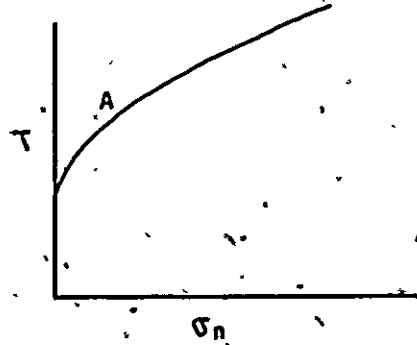


Fig. 7,29 Typical Shearing Responses of Soil in Direct Shear Test in Relation to Snow Type

strong; the model shown in Fig. 7,29(a) may also be applicable for semi-bonded snow. Actually the discontinuity lies through the specimen of those types of snow, but for convenience, it is considered only on the shear plane. In this case, $\tau - \sigma_n$ relationship is considered to be linear as shown in the figure. The apparent feature for this type of $\tau - \sigma_n$ curve is similar to that found in sand. Apparently, the shear strength may follow the Coulomb-Navier theory:

$$\tau = \sigma_n \tan \phi'$$

Where

τ is the shear strength

σ_n is the normal force acting on the shear plane

ϕ' is the apparent frictional angle.

It is remembered that ϕ' is a strong function of the shear velocity as pointed out in the preceding section. Then, Eq.(7,2) may be applicable for this case. Equation (7,2) is written as:

$$\tau = A_c S_e + \sigma_n \tan \phi$$

Where

τ is the shear strength,

A_c is the adhesion per unit area

S_e is the effective contact area of the specimen

σ_n is the normal force acting on the shear plane

ϕ is the inherent angle of friction from the macroscopic point of view.

as mentioned earlier. The density of the final condition is apparently higher than the initial density because of the microfractures due to intergranular slip which means compressibility. If initial density is greater than the critical density, apparently no microfracture under the normal load application would occur. Therefore, the shear strength can be obtained from the initial snow structure though there may be definitely creep deformation under the normal load (see Fig. 7.11).

For highly bonded snow or ice, the $\tau - \sigma_n$ curve may be identified as rock type-curve as shown in Fig. 7.29(e). This type is similar to Type A. It is considered that the $\tau - \sigma_n$ curve of high density snow obtained by Butkovich (1956) belongs to this type.

Thus the shearing characteristics in relation to snow types are divided into three main types, i.e., sand-type (granular snow), sensitive clay-type (moderately bonded snow) and rock-type (strongly bonded snow). Therefore, this must be taken into account for the evaluation of shear strength of snow.

Although some of the shearing characteristics of snow and test technique were discussed in this section, however, there are many problems remaining to be solved for the proper appreciation of snow strength. It is suggested that main problems to be solved are as follows:

- (a) to examine temperature effects in direct shear performance,
- (b) to evaluate adhesion force A_c and inherent angle of friction.

as mentioned earlier. The density of the final condition is apparently higher than the initial density because of the microfractures due to intergranular slip which means compressibility. If initial density is greater than the critical density, apparently no microfracture under the normal load application would occur. Therefore, the shear strength can be obtained from the initial snow structure though there may be definitely creep deformation under the normal load (see Fig. 7,11).

For highly bonded snow or ice, the $\tau - \sigma_n$ curve may be identified as rock type-curve as shown in Fig. 7,29(e). This type is similar to Type A. It is considered that the $\tau - \sigma_n$ curve of high density snow obtained by Butkovich (1956) belongs to this type.

Thus the shearing characteristics in relation to snow types are divided into three main types, i.e., sand-type (granular snow), sensitive clay-type (moderately bonded snow) and rock-type (strongly bonded snow). Therefore, this must be taken into account for the evaluation of shear strength of snow.

Although some of the shearing characteristics of snow and test technique were discussed in this section; however, there are many problems remaining to be solved for the proper appreciation of snow strength. It is suggested that main problems to be solved are as follows:

- (a) to examine temperature effects in direct shear performance,
- (b) to evaluate adhesion force A_c and inherent angle of friction.

- (c) to examine the effects of shear velocity in more wide ranges, and
- (d) to examine the effects of normal pressure in more high levels.

VII-4 Penetration Performance

VII-4.1 Thin Blade Penetration Performance into Snow

Field tests are of great importance in snow engineering problems. The true appreciation of snow properties should be obtained in-situ for the many reasons described in Chapter 1-2. At the present, the emphasis is on the application of soil testing techniques, such as vane shear, cone, plate penetration, etc. However, as described in the earlier sections, snow properties and behaviour are very complicated in terms of grain size, grain shape, bonding strength, and density, even at elevated temperatures. Since snow properties are generally not estimated from the initially fallen snow because of very complicated effects of temperature change and other external conditions, the only way to obtain snow properties is to perform in-situ-testing.

The grain characteristics of snow may be obtained rather easily. The grain size can be obtained using the sieve method as described previously. The grain shape may be judged by visual inspection because it is not difficult to distinguish fresh snow from metamorphic grains. There may be a few ways to obtain snow density in the field. Basically, snow density is obtained as the ratio of the weight of snow

mass to the volume of the mass as described previously. There is no information as to how much volume should be taken in the measurement of density. This may be judged for each case individually.

It may be rather difficult to evaluate bonding of snow. The direct way to measure snow bonding magnitude may be obtained from tensile tests. However, this method is not necessarily applicable because there is a difficulty of sampling, especially for poorly bonded or for low density snow. In addition, the performance of tensile tests is not always practical for in-situ testing.

Most of the testing techniques being used in soil mechanics has been introduced into the evaluation of snow properties. However, the data obtained from those techniques, in fact, have included the effects of speed, the change in density, and the change in bonding as found in the mechanical tests. Therefore, better in-situ technique for evaluation of snow properties is described in terms of:

- 1) simple techniques,
- 2) less effect of speed,
- 3) less effect of the change in density during testing, and
- 4) less effect of the change in bonding during testing,

and requires that:

- 1) the analyses are feasible, or
- 2) there is a relationship with other test results.

For these reasons, a blade penetration technique was developed in the present research. We might expect that thin blade penetration technique may satisfy the problems mentioned above because the small sectional area of thin blade at least decreases the problems encountered in the plate penetration performance.

The size of the thin blade used was 1.2 mm wide and 0.6 mm thick and the illustration of blade penetration performance is presented in Fig. 7,30.

Speed Effect in Thin Blade Penetration

Figure 7,31 shows the thin blade penetrating force into an age-hardened (sintered) snow as a function of penetration speed. As shown in the figure, the response characteristics of snow under thin blade penetration are divided into:

- (a) ductile type for penetration speeds of lower than 0.25mm/sec, and
- (b) brittle type for penetration speed of higher than 0.25 mm/sec.

It should be noted that the trend shown in the figure is similar to that obtained in the unconfined compression performances (see Figure 7,5)..

(a) Ductile Type

From the experimental results shown in Fig. 7,31, the ductile behaviour of snow under the thin blade penetration seems to be viscous

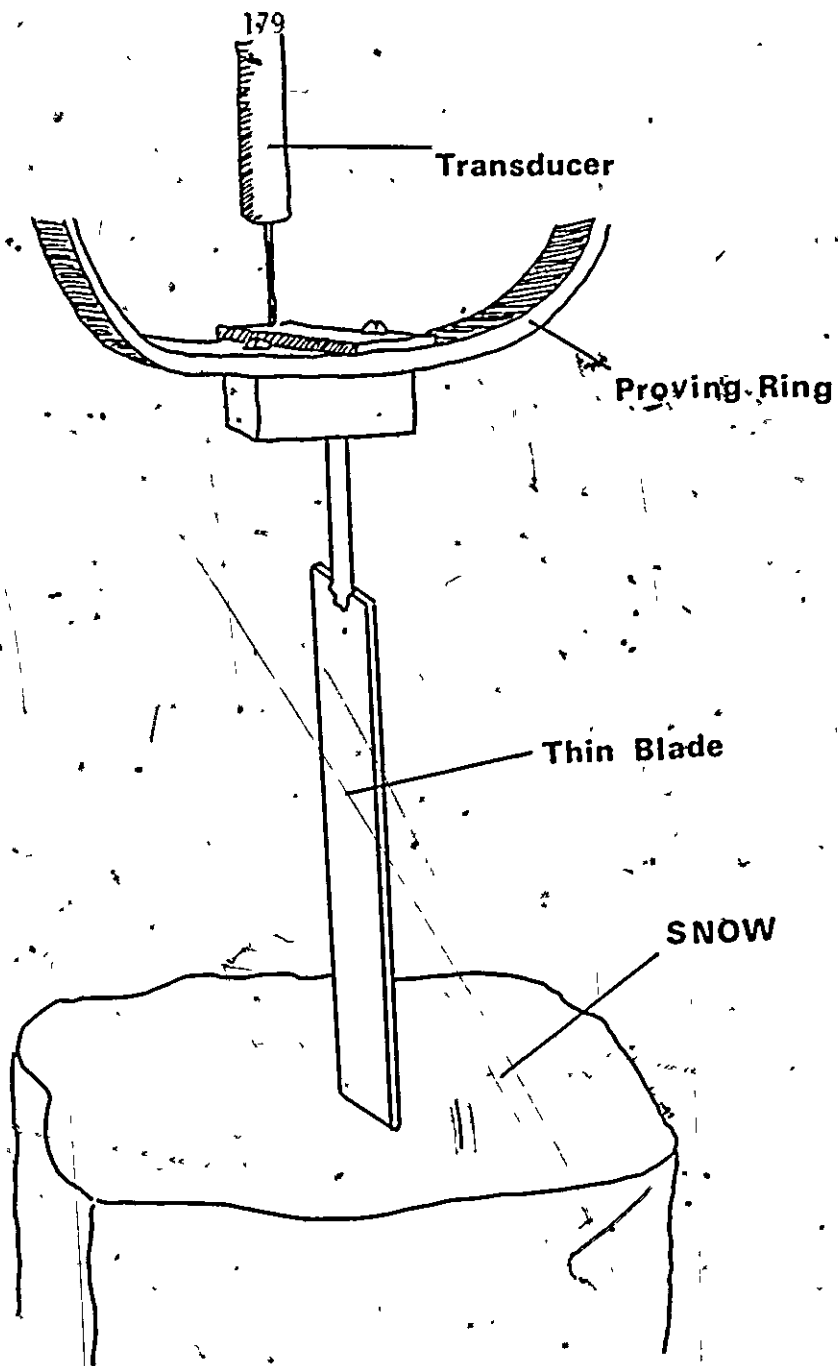


Fig. 7,30 Illustration of Thin Blade Penetration Performance

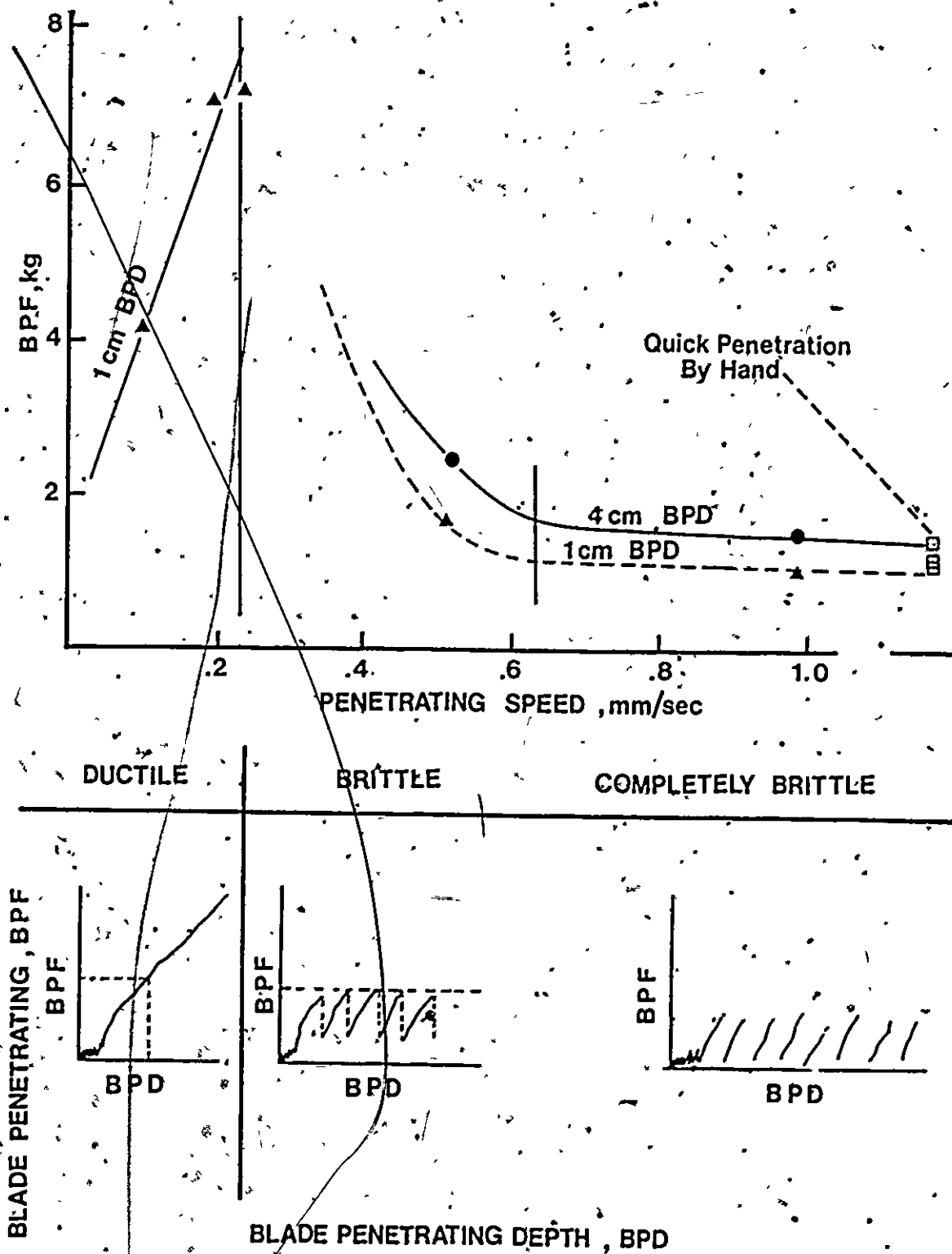


Fig. 7,31 Speed Effect of Thin Blade Penetration into Age Hardened Snow

because the penetrating force is a linear function of penetration speed.

It is noted that this trend is common to the experimental results obtained from the unconfined and confined compression tests. Basically, the ductile behaviour of snow can be explained by so-called crystalline flow as mentioned previously. The situation may not be dissimilar to the case of progressive low rate compression (see Process C in Fig. 7,18). The ductile behaviour of snow under confined compression can be described in terms of the hardening of snow structure. This means that snow structure changes under the ductile penetration. Therefore, a proper evaluation of snow properties can hardly be achieved by this low speed of penetration.

(b) Brittle Type

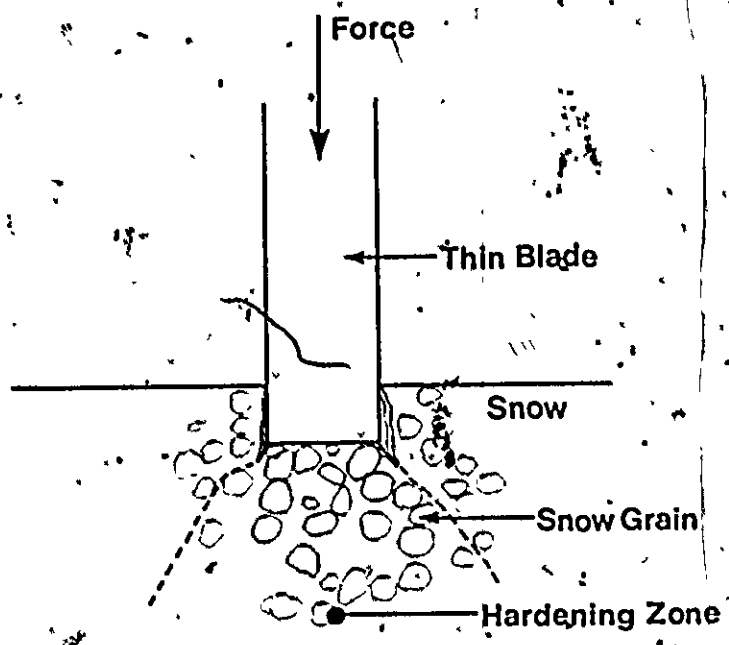
It is obvious from Fig. 7,31 that the blade penetrating force decreases as the penetrating speed increases in the range from 0.25 to 0.6 mm/sec. This trend is very similar to that found in the unconfined compression and direct shear tests (see Fig. 7,5 and Fig. 7,24). This is due to time effects in terms of the adhesion theory as described in Chapter VII-3. Therefore, it is expected that the brittle type of snow under the thin blade penetration is identified as that found in the brittle unconfined compressive behaviour as mentioned previously (see Fig. 7,2).

The experimental results shown in Fig. 7,31 indicate that the blade penetrating force is almost constant with respect to the penetrating speed in the range from 0.6 mm/sec to higher speeds. This may be described as completely brittle behaviour of snow which may not

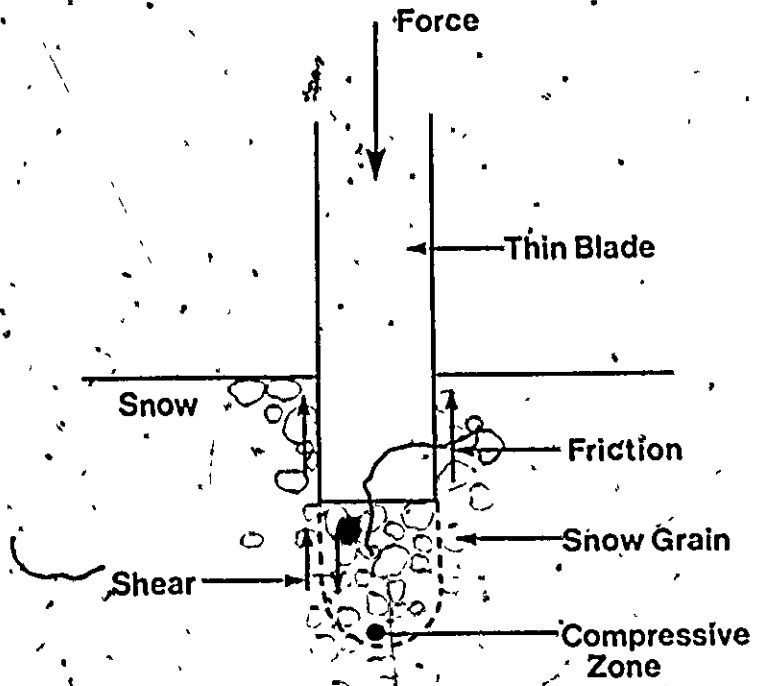
be dissimilar to that found in the dead load compressive behaviour of snow (see Process A in Fig. 7,18). In the completely brittle behaviour of snow, it may be expected that the thin blade penetrating force presents the actual snow properties without the change of initial properties. As shown in the figure, the blade penetrating force is almost constant with respect to the penetration depth and speed. Strictly speaking, very slight increase in force with respect to penetration depth was measured. This may be the frictional resistance between the surface of blade and snow. However, within 3 cm penetration depth, the increase in force is negligible.

Figure 7,32 shows a prediction of snow responses under the thin blade penetration performances. Since ductile behaviour of snow can be described in terms of the hardening of snow structure as mentioned in the previous sections, it may be expected that the hardening of snow under the tip of blade occurs as shown in Fig. 7,32(a). Whilst, since brittle behaviour of snow is described in terms of fractures, it may be expected that the fractures of snow occur under the tip of blade as shown in Fig. 7,32(b). In this sense, the blade penetrating force for relatively higher penetration speed can qualitatively be described by:

(B.P.F.) (compressive strength of snow under the tip of blade) +
 (cutting shear strength at the edges of blade) +
 (frictional resistance between the blade surface and
 snow).



(a) DUCTILE



(b) BRITTLE

Fig. 7.32 Prediction of Snow Behaviour under Thin Blade Penetration.

It was described earlier that the frictional resistance is negligible if the penetration depth is small. The deformation mechanisms of snow under a rigid plate penetration are discussed in the next section.

As described earlier, it is possible to obtain snow properties by using the high speed-thin blade penetration technique. In the present research, blade penetrating force is correlated to unconfined compressive strength because, at present, it may be difficult to evaluate proper snow properties by the blade penetrating force alone.

In order to obtain a relationship between blade penetrating force and unconfined compressive strength for various snows, a large number of snow specimens were subjected to both tests. Since the compressive velocity affects the unconfined compressive strength as pointed out previously, both the unconfined compressive strength and the blade penetrating force were obtained at 0.98 mm/sec for the compressive velocity and the penetration speed. It is noted that the penetration speed used provides for the completely brittle behaviour of snow under the tip of blade as mentioned earlier (see Fig. 7;31).

Figure 7,33 shows relationships between blade penetrating force and unconfined compressive strength for various snows. The figure shows that the blade penetrating force increases as the unconfined compressive strength increases. As pointed out previously, the unconfined compressive strength of snow is a strong function of bonding strength of snow (see Fig. 7,5). The bonding strength of snow was increased by sintering time after the preparation of specimens. This means that the bonding strength of snow can approximately be characterized

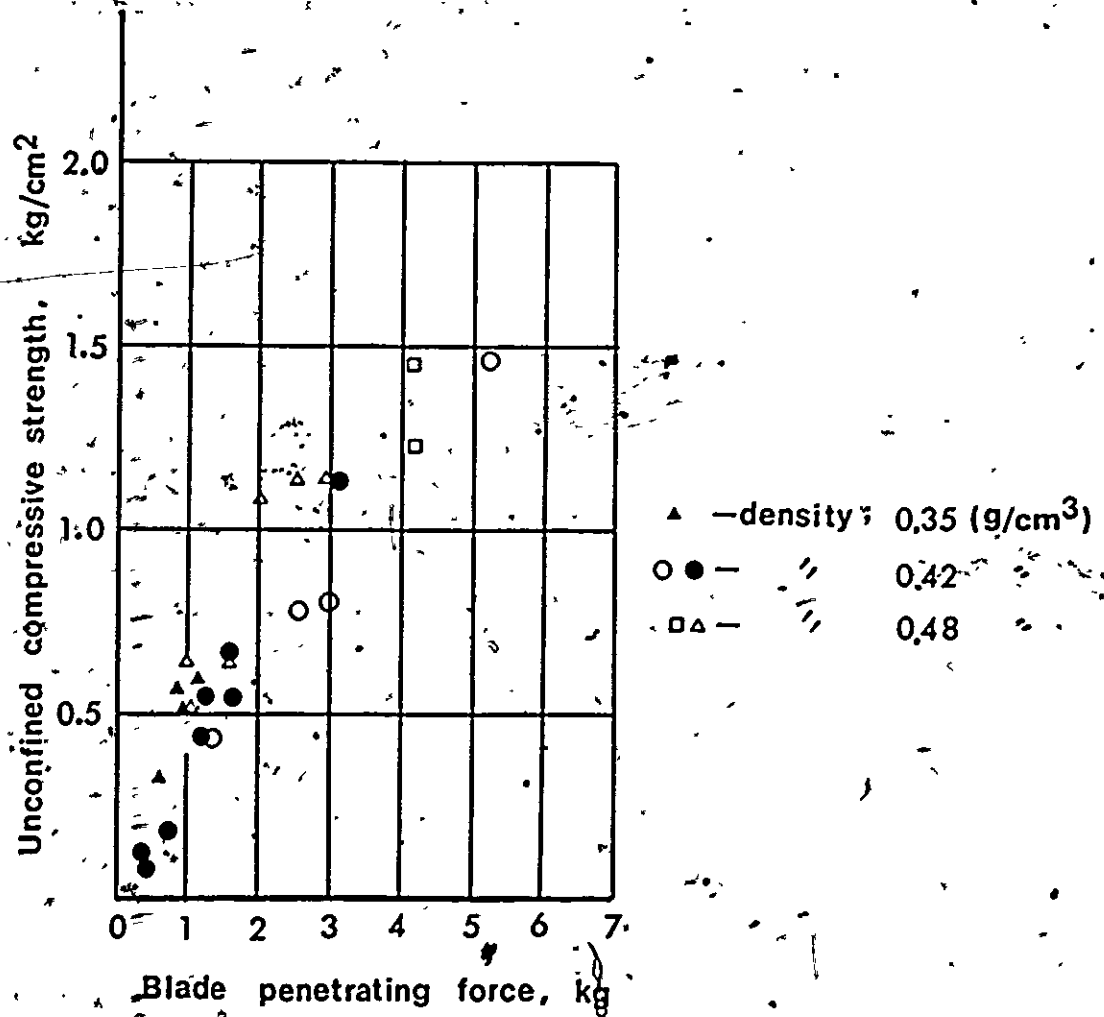


Fig. 7.33 Relationship between Unconfined Compressive Strength and Thin Blade Penetrating Force

by the blade penetrating force by considering the relationship between the blade penetrating force and unconfined compressive strength. For example, if the blade penetrating force obtained is negligible the corresponding unconfined compressive strength is also negligible as shown in the figure. This means that the snow is granular or fresh. It was described previously that the unconfined compressive strength of granular snow is negligible. Note that the unconfined compressive strength of fresh snow can often be negligible because of its very low density. In addition, the crystal of fresh snow is easily breakable as mentioned previously. It is also noted that it is not difficult to distinguish fresh snow from metamorphic grains (i.e., grains for granular and sintered snows) by visual inspection. On the other hand, if the blade penetrating force obtained is very high the corresponding unconfined compressive strength is also very high from the figure. This means that the snow is well sintered or strongly bonded.

Thus, snow properties in relation to the strength characteristics and bonding strength can be evaluated from the high speed-blade penetrating technique. However, general properties of snow should be based on the grain characteristics, density, blade penetrating force, etc. In addition, it may require the consideration of snow behaviour partially studied in the unconfined compression, confined compression, direct shear and penetration performances.

At present, many problems still remain to be solved. Those should be studied one by one in the future. Main problems to be solved for the thin blade penetration performance are cited as follows:

(a) Temperature Effect

It is considered that the effect of penetration speed is dependent on temperature because it may be dependent on the transition problems of snow (Chapter VII-1). The transition of snow is considered to be a strong function of temperature.

(b) Size Effect of Blade

In the present research, the size of blade used was 1.2 mm wide and 0.6 mm thick. However, it is obvious that the blade penetrating force is dependent upon the size of blade. Therefore, in order to design better instrument for the in-situ testing, it is necessary to examine the size effect of blade.

VII-4.2. Rectangular Rigid Plate Penetration Performance

Snow response under a plate penetration can be divided into two main types, i.e., cutting shear and compression shear, as mentioned previously (see Fig. 2,2). It was mentioned that the cutting shear may occur at the edges of plate while the compression shear may occur beneath the plate. These mechanisms were examined in the compression performances and the direct shear performance individually in the previous sections.

Plate penetration will provide for the more general snow response characteristics which are combined behaviour of the cutting shear and the compression shear. For these reasons, a rectangular rigid plate penetration into typical snows, i.e., fresh, granular and

sintered snow, was performed. Snow specimens were prepared by mechanically depositing of basic snow into glass sided-boxes as shown in Fig. 7,34. The size of rectangular rigid plate made of lucite plate was 3.5 cm long and 5.5 cm wide as shown in the figure. By using carbon powder, a grid system was used for the visual observation.

From the experimental results obtained in the mechanical tests presented in the previous sections, it is expected that the speed of plate penetration will affect the response characteristics of snow. Therefore, two ranges of penetration speeds, i.e., 0.097 and 0.98 mm/sec, were examined.

Fresh Snow

Figure 7,35 shows the rectangular rigid plate penetration into fresh snow (initial density $\gamma_0 = 0.12 \text{ g/cm}^3$). Figure 7,35(a) shows the apparent feature of densification of fresh snow under the plate penetration with a constant speed of 0.097 mm/sec, while Fig. 7,35(b) shows the densification of fresh snow under a speed of 0.98 mm/sec which is about ten times higher than the former. The distinct difference between the apparent features of these two penetration-performances can be clearly seen in the relationships between penetration force and depth as shown in Fig. 7,36. The results show that the higher resistance is obtained for the lower speed penetration. The curves indicated in the figure show that the penetration force of a low speed of 0.097 mm/sec is approximately five times greater than that of the higher penetration speed. This trend is common if the deformation rate

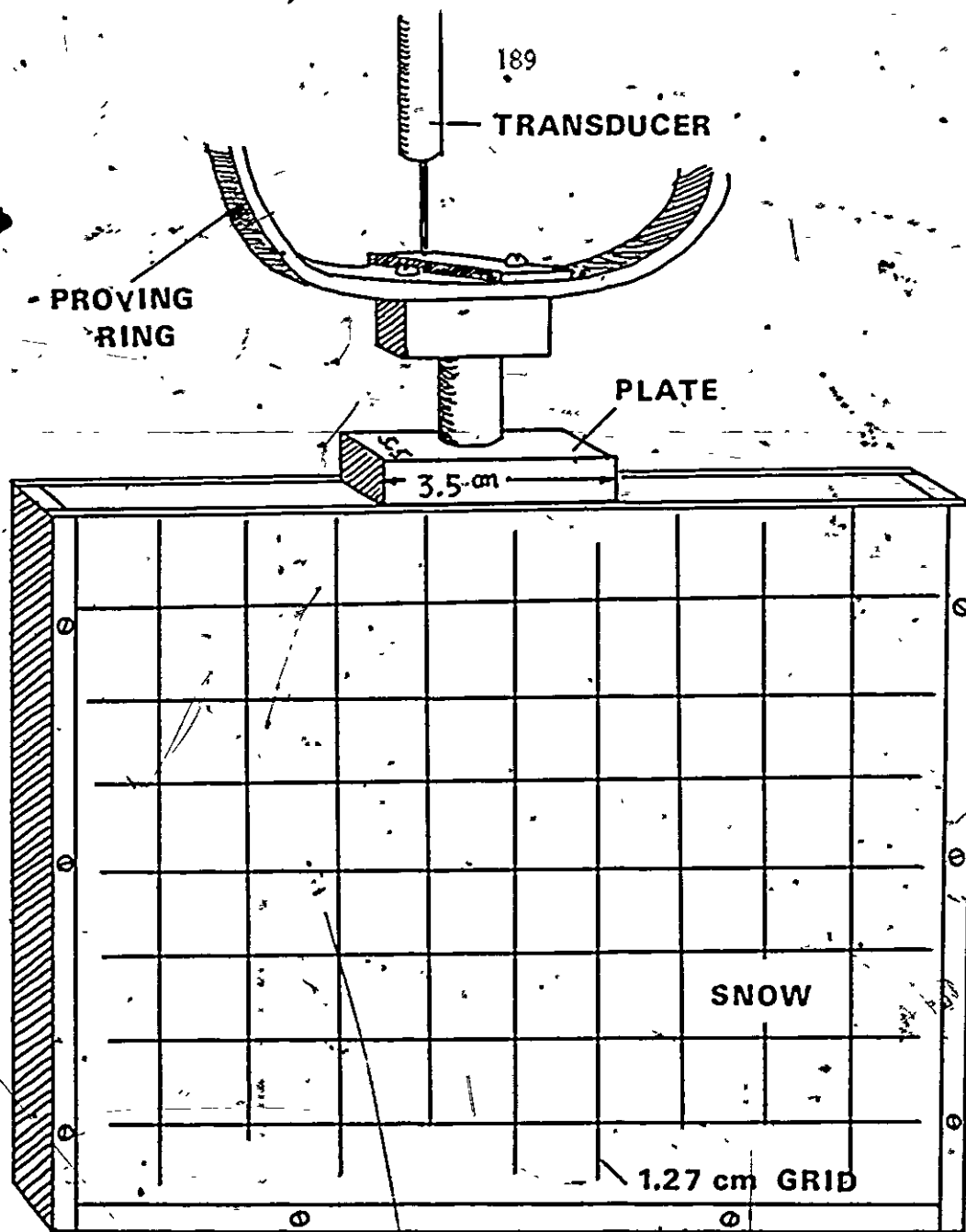
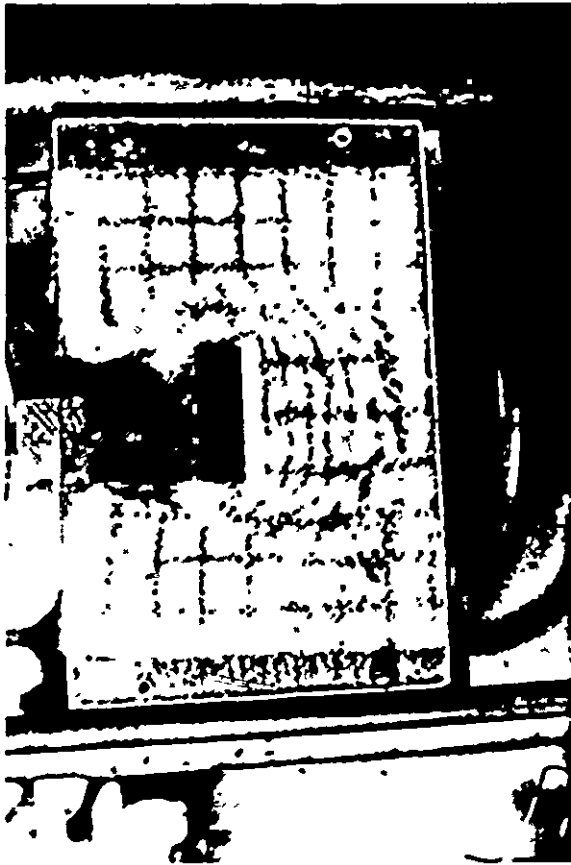
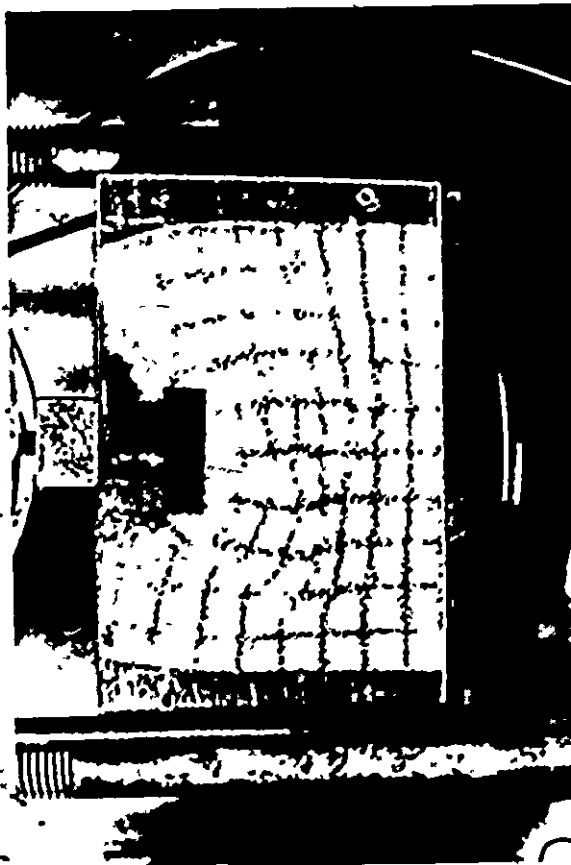


Fig. 7,34 Illustration of Rectangular Rigid Plate Penetration Performance (Glass-Sided Experiment)



(a)



(b)

Fig. 7.35 Plate Penetration into Fresh Snow

(a) Penetration Speed of 0.097 mm/sec

(b) Penetration Speed of 0.98 mm/sec

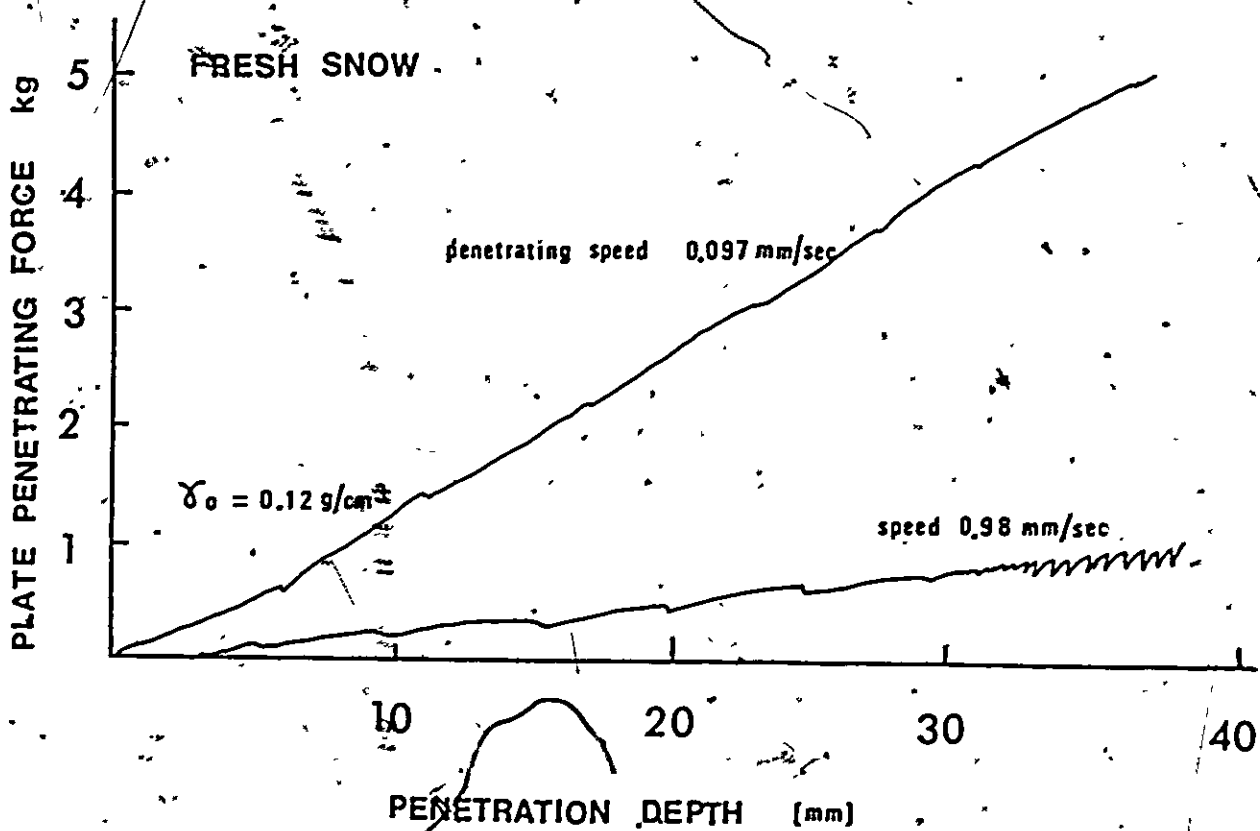


Fig. 7.36 Relationships between Penetrating Force and Depth for Fresh Snow in Rectangular Rigid Plate Penetration (Glass-Sided Experiment)

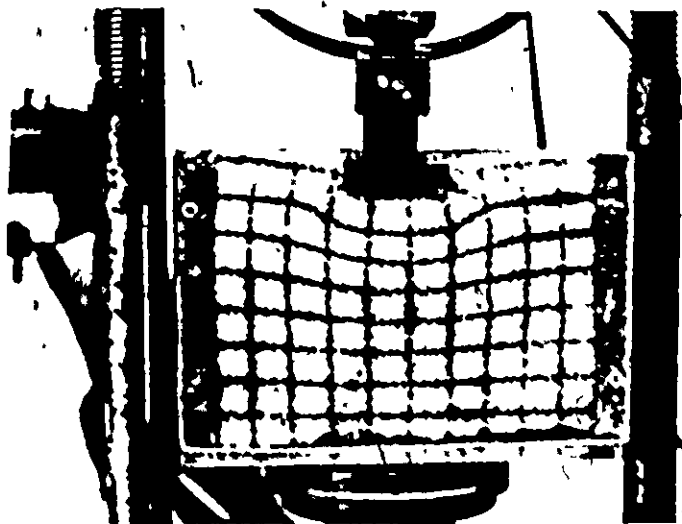
effect on snow is understood properly. The results obtained here are discussed with the results obtained from the other types of snow and is presented later in this section.

Granular Snow

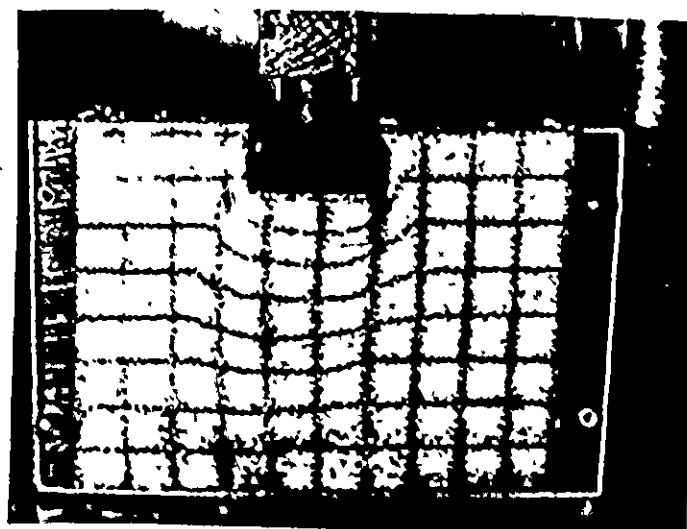
Figure 7,37 shows the plate penetration performances into granular snow (initial density 0.40 g/cm^3). The basic snow was three weeks old (see Chapter V-1). Figure 7,37(a) shows the penetration behaviour of granular snow with a penetration speed of 0.097 mm/sec , while Fig. 7,37(b) shows the behaviour under similar condition but at a penetrating speed of 0.98 mm/sec . The difference between these two performances lies in the modes of densification of snow.

Figure 7,38(a) illustrates the apparent features of snow densification under the lower penetration speed performance. The features of this lower penetration speed performance can be described as follows:

- (a) Snow surface was also densified in this low penetration speed performance. This is uncommon for the high penetration speed performance (see Fig. 7,37). Therefore, it is expected that, near the plate, tensile stress was exerted. As indicated in Fig. 7,38(a). The similar situation can be cited in the case of fresh snow (see Fig. 7,35).
- (b) Under the plate, the behaviour of snow is described as ductile. This is obvious from the relationship between penetration force and depth as shown in Fig. 7,39. The similar situation can be cited in the case of fresh snow (see Fig. 7,36).



(a)



(b)

Fig. 7.37 Plate Penetration into Granular Snow

(a) Penetration Speed of 0.097 mm/sec

(b) Penetration Speed of 0.98 mm/sec

The further discussion of ductile behaviour will be presented later in this section.

- (c) At the edges of plate, the occurrence of tension crack is obvious in both case of fresh snow and granular snow (see Figs. 7,35 and 7,37).
- (d) The densified zone spreads laterally and downward in this low penetration speed performance. The similar situation is cited in the case of fresh snow (see Fig. 7,35).

On the other hand, the apparent features of snow densification under the higher penetration speed performance is illustrated in Fig. 7,38(b).

The main features are as follows:

- (a) The densified zone under the plate narrows in comparison with the lower penetration speed performance. In addition, the snow surface near the plate is not densified. The similar situation can be cited in the performance of fresh snow.
- (b) The behaviour of snow under the plate is brittle. This is obvious from Fig. 7,39. It was described earlier that the behaviour of snow under the Tower speed penetration is ductile. The further discussion will be presented later.

The relationships between plate penetrating force and depth for the lower and the higher penetration speed performances are shown in Fig. 7,39. The figure shows that the penetrating resistance with a

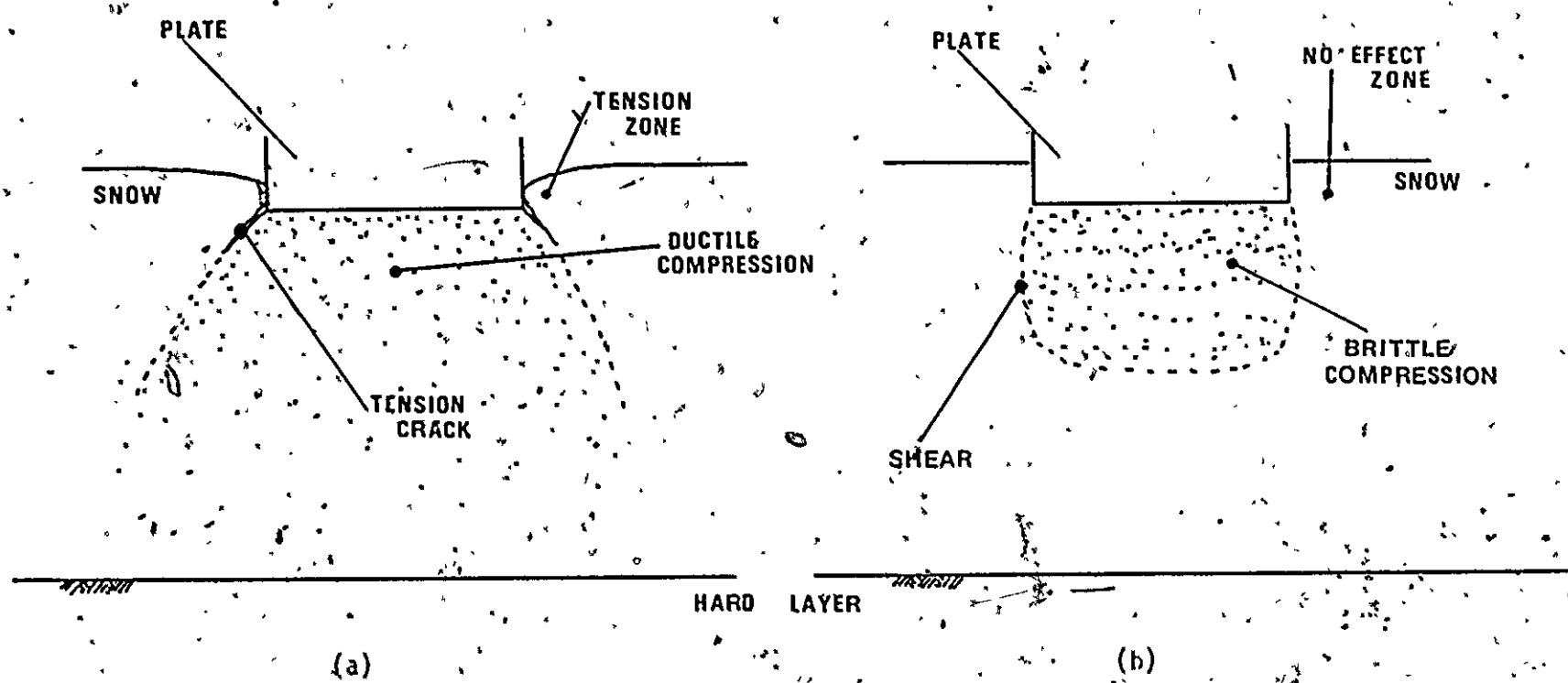


Fig. 7.38 Illustration of Apparent Snow Responses under Plate Penetration

(a) Lower Penetration Speed

(b) Higher Penetration Speed

195

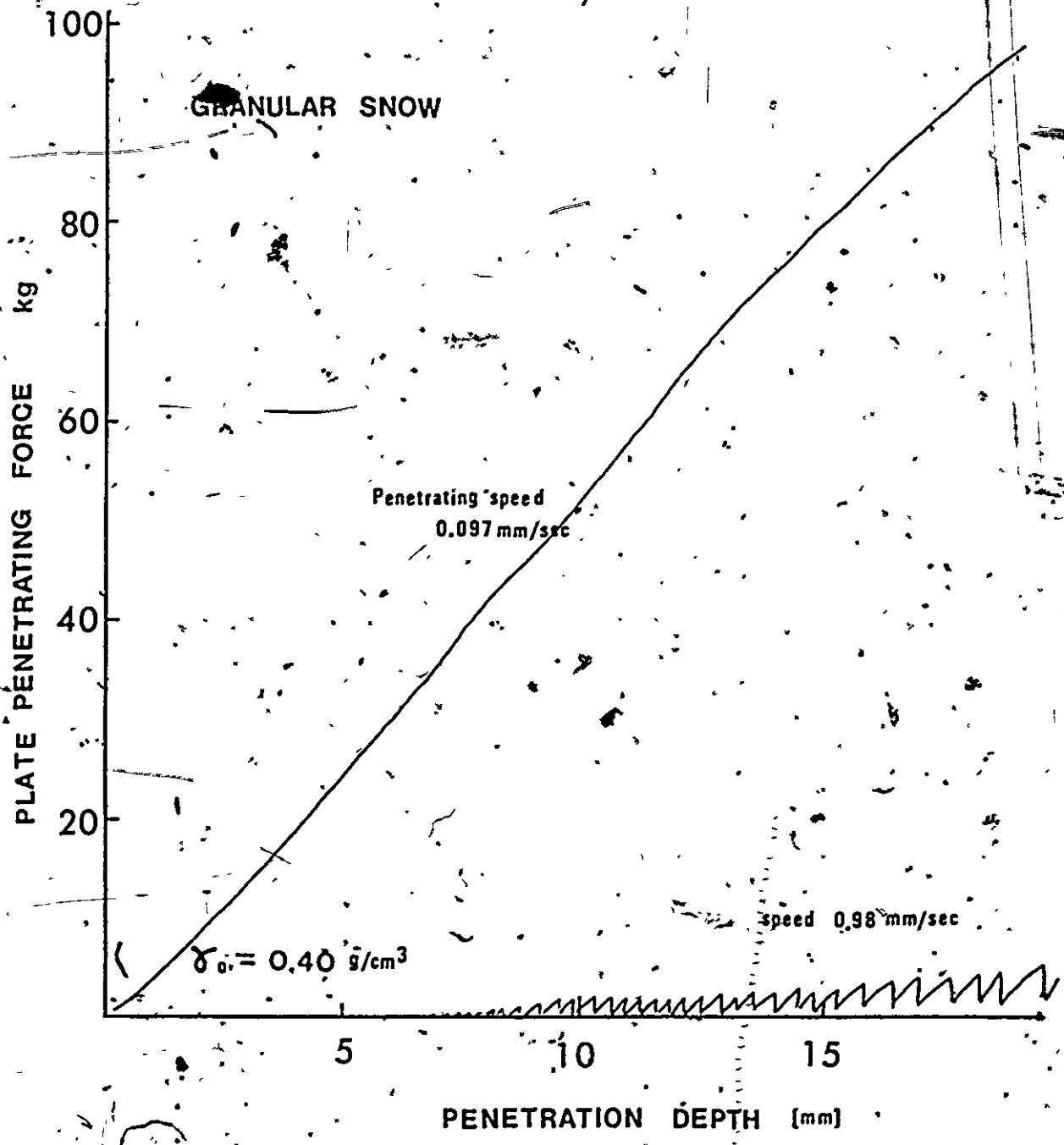


Fig: 7.39 Relationship between Penetrating Force and Depth for Granular Snow in Rectangular Rigid Plate Penetration Test (Glass-Sided Experiment)

speed of 0.097 mm/sec is remarkably higher than that obtained by the higher penetration speed. This trend is similar to that obtained from the ductile and brittle compression performances. Therefore, the lower penetration speed performance can be described as ductile, while the high speed penetration can be described as brittle. It was pointed out in the previous sections that the ductile behaviour of snow provides for the hardening of structure in relation to the adhesion theory, while the brittle behaviour of snow may result from the fracture. It is expected that the microscopic deformation mechanisms of these penetration performances are similar to those found in the confined compression tests. Therefore, under the lower speed penetration, the microscopic deformation mechanism can be described in terms of the increase in contact area between snow grains, especially for granular snow. On the other hand, the behaviour of snow under the higher penetration speed performance can be described as the microfractures resulting from the intergranular slippages or/and the breaking of grains.

To provide for more detailed response characteristics of snow under the plate penetration, the changes in snow properties during the plate penetration are examined by means of the blade penetrating technique.

Change in Snow Properties under Plate Penetration

The blade penetrating technique was established in the preceding section. It was found that the blade penetrating force (B.P.F.) is a function of unconfined compressive strength of snow. In addition,

the blade penetrating force may present the bonding strength of snow because unconfined compressive strength is a function of bonding strength of snow.

Figure 7,40 illustrates the blade penetration performance into snow densified by the plate penetration. By this method, the change in snow properties is examined. As mentioned earlier, the blade penetrating force presents the bonding strength of snow. Therefore, the change in bonding strength of snow densified by the plate penetration can be obtained from the blade penetrating technique.

Figure 7,41 shows the blade penetrating force contours of the granular snow densified by the plate penetration with a penetration speed of 0.097 mm/sec. The results indicates that B.P.F. is the greatest just below the plate and decreases downward and laterally. Note that B.P.F. denotes the blade penetrating force.

Figure 7,42 shows B.P.F. of granular snow densified by the higher speed (0.98 mm/sec) plate penetration. It is noted that it was impossible to obtain B.P.F. contour because large number of fracture planes or discontinuities in snow specimen resulting from the intergranular slippages or/and the breaking of grains. The profiles of B.P.F. obtained from Figs. 7,41 and 7,42 are presented in Fig. 7,43. Curve A indicated in this figure presents the profile of B.P.F. of granular snow densified by the lower speed (0.097 mm/sec) plate penetration, while Curve B presents the profile of granular snow densified by the higher speed (0.98 mm/sec) plate penetration. The penetration depth is approximately 2.2 cm for Curve A and 4.5 cm for Curve B.

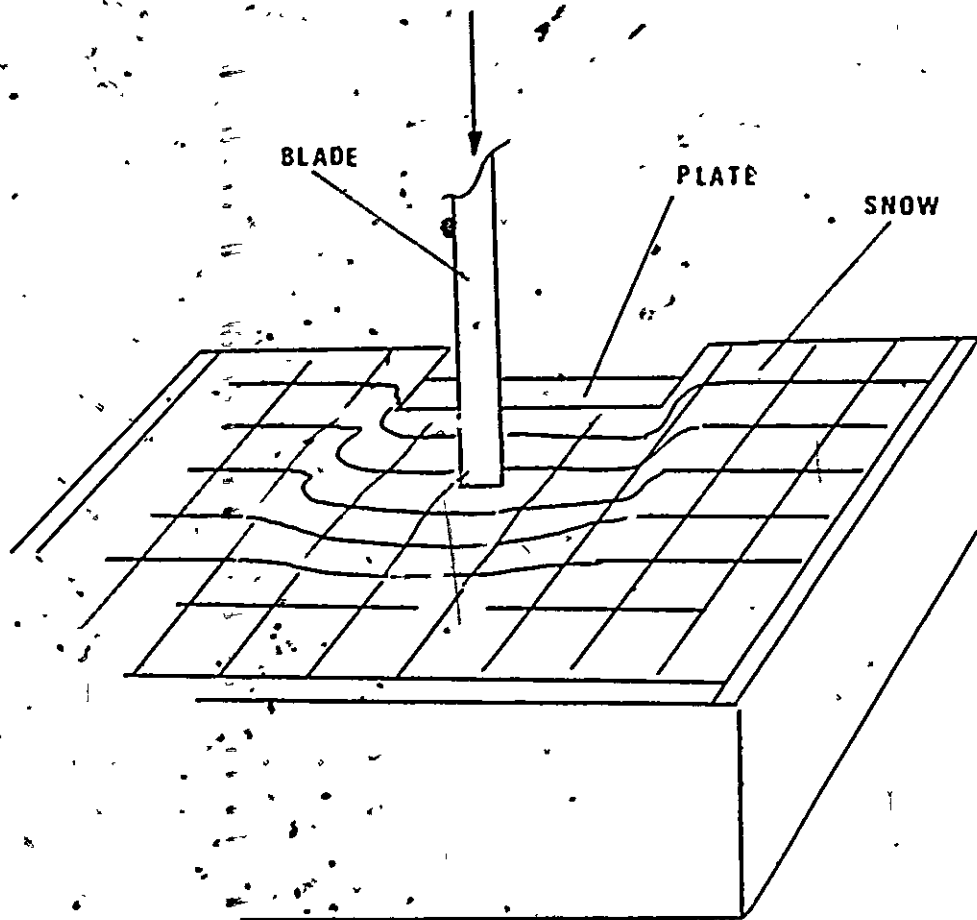


Fig. 7.40 Illustration of Thin Blade Penetration Performance
into Snow Previously Compressed by Plate Penetration

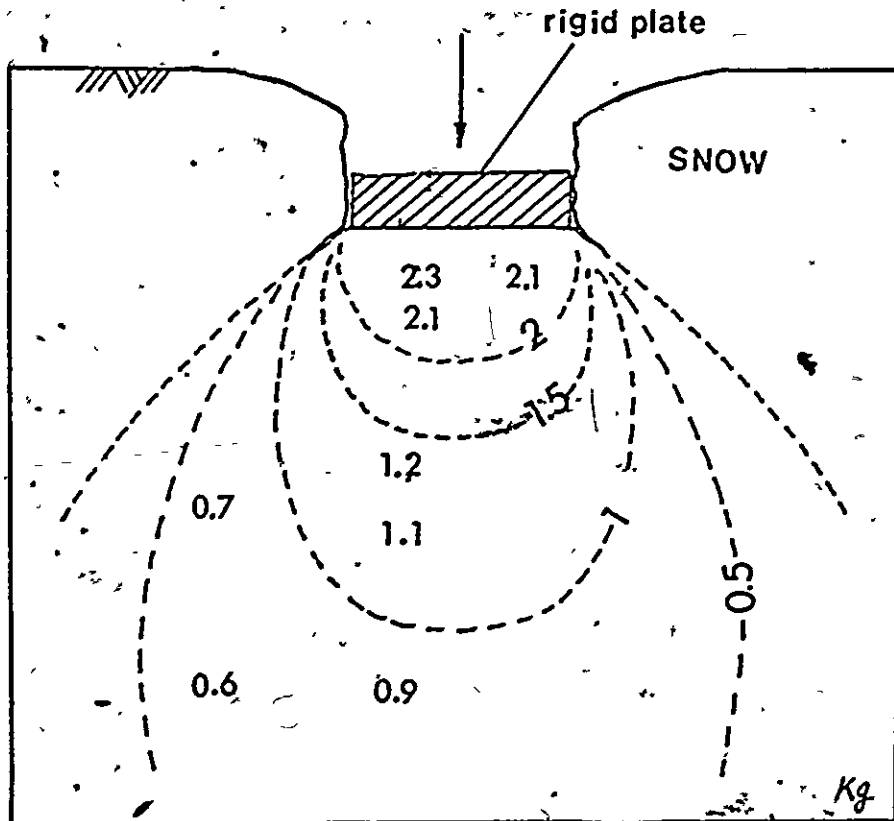


Fig. 7,41 Blade Penetrating Force Contours for Granular Snow Previously Compressed by Plate Penetration with a Speed of 0.097 mm/sec

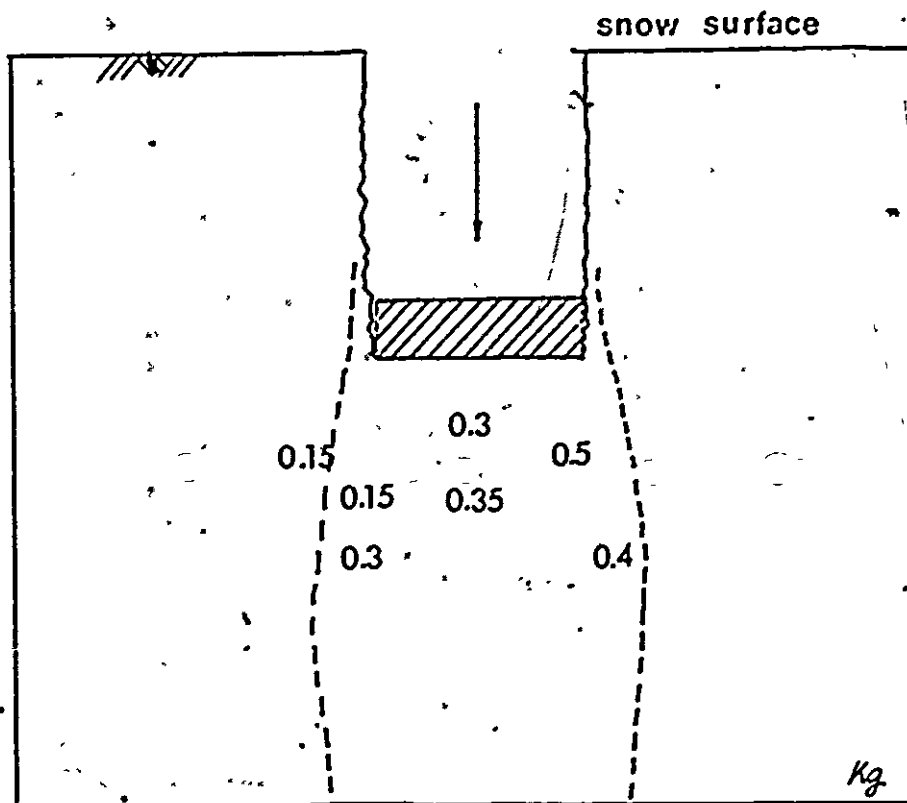


Fig. 7.42 Blade Penetrating Force for Snow Previously Compressed
by Plate Penetration with a Speed of 0.98 m/sec

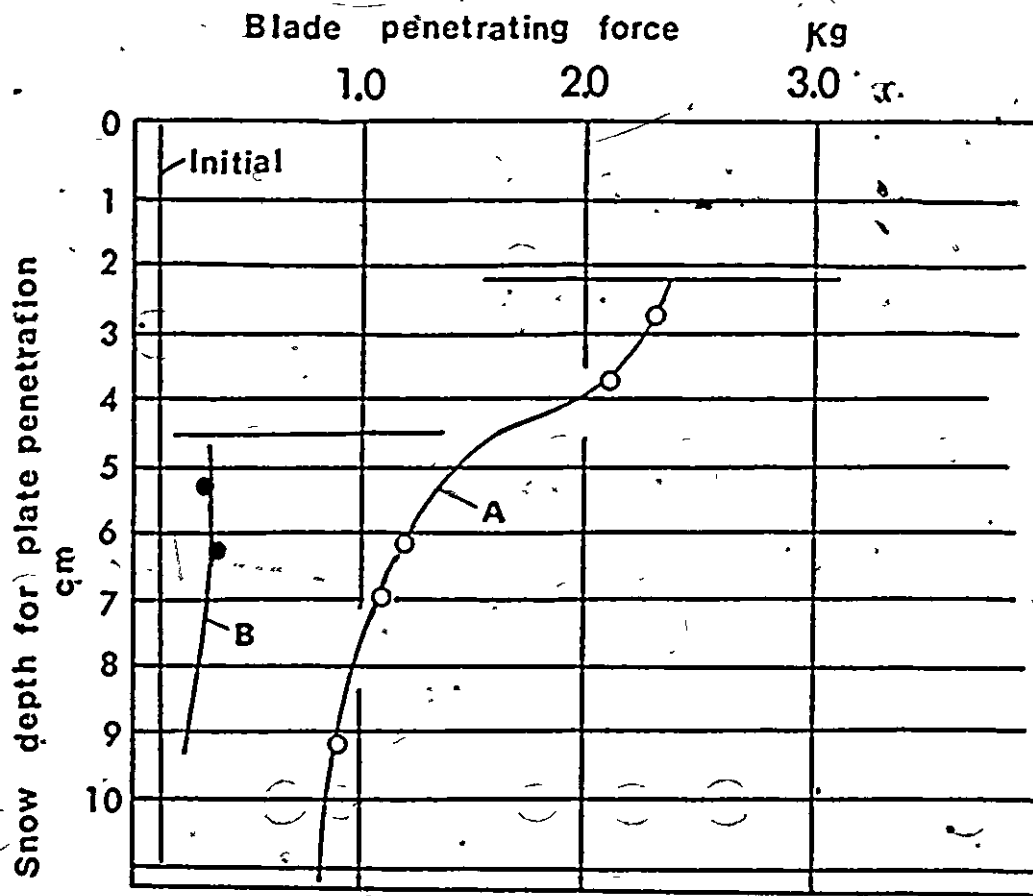


Fig. 7.43 Profiles of Blade Penetrating Force for Snow Previously Compressed
by Plate Penetration Obtained from Figs. 7.41 and 7.42

The large difference between Curves A and B is dependent upon the microscopic deformation mechanisms of snow. It was pointed out earlier that B.P.F. presents the bonding strength of snow. This means that considerable increase in bonding strength with respect to Curve A occurred but not to Curve B. This may be explained by the following:

- (a) with respect to Curve A, the microscopic deformation of snow was due to the increase in contact area between snow grains, and then the adhesive force in relation to the contact area increased, and
- (b) with respect to Curve B, the deformation of snow was brittle resulting from the intergranular slippages or/and the breaking of grains and then B.P.F. increased slightly because of the increase in density or/and the slightly increase in contact area between grains.

Thus, it is considered that the penetration behaviour of granular snow is similar to that found in the confined compression tests and is described in terms of the adhesion theory for relatively lower penetration speed performance and microfractures for relatively higher speed penetration performance. The discussion on the adhesion theory is presented in Chapter VII-1.

Sintered Snow

Figure 7,44 shows an apparent fracture mode for age-hardened snow for three days under the rigid plate penetration performance.

The basic snow was metamorphic snow for three weeks (see Chapter V-1).

This type of failure mode is apparently distinguishable from that obtained for fresh and initially granular snows. Thus the plate penetrating behaviour of snow is very much dependent upon snow type, penetration speed, and temperature.

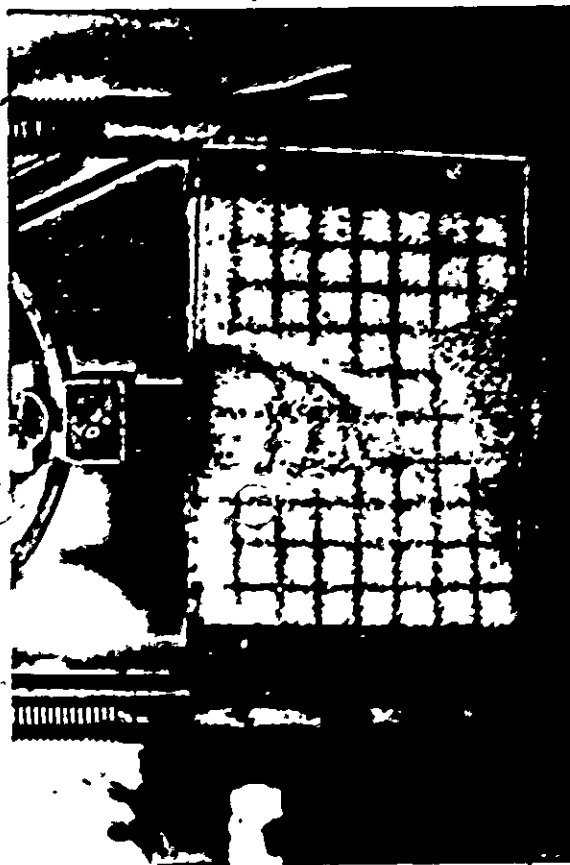


Fig. 7,44 Plate Penetration into Age Hardened Snow for 3 Days

CHAPTER VIII

GENERAL DISCUSSION AND CONCLUDING REMARKS.

VIII-1 Discussion on the Adhesion Theory

Any theory requires assumptions which often are true only to a limited degree. Thus, in theoretical ideas, questionable drawbacks can be verified only by actual experimentation.

The adhesion theory was developed in Chapter III. This theory is based on assumption that adhesive force acts on contact of two discrete solids and it depends on the area of contact, and is based on the work done by Bowden and Tabor (1950, 1964) who determined that metals adhere under the creep deformation. A similar concept was used by Trollope (1960) in the development of soil strength theory.

The experimental results obtained in this research concerning the adhesion theory are summarized as follows:

1. Contact area between snow grains under ductile compression increases (Chapter VI-1).
2. Strength of snow obtained from brittle condition is strongly dependent upon the deformation rate applied. The higher the deformation rate applied, the lower strength can be obtained (Chapter VII-1, 2, 3 & 4). It is expected that this trend is dependent upon the degree of increase in contact area at failure.

3. Under ductile condition, snow becomes strong with respect to strain. This hardening of snow is unlikely to occur under brittle condition. This suggests that the type of deformation, i.e., ductile or brittle, is very important to describe snow response characteristics.

Further experimental results obtained are discussed herein. Figure 8,1 shows a adhered granular snow specimen after ductile confined compression. It is apparent that if the specimen remains as granular the grains will disaggregate when the specimen was pushed out from the test cylinder. The figure, therefore, suggests that most of the snow grains adhered.

The increase in adhesive force with respect to ductile deformation is shown in Fig. 8,2. The basic procedure to obtain the results shown in the figure is described as below:

1. Initially granular snow was compressed in the standard test cylinder. The deformation rate used was relatively low (i.e., 0.097, 0.176 and 0.227 mm/sec) as indicated in the figure.
2. The compressed snow specimens were pushed out (Fig. 8,1) and then they were subjected to unconfined compression test.

In the unconfined compression test (Chapter VII-2), it was mentioned that unconfined compressive strength of snow is strongly dependent upon the bonding strength of snow. Therefore, Fig. 8,2.

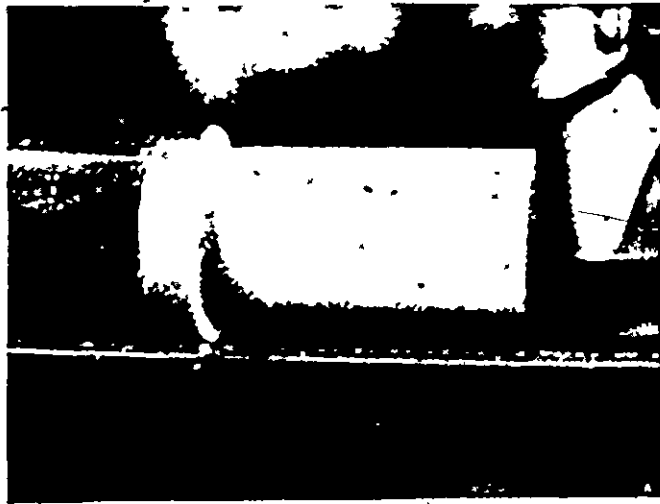


Fig. 8,1 Adhered Snow Specimen under Confined Compression

implies that the increase in unconfined compressive strength with respect to the maximum densified stress in the confined compression tests results from the increase in bonding strength of snow. There may be still arguments against the preceding statements because it may be true that the increase in density during the confined compression tests affected the increase in unconfined compressive strength. However, it is noted that density alone did not affect the unconfined compressive strength (see Fig. 7,6). For another example, Fig. 8,3 is presented. This figure shows stress-deformation relationships obtained by changing the compressive speeds during the confined compression. The curves shown in the figure were obtained from initially granular snow. The initial densities of both specimens are same (0.49 g/cm^3). The upper curve was compressed first with a compressive-velocity of 0.097 mm/sec and then the velocity was increased to 0.98 mm/sec only when the specimen was compressed up to 0.5 cm . Whereas in the case of lower curve the specimen was initially compressed with a velocity of 0.98 mm/sec and then the velocity was reduced to 0.097 mm/sec when the specimen was compressed up to 1.4 cm . Since the condition of compression was the standard confined compression used in Chapter VII-2, the deformation represents the density changes. Now we compare the stresses at a deformation of 0.65 cm for both curves indicated in the figure. Note that the densities at that deformation are same. As shown in the figure, the stress of upper curve indicates approximately 0.3 kg/cm^2 while the stress of lower curve is only 0.05 kg/cm^2 . The deformation rates of both curves are same (0.098 mm/sec), thereby the external

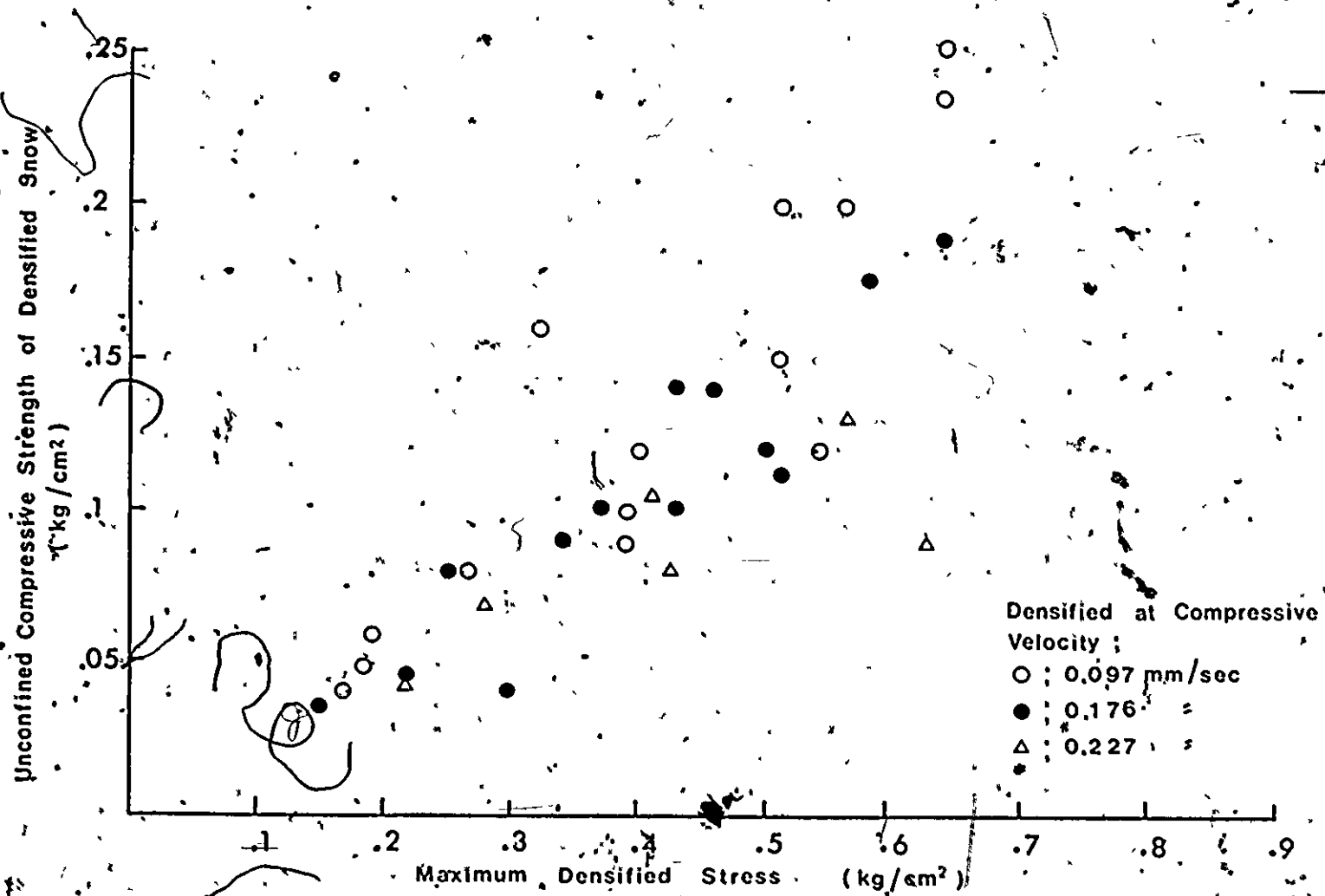
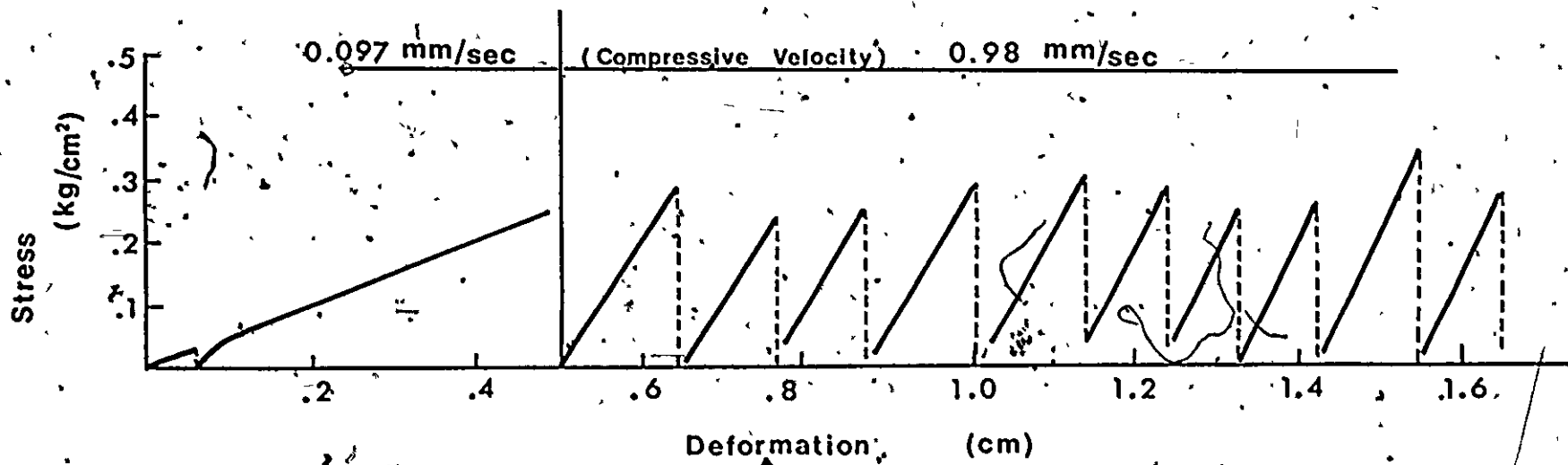
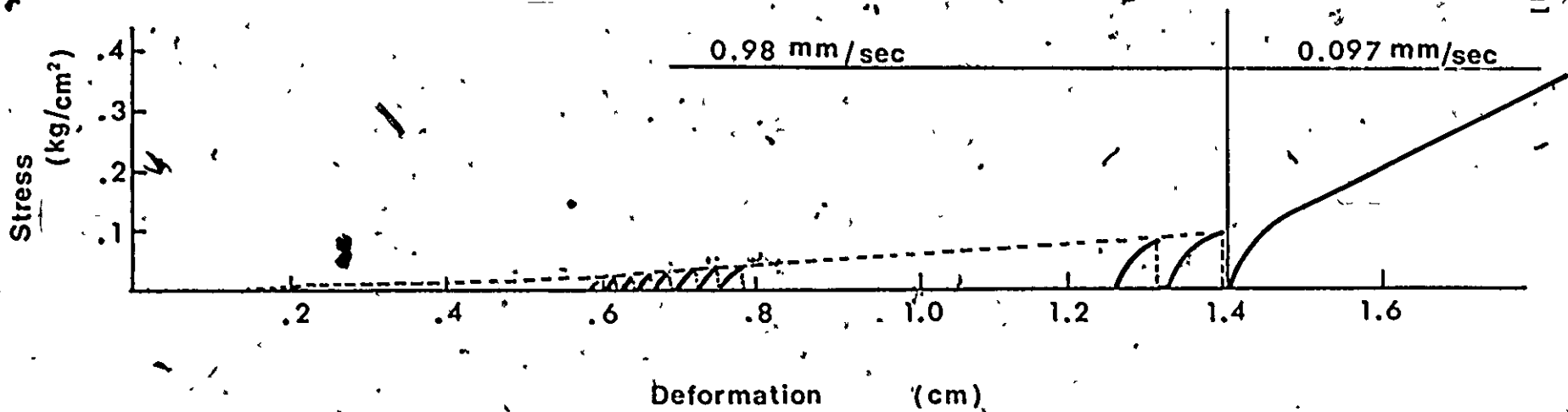


Fig. 8.2 Unconfined Compressive Strength of Snows Previously Compressed under Confined Condition



$h_0 = 12.9 \text{ cm}$



211

Fig. 8.3 Typical Rate Effect of Deformation in Confined Compression

conditions are same. The question is why the large difference between the observed stresses? This is explained by the fact that, for the upper curve, the ductile compression (with compressive velocity of 0.097 mm/sec) up to 0.5 cm prior to the brittle compression (at a velocity of 0.98 mm/sec) contributed to the increase in the adhesive force.

Thus it may be concluded that the ductile deformation contributes adhesion in snow and produces a different structure than with the brittle compression.

From the microscopic point of view, a simple model concerning with deformation mechanism of snow is illustrated in Fig. 8,4. The model illustrated in this figure indicates (a) initially point contact between grains, (b) sudden intergranular slippage, (c) increase in contact area followed by intergranular slippage and (d) continuous increase in contact area. Processes (a)-(b) and (a)-(c) are identified as brittle or semi-brittle behaviour of snow while process (a)-(d) is identified as the ductile behaviour of snow (see Chapter VII-1). It was found that the processes shown in the figure are strongly dependent upon deformation rate. Process (a)-(b) can be described in terms of completely brittle behaviour, as described in Chapter VII-4,1. In process (a)-(c), deformation required to initiate slip is very important because the deformation provides for the increase in contact area and the strength of snow is dependent upon the adhesive force in relation to the increase in contact area. This was mentioned in Chapter VII-3. It is considered that process (a)-(d) makes snow strong

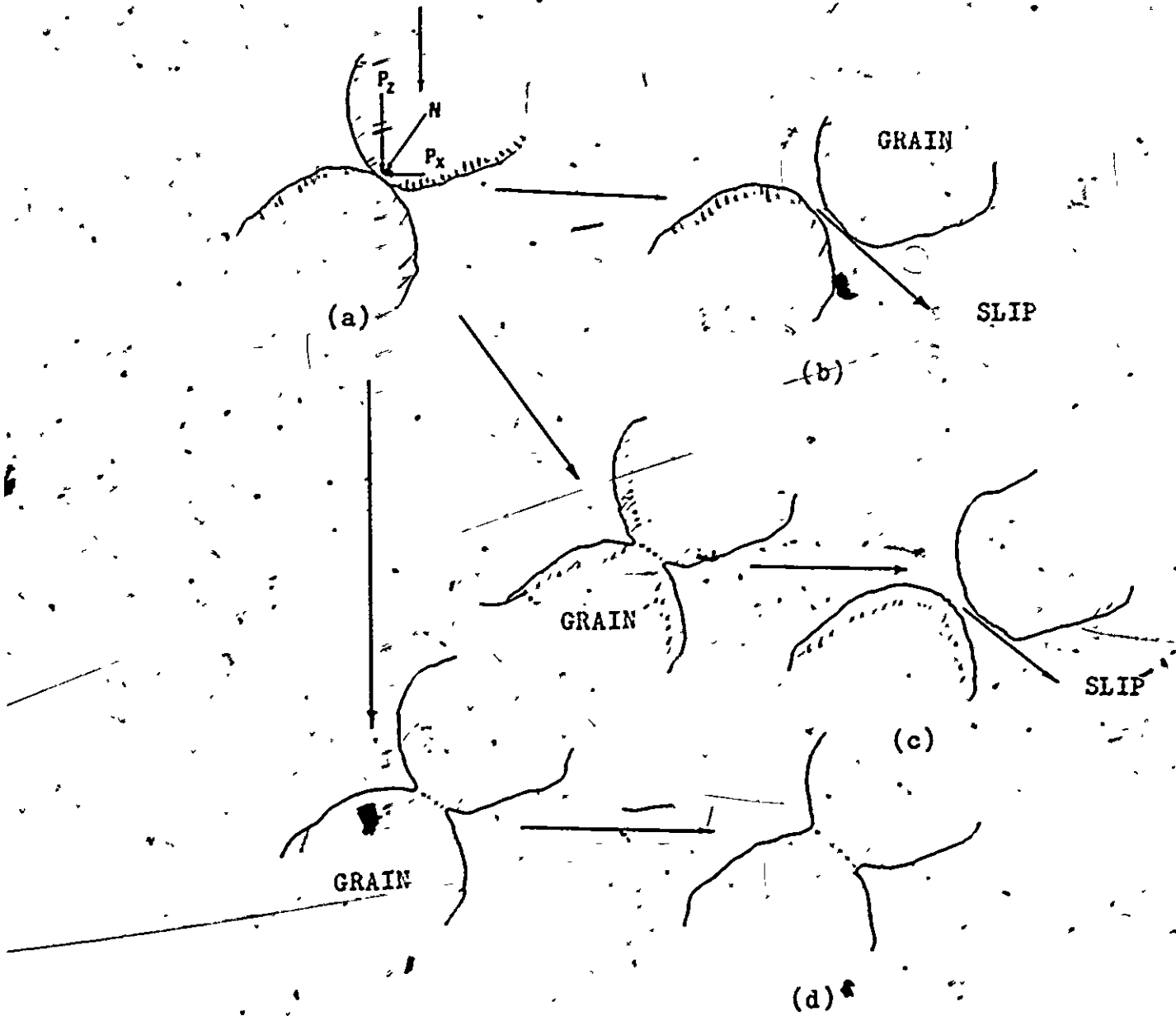


Fig. 8.4 Microscopic Model for Various Deformation Types of SnO₂

because of an increase in adhesive force with respect to the contact area. The apparent mechanical feature of this process is not too dissimilar to other viscous materials. From the macroscopic point of view, the model concerning with deformation mechanism was presented in Fig. 7,18.

In the case of shear performance of snow, basic deformation mechanism of snow may be similar to the model shown in Fig. 8,4. From the macroscopic point of view, the shear performance concerning with the adhesion theory is illustrated in Fig. 8,5. The model illustrated in this figure, in fact, neglects the effect of interlocking, however, it may be applicable to loose snow.

For granular snow, the shear strength in respect to the model illustrated in Fig. 8,5 can be presented by:

$$\tau = A_c S_e + \sigma_n \tan \phi \quad \dots (7,2)$$

Where

- τ is the shear strength
- A_c is the adhesion force per unit area acting on the effective contact area, S_e
- σ_n is the normal force applied
- ϕ is the inherent frictional angle.

As we know by now, the effective contact area is very complicated in terms of deformation exerted by the normal pressure, snow structure and temperature (Chapter VII-3).

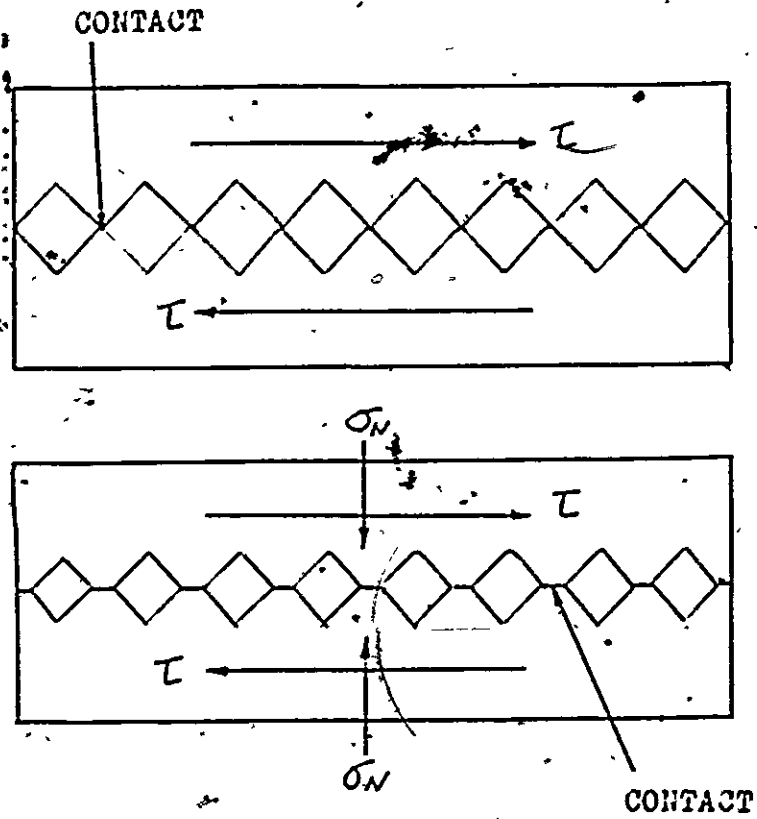


Fig. 8,5 Macroscopic Model of Snow for Direct Shear Test

Thus the adhesion theory is concerned with the most basic response characteristics of snow. In the present research, the adhesion theory was examined mostly for granular and poorly bonded snow. However, the concept can be applicable to fresh and strongly bonded snow.

VIII-2 Proposition of Snow Classification for Engineering Purposes

It was shown that the nature of snow, especially morphology as well as external conditions, is quite important in predicting engineering properties of snow. In this section, therefore, a classification of snow is proposed based on their constraints. At present, there are many problems to establish accurate classification of snow because of considerable lack of information on the properties and behaviour of snow. Therefore, snow classification in this section is not necessarily final and it should be changed when more information on snow properties are obtained in the future.

Basically snow is classified here based on factors governing snow structure and external conditions. The internal factors are (a) grain size, (b) grain shape, (c) intergranular interaction and (d) density, while the external factor is temperature.

With respect to grain characteristics, snow may be classified as:

- (a) fresh snow, and
- (b) metamorphic snow

as mentioned in Chapter V-1. It is not difficult to distinguish fresh snow from metamorphic grains by visual inspection. The grain size of snow can be obtained by the sieve analysis. Note that the sieve analysis is not applicable at higher temperature because grains adhere.

And from intergranular interaction point of view, snow may be classified as:

- (1) fresh snow,
- (2) granular snow,
- (3) semi-bonded snow,
- (4) sintered (bonded) snow, and
- (5) wet snow above the melting point.

It was found that the unconfined compressive strength of sintered snow is very dependent upon its sintering time. This means that unconfined compressive strength of snow is a function of the bonding strength of snow. It is noted that bonding strength of snow is very dependent upon sintering time (see Chapter II and Chapter VII-1). Therefore, sintered snow may be divided into (a) high sintered (bonded) snow (i.e., high strength snow) and (b) poorly sintered snow (i.e., low strength snow). Note that a typical poorly sintered snow is granular snow.

With respect to density, snow may be divided by the critical density of snow. The critical density (Chapter VII-2) is defined as the maximum packing density of snow without the bonds between grains. It was found previously that the critical density depends on snow type (Chapter VII-2). Basically, the critical density gives us not only the amount of compressibility but also the information whether or not microfractures of snow occur under the load. It should be noted that the threshold density of snow depends on the deformation rate as described previously but the critical density of snow can be uniquely determined. Therefore,

- (a) low density snow, $\gamma_0 < \gamma_{cr}$, and
- (b) high density snow, $\gamma_0 > \gamma_{cr}$.

Ramseier (1963) proposed that snow is divided into four types with respect to density from the unconfined compressive strength and the Young's Modulus of snow. However, his classification is based on natural processed snow obtained from Polar region. Therefore, he did not consider the existence of semi-bonded and granular snow. As mentioned previously, snow should not be classified from a single factor because there is no unique relationship between density and the other internal factors as found in the present study.

Now we examine entire nature of snow with respect to unconfined compressive strength and density with the information from the other internal factors governing snow structure. In Fig. 8.6, Curves a, b and c indicate relationships between unconfined compressive strength

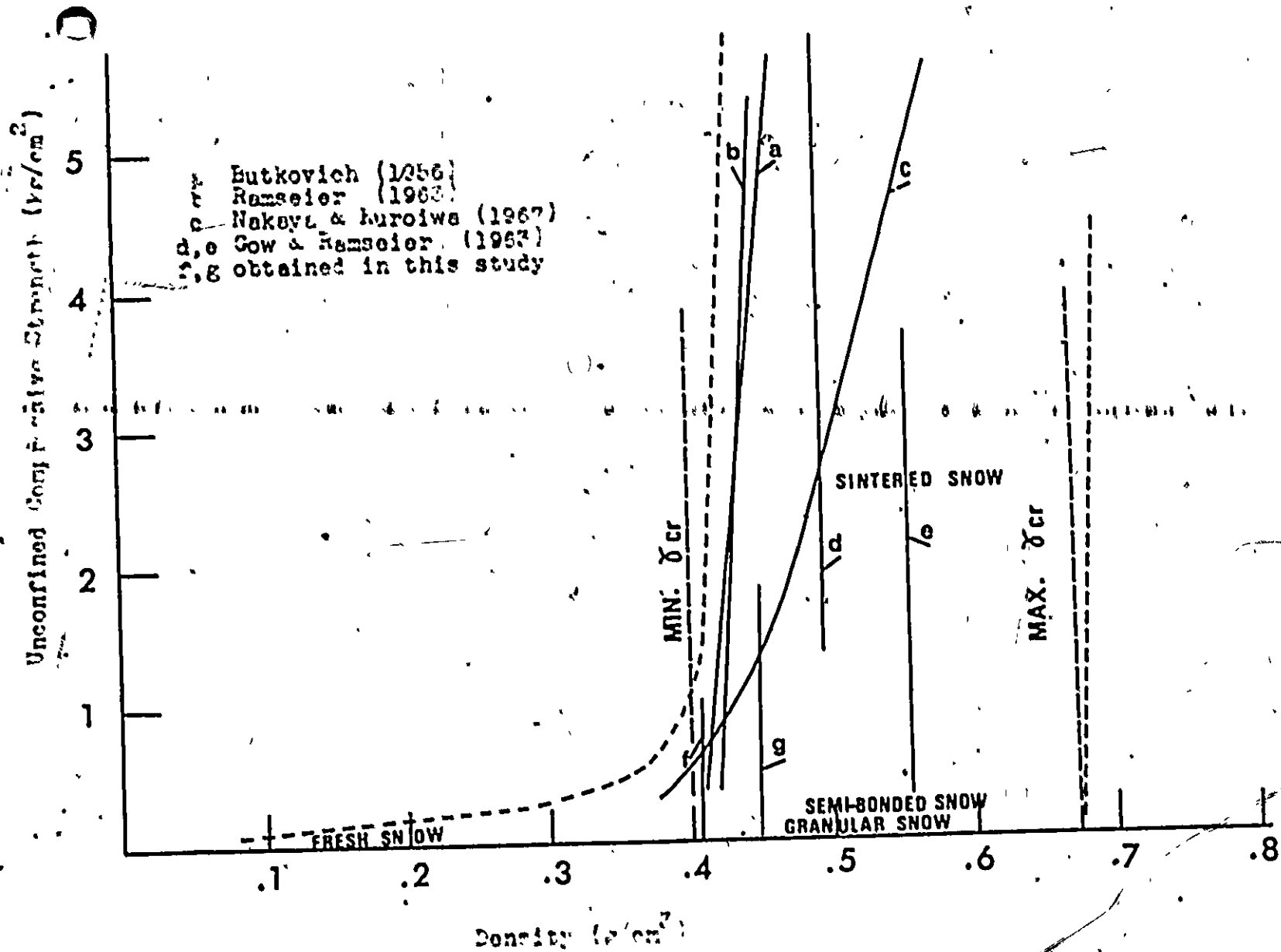


Fig. 8,6 Various Snow Nature in Relation to Unconfined Compressive Strength and Density

and density for natural processed snow obtained by Butkovich (1956), Ramseier (1963) and Nakaya and Kuroiwa (1967) respectively. Curve a obtained by Butkovich is very close to Curve b obtained by Ramseier though temperatures are different (-10°C by Butkovich and -49.4°C by Ramseier). However, Curve c obtained by Nakaya and Kuroiwa lies quite below Curves a and b. This may be explained by the varied nature of naturally processed snow though the test techniques used by them may also affect the strength of snow. Curves d and e shown in the figure indicate the age hardening of repacked snow obtained by Gow and Ramseier (1963). These two curves indicate that the unconfined compressive strength of snow increases with time without the large changes in density. This process in snow is identified as the sintering and is often called as the age hardening of snow. The detail of sintering process was presented in Chapter II. Same trend of age hardening of snow (Curves f and g) was also obtained in the present study as shown in the figure. It is apparent from the curves shown in the figure that strength of snow is independent of density. This suggests that snow should not be classified from the density alone.

The critical density of snow is defined as the maximum packing density without the bonding between snow grains. In other words, above the critical density, snow is always of bonded or sintered nature. It was found that the critical density of snow varies with respect to snow type. Therefore, we consider the maximum critical density and the minimum critical density. It is noted that the critical density is higher for well graded snow and is lower for uniformly graded snow

(Chapter VII-2). It is expected from the experimental results obtained in the research that the maximum critical density is approximately 0.67 g/cm^3 and 0.40 g/cm^3 for the minimum critical density as shown in the figure.

The unconfined compressive strength of fresh snow is very low as mentioned previously. The physical and mechanical properties of fresh snow can be described as follows:

- (a) very complex shape of crystals, consequently interlocking nature,
- (b) very low density (approximately 0.1 g/cm^3).
- (c) high compressibility because of initially low density.
- (d) low supportability because of low unconfined and confined compressive strength.

By considering the preceding statements, nature of snow can be indicated as shown in Fig. 8.6. For example, fresh snow lies on a low density range as indicated in the figure though higher density can also be obtained by densification. Granular snow lies on the density axis shown in the figure in a range of density from approximately 0.3 g/cm^3 to the maximum critical density (i.e., approximately 0.67 g/cm^3), while semi-bonded snow may lie above granular snow with respect to unconfined compressive strength axis in almost same density range to granular snow as indicated in the figure. Note that it is possible for semi-bonded snow to have higher density than granular snow because of

TABLE 8.1 Snow Classification Based on the Study

	Fresh Snow	Granular Snow	Semibonded Snow	Sintered Snow	
				poorly	strongly
grain	complex shape	METAMORPHIC GRAIN			
intergranular force	interlocking	friction and interlocking	adhesion by water film	bonding by sintering	
density [g/cm ³]	— 0.1 —	0.3 — 0.65	0.3 — 0.7 —	0.2—0.65	0.4 — 0.9
σ_c [kg/cm ²]	— 0.1 —	≈ 0	—	— 2	2 — 30
H / R [see Appendix C]	more than 3	— 1 —	temp. dependent	rock type	
δ_{cr} [g/cm ³]		0.4 — 0.65			
$\tau - \sigma_n$	SAND TYPE		sensitive clay type	sensitive clay type	
B.P.F. [kg]	≈ 0			— 8	8 +
	HIGH COMPRESSIBILITY MICROFRACTURE			high supportability	

B.P.F₁ - Thin blade penetrating force

222

the water content in the pores. Sintered snow, as shown in the figure, has high unconfined compressive strength in comparison with other types of snow as indicated by Curves a through g. The unconfined compressive strength of sintered snow depends on the bonding strength (i.e., sintering time) as mentioned previously.

From the practical point of view, unconfined compressive strength of snow can be represented by blade penetrating force (Chapter VII-4). Therefore, snow type can be obtained from B.P.F., density and additive grain characteristics.

To appreciate snow type properly, it is necessary to know the properties and behaviour with respect to type of snow. From the present research, main properties and behaviour of various types of snow, i.e., fresh, granular, semi-bonded and sintered snow, are presented in Table 8. It is noted that this table is not well established because there is still a lack of necessary information and apparently the table is not applicable for wet snow which was not studied in this research. Therefore, snow classification should be completed in future in such a way proposed in this study.

VII-3 Concluding Remarks

Theoretical and experimental investigations on properties and behaviour for various types of snow were made. From the study undertaken the following conclusions are drawn.

1. The adhesion theory based on the assumption that two discrete solids adhere under plastic, viscous or creep deformation, and as based on the work done by Bowden and Tabor (1950, 1964), is applicable to snow. It is concluded that ductile compression provides for an increase in contact area between snow grains. This causes a hardening of the snow structure.
2. Type of behaviour of snow is mainly described in terms of brittle or ductile. Brittle behaviour of snow is related to failure or fracture whereas ductile behaviour of snow is described in terms of the adhesion theory.
3. Unconfined compressive strength of snow is obtained from the brittle stress-strain curve and it is strongly dependent on snow type and deformation rate. Higher deformation rate will cause lower unconfined compressive strength. This trend is uncommon to other materials but is well explained by the adhesion theory.
4. Initial bonding of snow is very important for the strength characteristics much more than density.

Loose snow fails by microfailure which does not follow the conventional shear theories. Snow with a density less than the critical density possibly fails by microfailure. Critical density is defined as the maximum packing density of snow

without bond development between snow grains.

6. Transition from brittle to ductile behaviour in snow is described in terms of critical deformation rate, snow type and temperature. On the other hand, transition of snow is dependent on threshold density. Threshold density of snow denotes the density at the transition from brittle to ductile in confined compression with controlled deformation rate. Threshold density is strongly dependent upon deformation rate, snow type and temperature. The significance of threshold density is that it indicates increase in contact area between snow grains, which occurs above that density. It was mentioned that increase in contact area will cause increase in adhesion of snow.
7. Shearing response characteristics with respect to snow type are mainly divided into three types, i.e., sand type, sensitive clay type and rock type, from the apparent feature of $\tau - \sigma_n$ curves. On the other hand, shear strength of snow is very dependent on shear velocity. At temperature of -13°C , higher shearing velocity provides lower shear strength for granular snow. This trend is uncommon to other materials but it is explained by the adhesion theory.
8. Rigid plate penetration behaviour of snow is strongly dependent on penetrating speed and snow type. Generally, lower

penetration speed will provide higher penetration resistance. This trend is similar to the compressive and shear behaviour of snow, but not to other materials. Very low penetration speed will cause an increase in adhesion of snow below rigid plate while relatively high penetration speed will produce microfracture of snow below rigid plate.

9. Thin blade penetration behaviour into snow may be useful for evaluation of strength characteristics of snow, especially in the field. Thin blade penetrating force has a relationship with unconfined compressive strength as shown in Fig. 7,33.
10. The fact that there is an extremely varied nature of snow, inevitably requires classification of snow. Snow type may be described by:
 - a) grain characteristics,
 - b) intergranular interaction, and
 - c) density.

Grain characteristics of snow are divided into two types: i.e., fresh snow crystal, and metamorphic grain. So far as the intergranular force are concerned, snow is classified into four types: fresh snow, granular snow, semi-bonded snow and sintered snow. With respect to density, snow is divided into two types: i.e., high density snow ($\gamma_0 > \gamma_{cr}$) and low density snow ($\gamma_0 < \gamma_{cr}$).

APPENDIX

TABLE A-1. International Snow Classification
(see Fig. A-1)

For this purpose the tentative snow classification proposed by the International Commission of Snow and Ice is considered to be most convenient. In this classification all the solid precipitations are included.

Practical Classification of Solid Precipitation.

Code	Graphic symbol	Term	Remarks
F1		Plates	F1a, F1b, F1c, F4 of General classification of snow crystals
F2		Stellar crystals	F1d, F1e, F1f, F1g, F1h, F1i, F2a, F2b, F2c, F3a, F3b, F4
F3		Columns	C1a, C1b, C1c, C2a, C2b
F4		Needles	N1a, N1b, N2
F5		Spacial dendrites	F5a, F5b
F6		Capped columns	CP1a, CP1b, CP1c, CP2a, CP2b
F7		Irregular crystals	CP3, S, I1, I2, I3
F8		Graupel (Snow pellet)	R4a, R4b, R4c
F9		Sleet (Ice pellet)	U. S. definition; frozen raindrops, fairly small and transparent
F0		Hail a) small hail (opaque) b) hail (transparent)	Solid precipitation formed by the successive freezing of water layers
B		Broken	Broken crystals of type 1, 2, etc.
R		Rimmed	R1, R2, R3
F		Flake	Clusters of crystals of type 1, 2, etc.
w		Wet	Wet or partially melted crystals of type 1, 2, etc.
—		English sleet	Snow and rain falling together.
D			The size of particle means the greatest extension of a particle (or average when many are considered) measured in millimeters. For a cluster of crystals it refers to the average size of the crystals composing the flake.

Type of particle

Additional characteristics

Size of particle

APPENDIX A

N1a	N1b	N2	C1a	C1b	C1c	C2a		C2b
P1a	P1b	P1c	P1d	P1e	P1f	P1g	P1h	P1i
P2a	P2b	P2c	P3a	P3b	P4		P5a	P5b
CP1a	CP1b	CP1c	CP2a	CP2b	CP3	S	I1	I2
R1		R2		R3a	R3b	R4a	R4b	R4c

Fig. A-1 International Snow Classification (see Table A-1)

INTERGRANULAR SLIPPAGE BETWEEN SNOW GRAINS

Relating to Fig. B-1, the intergranular slippages between grains may depend on the true stresses acting on contact area, the intergranular interaction and the type of material.

If we assume that snow grains are viscous, the deformation of grains should depend on the rate of deformation. If a very rapid deformation rate is applied on snow, it is expected that the grains behave like rigid material. Note that elastic deformation of crystal is usually very small in comparison with its large viscous, plastic or creep deformation.

This appendix considers the conditions of intergranular slippage of snow grains under both rapid and slow rates of deformation.

Equilibrium Condition

In Fig. B-1, it is assumed that applied force F from the macroscopic point of view and true forces P_z from the microscopic point of view, on a plane, are in a state of equilibrium (Fig. B-1). Under an application of controlled deformation rate, the forces depend on the deformation rate. This is very common to other viscous materials. Referring to Fig. B-1, an equilibrium can be written by,

$$F = \sum_{i=1}^n P_{z_i} \quad \dots \quad (B-1)$$

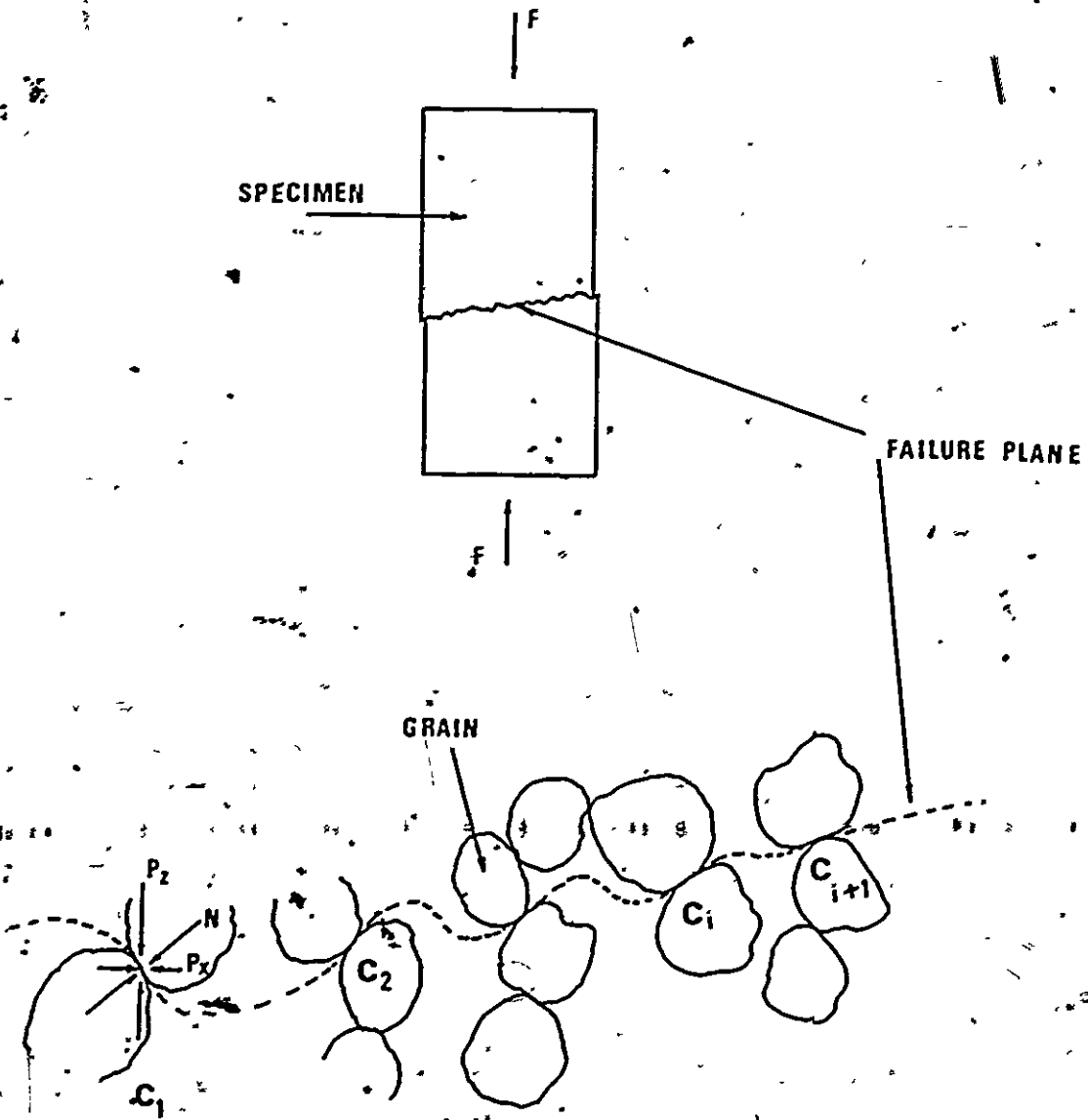


Fig. B-1 Stress Condition in Snow under Compression

Where i denotes i th contact and n denotes the total number of contacts on the equilibrium plane considered. Now, let us consider the following:

1. Rapid Deformation Rate

We assume that rapid deformation rate provides for the rigidity of snow grains for the following conditions:

(a) Uniaxial Force Condition ($P_z \neq 0$ and $P_x = P_y = 0$, Fig. B-2)

As a simple case, consider a point contact of grains as shown in Fig. B-2. By using the Amonton's law, an equilibrium condition of slippage can be given by,

$$\frac{P_z \sin \psi}{P_z \cos \psi} = \mu \quad \dots \dots (B-2)$$

If we represent as $\mu = \tan \phi$; Eq. B-2 becomes

$$\psi = \phi \quad \dots \dots (B-3)$$

Equation (B-3) may be concerned with Fig. B-3. The figure demonstrates that the cone shape of depositing granular material is uniquely determined by a ratio H^* / R^* where H^* is the height of the cone and R^* is the radius of bottom of deposits as shown in the figure. It is expected that the ratio H^* / R^* represents some properties of material.

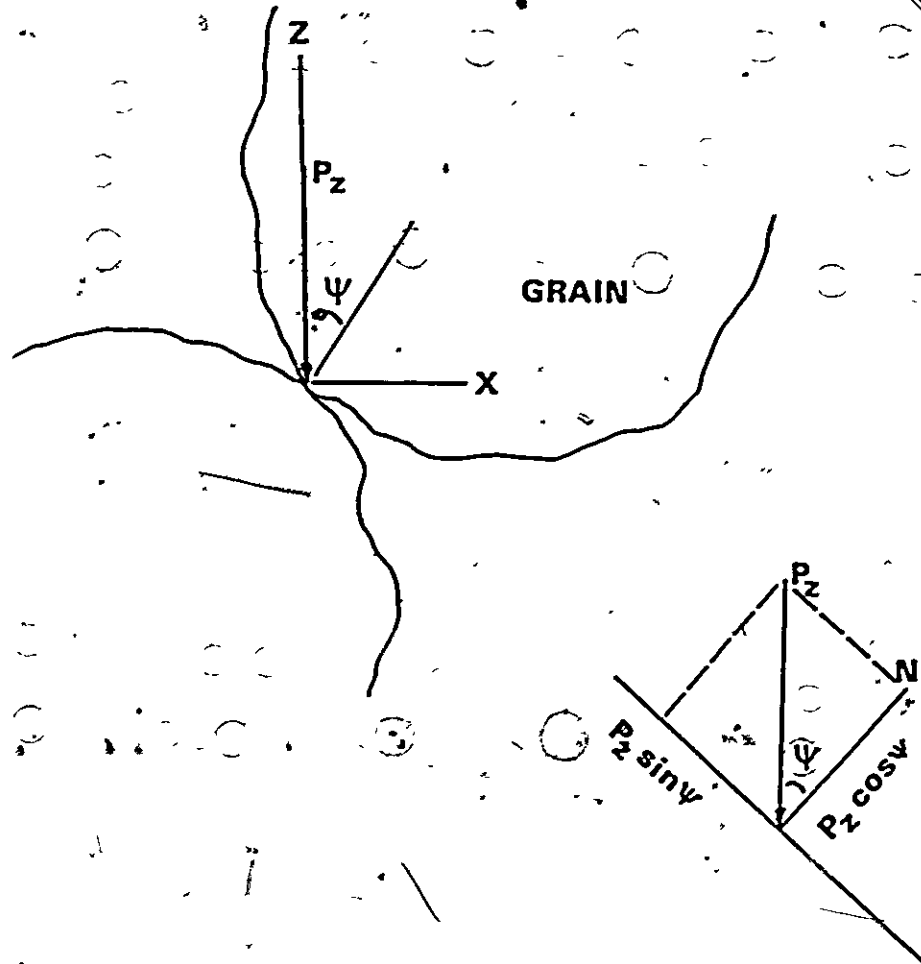


Fig. B-2 Intergranular Slip Condition under Uniaxial True Stress P_z at Contact between Grains

This idea is used in this study (Appendix C).

(b) Biaxial Force Condition ($P_z \neq 0, P_x \neq 0$ and $P_y = 0$, Fig.B-4)

With a similarity to the uniaxial force condition mentioned earlier, an equilibrium under biaxial force condition can be given by,

$$Pz_i \sin \psi = Px_i \cos \psi + \mu (Pz_i \cos \psi + Px_i \sin \psi)$$

$$\frac{Pz_i}{Px_i} = \frac{\cos \psi + \tan \psi \sin \psi}{\sin \psi - \tan \psi \cos \psi}$$

$$\tan \left(\frac{\psi}{2} + \psi' \right) \dots \dots \dots (B-4)$$

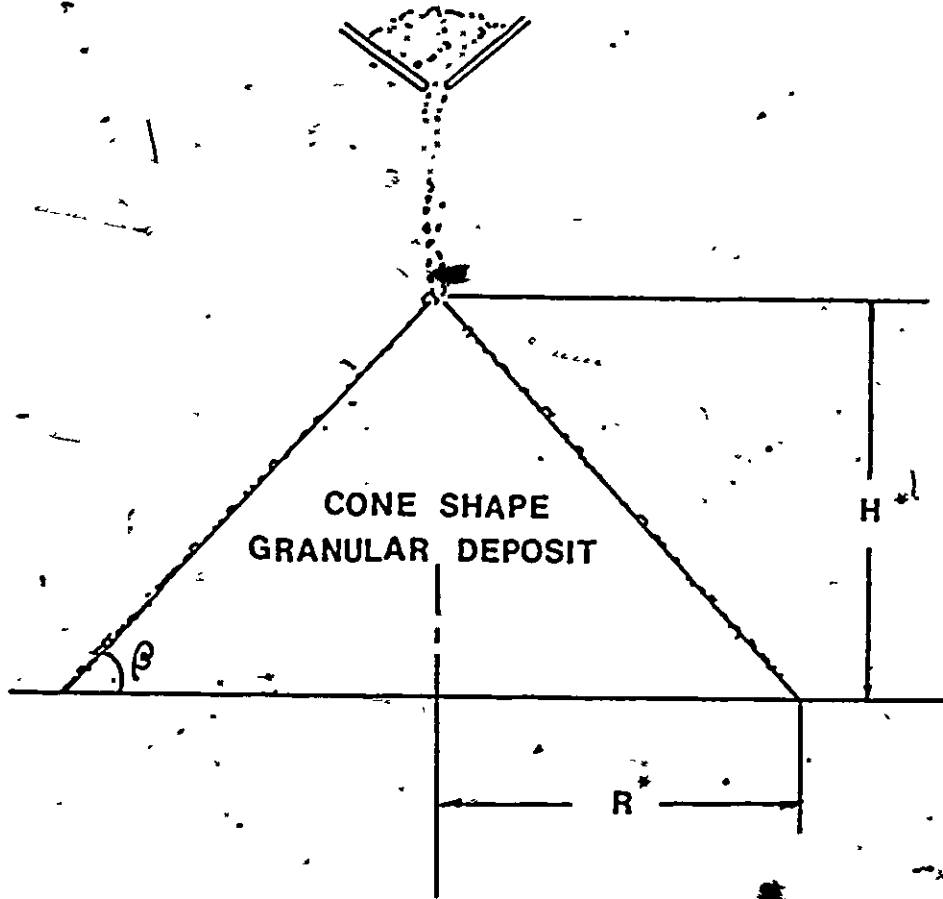
Equation (B-4) is being used by many researchers for the microscopic study of deformation mechanism of sands by assuming rigid sand particles.

2: Slow Deformation Rate

We assume that slow deformation rate provides for the viscous, plastic or creep deformation of snow grains for the following situations.

(a) Uniaxial Force Condition

We assume that a point contact increases up to S_c at a limiting equilibrium condition of slippage. Now we assume that an adhesive force is produced by the increase in contact area (the adhesion theory,



• Fig. 8-3 Depositing Performance of Granular Material

Fig. B-4). Then, the limiting equilibrium in relation to the increase in contact area can be given by,

$$Pz_i = A_c S_c + \mu P_z \cos \psi / (\sin \psi - \tan \psi \cos \psi)$$

where $\sin \psi - \tan \psi \cos \psi > 0$.

If the grains are spherical and the increase in contact area is expressed by Eq. (4,11) i.e., deformation with respect to P_x is assumed to be zero, Eq. (B-5) can be expressed by,

$$Pz_i = \frac{A_c \pi r^2 (3.9 \epsilon \cos^2 \psi - 1.785 \epsilon^2 \cos^4 \psi)}{(\sin \psi - \tan \psi \cos \psi)}$$

..... (B-6)

where A_c is adhesion force
 r is the radius of spherical grain
 ϵ is the strain applied
 ψ is the contact angle
 (see Chapter IV).

The equation assumed that no breaking of grain occurs under force P_z .

If

$$Pz_i < \frac{A_c \pi r^2 (3.9 \epsilon \cos^2 \psi - 1.785 \epsilon^2 \cos^4 \psi)}{(\sin \psi - \tan \psi \cos \psi)}$$

..... (B-6)

apparently, no intergranular slippage occurs.

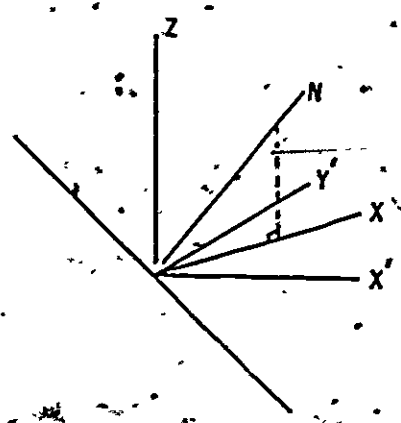


Fig: B-4 Intergranular Slippage Condition under Biaxial True Stress Condition

(b) Biaxial Force Condition

With a similarity to the case (a), the limiting equilibrium condition under biaxial force condition at a contact can be written as:

$$Pz_i = \frac{Px_i (\cos \psi + \tan \phi \sin \psi) + A_c S_c}{(\sin \psi - \tan \phi \cos \psi)} \dots (B-7)$$

From Eq. (4,11),

$$Pz_i = \frac{Px_i (\cos \psi + \tan \phi \sin \psi) + A_c \pi r^2 (3.9 \epsilon \cos^2 \epsilon - 1.785 \epsilon^2 \cos^4 \psi)}{(\sin \psi - \tan \phi \cos \psi)} \dots (B-7)'$$

Similar forms to Eqs. (B-5), and (B-7) may be applicable for sintered (bonded) snow as below:

$$Pz_i = \frac{A_s S_c}{\sin \psi - \tan \phi_e \cos \psi} \dots (B-8)$$

where A_s is the adhesion by sintering
 ϕ_e is the frictional angle for sintered snow.

$$Pz_i = \frac{Px_i (\cos \psi + \tan \phi_e \sin \psi) + A_s S_c}{(\sin \psi - \tan \phi_e \cos \psi)} \dots (B-9)$$

However, it should be noted that Eq. (4,11) is not applicable for sintered snow. Only qualitatively the concept of increase in contact area can be possible to apply for sintered snow.

DEPOSITING CHARACTERISTICS OF SNOW WITH RESPECT TO ITS GRAIN SIZE DISTRIBUTION AND GRAIN SHAPE

The depositing characteristics of snow depends on snow type. It is expected that the internal structure of the deposits may be influenced by the grain characteristics, i.e., grain size and shape. The attempt in this Appendix is to examine depositing characteristics of various snow in relation to prediction of snow type by knowing the depositing characteristics.

Experimental Procedure

1. Snow was sieved into cups as shown in Fig. C-1.
2. The maximum depositing height H^* (see Fig. C-1) was measured and a ratio H^* / R^* was obtained where R^* is the radius of cup. In addition, the depositing density of snow was also obtained.

Results

Figure C-2 shows apparent depositing figures of (a) fresh and (b) 2 year old snow.

The depositing density and H^* / R^* of various types of snow are presented in Table C-1.

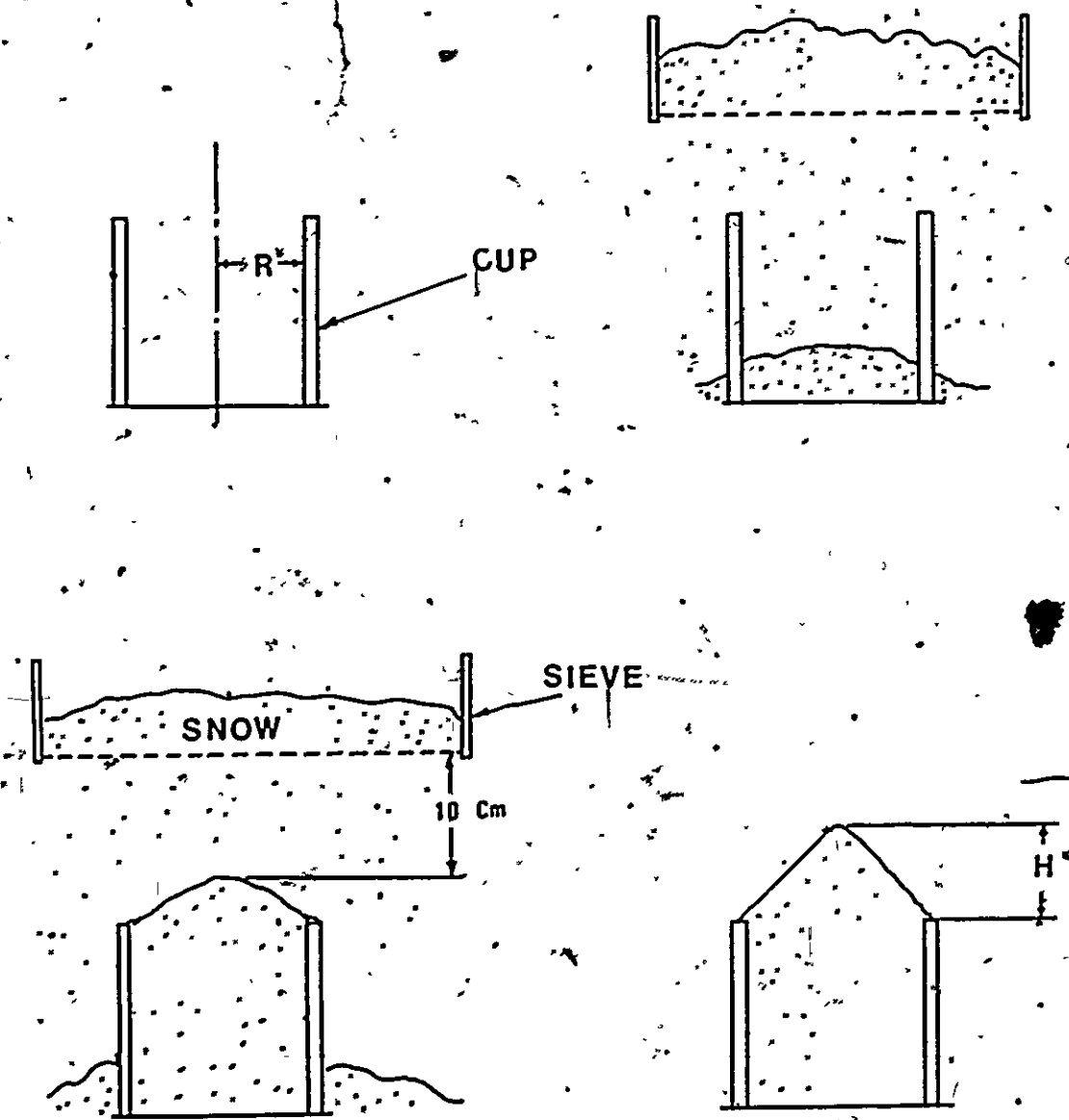
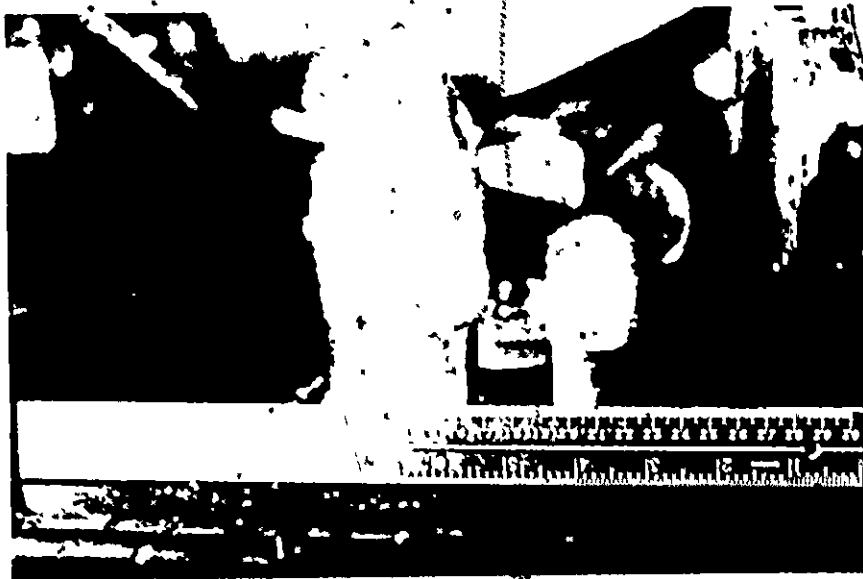
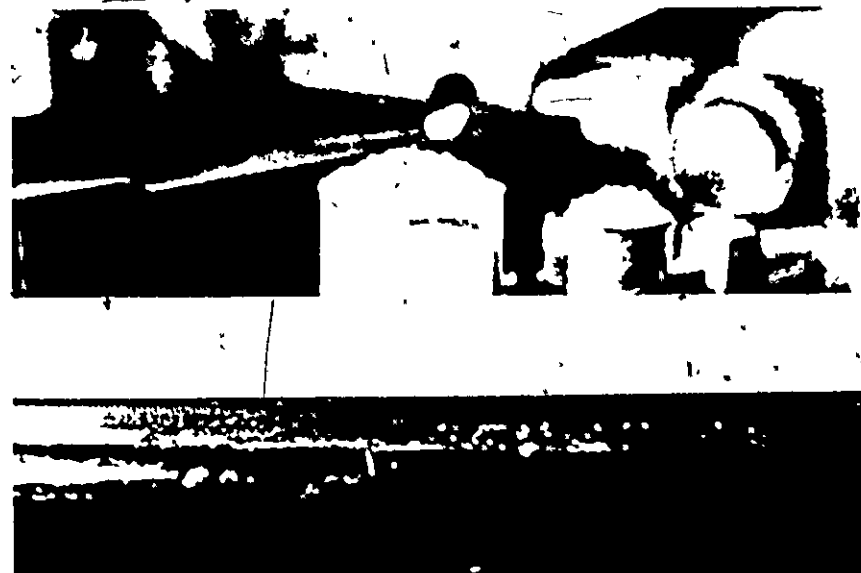


Fig: C-1 Depositing Performance of Snow into a Cup through a Sieve



(a)



(b)

Fig. C-2 Apparent Depositing Features of (a) Fresh Snow and
(b) Two Year Old Snow into Cups through a Sieve

TABLE C-1 DEPOSITING DENSITY AND H*/R* OF SNOW

SNOW TYPE	DENSITY (g/cm ³)	H*/R*	
		R* = 2.5 cm	R* = 1.3 cm
Fresh snow	0.12	more than 4	more than 3.2
3 week old	0.39	1.6	1.6
2 year old	0.49	0.6	0.9
1.19 < G < 2.38 mm	0.37	-	0.4
0.598 < G < 1.19 mm	0.44	-	0.8
0.417 < G < 0.598 mm	-	-	1.0

G denotes grain size.

TRUE GRAIN SIZE OF SNOW OBTAINED FROM THE MICROSCOPE ANALYSIS
AND APPARENT GRAIN SIZE FROM THE SIEVE ANALYSIS

The object to this Appendix is to compare grain size distributions obtained by the microscope analysis and by the sieve analysis which is being used for snow.

Snow Sample

Snow sample was uniformly graded by sieves (sieve openings of 0.598 and 1.19 mm, i.e., $0.598 < G < 1.19$ mm).

Microscope Analysis

Photographs of sufficient number of grains of the snow (i.e., $0.598 < G < 1.19$ mm) were taken through a microscope and then the short diameter D_s and the long diameter D_l of each grain were measured from the photographs.

Results

Figure D-1 shows the comparison between the true grain size obtained by the microscope analysis and the apparent grain size (i.e., $0.598 < G < 1.19$ mm) obtained by the sieve analysis. It should be noted that the distribution curves of true grain size cannot be compared with Fig. 5,2 because the curves of true grain size were obtained by number percentage of grains while the ordinary grain size distributions shown in Fig. 5,2 were obtained by weight percentage.

Figure D-2 shows the frequency distribution of D_s/D_l of snow sample used in this Appendix.

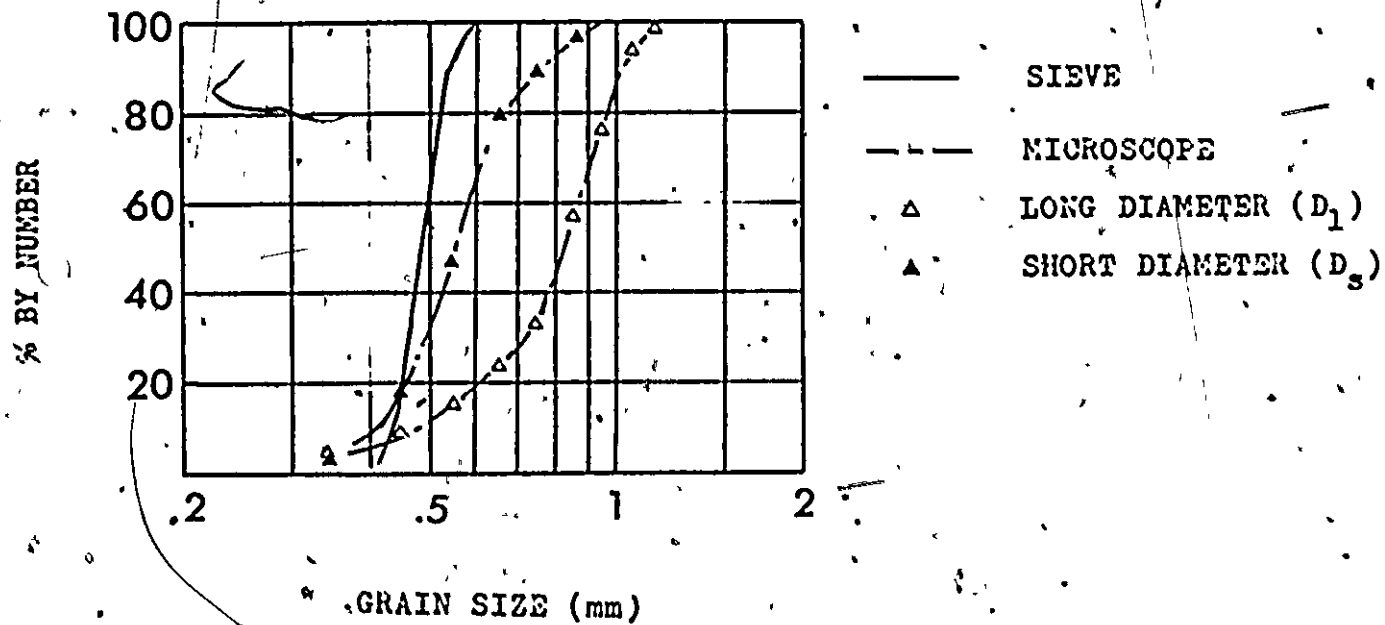
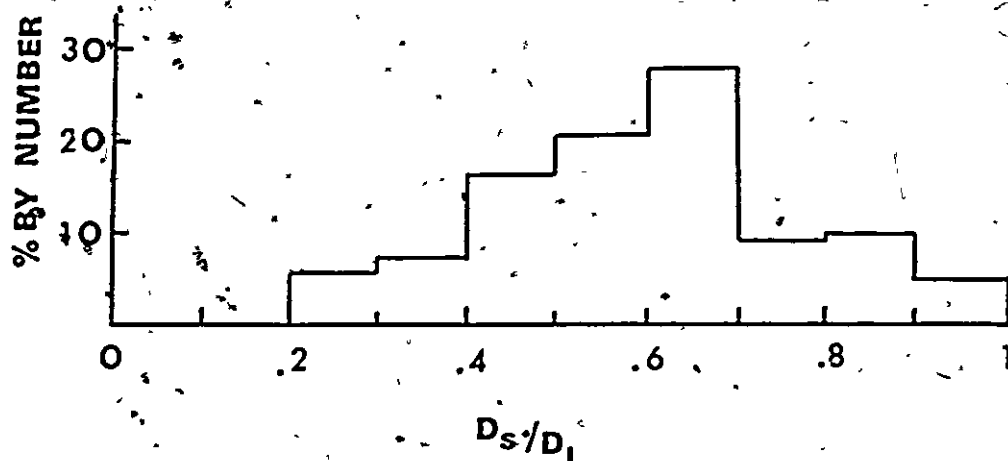


Fig. D-1 | A Comparison between Grain Size Distributions Obtained from the Microscope and the Sieve Analyses



D_s = SHORT DIAMETER OF SNOW GRAIN
 D_l = LONG

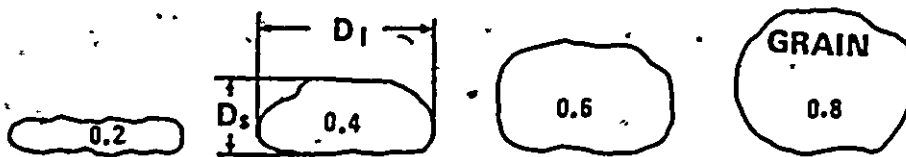


Fig. D-2 Frequency Distribution of Shape Factor (D_s/D_l) in Uniformly Graded Snow

MOHR'S ENVELOPE

The Mohr's theory assumes that the shearing stress at a yield is a function of the normal stress (σ) acting in the considered plane or

$$\tau = f(\sigma) \quad \dots (E-1)$$

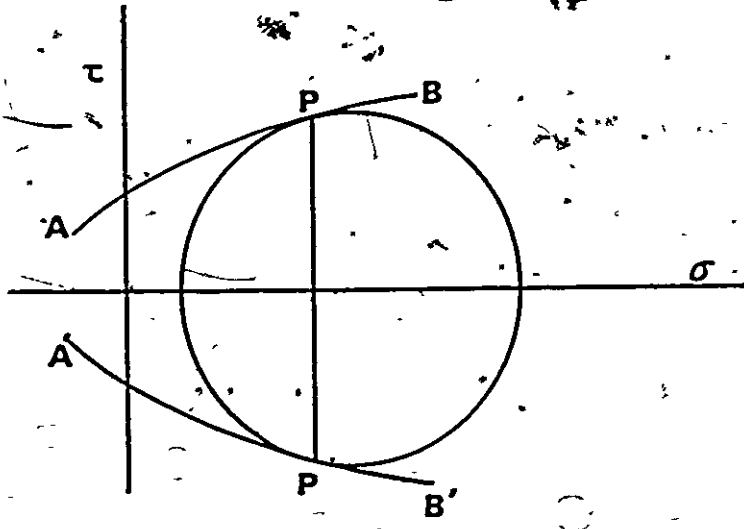
This relationship between τ and σ can be represented graphically by making a diagram in which τ and σ are taken as coordinates.

Figure E-1(a) shows such a diagram, called Mohr's circle.

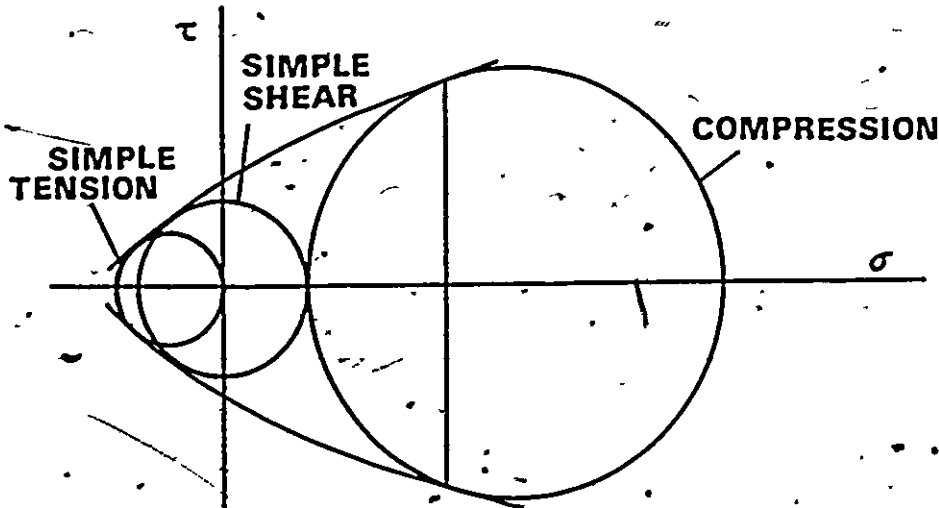
In Fig. E-1(a), Curves AB and A'B', called Mohr's envelope, are assumed to be parts of Eq. (E-1). Apparently, as a change of the sign of τ cannot influence failure. Curve A'B' is a mirror image of AB. Any state of stress can be represented by Mohr's circle in a $\tau - \sigma$ plane, it follows that for any circle lying wholly within Mohr's envelope the combination of shear and normal stresses will represent a stable condition. Because no portion of circle can lie beyond the envelope of the infinite number of possible circles passing through point P only the one tangent at that point can exist. Thus, the Mohr's envelope (or failure criterion) is the locus of the points of tangency corresponding to circles in the $\tau - \sigma$ plane. The circles shown in Fig. E-1(b) represent triaxial compression, simple shear and simple tension. In many cases, triaxial compression and direct shear

tests are being used for the obtaining the envelopes.

If Curves AB and A'B' are replaced by two straight lines inclined at an angle ϕ' with the σ axis, this envelope is described in terms of Coulomb-Navier theory. It is found that some of materials show the straight envelope and some do not.

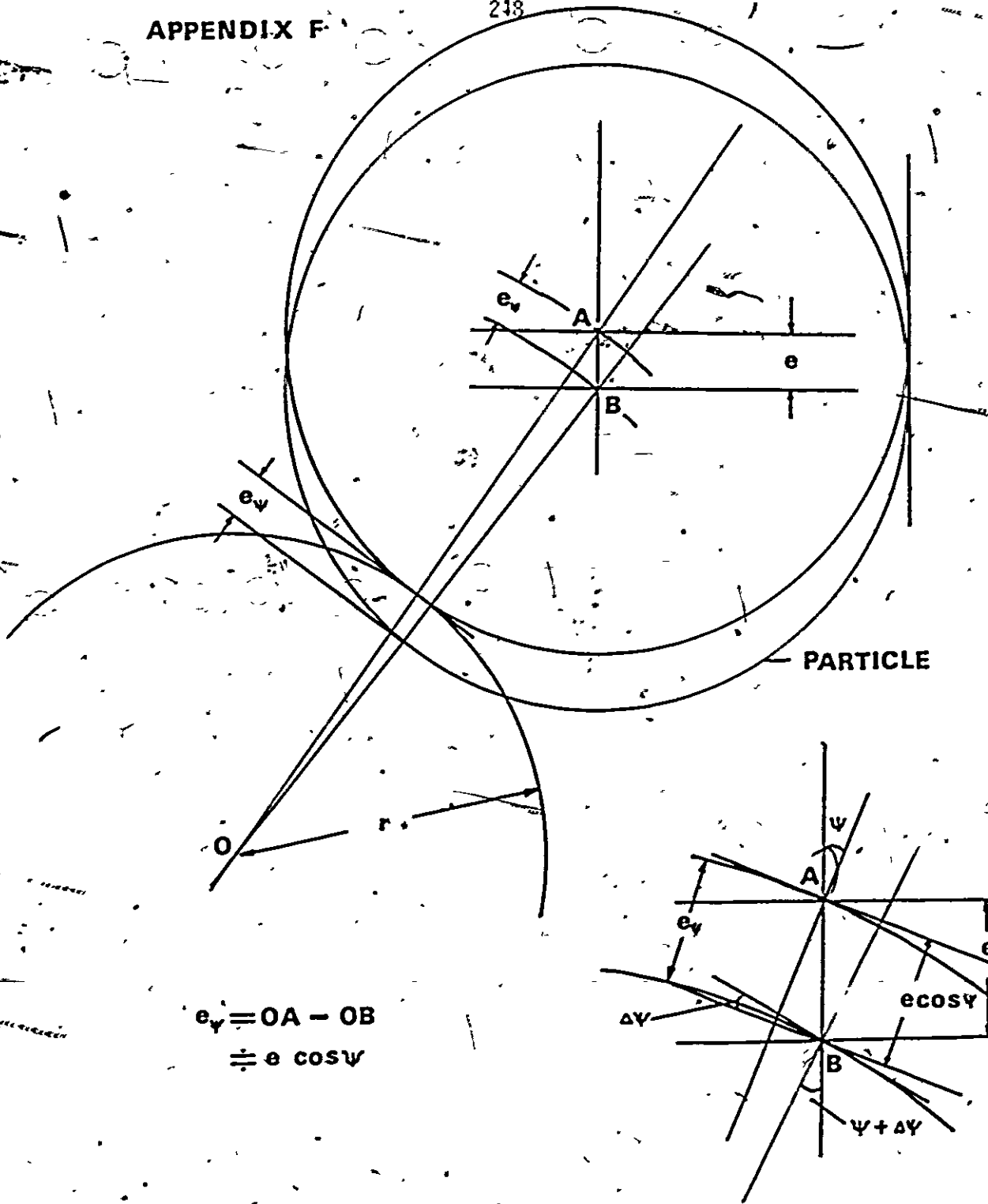


(a)



(b)

Fig. E-1 Mohr's Envelope



$$e_v = OA - OB$$

$$\cong e \cos \psi$$

Fig. F-1 Illustration that e_v Equals to $e \cdot \cos \psi$
 If $\Delta \psi$ is Assumed to be Small

BIBLIOGRAPHY

- Abele, G. and Gow, A.J. (1976). "Compressibility Characteristics of Compacted Snow", CRREL Report 76-21.
- Armstrong, R.W. (1969). "The Polycrystal Ductile-Brittle Transition", Fracture, Proc. 2nd Int. Conf. on Fracture Brighton. Ed. Pratt, P.L., Chapman & Hall Ltd.
- Bader, H. and Others. (1939). "Der Schnee und Seine Metamorphose", Beiträge zur Geologie der Schweiz", Geotechnische Serie. Hydrologie, Lief. 3. (English Translation: U.S. SIPRE. Translation 14, 1954).
- Ballard, G.E.H. and Feldt, E.D. (1966). "A Theoretical Consideration of the Strength of Snow", J. Glaciology, Vol. 6, No. 43, pp. 159-170.
- Ballard, G.E.H. and McGaw, R.W. (1965). "A Theory of Snow Failure", USA CRREL Research Report 137.
- Bowden, F.P. and Tabor, D. (1950). "The Friction and Lubrication of Solids", Part I, Oxford University Press, London.
- Bowden, F.P. and Tabor, D. (1964). "The Friction and Lubrication of Solids", Part II, Oxford University Press, London.
- Butkovich, T.R. (1956). "Strength Studies of High-Density Snow", USA SIPRE Research Report 18.
- Costes, N.C. (1963). "Confined Compression Tests in Dry Snow", Ice and Snow Properties, Processes, and Applications, Proc. of Conf. M.I.T., The M.I.T. Press, Cambridge, Massachusetts, pp. 594-612.
- Feldt, E.D. and Ballard, G.E.H. (1966). "A Theory of the Consolidation of Snow", J. of Glaciology, Vol. 6, No. 43, pp. 145-157.

- Flecher, N.H. (1973). "The Surface of Ice", Physics and Chemistry of Ice, Ed. Whalley, E. et al.; Royal Soc. of Canada, Ottawa.
- Gow, A.J. and Ramseier, R.O. (1963). "Age Hardening of Snow at the South Pole", J. Glaciology, Vol. 4, No. 35, pp. 521-526.
- Hayden, H.W. and Others. (1965). "The Structure and Properties of Materials, Vol. 111, John Wiley & Sons, Inc.
- Herring, C. (1950). "Diffusional Viscosity of a Polycrystalline Solid", J. Applied Phys., 21, pp. 437-445.
- Hobbs, P.V. and Mason, B.J. (1964). "The Sintering and Adhesion of Ice", Phil. Mag. Eight Ser., Vol. 9, No. 98, pp. 181-197.
- Hosler, C.L., Jensen, C.D.C. and Goldshlak, P.L. (1957). "On the Aggregation of Ice Crystal to Form Snow", J. Meteorol, 14, pp. 415-420.
- Jellinek, H.H.G. (1959). "Compressive Strength Properties of Snow", J. Glaciology, Vol. 3, No. 25, pp. 345-354.
- Jellinek, H.H.G. (1967). "Liquid-Like (Transition) Layer on Ice", J. Colloid Interface Sci., 25, pp. 192-205.
- Keeler, C.M. (1969). "The Growth of Bonds and the Increase of Mechanical Strength in Dry Seasonal Snow-Pack", J. Glaciology, Vol. 8, No. 54, pp. 441-450.
- Kingery, W.D. (1960). "Regelation, Surface Diffusion, and Ice Sintering", J. Appl. Phys., Vol. 31, No. 5, pp. 833-838.
- Kinosita, S. and Wakahama, G. (1959). "Thin Section of Deposited Snow Made by Use of Aniline", Teion-Kagaku, Low Temp. Sci. Ser. A., No. 18, pp. 35-45.
- Kuroiwa, D. (1961). "A Study of Ice Sintering", Tellus, 13, pp. 252-259.

- Kuroiwa, D., Mizuno, Y. and Takeuchi, M. (1967). "Micromeritcal Properties of Snow"; Phys. of Snow and Ice, Proc. the Int. Conf. on Low Temp. Sci., Vol. I, Part 2, Ed. Oura, H., The Inst. Low Temp. Sci., Hokkaido University.
- LaChapelle, F.R. (1969). "Field Guide to Snow Crystals", University of Washington Press.
- Mellor, M. (1964). "Properties of Snow", Cold Regions Science and Engineering, Part III, Engrg. Sect. A., Snow Engrg. U.S. Army Material Command, CRREL.
- Mellor, M. and Hendrickson, G. (1963). "Confined Creep Tests on Polar Snow", USA CRREL Research Report 138.
- Nabarro, F.R.N. (1948). "Report of a Conference on the Strength of Solids", Physical Society, London.
- Nakaya, U. and Kuroiwa, D. (1967). "Physical Properties and Internal Structure of Greenland Snow", Physics of Snow and Ice, Proc. the Int. Conf. on Low Temp. Sci., Vol. I, Part 2, Ed. Oura, H., The Inst. of Low Temp. Sci., Hokkaido University.
- Nakaya, U. and Matsumoto, A. (1954). "Simple Experiment Showing the Existence of Liquid Water Film on the Ice Surface", J. Colloid, Sci., 9, 41, pp. 41-49.
- Pasmore, E.M. (1965). "Correlation of Temperature and Grain Size Effects in the Ductile-Brittle Transition of Molybdeum", Phil. Mag., Vol. 11, pp. 441.
- Perutz, M.F. (1950). "Direct Measurement of the Velocity Distribution in a Vertical Profile through a Glacier", J. Glaciology, Vol. 1., No. 7, pp. 382-383.
- Petch, N.J. (1958). "The Ductile-Brittle Transition in the Fracture of α - iron", Phil. Mag., Vol. 3, pp. 1089.
- Ramseier, R.O. (1963). "Some Physical and Mechanical Properties of Polar Snow", J. Glaciology, Vol. 4, pp. 753-769.

- Ramseier, R.O. and Pavlak, T. (1964). "Unconfined Creep of Polar Snow", J. Glaciology, Vol. 5, No. 39, pp. 325-332.
- Ramseier, R.O. and Keeler, C.M. (1966). "The Sintering Process in Snow", J. Glaciology, Vol. 6, No. 45, pp. 421-424.
- Reiner, M. (1960). "Deformation, Strain and Flow", H.K. Lewis & Co., Ltd., London.
- Schytt, V. (1958). Glaciology, II. "Snow Studies at Maudheim. Snow Studies Inland", The Inner Structure of the Ice Shelf at Maudheim as Shown by Core-Drilling. Norwegian-British-Swedish Antarctic Expedition, 1949-52 Scientific Results, Vol. 3, A-C.
- Shumskii, P.A. (1964). "Principles of Structural Glaciology", Translated from Russian to English by Kraus, D., Dover Publications, Inc., New York.
- Sommerfeld, R.A. and LaChapelle, E. (1970). "The Classification of Snow Metamorphism", J. Glaciology, Vol. 9, No. 55, pp. 3-17.
- Taylor, D.W. (1948). "Fundamentals of Soil Mechanics", John Wiley & Sons, Inc., New York.
- Terzaghi, K. (1927). "Principles of Final Soil Classification", Public Roads, Washington, pp. 41-53.
- Tusima, K. (1973). "Tests of the Repeated Loadings on Snow", Low Temp. Sci. Ser. A 31. (Text in Japanese with English Summary).
- Trollope, D.H. (1960). "The Fabric of Clays in Relation to Shear Strength", Proc. 3rd Aust. - N.Z. Conf. S.M. & F.E., pp. 197-201.
- University of Minnesota (1951). "Review of the Properties of Snow and Ice", SIPRE Report 4, Ed. Mantis, T.

Wert, C.A. and Thomson, R.M. (1970). "Physics of Solids", 2nd Ed.,
McGraw-Hill Book Co. Ltd.

Yosida, Z. (1963). "Physical Properties of Snow", Ice and Snow -
Processes, Properties and Applications, Ed: Kingery, D.
Cambridge, Massachusetts, M.I.T. Press.